Applied Physics Laboratory University of Washington
Seattle, Washington 98105-6698

A Study of the Operator Expansion Method and its Application to Scattering from Randomly Rough Dirichlet Surfaces

by Peter J. Kaczkowski

Technical Report
APL-UW TR9406
June 1994

Applied Physics Laboratory University of Washington
1013 NE 40th Street Seattle, Washington 98105-6698

N00014-90-J-1252

FOREWORD

This report is a slightly revised version of the dissertation submitted in partial fulfillment of the requirements for the Doctoral degree in Electrical Engineering at the University of Washington in December 1993. Dr. Eric Thorsos, Principal Physicist at the Applied Physics Laboratory and Research Associate Professor of Electrical Engineering, was the chairman of the supervisory committee. Financial support for this research was provided by the Office of Naval Research, code 1125OA.

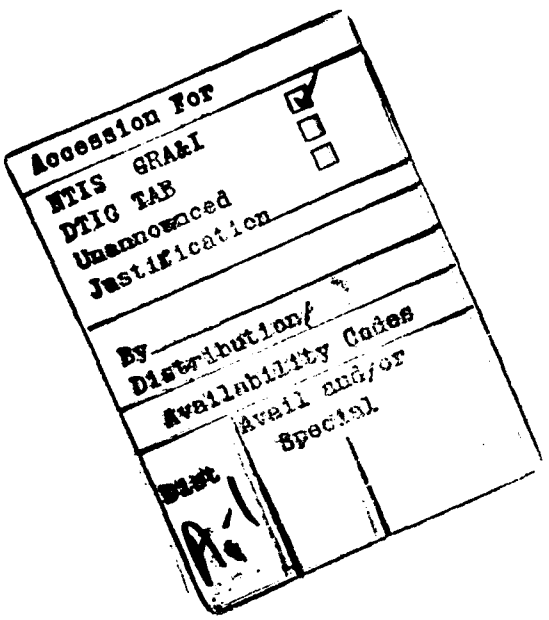

ABSTRACT

The Operator Expansion (OE) method, a new approximation introduced by Milder [J. Acoust. Soc. Am. 89(2), 529-541, 1991] for computing wave scattering from rough surfaces, is applied to acoustic scattering from one-dimensional randomly rough pressure release (Dirichlet) surfaces. The accuracy of the OE series solution is evaluated through comparison with exact numerical results obtained by solution of an integral equation. Studies of scattering from moderately rough surfaces with a Gaussian spectrum indicate that the first order OE solution is accurate when either small perturbation theory or the Kirchhoff approximation is accurate. The first order OE solution is also accurate in some cases when neither classical method is valid. In this moderate roughness regime, the OE series converges rapidly over all scattering angles for a broad range of incident angles, and numerical studies indicate that rapid convergence is always associated with an accurate solution. As roughness is increased, the OE series solution converges less rapidly overall but remains accurate for a wide range of scattering regimes, including some cases just rough enough to support backscattering enhancement. Studies of scattering from surfaces with a Pierson-Moskowitz spectrum used to model the sea surface interface roughness indicate that the OE method is very rapidly convergent over all angles for low frequency (200 Hz) acoustic scattering for wind speeds up to at least 20 m/s, and that the OE solution is accurate for very low grazing angle forward scattering for frequencies at least as high as 1000 Hz. The accuracy of simpler forms of the OE solution (also proposed by Milder) is investigated; these odd- or even-termed series are shown to be more efficient than the standard series at computing accurate solutions. The derivation of the operator series expansion is modified to provide an alternative, more intuitive, development. The connection to the Rayleigh hypothesis is discussed. OE estimates for the cross section are currently obtained using a Monte Carlo technique. The formal average for the lowest order cross section is presented, but the resulting expression is complicated and is not deemed practical. However, the OE method's efficiency and accuracy in one-dimensional tests suggest that this new approximation would be very useful, even as a Monte Carlo technique, for computing scattering from two-dimensional surfaces over a wide range of roughness regimes.

Table of Contents

List of Figures

List of Tables

Acknowledgments

I am very grateful to my advisor, Dr. Eric Thorsos, who spent many patient hours teaching me the mathematics and physics of surface scattering and the skills of scientific writing. I greatly benefited from his depth of understanding of the subject matter and from the generosity with which he gave of his time and effort. I also thank Dr. Darrell Jackson for his guidance in the course of many insightful discussions. I am grateful to Professors Akira Ishimaru and Leung Tsang for their excellent teaching of wave propagation and scattering. I feel very fortunate to have worked on my degree while at the Applied Physics Laboratory, and I particularly thank Dr. Terry Ewart and the Multi-Discipline Group for providing a supportive and stimulating environment for my studies.

Equally important has been the support and encouragement of my family and friends through the long and at times trying process. Most of all, I am very grateful and indebted to my wife, Sara Savage, for her unending patience, understanding, compassion, and faith. I would not have made it without her support and counsel, and look forward to our life together after the degree.

The dissertation is finally finished, and for that I am truly thankful.

CHAPTER 1

Introduction

1.1 Introductory Remarks

Many kinds of energy propagate as waves. These waves are modified by the changes in physical properties encountered as they propagate through a medium. In particular, an interface between two different media imposes boundary conditions on the wave field. Satisfaction of these boundary conditions is usually associated with the generation of fields reflected by and transmitted through the boundary. Because few physical surfaces are smooth, the interaction of waves with rough boundaries, called scattering, is a commonly occurring phenomenon. The essence of the rough surface scattering problem is the determination of the field scattered by a rough boundary of known shape, given a known field incident upon it.

Rough surface scattering applications are diverse. Periodic rough surfaces have long been used as diffraction gratings [Petit, 1980]. Roughness of the sea surface complicates propagation of radio waves, and rough interfaces between different tissue types affect the propagation of acoustic waves in biological media [Ishimaru, 1978]. Scattering from rough waveguide boundaries leads to loss of signal strength and coherence in integrated optics [Marcuse, 1982], as well as in ocean acoustics [DeSanto, 1979].

Many applications emphasize the solution of the inverse problem: the use of the scattered field to extract information about the shape of the surface or the properties of the medium beyond the surface. Examples include the use of satellite radar in remote sensing of the polar ice caps to determine the age or thickness of the ice [Carsey, 1992]; the use of airborne radar scattering from the sea surface to infer wind speed and other environmental conditions [Geernaert and Plant, 1990]; analysis of elastic and acoustic wave echoes in seismic exploration to search for oil bearing structures in the earth [Claerbout, 1985]; and the use of ultrasound to produce images of the human body to conduct noninvasive medical examinations [Kuttruff, 1991].

The deterministic problem treats scattering from a single surface, as for example in computing scattering from a periodic grating [Petit, 1980]. Yet in many situations an averaged solution is preferred, in which moments of the scattered field provide a more useful description of the scattering results. This is true for applications in which the scattering comes from a portion of a random surface that is large compared with the surface correlation length, and in applications that regard the surface-scattered field as noise in imaging or navigation problems. For example, a ship-borne radar system is often used to locate navigation markers or other vessels. Under stormy conditions, the

radar pulse scattered by the ocean surface waves can return as bright echoes that clutter the radar image, obscuring the desired signal. Surface scattering can become an important source of noise in active sonar systems. The backscattered sound from the ocean surface and bottom, called reverberation, often limits the detection performance of these systems [Ellis et al., 1993], [McDaniel, 1993]. Understanding the physics of scattering, and consequently gaining knowledge about the statistics of the scattered field, may help improve signal processing schemes that seek to increase the signal-to-noise ratio in similar imaging applications.

The exact solution of the rough surface scattering problem can only be obtained numerically. As discussed in Chapter 2 for the acoustic case, the scattering process is governed by integral equations that cannot be solved analytically for a general surface profile. Exact solutions can only compute scattering from one surface at a time. Thus, exact solutions of the stochastic scattering problem are approached by averaging scattering results from a large number of individual realizations of the random process. This procedure, called the Monte Carlo method, is very computationally intensive, even for computing two-dimensional (2-D) scattering from one-dimensional (1-D) surfaces. Most scattering applications require treating three-dimensional (3-D) scattering from 2-D surfaces. Such applications almost always result in too large a problem to solve using exact methods.

Many approximations have been proposed to address the rough surface scattering problem in order to simplify the solution for scattering from a single surface or to obtain a formally averaged solution. A formally averaged solution is one in which the statistical properties of the surface roughness, such as the height correlation function or the surface height spectrum, are used to determine the average properties of the scattering. Most approximate methods are restricted to treating a small range of roughness regimes and very few methods can accurately treat scattering from surfaces that are are rough on many scales (such multiscale surfaces commonly occur in nature) over a wide range of incident and scattering angles.

Though often too computationally intensive to be practical in most applications, exact numerical solutions have been very useful in evaluating the accuracy of approximations for scattering from 1-D surfaces. The results of such studies are often presumed to carry over to scattering from 2-D surfaces, where the approximations are used to interpret experimental measurements. In this dissertation we use a numerically exact integral equation technique to study the accuracy of a new approximation called the Operator Expansion (OE) method, introduced by Milder [1991]. The OE method is currently only applied in a Monte Carlo technique, because the formally averaged solution is too complex to be practical (see Chapter 6), and only for the acoustic Dirichlet

problem (pressure release surface). The many favorable attributes of the OE method, which are discussed in more detail below, prompted this investigation. We find that the method is very efficient at computing an accurate scattering solution over a wide range of incident and scattering angles and roughness regimes. We conclude that the method is well suited in its present form to address practical Dirichlet scattering problems such as scattering of moderate frequency sound (up to a few kHz) from realistic 2-D ocean surfaces. Further development of the method to treat other boundary conditions is warranted.

1.2 Rigorous Numerical methods

Recent advances in computer technology have made computationally intensive rigorous solutions practical, at least for scattering from 1-D surfaces. The rigorous methods provide exact numerical solutions in the sense that no approximations have been made in the scattering physics, but significant care must always be used in their implementation. For example, the scattering problem is governed by integral equations (see Sec. 2.2.4) that can be solved in coordinate space or in Fourier transform space by discretization and subsequent solution of a large system of equations; such methods can be limited by ill-conditioning [Garcia et al., 1978].

Exact numerical methods estimate moments of the scattered field by averaging over a finite number of scattering experiments in a Monte Carlo method. This procedure always results in the presence of statistical fluctuations in the solution (experimental data has similar limitations), but these can be made very small by calculating scattering for a large number of surfaces. However, in many cases it is not necessary to reduce the fluctuations to exceedingly small levels in order to adequately ascertain the accuracy of a formally averaged solution. Furthermore, the number of required surface realizations can be quite small if the approximate method is implemented to compute scattering from single surfaces. The fluctuations can then be reduced by taking the difference between the exact solution and the approximate solution.

All methods using randomly rough surfaces must rely on a stochastic process to generate the realizations. Here, a Fourier transform based method is used to generate random phase (and amplitude) realizations consistent with a given spectrum [Thorsos, 1988], [Macaskill and Ewart, 1984]; the generated surfaces have Gaussian statistics.

The following summary of exact numerical methods is not intended to be an exhaustive list but rather is provided as background for the tapered plane wave integral equation method used in this dissertation. Here, the discussion is specialized to the Dirichlet surface but the methods are applicable to other boundary conditions as well.

Extended Boundary Condition (EBC) -- T-matrix method

The EBC method, proposed by Waterman [1975], is based on the use of an exact integral identity derived for the scattering problem using Green's theorem (see Sec. 2.2.3, and Ishimaru [1991]). The identity, also called the extinction theorem because it is obtained by considering field points below the surface where no real field exists, places integral constraints on the surface values of the normal derivative field. The solution was developed for scattering from finite objects or periodic surfaces, and thus is effected in the Fourier transform domain. The method is well known to become ill-conditioned for sufficiently rough surfaces [Garcia et al., 1978], [Chuang and Kong, 1981]. The method has recently been applied to scattering from 2-D surfaces [Lou, 1991].

Least-Squares methods, Rayleigh-Fourier method

The least-squares method expands the surface values of the scattered field in a truncated sum of outgoing plane waves, and solves for the plane wave coefficients by solving a least-squares problem. (This method does not invoke the Rayleigh hypothesis, and works well beyond the Rayleigh hypothesis validity limit; more details are presented in Sec. 3.5.2). Meecham [1956b] first proposed this solution, but was unaware of the fact that the least-squares method is rigorous. Ikuno and Yasuura [1973], Millar [1973], Petit [1980] and others developed the underlying theory. Recently, Berman and Perkins [1990] have extended the method (in both coordinate space and Fourier space) to fluid-fluid and fluid-solid interfaces with good results. Generally, the least-squares method can treat rougher surfaces than the EBC method.

Finite Element Method (FEM)

Recently, a hybrid method using a finite element technique has been used to compute scattering from rough surfaces [Lou et al., 1991a]. Given a down-going incident field, the finite element method is used to compute the scattered field in the near-surface region and is then matched to an up-going plane wave solution on a plane a small distance above the highest point of the rough surface. This method exploits the large ratio between surface length and surface height to provide an efficiently computable solution for 1-D surfaces. The method could perhaps be practical in computing scattering from 2-D surfaces, though the partitioning of the 3-D volume in the near-surface region into small elements is substantially more complicated than the corresponding process for 1-D surfaces. The method can be extended to penetrable surfaces [Lou et al., 1991b], and could in principle include inhomogeneities in the medium near the surface.

Integral equation iterative series

The integral equation of the second kind for the surface values of the unknown scattered field normal derivative (Dirichlet boundary condition) provides a way of solving the scattering problem by iteration [Meecham, 1956a]. The Kirchhoff approximation arises naturally as the first term in this iterative series, which, when examined in the high frequency limit, is shown to be a multiple scattering series [Liszka and McCoy, 1982]. The iterative method can be used to provide a numerical exact solution by repeating the iteration until the changes in the normal derivative field are deemed sufficiently small from one iteration to the next. The iterative technique is combined with an efficient matrix solution in the Banded Matrix Iterative Approach (BMIA) [Tsang et al., 1993a, 1993b] that solves the strongly coupled local interactions by banded matrix techniques, and iterates to find the weaker, more distant interactions. The method is very promising because of its speed in providing a rigorous solution for a wide range of scattering regimes.

Tapered Wave Integral Equation

The tapered wave integral equation method [Axline and Fung, 1980], [Thorsos, 1988] solves an integral equation governing the scattering problem. The problem is generally nonperiodic and the solution is effected in coordinate space. The incident field is tapered to reduce edge effects, directly leading to a trade-off between surface length (and hence computation time) and angular resolution of the scattering results in the far field. Though the method is appealing because realistic experimental scenarios can easily be constructed, its usefulness comes from the great range of surface roughness that can be treated without ill-conditioning. The method has been used to study scattering from very rough surfaces that exhibit backscattering enhancement for the Dirichlet boundary condition [Thorsos and Jackson, 1991], [Chen and Ishimaru, 1990] and for electromagnetic scattering from metallic and dielectric surfaces [Maradudin et al., 1990]. For the Dirichlet boundary condition, the method can be implemented for two formally equivalent integral equations of the first and second kind [Meecham, 1956a], [Thorsos, 1988]. As with any numerical method, convergence tests (in this case changing the number of surface partitions per acoustic wavelength) must be performed to ensure accuracy. These tests show that the two implementations converge differently. Thus, direct comparison between the first and second kind integral equation solutions provides a useful numerical test of the accuracy of the solution. The principal drawback of the integral equation method is its computational expense (computation time is proportional to the number of surface partitions cubed), practically limiting it to 1-D surfaces. Here, we use the solution for both kinds of integral equations, as presented by Thorsos [1988], to evaluate the accuracy of approximate solutions.

1.3 The Classical Approximations

Two approximate methods, the small perturbation method and the Kirchhoff approximation, have been used extensively in surface scattering. Though many applications are beyond the scope of these classical approximations, they are fundamental in providing accurate, physically based solutions in important scattering regimes.

Perturbation theory

Introduced by Rayleigh [1945, 1907] for the case of sinusoidal surfaces and by Rice [1951] for the case of periodic randomly rough surfaces, the perturbation theory solution is an orderly expansion in terms of the small parameter kh, where k is the acoustic wave number and h is the rms (root mean square) surface height. Though the radius of convergence of the perturbation series has not been established analytically, numerical studies have shown through comparison with exact calculations that the method is valid in many regions of interest in low-frequency ocean acoustics [Thorsos and Jackson, 1991], [Thorsos, 1990a], and in electromagnetic scattering [Soto-Crespo et al., 1990]. The Rayleigh-Rice method invokes the Rayleigh hypothesis, but nevertheless provides a solution that has been shown to be identical through fifth order to the perturbation solution derived rigorously using the EBC [Jackson et al., 1988]. The small perturbation method is also called field perturbation when it is important to distinguish it from the phase perturbation method, discussed in Sec. 1.4. The Rayleigh-Rice approach is used to derive the perturbation solution for scattering from a single surface in Sec. 2.5 and in Sec. 3.4.

The Kirchhoff approximation

The Kirchhoff approximation for rough surface scattering was studied first by Brekhovskikh [1952] and also by Eckart [1953] for acoustic scattering, and by Beckmann and Spizzichino [1963] for electromagnetic scattering. Named after Kirchhoff because of the similarity to the approximation bearing his name in the problem of light diffraction by an aperture [Born and Wolf, 1980], the Kirchhoff approximation in surface scattering is based on the assumption that a smooth, slowly varying surface can be locally approximated as planar; thus, the Kirchhoff approximation is also called the tangent plane approximation [Bass and Fuks, 1979]. It is assumed valid when the local radius of curvature is everywhere large compared to a wavelength, and when the angles of incidence and scattering are not so close to the surface slope angles as to cause shadowing or other multiple scattering effects. The radius of curvature criterion can be relaxed when accuracy of the average angular distribution of the scattered intensity far from the surface is desired; numerical comparisons to integral equation results have

shown that for randomly rough surfaces with a Gaussian spectrum [Thorsos, 1988], the surface correlation length is the quantity that should be compared with the wavelength in order to establish validity of scattering cross section calculations. The Kirchhoff approximation is often used in computing forward scattering; numerical studies show that for certain power law surfaces [Thorsos, 1990a] for which the local radius of curvature is rarely, if ever, large compared to the acoustic wavelength, the Kirchhoff approximation is still valid for near specular scattering. The Kirchhoff approximation solution is developed in Sec. 2.4 for scattering from a single surface, which is convenient for Monte Carlo studies. Like perturbation theory, the Kirchhoff approximation is readily averaged and provides a useful solution in regimes where it is accurate.

Though these two fundamental approximations are useful in their respective regions of validity, many cases of interest fall outside the scattering regimes in which either the small perturbation method or the Kirchhoff approximation apply. The roughness regimes for which the classical methods are accurate over all scattering angles for 45° incidence are depicted in Fig. 4.2 for surfaces with a Gaussian spectrum. For such surfaces, the classical methods' accuracy regions do not overlap except for very small roughness. In low frequency acoustic scattering from 1-D Pierson-Moskowitz surfaces (whose spectrum is used to model the sea surface height spectrum) the Kirchhoff approximation is more accurate for near specular scattering whereas the perturbation solution is more accurate for scattering in directions away from specular.

Composite roughness model

A heuristic model attempting to combine the abilities of these two fundamental approximations was developed for particular applications in which the surface height function can be usefully decomposed into two roughness scales: a large scale surface for which the Kirchhoff approximation holds, and a small scale surface (on the scale of the irradiating wavelength) for which perturbation theory applies. The composite roughness model has long been applied to scattering of acoustic [Kur'yanov, 1963] or electromagnetic [Guinard et al., 1971] waves from the sea surface (or both [McDaniel and Gorman, 1982]); a rigorous derivation of the method which presents an estimate of the contribution from neglected terms was provided by McDaniel and Gorman [1983]. Accuracy of such a composite roughness model has been examined for low frequency acoustic monostatic backscattering from 1-D Pierson-Moskowitz surfaces [Thorsos, 1990a] and found to be good except near grazing. Comparisons for shorter wavelength scattering have been made with data, but scattering from bubbles usually dominates the acoustic backscattering signal above a certain wind speed [Nutzel et al., 1993], [McDaniel and Gorman, 1982], and the lack of complete understanding of surface hydrodynamics and coupling of water waves to the wind (leading to an inaccurate

representation of the surface height) may contribute substantially to the inaccuracy of electromagnetic composite roughness models at lower grazing angles [Weissman et al., 1993]. In general, the composite roughness model does not include a systematic way of partitioning a realistic spectrum into the two spectral bands, and yet the results depend on the choice of the partition wavenumber, principally through its effect on the slope of the large scale surface. Furthermore, a "good" choice for the partitioning also depends on the angle of incidence [Thorsos, 1990a], [Dashen et al., 1990].

Great effort has been directed at finding a systematic approximation that has properties of both classical methods in their respective regions of validity (while retaining computational efficiency!) so as to be useful in treating scattering from a broad class of 2-D surfaces. We now turn to a brief description of some of the most notable modern approximations. The following list is by no means complete; for a review of many other methods see Winebrenner [1985].

1.4 Recent Approximate Methods

Phase perturbation method

The phase perturbation method, developed by Winebrenner and Ishimaru [1985a, 1985b] from an earlier suggestion† by Shen and Maradudin [1980], expands a quantity related to the phase of the unknown surface field in a power series in kh. (The standard perturbation method expands the field itself in a series in kh.) Each term of the phase perturbation series solution contains a partial sum of higher order terms in the field perturbation series; this resummation leads to improved convergence over the standard field perturbation solution, and consequently to accuracy over a greater range of normalized surface height kh than possible with field perturbation. Indeed, Winebrenner and Ishimaru [1985b] showed that the (second order in kh) backscattering cross section reduces to each of the classical approximation solutions in their respective limits; this appears to be the first systematic theory to have this important property. The phase perturbation solution was compared in detail to the classical approximations [Broschat et al., 1987] and to an exact numerical solution [Broschat et al., 1989] for scattering from surfaces with a Gaussian spectrum. The method is accurate when the Kirchhoff approximation and perturbation method are accurate, and for some roughness regimes beyond the reach of the classical approximations. The phase perturbation method has also been tested in scattering from Pierson-Moskowitz surfaces [Broschat, 1993] and

† Shen and Maradudin [1980] followed their initial phase expansion by an expansion of the complete exponential terms, limiting the resulting solution to the height perturbation regime.

has typically been found, for a wind speed of 20 m/s and incident grazing angles between 10° and 20°, to be accurate for all scattering angles except those closer than 10° from grazing. The phase perturbation solution developed by Winebrenner and Ishimaru [1985a, 1985b] has one theoretical drawback in that it is not reciprocal. A heuristic algorithm which combines the phase perturbation solution and its "reversed phase" formulation to provide a reciprocal solution has been proposed, and is found to be somewhat more accurate than the original solution [Broschat et al., 1990].

Bahar's "Full-Wave" method

In a series of papers, Bahar developed a technique for computing scattering called the "full-wave" method [e.g., Bahar, 1980, 1991]. Though the method's name has not changed, the full-wave solution has actually appeared in several different forms [Thorsos and Winebrenner, 1991], [Thompson and Chapman, 1993]: one form before 1980 [e.g., Bahar, 1978], a second between 1980 and 1991 [e.g., Bahar, 1980], and a third form [Bahar, 1991]. In general, the method attempts to provide an approximation which reduces to both classical approximations in their appropriate limits, and Bahar has repeatedly made the claim that the (1980) full-wave solution has this property [Bahar, 1980, 1981, 1987]. However, it has been shown [Thorsos and Winebrenner, 1991] that for scattering from 1-D Dirichlet surfaces the 1980 full-wave solution does not reduce to first order perturbation theory when the latter is known to be valid; instead, calculations of the cross section show that the full-wave solution agrees closely with the Kirchhoff approximation result (which is inaccurate in the regime examined). These results, in direct contradiction to Bahar's conclusions, are supported by the work of others [Thompson and Chapman, 1993]. The third form of the full-wave solution [Bahar, 1991] has yet to be fully discussed by other investigators.

Kirchhoff iterate

The integral equation iterative method discussed in Sec. 1.2 can be used to provide a numerically exact solution. Several investigators have examined the accuracy of the solution which uses just the first two terms in the series, the Kirchhoff approximation and the first iterate. Holliday [1987] showed that the Kirchhoff plus first iterate solution reduces to the first order perturbation solution for backscattering when roughness is small, and Thorsos and Jackson [1991] show numerically that this reduction occurs for bistatic scattering when kh is sufficiently small. The first iterate solution has also been investigated in scattering from very rough surfaces where enhanced backscatter is observed [Thorsos and Jackson, 1991], [Chen and Ishimaru, 1990], [Ishimaru and Chen, 1990], and has been shown to contribute an essential part of the enhancement mechanism, thus providing an approximation which may be useful over a wide range of

roughness regimes. However, Thorsos and Jackson [1991] have shown that the scattering cross section obtained from the first iterate depends on surface length; higher order iterations are required to cancel this dependence, but a shadowing function may be used instead to approximate the effects of the higher order terms [Ishimaru and Chen, 1990].

Unified perturbation method

The unified perturbation method [Rodriguez and Kim, 1992] is another method which seeks to systematically treat scattering from surfaces rough on many scales. The method evolved from a perturbation treatment in which the small parameter is the momentum transfer in the horizontal direction [Rodriguez, 1989]; for near vertical incidence, this can be interpreted as an expansion about the specular direction. The small momentum transfer expansion leads formally to a series which has the Kirchhoff approximation as its first term, and a curvature dependent correction at next order. Nevertheless, the relation between this series and the integral equation iterative series which also has the Kirchhoff approximation as its first term is not obvious [Rodriguez and Kim, 1992]. Rodriguez [1989] states that the small momentum transfer method is not applicable for incident angles which are close to grazing because of the singular behavior of a geometric factor at grazing incidence. The accuracy of the unified perturbation method has been tested for certain power law surfaces using an exact numerical method (method of moments, or, integral equation method), and inaccuracies (error $\geq$ 1 dB) of the first and second order solutions appear for scattering angles further than about 65° from vertical, for several surface roughnesses, even when the incident angle is less than or equal to 50° from vertical [Rodriguez and Kim, 1992].

Small-slope approximation

The small-slope approximation was developed by Voronovich [1985] with the objective of finding an approximation which could treat scattering from multiscale surfaces without having to appeal to a composite roughness model. In performing the small slope expansion of the scattering amplitude, Voronovich succeeded in deriving a systematic series solution which is constrained to reduce to the perturbation solution for small height, and yet is valid for arbitrary surface height so long as the surface slope remains small. Furthermore, the solution is manifestly reciprocal. The first two terms in the series solution for the cross section have been investigated numerically [Broschat and Thorsos, 1991], [Berman, 1991], and further studies indicate that it may indeed be a very accurate formally averaged theory [Thorsos, 1993a].

Dashen's method

In a series of papers, Dashen and Wurmser [1991a, 1991b, 1991c] and Dashen, Henyey, and Wurmser [1990] describe an approximation which is constructed to be manifestly reciprocal, and which is obtained by examining a perturbation (variation) about a known reference surface solution. This reference surface need not be flat; indeed, a slowly varying reference surface leads to a series solution expanded in the radius of curvature. At lowest order, that is, when neglecting curvature dependent terms, the solution is constrained to "reproduce the traditional composite model" [Dashen and Wurmser, 1991b], in the following sense. The lowest order solution for the scattering amplitude is expressed as a single integral over a product of exponential functions of the surface height and a function of slope; this function of slope is determined such that the lowest order solution reduces to the perturbation and Kirchhoff approximation solutions in the appropriate limits. At lowest order, both the small slope approximation (Voronovich) and Dashen's solution are "local" approximations, resulting in single integral forms for the scattering amplitude. In contrast, the operator expansion method described below is a nonlocal solution even at lowest order.

1.5 The Operator Expansion method

The operator expansion method is a new formalism for computing scattering from Dirichlet rough surfaces [Milder, 1991], and is based on an approximation used in surface wave hydrodynamics [Milder, 1990]. Similar surface scattering approximations were introduced long ago by Lysanov [1956] and also by Meecham [1956c], and further examined by Urusovskii [1960]. In these approaches, an approximate solution to the integral equation for the surface field was developed for rough surfaces with small slope and small height and was written in terms of Fourier transforms. Much later, Voronovich [1987] developed a small slope series solution for nonlocal vertical derivative operator (denoted $\hat{Z}$ by Voronovich and $\hat{D}$ by Milder and in this dissertation), an approach which subsequently led to a different approximation called the Small Slope Approximation (SSA) [Voronovich, 1985].[†] We do not examine any of these related approximations here, nor do we compare the above methods to the operator expansion method though such a study would likely prove valuable.

[†] In a personal communication, Voronovich clarified the evolution of the work on the SSA: though the two papers were published in reverse chronological order, the submission dates reflect the order of development. The two papers have similar titles but the methods themselves are quite different, the SSA lending itself much more readily to formal averaging than the vertical derivative operator method. Similarly, the OE method does not easily lead to a practical formal average; see Chapter 6.

The OE method has several attributes of a promising technique:

- Milder [1991] showed that the OE solution reduces analytically to the classical solutions to the surface scattering problem in their respective asymptotic limits, that is, to the perturbation solution in the limit of small rms surface height, and to the Kirchhoff approximation (plus a curvature dependent correction term) in the limit of very smooth surfaces varying slowly on the scale of the acoustic wavelength. This fundamental analytical property of reduction to both classical theories in their respective regions of validity indicates that the operator expansion solution might well be valid over a wide range of scattering regimes. Indeed, this reduction to *both* classical solutions must be a property of any method which can accurately treat scattering from multiscale surfaces, yet has historically been very difficult to achieve.

- The operator expansion solution is presented as a systematic series of terms containing powers of an integral operator, from which the method derives its name. Numerical tests presented in Chapters 4 and 5 indicate that the convergence of the series (observed by examination of the rate of decay of these terms) is useful in determining the accuracy of the OE solution at any given order.

- Milder [1991] indicated that the solution is reciprocal at each order in its expansion (analytically verified in our work through third order). Reciprocity is a physical property of the scattering problem which is not always easy to retain in an approximation; in the case of the OE, reciprocity is a natural consequence of the construction of the expansion and is not "forced" in any way.

- The OE solution is implemented using Fast Fourier Transforms (FFTs) and is extremely fast to compute for scattering from 1-D surfaces, making it practical for 3-D scattering from 2-D surfaces. For example, for a 1-D surface divided into only 400 intervals, the second order solution for the surface field is about two orders of magnitude faster than the corresponding integral equation calculation.

These features make the OE method a very promising approximation and have motivated the current study of its accuracy. Milder tested the method for scattering from 1-D sinusoidal surfaces and wedge shaped gratings [Milder, 1991], and from 2-D sinusoidal surfaces [Milder and Sharp, 1992], and found that the method proved to be both fast and accurate for those surface types. We examine the method in computing scattering from randomly rough surfaces. In particular, the application to scattering from multiscale surfaces, such as those encountered in scattering of sound from the ocean surface, is of great interest. In this study, accuracy of the OE method is determined through comparison to the exact solution obtained by an integral equation

technique; as discussed above, this solution is practically limited to treating scattering from 1-D surfaces. Our study was performed for 2-D scattering from 1-D surfaces, but the results are expected to carry over to 3-D scattering from 2-D surfaces.

1.6 Overview of the dissertation

The basic equations governing the scattering problem, and the two classical approximations used to solve it, are presented in Chapter 2. Specializing the problem to the 1-D Dirichlet boundary, Green's theorem is used to develop the scattering integrals and other important integral identities relating the incident, scattered, or total fields, and their normal derivatives, on the rough surface boundary. The scattering results in subsequent chapters are presented in the far field of the scattering surface; the scattering amplitude and the scattering cross section are defined and examined for series solutions. Numerical results presented in later chapters indicate that the operator expansion solution for the cross section does not require consistency in the surface field expansion parameter to maintain accuracy. Consequently, the computational efficiency of the method can be increased by making use of an "inconsistent" series solution. The Kirchhoff approximation and the small perturbation method are presented as "Monte Carlo" methods, to assist in comparing them to the operator expansion solution in later chapters.

The broad range of accuracy of the operator expansion, observed in numerical tests presented in Chapters 4 and 5, prompted a closer look at the derivation of the method. We find that insight into the method's accuracy can be gained by examining the construction of the operator solution; this construction is performed in Chapter 3 in a somewhat less rigorous but more intuitive manner than in Milder's derivation. (The expression for an additional order (third) in the operator expansion beyond that given by Milder is also included.) The decomposition of the fundamental nonlocal operator into its component operators is carried a little further than necessary to obtain the actual series expansion, so that the role of the various components can be examined. A comparison between the Monte Carlo perturbation method and a method based on one of the operator component solutions brings to light some of the similarities and some of the differences between the OE and the perturbation method, and hints at why the OE method has a much broader range of validity than the standard perturbation expansion: the perturbation expansion can be viewed as a one-way analytic continuation from the rough surface to a plane, whereas the OE makes use of a two-way continuation (to a plane and then back to the rough surface) which greatly reduces the height dependence of the solution.

Numerical implementation notes also appear in Chapter 3, and include a description of the tapered plane wave incident field, use of the FFT in the solution, factoring of operator terms for increased efficiency, surface height tapering requirements, and other details pertaining to the difficulties associated with evaluating the third order term.

An extensive discussion of the two principal differences between Milder's derivation and our own appear at the end of Chapter 3. The first has to do with the method of finding the operator series expansion. Milder uses a variational technique, obviating the need to find an explicit series representation for one of the operator components, whereas we employ a backsubstitution technique used in similar derivations [West et al., 1987]. We present an expanded version of Milder's variational method for completeness, and because of its elegance in solving for the operator series expansion. The second difference concerns the application of the Rayleigh Hypothesis (RH) in deriving the OE solution. In performing the derivation, we explicitly assume that the RH holds, and rely on numerical tests to evaluate the impact of this assumption on the accuracy of the solution in cases where the RH is invalid. Milder attempted to avoid making the RH assumption by using a transformation of the extended boundary condition (extinction theorem) integral theorem. We find that in his derivation, the RH is imposed on an arbitrary down-going plane wave which, by analogy with the scattering problem, is equivalent to imposing the RH on the scattered field. Thus we show that all available derivations of the operator expansion invoke the Rayleigh hypothesis. A careful examination of this subtle issue is presented in the concluding section of Chapter 3, along with a review of some of the most relevant work of other investigators regarding the Rayleigh hypothesis and the use of up-going wave expansions in providing rigorous solutions to the scattering problem.

The cornerstone of the dissertation is the extensive numerical testing of the operator expansion solution through comparisons with a numerically exact integral equation solution. Without such tests, the accuracy of the OE method in roughness regimes where classical solutions are no longer accurate is largely a matter of speculation, particularly when questions about the method's formal validity arise in connection with the Rayleigh hypothesis. However, numerical experiments have shown that the operator expansion method is indeed accurate over a wide range of scattering parameters. These results are reported in Chapters 4 and 5, which treat scattering from randomly rough 1-D Dirichlet surfaces with Gaussian and Pierson-Moskowitz spectra, respectively.

The study of scattering from surfaces with a Gaussian spectrum (Chapter 4) is guided by the use of a single "slope-height" roughness parameter khs, which was suggested by Milder [1991] as a general indicator of the OE method's roughness regime. Milder and Sharp [1992] find that the OE method is generally applicable if $khs \leq 1$.

Here, numerical examples are chosen on contours of constant *khs* which appear as straight lines in the (log-log) *kl*-*kh* plane (see Fig. 4.2). The classical methods are known to be accurate in certain regions of the *kl*-*kh* plane, broadly corresponding to $khs \leq 0.25$. Thus, the first series of tests examines the reduction to the classical approximations numerically, and indicates that when $khs = 0.15$ the first order OE solution is generally accurate when the Kirchhoff approximation and perturbation methods are accurate, and is also accurate for some cases when the classical methods are not. When $khs = 0.15$, the OE series solution is found to converge very rapidly over all scattering angles. As the value of *khs* is increased to well beyond the range of roughnesses which can be treated accurately by the classical methods, the operator expansion solution still provides an accurate solution for many situations. In general, the rapid convergence of the series is associated with an accurate solution; this self-consistent property is hoped to be very useful in applying the method to scattering from 2-D surfaces for which exact solutions are very costly.

Tests have been carried out for values of $khs \lesssim 10$, but the highest value reported is $khs \approx 3.5$, for an example which is just rough enough to support backscattering enhancement. The OE method is able to accurately compute scattering for this case (for an incident grazing angle of 60°) for all scattering angles more than 40° from grazing; the backscattering enhancement peak is clearly visible and accurately computed. However, this example is near the limit of the maximum roughness for which the OE method can accurately compute scattering.

The OE method is applied to scattering from a form of multi-scale surface used to model the ocean surface (Pierson-Moskowitz spectrum) in Chapter 5. Scattering is considered for surface roughness due to wind speeds up to 20 m/s and for acoustic frequencies up to 1000 Hz. The low frequency tests (200 Hz) are conducted over all scattering angles for incident grazing angles from 10° to 90° using the integral equation technique, and the OE method is found to converge rapidly over nearly all scattering angles leading to an accurate solution over those same angles. The higher frequency examples are examined using a recently developed parabolic equation integral equation method [Thorsos, 1993b] which can accurately compute forward scattering (within about 45° of grazing) for surfaces partitioned into a number of intervals an order of magnitude greater than possible with the Helmholtz equation method. For incident angles as low as 5°, for a 15 m/s surface and 1 kHz scattering requiring 20,000 surface intervals, the OE method is accurate over all forward scattering angles examined. The OE method is thus seen to be very promising in computing scattering from realistic 2-D ocean surfaces at moderate frequencies, even at very low grazing angles.

Milder [1991] showed that the OE solution could be simplified by taking advantage of an inversion symmetry of the solution with respect to the surface height function. The resulting series solutions contain only odd or only even terms from the original operator series expansion. We examine the accuracy of these "short" forms for both types of surface height spectra and find that they provide a more efficient solution than the standard series. In the case of Pierson-Moskowitz surfaces, the improvement in accuracy for solutions computed to the same order in the surface field is quite dramatic; the short forms almost get "an order for free".

The operator expansion method is currently developed as a numerical technique, that is, it computes scattering from one surface at a time. While this makes comparisons with the exact integral equation solution particularly convenient, the OE method can only be used to compute moments of the scattered field using the Monte Carlo method. Most other approximations are formally averaged, that is, the statistical properties of the randomly rough surface height are used to analytically evaluate the moments of the scattered field. The demonstrated accuracy of the OE method is further incentive to find an averaged solution. An attempt at formally averaging the lowest order operator expansion solution (even series solution EV_0) is presented in Chapter 6; the resulting expression for the scattering cross section is not simple enough to be practical. The nonlocal nature of the OE solution, in great part responsible for the method's broad range of accuracy, leads to an expression for the scattering amplitude with several integrals over the transverse coordinate and its Fourier conjugate variable (the transverse wavenumber), even at lowest order.

A detailed summary of the results of each chapter appears in Chapter 7; summaries do not appear at the end of each chapter for the sake of brevity. The final chapter concludes with a few suggestions for future work on this promising method, which include extending the technique to other boundary conditions and examining the method's behavior in 3-D scattering from 2-D surfaces. The operator expansion method is currently seen as a very efficient numerical method providing an accurate solution to the Dirichlet surface scattering problem over a very broad range of scattering regimes, far broader than possible with the classical approximations. The OE solution is much faster to compute than the exact integral equation solution and is practical for computing scattering from realistic 2-D surfaces, even when applied in a Monte Carlo approach.

CHAPTER 2

Basic Equations for Rough Surface Scattering

2.1 Introduction to Chapter 2

In this chapter we present the fundamental equations governing the rough surface scattering problem which we address throughout this dissertation. We consider the scattering of acoustic waves from surfaces rough in one dimension only. The methods themselves are not restricted to this dimensionality, but computer limitations arise in calculating the exact solution to the problem of scattering from a single surface, obtained by solving an integral equation. Use of this exact solution is central to the determination of the accuracy of various approximate methods considered here; for consistency and simplicity we will develop all equations for two-dimensional (2-D) scattering from one-dimensional (1-D) surfaces. The operator expansion method has not yet been extended beyond the scalar Dirichlet scattering problem[†], while the perturbation method, Kirchhoff approximation, and the integral equation technique have all been developed for more complicated environments, and for vector fields. We will only treat the scalar case here, specializing many of the equations to the Dirichlet boundary condition.

2.2 Fundamental Integral Relations

2.2.1 The surface scattering problem

The geometry for 2-D scattering from a 1-D surface is sketched in Fig. 2.1, where we consider the acoustic pressure field $p(\mathbf{r})$ in region V_1 bounded by the physical rough surface S and by the hemisphere H. The time-harmonic ($e^{-i\omega t}$) sources P of acoustic pressure p are confined to a finite space V_3 within V_1. The problem is to determine the field $p(\mathbf{r})$ in region V_1 given the sources $P(\mathbf{r})$, the shape of the rough surface S, and the physical boundary condition on S.

The acoustic field $p(\mathbf{r})$ satisfies the inhomogeneous Helmholtz Equation (HE)

$$\left[\nabla^2 + k^2\right] p(\mathbf{r}) = -P(\mathbf{r}) \ , \quad \mathbf{r} \in V_1 \tag{2.1}$$

[†] Milder [1991] presented some formal equations for the Neumann boundary condition, but certain practical aspects of the Neumann solution which are fundamentally different from those encountered in the Dirichlet case were not addressed.

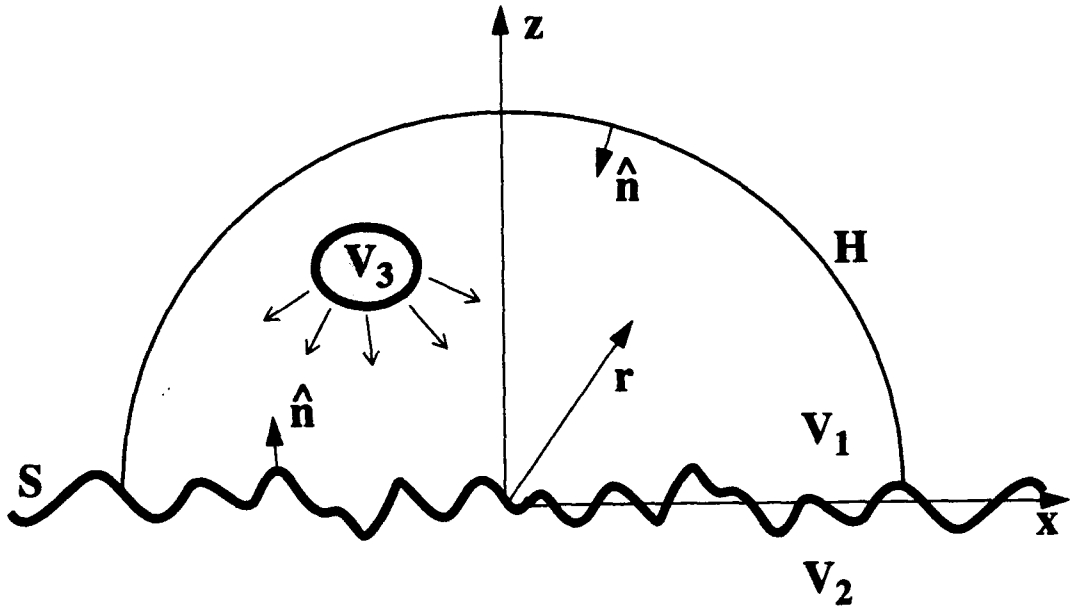

Figure 2.1 : Geometry for 2-D scattering from a 1-D rough surface. The sources of the field incident on surface S are distributed in volume V_3. The field scattered by the rough surface is to be determined at various points $\mathbf{r}$. Hemisphere H is a mathematical surface closing volume V_1 above S.

for all points $\mathbf{r}$ in V_1, where $k = \omega/c$ is the acoustic wavenumber, ω is the angular frequency, and c is the sound velocity in V_1. The field p also satisfies a boundary condition on S which will be used below. The free space Green function for the HE satisfies the inhomogeneous equation with a point source at point $\mathbf{r}'$:

$$\left[\nabla^2 + k^2\right] G_0(\mathbf{r},\mathbf{r}') = -\delta(\mathbf{r}-\mathbf{r}') . \tag{2.2}$$

For two-dimensional problems, the free space Green function for outgoing waves is

$$G_0(\mathbf{r},\mathbf{r}') = \frac{i}{4} H_0^{(1)}(k|\mathbf{r}-\mathbf{r}'|) , \tag{2.3}$$

where $H_0^{(1)}$ is the zero order Hankel function of the first kind.

2.2.2 Green's theorem — Helmholtz-Kirchhoff scattering integrals

Green's theorem allows us to express the relation between a field and its sources, which can be distributed in volumes or on surfaces. Continuous source distributions can be constructed by superposition of singularities of the field (such as the point source term $\delta(\mathbf{r}-\mathbf{r}')$), which are understood to be points at which the field or one of its first or second partial derivatives is discontinuous [Baker and Copson, 1950, p. 23]. Surface source distributions have no discontinuity along the surface, but are discontinuous across the surface; indeed, they can be interpreted as surface distributions of monopole and dipole sources [Jackson, 1975, p. 41] giving rise to a field in the manner of

Huygens' principle [Baker and Copson, 1950]. In this dissertation we shall refer to distributed volume sources or to point singularities of the field simply as *sources* of the field. The word *surface* will always be attached to surface source distributions.

To obtain an equation relating a field to its sources, subject to the presence of the physical boundary S, consider two scalar fields ϕ and ψ defined in a closed volume V bounded by the surface Σ. Green's theorem for ϕ and ψ is given by

$$\int_V [\phi\nabla^2\psi - \psi\nabla^2\phi]\, dv = \oint_\Sigma [\psi\frac{\partial\phi}{\partial n} - \phi\frac{\partial\psi}{\partial n}]\, d\sigma\ , \tag{2.4}$$

where $\partial/\partial n \equiv \hat{\mathbf{n}}\cdot\nabla$ is the normal derivative along the *inward* surface normal, that is, into volume V. If we apply Green's theorem to fields $p(\mathbf{r})$ and $G_V(\mathbf{r},\mathbf{r}')$, defined as in (2.1) and (2.2) but for a general volume V in which $G_V(\mathbf{r},\mathbf{r}')$ is a Green function, we obtain

$$\int_V p(\mathbf{r}')\,\delta(\mathbf{r}-\mathbf{r}')\, dv' = \int_V P(\mathbf{r}')\, G_V(\mathbf{r},\mathbf{r}')\, dv'$$

$$+ \oint_\Sigma \left[p(\mathbf{r}')\frac{\partial G_V(\mathbf{r},\mathbf{r}')}{\partial n'} - G_V(\mathbf{r},\mathbf{r}')\frac{\partial p(\mathbf{r}')}{\partial n'} \right] ds'\ . \tag{2.5}$$

Through specification of the volume of integration V (and hence its bounding surface Σ and Green function $G_V(\mathbf{r},\mathbf{r}')$) and choice of field point location $\mathbf{r}$, this general form [Wolf, 1973] allows us to generate several important integral relationships, and in so doing, gain useful insights regarding the behavior of field integrals. For volume $V = V_1$ and field point $\mathbf{r}$ in V_1, (2.5) becomes

$$p(\mathbf{r}) = \int_{V_3} P(\mathbf{r}')\, G_0(\mathbf{r},\mathbf{r}')\, dv'$$

$$+ \oint_{S+H} \left[p(\mathbf{r}')\frac{\partial G_0(\mathbf{r},\mathbf{r}')}{\partial n'} - G_0(\mathbf{r},\mathbf{r}')\frac{\partial p(\mathbf{r}')}{\partial n'} \right] ds'\ ,\ \mathbf{r}\in V_1\ , \tag{2.6}$$

which we write as $p(\mathbf{r}) = p_i(\mathbf{r}) + p_s(\mathbf{r})$ (total = incident + scattered), where the volume integral is identified as the direct incident field $p_i(\mathbf{r})$ at point $\mathbf{r}$ due to the sources inside V_3. This direct field is also incident on the physical surface S and on the mathematical surface H. The surface integral $p_s(\mathbf{r})$ expresses the contribution to the total field due to the scattering of the incident field by S, and any contribution due to the integral over H.

The conventional way of demonstrating that the integral over hemisphere H is zero consists of taking H to "infinity" (such that $|\mathbf{r}'| \gg L$ and $|\mathbf{r}'| \gg |\mathbf{r}|$) and recognizing that the integral is zero in this far-field limit. The far-field evaluation of the large argument form of the Hankel function

$$H_0^{(1)}(k|\mathbf{r}'-\mathbf{r}|) \rightarrow \frac{e^{ikr'}}{\sqrt{r'}} \sqrt{\frac{2}{\pi k}}\, e^{-i\pi/4}\, e^{-ik\hat{\mathbf{r}}'\cdot\mathbf{r}} \tag{2.7a}$$

leads to the evaluation of the integral (with $ds' \rightarrow r'\, d\theta'$)

$$\int_H \sqrt{r'} \left[\frac{\partial p(\mathbf{r}')}{\partial r'} - p(\mathbf{r}')\left(ik - \frac{1}{2r'}\right)\right] e^{ikr'}\, e^{-ik\hat{\mathbf{r}}'\cdot\mathbf{r}}\, d\theta' \,. \tag{2.7b}$$

If the scattered energy comes from a finite region of length L, then for $r' \gg L$ (the far field) the field p behaves as an outgoing cylindrical† wave on H:

$$\lim_{r'/L\rightarrow\infty} p(\mathbf{r}') = \frac{e^{ikr'}}{\sqrt{r'}} F(\theta'), \quad \text{and} \quad \lim_{r'/L\rightarrow\infty} \frac{\partial p(\mathbf{r}')}{\partial n'} = -\frac{\partial}{\partial r'}\left[\frac{e^{ikr'}}{\sqrt{r'}}\right] F(\theta') \,, \tag{2.7c}$$

where F is the scattering amplitude which only depends on the angle θ' defined in Fig. 2.2. Using (2.7c) in (2.7b) shows that the integral over H vanishes in the far field.

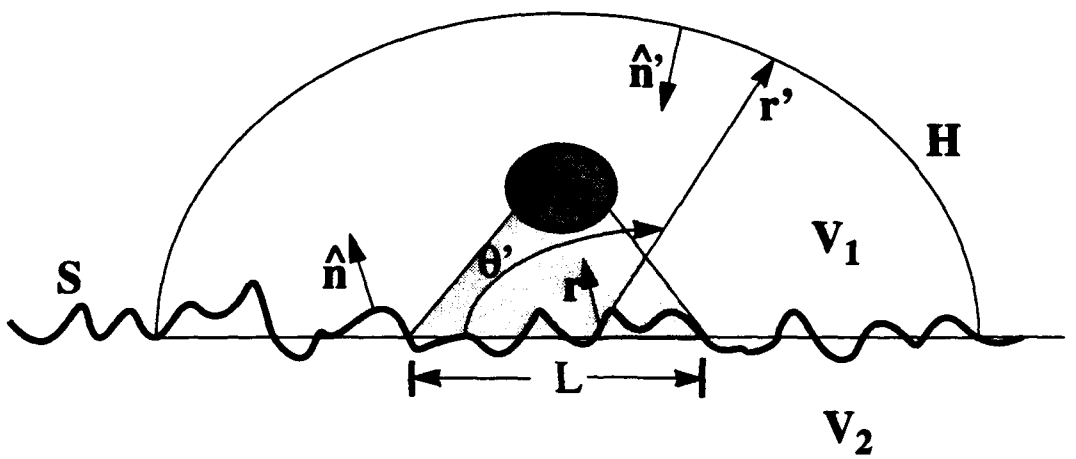

Figure 2.2 : Far-field geometry for scattering from an ensonified region of length L. Here, $|\mathbf{r}'| \gg L$ and $|\mathbf{r}'| \gg |\mathbf{r}|$.

An argument can also be constructed using the radiation condition and (2.5) to show that the surface closing V_1 above S need not be in the far field to give zero

† The field p is said to satisfy the Sommerfeld radiation condition, which is usually stated as $\lim_{r'\rightarrow\infty} r'\left(\frac{\partial p}{\partial r'} - ikp\right) = 0$, for 3-D propagation where the field behaves as $\exp(ikr')/r'$ for $r'/L \rightarrow \infty$. [Sommerfeld, Vol. IV, 1954], [Jackson, 1975], [Courant and Hilbert, Vol. II, 1962].)

contribution to the field at point **r**; indeed, it is instructive to see that it can be of *arbitrary* shape and location as long as it lies above the sources in V_3 and the field point **r**. Consider enclosing volume V_1 by the original boundary S and an arbitrary surface S' depicted in Fig. 2.3. We now define V_0 to be the region above V_1 enclosed by S' and the hemisphere H which is taken to "infinity" as before. For points **r** in V_1 we integrate (2.5) over volume V_0 to find :

$$0 = \oint_{S'+H} \left[p(\mathbf{r}') \frac{\partial G_0(\mathbf{r},\mathbf{r}')}{\partial n'} - G_0(\mathbf{r},\mathbf{r}') \frac{\partial p(\mathbf{r}')}{\partial n'} \right] ds' \ . \tag{2.8}$$

Since the H integral is zero as before, the integral over S' must be zero as well. This result shows that the S' surface integral is zero as long as, from the point of view of an observer at **r** in V_1, there are no *incoming* fields traversing S', that is, when there are no field sources in volume V_0. The integral over S' will only contribute to the field at **r** if there are sources beyond (and therefore "visible" through) S'. We now return to the use of H to denote that surface which closes V_1 above sources P and field point **r**, with the understanding that H can be of arbitrary shape. We remark that the infinitely long surface S divides all of space into two closed regions, V_1 above S and V_2 below S, and that to use Green's theorem it suffices to integrate over S alone because the surface integrals over either of the closing surfaces above or below do not contribute to the field at any point inside them.

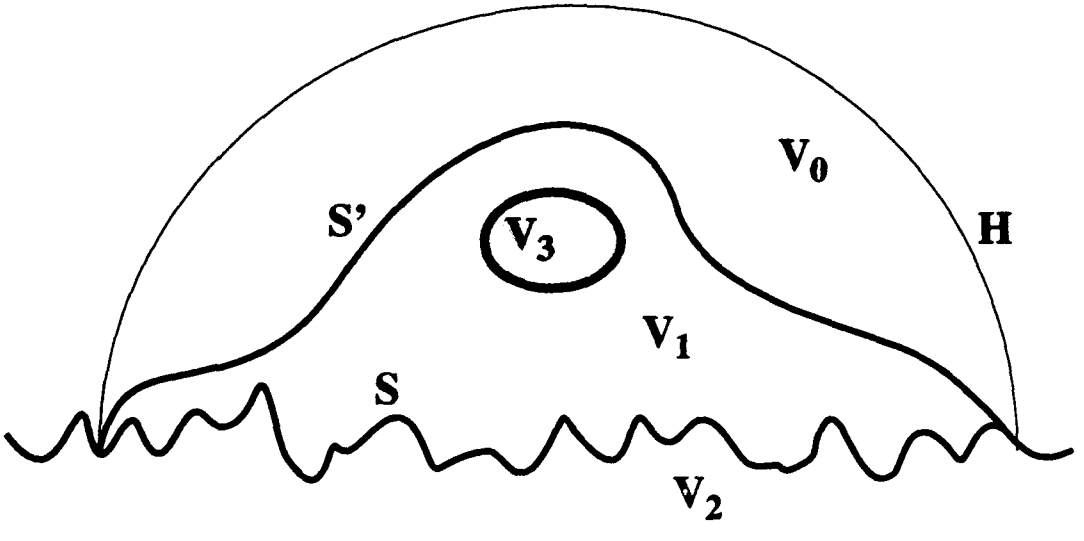

Figure 2.3 : Diagram of surfaces and volumes used in the application of Green's theorem to the infinite (mean horizontal) rough surface scattering problem.

One further consideration arises in the case of scattering from an infinitely long (zero mean) rough surface, in contrast to the problem of scattering from a finite body. To ensure that no incoming waves traverse H, we require that the sources of field p be confined to a finite volume. Thus, p_i only *effectively* ensonifies a limited portion of the surface. This theoretical restriction is only rigorously necessary because the hemisphere can never enclose the entire infinitely long rough surface. The idea is to reduce the scattered energy coming back from S through H (as illustrated in Fig. 2.4) to arbitrarily small levels. Strictly speaking, p_i can not be a single plane wave. The case of plane wave incidence, commonly used in scattering work, can be reached in the limit of a process which always takes the diameter of H to be sufficiently greater than the extent of the surface region over which most of the incident energy is concentrated; see Fig. 2.2 for a schematic view of one such configuration. Alternatively, to ensure that no energy returns back through H, the surface S can be made flat outside surface H, but in this case as well the incident field should be tapered to reduce any edge effects.

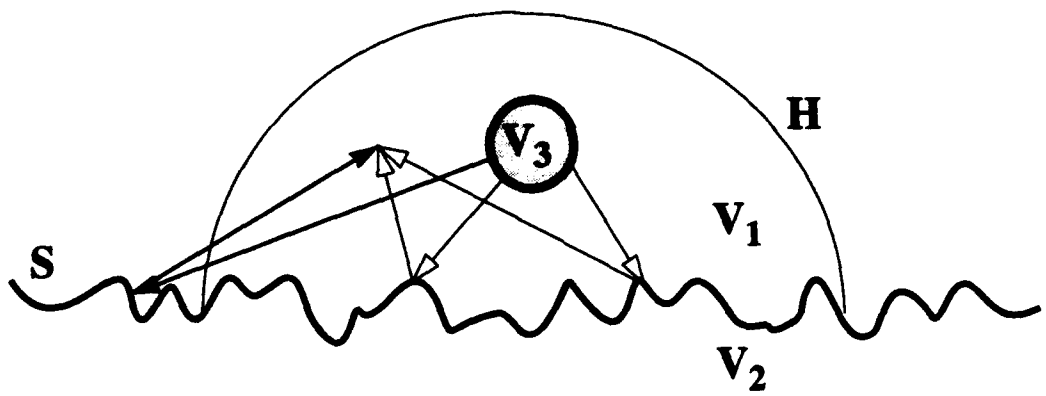

Figure 2.4 : Diagram of possible paths for incident and scattered energy. The paths with white arrowheads lead to surface contributions from S only, whereas the path with black arrowheads gives rise to (unwanted) contributions from H as well.

2.2.3 Integral forms using scattered or incident fields

The boundary S reverses part or all of the downward energy incident upon it, giving rise to a scattered field whose sources are distributed over the surface S, but which *appears* to emanate from image sources below S (see Fig. 3.2). These "virtual" sources of the scattered field can in principle be located by continuing the scattered field below the surface. The boundary condition ensures that all of the real surface sources of p_s lie on S. Alternatively, all of the image sources lie below the surface S; thus, p_s is homogeneous in V_1. A mathematical statement of this fact can be obtained by applying (2.5) (a direct consequence of Green's theorem) to the scattered field, setting $V = V_1$ and placing field point $\mathbf{r}$ in V_2 to obtain

$$0 = \int_S \left[G_0(\mathbf{r},\mathbf{r}') \frac{\partial p_s(\mathbf{r}')}{\partial n'} - p_s(\mathbf{r}') \frac{\partial G_0(\mathbf{r},\mathbf{r}')}{\partial n'} \right] ds' \,, \quad \mathbf{r} \in V_2 \,. \qquad (2.9)$$

This is the scattered field form of the extinction theorem (2.12) discussed below; the extinction theorem is an integral relation used as an "extended" boundary condition to solve scattering problems [Ishimaru, 1991]. We can also apply (2.5) to the scattered field in volume V_1 for $\mathbf{r}$ in V_1, recognizing that p_s satisfies the homogeneous HE in V_1, to obtain

$$p_s(\mathbf{r}) = - \int_S \left[G_0(\mathbf{r},\mathbf{r}') \frac{\partial p_s(\mathbf{r}')}{\partial n'} - p_s(\mathbf{r}') \frac{\partial G_0(\mathbf{r},\mathbf{r}')}{\partial n'} \right] ds' \,, \quad \mathbf{r} \in V_1 \,, \qquad (2.10)$$

which expresses the scattered field above S in terms of the surface sources of p_s on S. This expression, as well as the surface integral over S in (2.6), is the Helmholtz integral (or the Helmholtz-Kirchhoff integral) for the scattered field.

Applying Green's theorem over volume V_1 to the incident field $p_i(\mathbf{r})$ for field points $\mathbf{r}$ in volume V_1, with p_i satisfying the same inhomogeneous HE (2.1) as total field p but *without a boundary condition* on S, we obtain

$$p_i(\mathbf{r}) = p_i(\mathbf{r}) + \int_S \left[G_0(\mathbf{r},\mathbf{r}') \frac{\partial p_i(\mathbf{r}')}{\partial n'} - p_i(\mathbf{r}') \frac{\partial G_0(\mathbf{r},\mathbf{r}')}{\partial n'} \right] ds' \,, \text{ or}$$

$$0 = \int_S \left[G_0(\mathbf{r},\mathbf{r}') \frac{\partial p_i(\mathbf{r}')}{\partial n'} - p_i(\mathbf{r}') \frac{\partial G_0(\mathbf{r},\mathbf{r}')}{\partial n'} \right] ds' \,, \mathbf{r} \in V_1 \,, \qquad (2.11)$$

which reflects the fact that the incident field has no sources below S, a statement analogous to relation (2.9) for the scattered field. It is interesting to note that because of identity (2.11), the scattered field surface integral can either be written in terms of the total field (2.6), or equivalently, in terms of the scattered field (2.10).

Finally, by applying (2.5) to the total field p and integrating over volume $V = V_1$ for $\mathbf{r} \in V_2$, we obtain the integral identity known as the (Ewald-Oseen) extinction theorem:

$$0 = p_i(\mathbf{r}) + \int_S \left[p(\mathbf{r}') \frac{\partial G_0(\mathbf{r},\mathbf{r}')}{\partial n'} - G_0(\mathbf{r},\mathbf{r}') \frac{\partial p(\mathbf{r}')}{\partial n'} \right] ds' \,, \mathbf{r} \in V_2 \,. \qquad (2.12)$$

Wolf [1973] exposed the commonly held misconception that the scattered field "extinguishes" the incident field below S. As we can see from (2.9), there is no surface integral contribution to the scattered field in V_2. Rather, the surface integral over the

incident field itself cancels the incident field (obtained from the volume integral) below S.

2.2.4 Dirichlet boundary condition

If we now restrict ourselves to the Dirichlet boundary condition (pressure release surface) for which the total field on the surface is zero, then $p_s(\mathbf{r}') = -p_i(\mathbf{r}')$, for $\mathbf{r}' \in S$, and the scattered field integral from (2.6) becomes

$$p_s(\mathbf{r}) = -\int_S G_0(\mathbf{r},\mathbf{r}') \frac{\partial p(\mathbf{r}')}{\partial n'} ds' = -\int_S G_0(\mathbf{r},\mathbf{r}') \left[\frac{\partial p_i(\mathbf{r}')}{\partial n'} + \frac{\partial p_s(\mathbf{r}')}{\partial n'} \right] ds', \quad (2.13)$$

where the only unknown component under the integral is the normal derivative of the scattered field on the rough surface. An exact numerical solution can be obtained by solving the following integral equation [Thorsos, 1988], which is derived by taking field point $\mathbf{r}$ to the rough surface S in (2.13) and using $p_s = -p_i$ on S:

$$p_i(\mathbf{r}) = \int_S G_0(\mathbf{r},\mathbf{r}') \frac{\partial p(\mathbf{r}')}{\partial n'} ds', \quad \mathbf{r},\mathbf{r}' \in S. \quad (2.14)$$

The numerical solution by matrix inversion of this integral equation of the first kind (or the solution of an equivalent integral equation of the second kind [Thorsos, 1988]) is used in later chapters to evaluate the accuracy of various approximations.

Another integral equation of the first kind can be derived from scattered field forms (2.9) or (2.10) by taking point $\mathbf{r}$ to the surface S:

$$\frac{1}{2} p_s(\mathbf{r}) - \int_S p_s(\mathbf{r}') \frac{\partial G_0(\mathbf{r},\mathbf{r}')}{\partial n'} ds' = -\int_S G_0(\mathbf{r},\mathbf{r}') \frac{\partial p_s(\mathbf{r}')}{\partial n'} ds', \quad \mathbf{r},\mathbf{r}' \in S. \quad (2.15)$$

It is worth remarking that taking $\mathbf{r}$ to the surface requires special care in evaluating contributions from the (integrable) singularity in the Green function (or its normal derivative) at $\mathbf{r} = \mathbf{r}'$. The results are summarized as follows, for an inward ($+\hat{z}$ directed) surface normal. Setting

$$I_1 = \frac{i}{4} \int_S H_0^{(1)}(k|\mathbf{r}-\mathbf{r}'|)\, \psi(\mathbf{r}')\, ds' , \quad (2.16a)$$

$$I_2 = \frac{i}{4} \int_S \frac{\partial H_0^{(1)}(k|\mathbf{r}-\mathbf{r}'|)}{\partial n'} \psi(\mathbf{r}')\, ds' , \quad (2.16b)$$

then

$$\lim_{\mathbf{r}\to S} I_1 = I_1(\mathbf{r}\in S)\ , \tag{2.17a}$$

$$\lim_{\mathbf{r}_1\to S} I_2 = I_2(\mathbf{r}\in S) + \frac{1}{2}\psi(\mathbf{r})\ , \quad \lim_{\mathbf{r}_2\to S} I_2 = I_2(\mathbf{r}\in S) - \frac{1}{2}\psi(\mathbf{r})\ , \tag{2.17b}$$

where the limiting process (left hand side of (2.17)) takes $\mathbf{r}$ arbitrarily close to the surface but not on the surface, and the notation $I(\mathbf{r}\in S)$ on the right indicates that the point $\mathbf{r}$ is on the surface. The singular contributions for $\mathbf{r}\in S$ are obtained by integrating the small argument expansion of the Hankel function (or its normal derivative) over a small interval centered on the singular point $\mathbf{r}=\mathbf{r}'$. The subscript i on $\mathbf{r}_i$ in (2.17b) indicates the region V_i from which $\mathbf{r}$ approaches the surface. Note that because the singularity in the Hankel function (or its normal derivative) is integrable, the integrals in (2.16) are written in the same way whether $\mathbf{r}$ is on or off the surface; however, the result of performing the integrals in (2.17b) shows that the "limit of the integral" is not the same as the "integral of the limit" in the case of I_2.

It is clear from (2.15) that specifying the scattered field on the surface S (by relating it to the incident field through the Dirichlet boundary condition) suffices to determine the normal derivative $\partial p_s/\partial n$: the scattered field normal derivative can be obtained by solving the integral equation.[†] While (2.15) is somewhat less convenient to solve numerically than (2.14) because of the additional integral evaluation in the left hand side, it does serve to relate the surface values of the normal derivative of the scattered field to the scattered field evaluated on the rough surface alone, that is, without any direct knowledge of p_s in the neighborhood of S. This relationship is inherently nonlocal; the values of the scattered field over the entire surface influence the value of the normal derivative field at each point on the surface. The operator expansion method seeks to approximate $\partial p_s/\partial n$ by retaining only the most important elements of this nonlocal character, thereby providing a much quicker evaluation than is possible by solving the integral equation itself. This is accomplished by using a plane wave representation of the scattered field, approximately obtained from its surface values in a manner closely related to the "spectral" solution for a flat surface. In the latter case the decomposition into plane waves can be simply and exactly obtained by Fourier transform. As we shall see in the next chapter, a key to understanding the operator expansion method lies in the relationship between this flat surface solution and the rough surface scattering problem.

[†] The Neumann condition ties $\partial p_s/\partial n$ to $\partial p_i/\partial n$ on the surface, leading to an integral equation of the second kind for p_s. It is also possible to derive an integral equation of the second kind, equivalent to (2.15), for the Dirichlet problem, but we will not pursue that here.

2.3 The scattering cross section and related far field quantities

The integral relations in the preceding section indicate how the scattered field (and hence the total field) is related to the shape of the boundary S and the field p_i incident upon it. Of particular interest in many scattering problems is the evaluation of the scattered field far from the scattering region. Most of the comparisons between exact integral equation solutions and approximate solutions in later chapters will be performed using far field quantities. Such studies can be done for a single surface, or by averaging results for several different random surfaces chosen from a stochastic ensemble. We will present results in terms of the scattering strength, defined by $SS = 10 \log \sigma(\theta_i,\theta_s)$, where σ is the dimensionless scattering cross section per unit scattering angle per unit surface length. An estimate for σ can be obtained by averaging over the far field scattered intensity $I_s(\mathbf{r},\theta_i)$ which contains both coherent and incoherent energy; an average over surface realizations is denoted by $\langle I_s(\mathbf{r},\theta_i)\rangle$. For 1-D surfaces ensonified by a plane wave we recall the definition of the cross section

$$\sigma(\theta_i,\theta_s) = \frac{\langle I_s \rangle}{I_{inc}} \frac{r}{L} = \frac{\langle I_s \rangle r \sin\theta_i}{E_f} \tag{2.18}$$

where $r = |\mathbf{r}|$ is the (far-field) distance from the surface of length L, and where E_f is the incident energy flux through the surface. The expression on the right is the appropriate generalization when the incident field is not a plane wave. Using the large argument form for $H_0^{(1)}(k|\mathbf{r}-\mathbf{r}'|)$ we write the scattering integral (2.13) in the far field of the surface as

$$p_s(\mathbf{r}) = \frac{e^{ikr}}{\sqrt{r}} \frac{e^{i\pi/4}}{\sqrt{8\pi k}} \int_S \exp[-i\,\mathbf{k}_s\cdot\mathbf{r}'] \frac{\partial p(\mathbf{r}')}{\partial n'} ds' \equiv \frac{e^{ikr}}{\sqrt{r}} F(\mathbf{k}_s) \,, \tag{2.19}$$

where the scattered field wave vector $\mathbf{k}_s = k\mathbf{r}/r$, and where we have defined the scattering amplitude F for the 2-D scattering geometry; p_s and F are implicitly dependent on the incident field. The averaged far-field scattered intensity is then

$$\langle I_s \rangle = \frac{\langle |F|^2 \rangle}{2\rho c} \frac{1}{r} \,, \tag{2.20}$$

where ρc is the acoustic impedance of the medium, and where the factor of two results from taking a time average.

Some approximate methods (for example, perturbation theory and the operator expansion) provide a series solution for the surface values of the normal derivative field, and hence a series for the scattering amplitude as well. We can write these series as

$$\frac{\partial p}{\partial n} = \frac{\partial p_0}{\partial n} + \frac{\partial p_1}{\partial n} + \frac{\partial p_2}{\partial n} + \cdots , \tag{2.21a}$$

$$F = F_0 + F_1 + F_2 + \cdots , \tag{2.21b}$$

where the order is determined by the power of an implicit expansion parameter. Truncating the series for $\partial p/\partial n$ to a given order results in a solution for F to the same order. Then, the terms in the series for the scattered intensity constructed from the product of truncated series for F are

$$I_0 \propto |F_0|^2 , \tag{2.22a}$$

$$I_1 \propto I_0 + 2\,\mathrm{Re}(F_0 F_1^*) + |F_1|^2 , \tag{2.22b}$$

$$I_2 \propto I_1 + 2\,\mathrm{Re}(F_0 F_2^*) + 2\,\mathrm{Re}(F_1 F_2^*) + |F_2|^2 , \tag{2.22c}$$

$$I_3 \propto I_2 + 2\,\mathrm{Re}(F_0 F_3^*) + 2\,\mathrm{Re}(F_1 F_3^*) + 2\,\mathrm{Re}(F_2 F_3^*) + |F_3|^2 , \tag{2.22d}$$

$$\cdots$$

in which the proportionality symbol indicates that factors which cancel in the expression for the cross section have been suppressed. (The s subscript was dropped from I_s for simplicity, and an asterisk denotes complex conjugation.)

The "truncated series" scattered intensity terms are formed using all possible products from the scattering amplitude computed to a given order. However, one can also construct the scattered intensity series in *consistent* orders of the series expansion parameter by only including cross terms $F_n F_m^*$ for which the sum of indices $n+m$ is less than or equal to the given order:

$$I^{(0)} \propto |F_0|^2 , \tag{2.23a}$$

$$I^{(1)} \propto I^{(0)} + 2\,\mathrm{Re}(F_0 F_1^*) , \tag{2.23b}$$

$$I^{(2)} \propto I^{(1)} + |F_1|^2 + 2\,\mathrm{Re}(F_0 F_2^*) , \tag{2.23c}$$

$$I^{(3)} \propto I^{(2)} + 2\,\mathrm{Re}(F_1 F_2^*) + 2\,\mathrm{Re}(F_0 F_3^*) , \tag{2.23d}$$

$$I^{(4)} \propto I^{(3)} + |F_2|^2 + 2\,\mathrm{Re}(F_1 F_3^*) + 2\,\mathrm{Re}(F_0 F_4^*) , \tag{2.23e}$$

$$\cdots$$

Terms in both series (2.22) and (2.23) are indexed by the highest order of the surface field included in the solution. Examples in chapters 4 and 5 illustrate that, in the case of the operator expansion method, the I_n "truncated" series (2.22) often makes better use of the n'th order surface field than does the $I^{(n)}$ "consistent" series (2.23). In particular, we compare the accuracy of the I_1, $I^{(2)}$, and I_2 solutions and find that, in general, consistently including terms of like powers is not required in order to maintain

accuracy, in contrast to standard perturbation theory [Thorsos, 1990a]. There it was shown that a major cancellation between terms containing fourth powers of the perturbation expansion parameter kh requires careful computation of both terms at that order, σ_{22} and σ_{13}, necessitating calculation of the second *and* third order fields to obtain the second term in the series for the incoherent cross section $\sigma^{(4)}$ †.

To evaluate the cross section one must first solve for the surface sources of p_s distributed on S. As was discussed above, this can be done exactly by numerically solving an integral equation. This is a computationally intensive solution, practically limited to scattering from 1-D surfaces. Furthermore, it requires computing scattering from one surface realization at a time, since no formally averaged solution is possible. The Kirchhoff Approximation (KA) and perturbation theory are two classical approximations which have been used extensively, and we briefly review them here because of their usefulness in computing scattering in complementary roughness regimes, and because of their analytical ties to the much newer operator expansion method. Though these classical approximations do lend themselves to formal averaging, we develop them here as numerical techniques in order to make comparisons to the exact integral equation result and to the operator expansion solution more straightforward. We begin with the Kirchhoff approximation.

2.4 Kirchhoff approximation

In the Kirchhoff approximation, the unknown normal derivative in (2.13) is set to the value it would have for reflection from the locally tangent plane

$$\frac{\partial p_s(\mathbf{r}')}{\partial n'} = \frac{\partial p_i(\mathbf{r}')}{\partial n'} \quad , \quad \mathbf{r}' \in S \quad . \tag{2.24}$$

Using the integral identity (2.11) for the incident field we can write the Kirchhoff solution for the scattered field in three equivalent ways :

$$p_s(\mathbf{r}) = -2 \int_S G_0(\mathbf{r},\mathbf{r}') \frac{\partial p_i(\mathbf{r}')}{\partial n'} ds' \tag{2.25a}$$

$$= -2 \int_S p_i(\mathbf{r}') \frac{\partial G_0(\mathbf{r},\mathbf{r}')}{\partial n'} ds' \tag{2.25b}$$

† In the operator expansion solution, term F_0 contains incoherent energy, whereas in perturbation theory it does not. In the perturbation method all F_0 terms drop out in the series for the incoherent intensity, as do all odd order terms such as $F_1 F_2^*$.

$$= -\int_S \left[G_0(\mathbf{r},\mathbf{r}') \frac{\partial p_i(\mathbf{r}')}{\partial n'} + p_i(\mathbf{r}') \frac{\partial G_0(\mathbf{r},\mathbf{r}')}{\partial n'} \right] ds' . \qquad (2.25c)$$

To illustrate the symmetry of these forms in the far field, we choose the incident field to be a single plane wave for clarity. Setting $p_i(\mathbf{r}) = \exp[i\,\mathbf{k}_i \cdot \mathbf{r}]$, the scattering amplitude (2.19) is proportional to :

$$F_{KA}(\mathbf{k}_s) \propto -i \int_S \exp[i\,(\mathbf{k}_i - \mathbf{k}_s)\cdot\mathbf{r}']\; 2\mathbf{k}_i \cdot \hat{\mathbf{n}}'\, ds' \qquad (2.26a)$$

$$= -i \int_S \exp[i\,(\mathbf{k}_i - \mathbf{k}_s)\cdot\mathbf{r}']\; (-2\mathbf{k}_s)\cdot\hat{\mathbf{n}}'\, ds' \qquad (2.26b)$$

$$= -i \int_S \exp[i\,(\mathbf{k}_i - \mathbf{k}_s)\cdot\mathbf{r}']\; (\mathbf{k}_i - \mathbf{k}_s)\cdot\hat{\mathbf{n}}'\, ds' . \qquad (2.26c)$$

Though the integrands of these three forms are not the same at any given surface point $\mathbf{r}'$, the scattering amplitudes are rigorously identical. These three expressions seem to give *different* results in part because of the apparent lack of reciprocity in (2.26a) and (2.26b) — this property has led to erroneous statements in the past; for example, see DeSanto and Brown [1986, Sec. 3.3].

2.5 Rayleigh-Rice perturbation theory

There are many ways to present a derivation of Rayleigh-Rice perturbation theory, but we will choose one which leads directly to a Monte Carlo solution. This formulation is compared to a component of the operator expansion solution in chapter 3. The approach taken here follows that outlined by Thorsos and Jackson [1989], which was in turn motivated by the development of Harper and Labianca [1975a, 1975b].

The Rayleigh-Rice perturbation method can be interpreted as a transformation of the scattering problem from one posed on the rough surface $z = \zeta(x)$ with the Dirichlet boundary condition, to one posed on the mean plane $z = 0$ with a new set of boundary conditions determined by the small perturbation method. In other words, the complexity of the original boundary shape, on which is specified a simple boundary condition, is exchanged for complexity of a new set of boundary conditions specified on a simple boundary. The connection between the two problems is established by continuation of the total field between the mean plane and the rough surface. Because the field is written as an expansion in a power series in small roughness parameter kh, where k is the

acoustic wavenumber and h is the rms surface height, the original Dirichlet boundary condition on the rough surface can be enforced order by order. The solution requires analytic continuation of the field in the entire region between surface extrema, and invokes the Rayleigh hypothesis on the scattered field to perform that continuation.

We write the expression for the total field as in (2.6), but assume that the scattering comes from a flat surface with a set of boundary conditions to be determined. Thus,

$$p(\mathbf{r}) = \int_{V_3} P(\mathbf{r}')\, G_0(\mathbf{r},\mathbf{r}')\, dv' + \int_{z=0} \left[p(\mathbf{r}') \frac{\partial G_0(\mathbf{r},\mathbf{r}')}{\partial z'} - G_0(\mathbf{r},\mathbf{r}') \frac{\partial p(\mathbf{r}')}{\partial z'} \right] dx' , \tag{2.27}$$

where the normal derivatives are vertical derivatives. In general, both terms (field and normal derivative of the field) are present in the surface integral. However, the surface integral can be simplified by choosing the Green function which is zero on the mean plane[†]:

$$G_1(\mathbf{r},\mathbf{r}') = G_0(\mathbf{r},\mathbf{r}') - G_0(\mathbf{r},\mathbf{r}'') , \tag{2.28}$$

where point $\mathbf{r}''$ in V_2 is the image of $\mathbf{r}'$ in V_1 reflected in the $z = 0$ plane. The total field is written as a perturbation about the flat plane solution

$$p(\mathbf{r}) = p_0(\mathbf{r}) + p_{si}(\mathbf{r}) , \tag{2.29}$$

where p_0 is the flat surface solution, and p_{si} is the scattered field due to the roughness of the original surface as follows. (Note that $p_{si} \neq p_s$ defined by (2.6) and (2.10). The scattered field p_s includes the reflected field p_r, defined below.) The volume integral in (2.27) becomes

$$p_0(\mathbf{r}) = \int_{V_3} P(\mathbf{r}')\, G_1(\mathbf{r},\mathbf{r}')\, dv' = p_i(\mathbf{r}) + p_r(\mathbf{r}) , \tag{2.30}$$

where p_r is the up-going field due to a flat surface reflection of the incident field. Using $G_1(\mathbf{r},\mathbf{r}')$ in the surface integral in (2.27) gives the scattered field p_{si} due to the roughness alone:

$$p_{si}(\mathbf{r}) = \int_{z=0} p(\mathbf{r}) \frac{\partial G_1(\mathbf{r},\mathbf{r}')}{\partial z'} dx' , \tag{2.31}$$

[†] This procedure can be interpreted as finding the image sources of the scattered field due to a point source above the surface, thereby solving the scattering problem; hence, $G_1(\mathbf{r},\mathbf{r}')$ is often called the image Green function. However, G_1 is only readily available for a flat surface.

which contains all the incoherent scattered field but also includes coherent components of the scattered field. These coherent components are small corrections to the reflected field p_r for small surface roughness, but effectively cancel the reflected field for very rough surfaces. We recognize that

$$\frac{\partial G_1(\mathbf{r},\mathbf{r}')}{\partial z'} = 2\left[\frac{\partial G_0(\mathbf{r},\mathbf{r}')}{\partial z'}\right]_{z'=0}, \tag{2.32}$$

which has a far-field limit easily obtained from (3.48).

In order to connect the flat surface values of the total field to its values on the rough surface (where the original boundary condition sets $p(x,\zeta(x))=0$), we write the total field in the neighborhood of the mean plane as a Taylor expansion about the $z=0$ plane, and evaluate this expansion on the rough surface $z=\zeta(x)$:

$$p(\mathbf{r})\Big|_{z=\zeta(x)} = \left[p(\mathbf{r}) + \zeta(x)\frac{\partial p(\mathbf{r})}{\partial z} + \frac{\zeta^2(x)}{2!}\frac{\partial^2 p(\mathbf{r})}{\partial z^2} + \cdots\right]_{z=0}. \tag{2.33}$$

We also write the total field in a power series in small roughness parameter kh as

$$p(\mathbf{r}) = p_0(\mathbf{r}) + (kh)\,p_1(\mathbf{r}) + \frac{(kh)^2}{2!}p_2(\mathbf{r}) + \cdots \tag{2.34}$$

and substitute (2.34) into (2.33) to obtain:

$$\begin{aligned} p(\mathbf{r})\Big|_{z=\zeta} = {} & p_0(\mathbf{r}) + \varepsilon_1 p_1(\mathbf{r}) + \varepsilon_2 p_2(\mathbf{r}) + \varepsilon_3 p_3(\mathbf{r}) \\ & + \zeta\frac{\partial p_0(\mathbf{r})}{\partial z} + \varepsilon_1\zeta\frac{\partial p_1(\mathbf{r})}{\partial z} + \varepsilon_2\zeta\frac{\partial p_2(\mathbf{r})}{\partial z} \\ & + \frac{\zeta^2}{2!}\frac{\partial^2 p_0(\mathbf{r})}{\partial z^2} + \varepsilon_1\frac{\zeta^2}{2!}\frac{\partial^2 p_1(\mathbf{r})}{\partial z^2} \\ & + \frac{\zeta^3}{3!}\frac{\partial^3 p_0(\mathbf{r})}{\partial z^3} + O(\varepsilon_4)\Big|_{z=0} \end{aligned} \tag{2.35}$$

where $\varepsilon_n \equiv \dfrac{(kh)^n}{n!}$, and $\zeta \equiv \zeta(x)$.

Using the Dirichlet boundary condition on the rough surface $p(x, z=\zeta(x))=0$, and collecting like powers of kh (organized by column in (2.35)), we obtain a new series of boundary conditions for the total field organized by order in kh. Through third order these are:

$$p_0(x,0) = 0, \tag{2.36a}$$

$$\varepsilon_1 p_1(x,0) = \left[-\zeta\frac{\partial p_0(\mathbf{r})}{\partial z}\right]_{z=0}, \tag{2.36b}$$

$$\varepsilon_2 p_2(x,0) = \left[-\varepsilon_1 \zeta \frac{\partial p_1(\mathbf{r})}{\partial z} \right]_{z=0}, \tag{2.36c}$$

$$\varepsilon_3 p_3(x,0) = \left[-\varepsilon_2 \zeta \frac{\partial p_2(\mathbf{r})}{\partial z} - \varepsilon_1 \frac{\zeta^2}{2!} \frac{\partial^2 p_1(\mathbf{r})}{\partial z^2} - \frac{\zeta^3}{3!} \frac{\partial^3 p_0(\mathbf{r})}{\partial z^3} \right]_{z=0}. \tag{2.36d}$$

This set of boundary conditions must now be solved for the total field (2.34) to a given order, and used in (2.31) to find the scattered field p_{si} to the same order. The Dirichlet boundary condition on the rough surface and the perturbation analysis lead to $p_0(x,0) = 0$; this is simply a restatement of the fact that the rough surface scattering solution is obtained by perturbation about the flat surface reflection from a Dirichlet boundary. The zeroth order total field p_0 is zero on the mean plane; because p_0 is the sum of incident and reflected fields it can easily be shown that all even order z-derivatives of p_0 evaluated on the plane $z = 0$ are also zero. The (nonzero) derivative $\partial p_0 / \partial z = 2\, \partial p_i / \partial z$ is readily obtained analytically for a given incident field. Because the vertical derivatives are sought on the plane $z = 0$, they can also be computed by Fourier transform [Thorsos and Jackson, 1989]. This transform technique will be used extensively in the operator expansion method, and is discussed in detail in chapter 3.

CHAPTER 3

The Operator Expansion Method

3.1 Introduction to Chapter 3

The operator expansion is a new approximation for computing scattering from rough surfaces. Proposed by Milder [1991], it is based on a technique used by Milder [1990] and colleagues [West et al., 1987] in surface wave hydrodynamics. The Dirichlet (pressure release) scattering problem is solved using a nonlocal operator which computes the normal derivative of the scattered field given *only* the boundary values of the scattered field; these are tied to the incident field through the boundary condition. The nonlocal normal derivative operator which performs this transformation is expressed in a systematic series expansion whose terms contain powers of the surface height function and powers of a Fourier integral operator. In this chapter we derive the expansion and show how it is used to solve the Dirichlet scattering problem. Our presentation differs from that given by Milder in two fundamental respects. First, we derive and apply the operator expansion assuming that the scattered field satisfies the Rayleigh hypothesis. Second, the series expansion itself is obtained in a more straightforward but less rigorous way. Though this approach seems to make unnecessarily restrictive assumptions, the solution thus obtained is identical to Milder's and provides an alternative way of deriving the expansion which we feel is simpler. We discuss Milder's approach in Sec. 3.5 and contrast it with our own.

The operator expansion method attempts to solve the rough surface scattering problem much more efficiently than possible with a rigorous integral equation method by retaining only the most important parts of the nonlocal relationship (embodied in the integral relationships (2.9) or (2.15)) between the surface values of scattered field and the surface values of its normal derivative. This is accomplished using a plane wave representation of the scattered field, approximately obtained from its surface values in a manner closely related to the spectral solution for a flat surface, described in Sec. 3.2.1. In that unique situation, the decomposition into plane waves can be simply and exactly obtained by Fourier transform. Once the plane wave representation for the exact field is known, the field or any of its derivatives can be evaluated anywhere the representation is valid, namely above the flat surface. The rough surface scattering problem then reduces to finding an approximate plane wave representation for the scattered field, the latter being specified only on the rough surface. To this end, the scattered field is first continued to a flat plane. There, the vertical derivative is obtained by Fourier transform and then is continued back to the rough surface where it is related to the desired normal

derivative using the known tangential derivative of the surface field. The analytic continuation steps are expressed as Taylor series, leading to a series expansion for the normal derivative operator. Though the plane wave coefficients for the scattered field are never explicitly solved for, the representation of surface fields in up-going waves underlies the entire derivation as we shall see below.

3.2 Derivation of the Operator Expansion Series

3.2.1 Spectral solution for a flat surface

In this section we solve the problem of reflection from a flat Dirichlet surface depicted in Fig. 3.1 by a method which we later extend to the rough surface case. While we know the solution for the normal derivative of the scattered field in this simple case to be

$$\frac{\partial p_s(\mathbf{r})}{\partial z} = \frac{\partial p_i(\mathbf{r})}{\partial z} \tag{3.1}$$

at every point on the surface, a "local" relationship, we do not make use of the normal derivative of the incident field. Rather, the solution is obtained by using just the surface values of the incident field itself, the latter chosen because it is directly tied to the scattered field via the boundary condition. (Conversely, in the Neumann problem one would use just the surface values of the normal derivative of the incident field.)

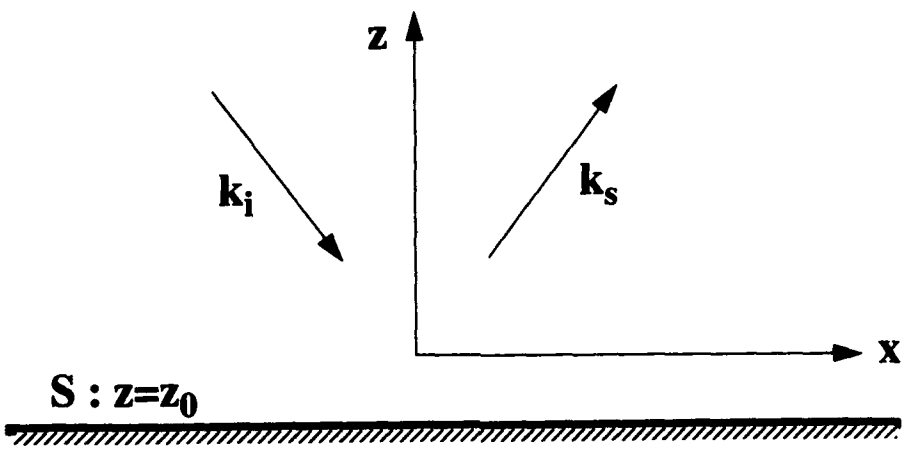

Figure 3.1 : Reflection of an incident field by a flat surface at height $z = z_0$.

Considering reflection of down-going incident energy (which we take to be more general than a single plane wave) by a flat surface located at height z_0 it is clear that, even very close to the surface, all scattered energy propagates upward. The scattered

field can then be written as a sum of upward directed plane waves, both propagating and evanescent,

$$p_s(\mathbf{r}) = \int_{-\infty}^{+\infty} \exp[ik_x x]\exp[ik_z z]\,\tilde{p}_s(k_x)\,dk_x\,, \tag{3.2}$$

where for up-going waves we have $k_z = +\sqrt{k^2 - k_x^2}$ and $\mathrm{Im}(k_z) \geq 0$, and where the $\tilde{p}_s(k_x)$ are the complex plane wave coefficients given by a Fourier transform over the values of the scattered field specified on any horizontal surface, and in particular on the flat reflecting surface located at $z = z_0$:

$$\tilde{p}_s(k_x) = \frac{\exp[-ik_z z_0]}{2\pi} \int_{-\infty}^{+\infty} \exp[-ik_x x']\,p_s(x', z_0)\,dx'\,. \tag{3.3}$$

Note that as defined by (3.3) the coefficients $\tilde{p}_s(k_x)$ are independent of z_0. We also refer to (3.2) as the spectral representation of the field[†].

Once the complex amplitudes $\tilde{p}_s(k_x)$ are known, the scattering problem is solved because the scattered field, or any of its derivatives, can be computed anywhere in the scattering region for $z \geq z_0$. To make use of the scattering integral (2.13) we require the normal (vertical) derivative on $z = z_0$. The vertical derivative of the field is easily obtained by differentiating (3.2) and evaluating for $z = z_0$:

$$\left[\frac{\partial p_s(\mathbf{r})}{\partial z}\right]_{z=z_0} = \int_{-\infty}^{+\infty} dk_x \exp[ik_x x]\,(ik_z) \int_{-\infty}^{+\infty} \frac{dx'}{2\pi} \exp[-ik_x x']\,p_s(x', z_0)$$

$$\equiv \hat{Q}\,p_s(x', z_0)\,. \tag{3.4}$$

Equation (3.4) defines the Fourier integral operator $\hat{Q}$ which, when applied to the scattered field on the surface $z = z_0$, yields the vertical (normal) derivative of the scattered field on the flat surface directly usable in (2.13) as

$$p_s(\mathbf{r}) = -\int_{z_0} G_0(\mathbf{r}, \mathbf{r}') \left[\frac{\partial p_i(\mathbf{r}')}{\partial z'} - \hat{Q}\,p_i(x', z_0)\right] dx'\,, \tag{3.5}$$

[†] The plane wave coefficients $\tilde{p}_s(k_x)$ are equivalent to the elements of the transition or T-matrix [Thorsos and Jackson, 1989] when the incident field is a plane wave; here, we consider more general forms of the incident field.

where we have used the Dirichlet boundary condition $p_s = -p_i$.

In the flat surface example above we show how the nonlocal Fourier integral operator $\hat{Q}$ is used to solve the scattering problem from surface values of p_s alone. (Note that $\hat{Q}$ is related to $\hat{q}$ used by Milder by $\hat{Q} \equiv i\hat{q}$.) It is straightforward to show, using equations (3.2) and (3.3) written for the incident field in terms of down-going waves, (3.4), and the Dirichlet boundary condition, that the solution (3.1) is recovered. We note that applying $\hat{Q}$ to flat surface values of entirely down-going fields produces the negative of the normal derivative; indeed, while the effect of $\hat{Q}$ on p_s is to produce $\partial p_s/\partial z$, when applied to p_i it produces $-\partial p_i/\partial z$. Consequently, when applied to a field which is a mixture of up- and down-going energy, $\hat{Q}$ does not produce the normal derivative, as can be trivially illustrated by operating on the total field: $\hat{Q}p = 0$. In general, operator $\hat{Q}$ is unsuitable for computing the normal derivative of a flat surface field resulting from an arbitrary combination of up- *and* down-going waves. All up-going wave operators we define have similar limitations but may nevertheless provide useful approximations in situations where both up-going and down-going waves are present.

In order to compute the normal derivative of the scattered field on the rough surface we apply up-going wave operators like $\hat{Q}$ to the surface values of the scattered field, under the assumption that the scattered field can be represented by strictly upward directed waves at the surface. This up-going wave assumption becomes important in the rough surface case when, because of multiple scattering, the scattered field may also contain down-going energy in the neighborhood of the surface. Stepping back to consider the case of an arbitrary field traversing a mathematical surface, it is clear that one cannot determine from the surface values of the field alone which way the field is propagating; because the field could have sources on either side of the surface, the normal derivative is required to sort out the partitioning of up-going and down-going energy. However, if the field is known to be homogeneous on one side of the surface, as is the case for the scattered field which has no sources in the scattering region, then the integral equation (2.6) shows that the normal derivative can be obtained from the field on the surface, and therefore contains no independent information, *in spite* of the mix of upward and downward traveling energy inside the wells of the surface. The solution of the integral equation makes no assumption about the plane wave representation of the scattered field, and for this reason will likely be more robust (as surface roughness increases) than an up-going wave operator solution. The up-going wave representation raises questions about the connection between the operator expansion method and the Rayleigh hypothesis; this topic is discussed in greater detail in Sec. 3.5.

3.2.2 Extension of the spectral solution to the rough surface problem

The scattering problem posed on a rough surface immediately becomes more difficult; the spectral solution method is complicated by the phase term containing the x-dependent surface height function. The field can still be expressed as an expansion in up-going plane waves

$$p_s(x, \zeta(x)) = \int_{-\infty}^{+\infty} dk_x \exp[ik_x x] \exp[ik_z \zeta(x)] \tilde{p}_s(k_x) \tag{3.6}$$

but in this case the spectral coefficients $\tilde{p}_s(k_x)$ are no longer simply related to the boundary field $p_s(x, \zeta(x))$ through a Fourier transform. While the solution for the flat surface problem does not require the machinery of the Fourier integral operator, a similar approach for the rough surface problem would be a welcome simplification. Following Milder [1991], and by analogy to the definition of $\hat{Q}$ in (3.4), we define the rough boundary normal derivative operator $\hat{N}_b$ by its effect on the scattered field :

$$\hat{N}_b \; p_s(x, \zeta(x)) \equiv \left[\frac{\partial p_s(\mathrm{r})}{\partial n} \right]_{z = \zeta(x)} . \tag{3.7}$$

In order to arrive at a Fourier integral operator expression for $\hat{N}_b$ we extend the methodology used in the flat surface case to the rough surface case by using an up-going plane wave representation of the scattered field to solve for the normal derivative. As before, the plane wave coefficients are obtained from the rough surface values of the scattered field, but the coefficients can only be computed by Fourier transform if the scattered field is known on a flat plane; therefore, we continue the scattered field from the rough surface to a reference flat surface. For reasons discussed later (see Sec. 3.4), the spectral form thus obtained is not directly used to evaluate the normal derivative $\partial p_s / \partial n$ on the rough surface; rather, the vertical derivative field $\partial p_s / \partial z$ is evaluated on the reference plane using $\hat{Q}$ and is then continued back to the rough surface S, where it is finally related to the normal derivative. Because the reference plane is only used as an intermediary in the estimation of $\partial p_s / \partial n$, its location is arbitrary. For example, it could be placed entirely above the rough surface, or, it could be placed on the mean plane $z = 0$; in fact, specification of its location is not required in the operator expansion. Nevertheless, we will see that continuation of the scattered field is required into some regions *below* the rough surface S and therefore beyond the acoustic medium, where no real fields exist.

To visualize the continuation process we imagine extending the acoustic medium below the surface S, and consider the surface sources of the scattered field (i.e.,

scattered field and normal derivative values) to be "secondary" sources in the sense of Huygens' principle; see Fig. 3.2. In other words, the physical boundary between the acoustic medium and vacuum is replaced by a mathematical contour (of same shape $z = \zeta(x)$) embedded in the extended acoustic medium, on which are present the same values of the scattered field and of the scattered field normal derivative as before. Above the contour S, the scattered field given by the scattering integral (2.10) is therefore the same. Below S lies the continued scattered field; the continuation is straightforward so long as no sources are encountered, yet studies of the validity of the Rayleigh hypothesis indicate that singularities of the continued scattered field do exist below the rough surface [Millar, 1973], [van den Berg and Fokkema, 1980]. It is possible to continue the scattered field numerically and thereby "image" the virtual sources of the scattered field. One such technique first solves for the unknown normal derivative using an exact method, and then computes the scattered field on a plane just above the highest point on the surface using (2.10). The spectral coefficients $\tilde{p}_s(k_x)$ are obtained by Fourier transforming those scattered field values using (3.3), and the field is continued below the plane and below the rough surface using (3.2). It is important not to confuse the continued field given by the upward wave representation (3.2) (nonzero below S) with the field given by the Helmholtz surface integral over S (2.9), which is always zero below S. Such an error was the cause of some of the controversy over the validity of the Rayleigh hypothesis [Millar, 1971].

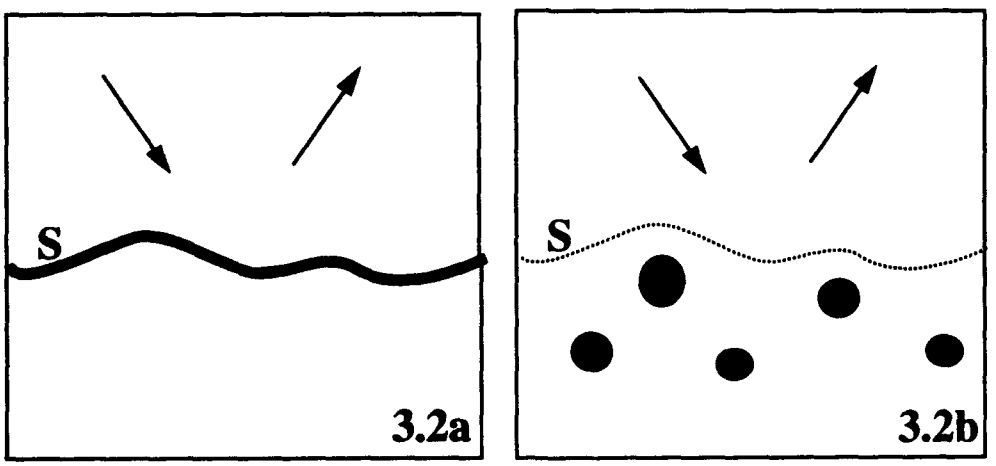

Figure 3.2 : Replacing a surface distribution of sources by a volume distribution of image sources. In the depiction of the real scattering process on the left, all of the energy incident upon the Dirichlet surface S (a physical boundary) is ultimately scattered upward; all scattered field sources are distributed on the surface S, and there is no scattered field below S (3.2a). Alternatively, the scattered field above the surface S *can be thought of* as emanating from image sources distributed in the continued acoustic medium below the now mathematical surface S (3.2b).

For the purpose of the derivation, we assume that all singularities of the continued scattered field lie below the plane passing through the lowest point on the rough surface $z = \zeta_{min}$. This assumption is equivalent to making the Rayleigh hypothesis and allows the continuation of p_s throughout the region between surface extrema. The operator expansion solution obtained in this way is identical to Milder's, though Milder tried to avoid making the Rayleigh hypothesis on p_s by using an integral identity derived from (2.9), an exact relation obtained using Green's theorem. It turns out that Milder's approach still assumes that the Rayleigh hypothesis is valid; we discuss his argument in Sec. 3.5.

The details of the continuation procedure and the development of a series expansion for $\hat{N}_b$ are given in the following sections; here we wish to outline our derivation of the operator expansion solution. The mathematical formulation presented in this work is occasionally identical to Milder's [1991]. However, we provide an expanded discussion and an alternative interpretation of the derivation in the hope that it will be easier to follow. We develop the expansion for $\hat{N}_b$ for strictly up-going fields which satisfy the Rayleigh hypothesis. We then assume that $\hat{N}_b$ can be applied to $p_s(x, \zeta(x))$ and investigate the usefulness of this solution numerically in Chapters 4 and 5.

Beginning with the scattered field known on the rough surface through the Dirichlet boundary condition ($p_s = -p_i$), the operation embodied by the symbol $\hat{N}_b$ can be conceptually decomposed into four separate steps which are schematically illustrated in Fig. 3.3:

1. Continuation of the scattered field from the rough surface $z = \zeta(x)$ to a reference plane located at $z = z_0$.

2. Evaluation of the vertical derivative of the scattered field on the reference plane using the flat surface vertical derivative operator $\hat{Q}$.

3. Continuation of the vertical derivative field from the flat surface $z = z_0$ back to the rough surface $z = \zeta(x)$.

4. Evaluation of the normal derivative field on the rough surface using the newly determined vertical derivative and the known tangential derivative fields.

Steps 1 and 3 are inverse procedures (though the fields being continued are not the same); indeed, these operations correspond to Milder's operators $\hat{Z}^{-1}$ and $\hat{Z}$, respectively. As we shall see, operator $\hat{Z}$ has a series representation that is straightforward to obtain, whereas $\hat{Z}^{-1}$ does not; consequently, we will treat step 3 before step 1. An

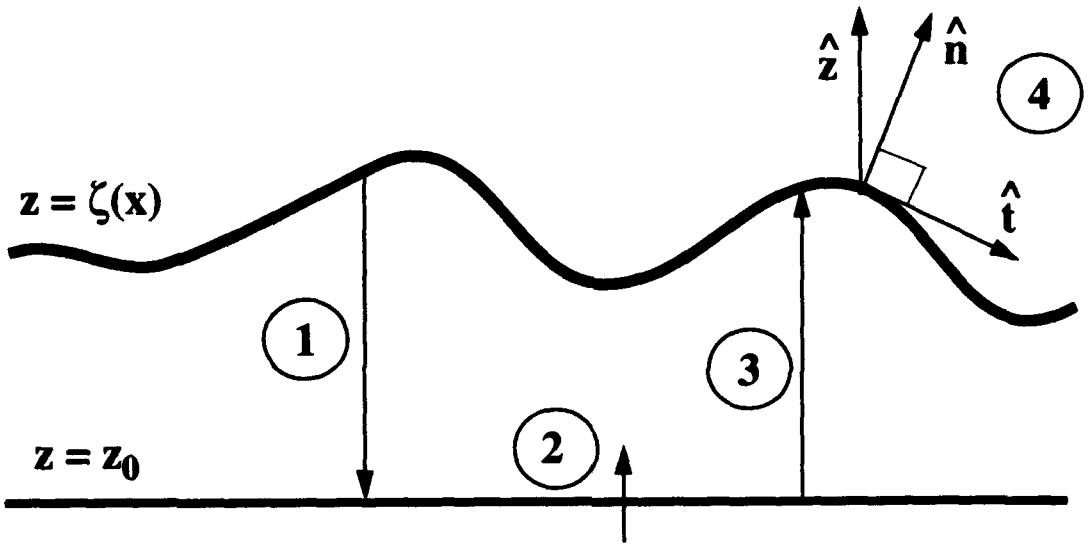

Figure 3.3 : Diagram illustrating the four operations which are combined in operator $\hat{N}_b$.

expansion for the operator $\hat{N}_b$ is obtained as a series of terms containing powers of the Fourier integral operator $\hat{Q}$ and the surface height function $\zeta(x)$. We now turn to the details of the derivation, beginning with the treatment of step 3.

3.2.3 Continuation of a field from a flat surface to an arbitrary contour

The continuation of fields is fundamental to the operator expansion method. Operators for field continuation between the rough surface and a reference plane are developed as Taylor series expansions, leading to a series for normal derivative operator $\hat{N}_b$. Truncation of the series for $\hat{N}_b$ is directly interpretable as an approximation of the continuation operations, and consequently, as an approximation of the plane wave coefficients $\tilde{p}_s(k_x)$. Examples in Chapters 4 and 5 illustrate that the series for $\hat{N}_b$ converges rapidly for many problems of interest. Retaining just a few terms in the series leads to an accurate solution for the surface values of the normal derivative field, and hence for the scattering cross section as well.

Like differentiation of fields, continuation of fields in the operator expansion method also relies on a field representation in terms of up-going plane waves; the idea is simply that an up-going field can be evaluated anywhere *above* its sources given its plane wave coefficients. We assume that an entirely up-going field p_+ is known on a flat surface picked for convenience to be the plane $z_0 = 0$, and recall that its spectral representation can be obtained as in (3.3). There are two reasons for not simply using (3.6) to perform the continuation. First, we wish to develop a series form for the continuation operator which can be used to find a series for its inverse. Second, the series is cast in terms of Fourier transforms which are convenient and efficient to evaluate

numerically. To find a series representation for the field $p_+(x, \zeta(x))$ which has been continued up to the mathematical surface $z = \zeta(x) \geq 0$, we first write (3.6) for p_+ and expand the height dependent exponential, and then interchange the order of integration and summation:

$$p_+(x, \zeta(x)) = \int_{-\infty}^{+\infty} dk_x \exp[ik_x x] \sum_{n=0}^{+\infty} \frac{(ik_z \zeta(x))^n}{n!} \tilde{p}_+(k_x)$$

$$= \sum_{n=0}^{+\infty} \frac{\zeta(x)^n}{n!} \int_{-\infty}^{+\infty} dk_x \exp[ik_x x] \ (ik_z)^n \ \tilde{p}_+(k_x) \ . \tag{3.8}$$

The convergence of the series in (3.8) and the validity of the interchange of the order of operations are both dependent on the condition that the plane $z_0 = 0$ lie above all singularities (sources) of the field p_+. For the purpose of this derivation we shall restrict ourselves to such a case. Nevertheless, we shall apply the resulting expressions to situations in which the location of the singularities is unknown *and could violate the stated assumption*, and rely on numerical tests to assess the accuracy of the solution obtained in this way.

The remaining integral in (3.8) is a spectral representation of the n'th vertical derivative of the field evaluated on the flat surface $z = 0$, as can be verified by repeated differentiation of (3.2) written for p_+. Using (3.4), we see that these derivatives can also be written as the operator $\hat{Q}$ operating n times on field p_+ so that

$$p_+(x, \zeta(x)) = \sum_{n=0}^{+\infty} \frac{\zeta(x)^n}{n!} \left[\frac{\partial^n}{\partial z^n} \ p_+(x, z) \right]_{z=0}$$

$$= \sum_{n=0}^{+\infty} \frac{\zeta(x)^n}{n!} \hat{Q}^n \ p_+(x,0) \ . \tag{3.9}$$

Equation (3.9) is a Taylor series expansion of the field about the horizontal reference surface using nonlocally computed vertical derivatives, and provides a continuation of the field from the surface $z = 0$ to an arbitrary surface $z = \zeta(x)$. Following Milder, we designate this continuation operation on up-going flat surface fields by operator $\hat{Z}$:

$$\hat{Z} \ p_+(x,0) \ = \ \exp[-ik_z z_0] \ \hat{Z} \ p_+(x, z_0) \ \equiv \ p_+(x, \zeta(x)). \tag{3.10}$$

The definition for $\hat{Z}$ remains essentially unchanged in the generalization to an arbitrary location of the flat surface on which the field is specified, except for a simple z_0 dependent phase term; the formal restriction is simply that both z_0 and ζ_{min} (the height of the

lowest point on the rough surface) be above all singularities of the continued field. In other words, $\hat{Z}$ is an exact continuation operator only for entirely up-going fields. In developing the expansion for $\hat{N}_b$, operator $\hat{Z}$ is applied to the vertical derivative of the scattered field $\partial p_s/\partial z$ (step 3). We shall see that the height z_0 does not appear in the expansion for the operator $\hat{N}_b$ because of the two-way continuation. (See the algebraic property of commutators in the expansion for $\hat{D}$ in (3.74).) Thus, the location of the flat plane is truly arbitrary in the operator expansion solution. However, the location of the flat plane does matter for a single continuation step, and appears in the expressions for fields continued using $\hat{Z}$ or $\hat{Z}^{-1}$ alone.

3.2.4 Continuation of the rough surface scattered field to a reference flat surface

In sketching out the construction of the expansion for $\hat{N}_b$, the first step is to continue the scattered field from the rough surface to a reference plane. The difficulty with performing this step using a plane wave decomposition is that the latter is obviously unknown. However, we recognize that the desired continuation operator is the inverse of $\hat{Z}$ defined above. Indeed, if we define operator $\hat{Z}^{-1}$ by

$$\hat{Z}\hat{Z}^{-1} = \hat{Z}^{-1}\hat{Z} = 1 \ , \tag{3.11}$$

then we have defined an operator which takes an up-going field specified on the rough surface $z = \zeta(x)$ and produces the values of the field on the flat surface $z = 0$:

$$\hat{Z}^{-1} p_+(x, \zeta(x)) = p_+(x,0) \ . \tag{3.12}$$

We can see that by applying $\hat{Z}^{-1}$ to the rough surface scattered field we would hope to obtain the scattered field evaluated on the reference plane $z = 0$ where its plane wave coefficients can easily be found. In principle, these coefficients could then be used to evaluate the desired scattered field normal derivative on the rough surface, or, they could be used to find the far field scattered field directly, and hence, the scattering cross section†. Instead, in the operator expansion method the vertical derivative of the continued scattered field is computed on the reference plane by applying operator $\hat{Q}$ to $p_s(x,0)$, and then operator $\hat{Z}$ is used to continue the vertical derivative $\partial p_s/\partial z$ to the rough surface. Thus, Milder defines a nonlocal vertical derivative operator $\hat{D}$ operating on up-going rough surface fields such that

$$\hat{D}\ p_+(x, \zeta(x)) = \hat{Z}\hat{Q}\hat{Z}^{-1} p_+(x, \zeta(x)) \equiv \left[\frac{\partial p_+(\mathbf{r})}{\partial z}\right]_{z=\zeta(x)} \ . \tag{3.13}$$

† This approach is outlined in Sec. 3.4, and numerically examined in Sec. 4.6. It is shown to be inferior to the operator expansion solution in terms of rate of convergence and domain of validity. Nevertheless, it is an improvement over standard perturbation theory which it closely resembles.

Under the assumption that the scattered field is up-going at the rough surface, $\hat{D}$ provides a means of obtaining the needed information regarding the behavior of the scattered field *in the neighborhood* of the surface, and thus can be related to the normal derivative operator $\hat{N}_b$ (see the following section). Here we wish to solve for the expansion for $\hat{D}$ using a method which, though less rigorous than the variational approach used by Milder [1990] and [1991], is simple and still provides the same solution. A series representation for $\hat{Z}^{-1}$ is obtained by expanding $\hat{Z}$ and $\hat{Z}^{-1}$ in (3.11) in series and solving for the terms in $\hat{Z}^{-1}$ by successive substitution, following the method outlined by Watson and West [1975], discussed in more detail by West et al. [1987], and reviewed by Milder [1990]. As Milder [1991] pointed out, the convergence of this expansion is not well established, and in Chapter 4 we demonstrate numerically that it is not as good as the convergence of the expansion for $\hat{N}_b$. The strength of Milder's variational approach is to show that a series expansion for $\hat{Z}^{-1}$ is not required to find the series expansion for $\hat{D}$ (and hence for $\hat{N}_b$); existence of operator $\hat{Z}^{-1}$ is all that is needed. Nevertheless, the series for $\hat{Z}^{-1}$ formed by backsubstitution leads to exactly the same series for $\hat{D}$ and provides an independent, if not rigorous, method of obtaining the terms of the operator expansion.

We write operators $\hat{Z}$ and $\hat{Z}^{-1}$ as series in powers of ζ and $\hat{Q}$. When using operator notation the fields being operated on are often omitted for the sake of brevity, but in all cases it is understood that the operator symbols operate on fields to their right. We multiply the series for $\hat{Z}$ and $\hat{Z}^{-1}$, given by

$$\hat{Z} = \sum_{n=0}^{+\infty} \hat{Z}_n \quad \text{with} \quad \hat{Z}_n = \frac{\zeta^n \hat{Q}^n}{n!}, \tag{3.14}$$

and

$$\hat{Z}^{-1} = \sum_{n=0}^{+\infty} \hat{Z}_n^{-1}, \tag{3.15}$$

to obtain the identity operator

$$\left[\hat{Z}_0 + \hat{Z}_1 + \hat{Z}_2 + \cdots\right]\left[\hat{Z}_0^{-1} + \hat{Z}_1^{-1} + \hat{Z}_2^{-1} + \cdots\right] = 1, \tag{3.16}$$

then expand, collect orders, and backsubstitute to find to third order:

$$\hat{Z}_0^{-1} = 1, \tag{3.17a}$$

$$\hat{Z}_1^{-1} = -\zeta\hat{Q}, \tag{3.17b}$$

$$\hat{Z}_2^{-1} = \zeta\hat{Q}\,\zeta\hat{Q} - \tfrac{1}{2}\zeta^2\hat{Q}^2, \tag{3.17c}$$

$$\hat{Z}_3^{-1} = -\zeta\hat{Q}\,\zeta\hat{Q}\,\zeta\hat{Q} + \tfrac{1}{2}\zeta\hat{Q}\,\zeta^2\hat{Q}^2 + \tfrac{1}{2}\zeta^2\hat{Q}^2\zeta\hat{Q} - \tfrac{1}{6}\zeta^3\hat{Q}^3. \tag{3.17d}$$

Manipulations involving operators are not commutative. For example, $\zeta\hat{Q} \neq \hat{Q}\zeta$ when $\zeta(x) \neq 0$, as can be verified by operating on a test function; in operator $\zeta\hat{Q}$, ζ only acts as a local factor, whereas in $\hat{Q}\zeta$ it enters nonlocally through a convolution. The commutator of ζ and $\hat{Q}$, denoted by

$$[\zeta,\hat{Q}] \equiv \zeta\hat{Q} - \hat{Q}\zeta, \tag{3.18}$$

is a fundamental component of the operator expansion, and the use of this notation simplifies the expansion for $\hat{D}$ (3.20) and $\hat{N}$ (3.28) below.

Though ζ and $\hat{Q}$ do not commute in general, we note that the terms for $\hat{Z}_n^{-1}$ are the same whether obtained from $\hat{Z}\hat{Z}^{-1} = 1$ or from $\hat{Z}^{-1}\hat{Z} = 1$.

3.2.5 The series expansion for vertical derivative operator $\hat{D}$

The series for $\hat{Z}$ and $\hat{Z}^{-1}$ can now be combined to find the terms in the series for $\hat{D}$, using $\hat{D} = \hat{Z}\hat{Q}\hat{Z}^{-1}$ (3.13). To third order we find:

$$\hat{D}_0 = \hat{Q}, \tag{3.19a}$$

$$\hat{D}_1 = \zeta\hat{Q}^2 - \hat{Q}\zeta\hat{Q}, \tag{3.19b}$$

$$\hat{D}_2 = \hat{Q}\zeta\hat{Q}\zeta\hat{Q} - \tfrac{1}{2}\hat{Q}\zeta^2\hat{Q}^2 - \zeta\hat{Q}^2\zeta\hat{Q} + \tfrac{1}{2}\zeta^2\hat{Q}^3, \tag{3.19c}$$

$$\begin{aligned}\hat{D}_3 = {} & -\hat{Q}\zeta\hat{Q}\zeta\hat{Q}\zeta\hat{Q} + \zeta\hat{Q}^2\zeta\hat{Q}\zeta\hat{Q} + \tfrac{1}{2}\hat{Q}\zeta\hat{Q}\zeta^2\hat{Q}^2 + \tfrac{1}{2}\hat{Q}\zeta^2\hat{Q}^2\zeta\hat{Q} \\ & - \tfrac{1}{2}\zeta\hat{Q}^2\zeta^2\hat{Q}^2 - \tfrac{1}{2}\zeta^2\hat{Q}^3\zeta\hat{Q} - \tfrac{1}{6}\hat{Q}\zeta^3\hat{Q}^3 + \tfrac{1}{6}\zeta^3\hat{Q}^4.\end{aligned} \tag{3.19d}$$

These terms can be written more compactly using the commutator notation. In particular, applying the variational method used by Milder leads directly to an elegant recursive form [Milder, 1990] for the terms in the expansion for $\hat{D}$:

$$\hat{D}_n = \frac{1}{n}\sum_{m=0}^{n-1}[\zeta,\hat{D}_m]\,\hat{D}_{n-m-1}, \quad n \geq 1, \tag{3.20}$$

with $\hat{D}_0 = \hat{Q}$ and $\hat{D} = \hat{D}_0 + \hat{D}_1 + \hat{D}_2 + \cdots$. This expression (and (3.26) for $\hat{N}$) is useful for generating terms in the operator expansion to arbitrary order. We present the variational approach in Sec. 3.5.1.

3.2.6 The expansion for normal derivative operator $\hat{N}$

The essential part of the operator expansion solution is the expansion for the nonlocal vertical derivative operator $\hat{D}$. It provides information about the behavior of the scattered field in the neighborhood of the surface given only the values of the field on the surface. The vertical derivative can be combined with the linearly independent

tangential derivative along the surface to construct the desired normal derivative (see step 4 in Fig. 3.3). The tangential derivative of the scattered field is known in the sense that the field is given on the boundary by the negative of the incident field. In numerical implementations, this field is sampled at many points along the surface, and the tangential derivative could be obtained by a finite difference method; here, we use an FFT technique. Formally, the normal and tangential derivatives are given by

$$\frac{\partial p_s(\mathbf{r})}{\partial n} = \hat{\mathbf{n}}\cdot\nabla p_s(\mathbf{r}) = \frac{1}{\sqrt{1+\zeta_x^2}}\left[-\zeta_x\frac{\partial}{\partial x} + \frac{\partial}{\partial z}\right]p_s(\mathbf{r}) \ , \tag{3.21a}$$

$$\frac{\partial p_s(\mathbf{r})}{\partial s} = \hat{\mathbf{t}}\cdot\nabla p_s(\mathbf{r}) = \frac{1}{\sqrt{1+\zeta_x^2}}\left[\frac{\partial}{\partial x} + \zeta_x\frac{\partial}{\partial z}\right]p_s(\mathbf{r}) \ , \tag{3.21b}$$

where $\zeta_x \equiv d\zeta(x)/dx$ is the surface slope at each point, and $\sqrt{1+\zeta_x^2} = ds/dx$ is the required normalization factor. The normal derivative can then be written using the tangential and vertical derivatives as

$$\left[\frac{\partial p_s(\mathbf{r})}{\partial n}\right]_{z=\zeta(x)} = \left[-\zeta_x\frac{\partial}{\partial s}p_s(\mathbf{r}) + \sqrt{1+\zeta_x^2}\frac{\partial}{\partial z}p_s(\mathbf{r})\right]_{z=\zeta(x)} . \tag{3.22}$$

It proves convenient to define the nonlocal operator $\hat{N}$ without the normalization factor $(ds/dx)^{-1}$ because of a change of variables in the surface integrals from surface coordinate s to transverse coordinate x. We define the "scaled" normal derivative (indicated by a prime) of the scattered field

$$p_s'(\mathbf{r})\,dx \equiv \frac{\partial p_s(\mathbf{r})}{\partial n}\,ds \ . \tag{3.23}$$

Recalling definition (3.7) and using (3.22), we write the expression for scaled normal derivative operator $\hat{N}$ as

$$\hat{N}\,p_s(x,\zeta(x)) \equiv \frac{ds}{dx}\hat{N}_b\,p_s(x,\zeta(x)) = \left[-\zeta_x\frac{d}{dx} + (1+\zeta_x^2)\,\hat{D}\right]p_s(x,\zeta(x)) , \tag{3.24}$$

where we use $\hat{D}$ to evaluate the vertical derivative $\partial/\partial z$, and use an FFT to evaluate the x-derivative of the complex function $p_s(x,\zeta(x))$. (Note that this is not the x-derivative of the scattered field, which is then evaluated on the rough surface; to obtain that quantity would require a nonlocal operator analogous to $\hat{D}$.) Operator $\hat{D}$ is an approximation of the vertical derivative if p_s does not satisfy the Rayleigh hypothesis, and to the extent that the series for $\hat{D}$ is truncated. It is important to recognize that to evaluate (3.22) the scattered field must be known in the neighborhood of the surface, whereas (3.24) only requires knowledge of the field on the rough surface itself.

Operator $\hat{D}$ is written as a series expansion in powers of ζ and $\hat{Q}$ (3.19), such that at n'th order the terms contain ζ^n and $\hat{Q}^{n+1}$. Milder [1991] showed that the slope squared ζ_x^2 can be expanded in terms of ζ and $\hat{Q}$ as a second order term:

$$\zeta_x^2 = -\frac{1}{2}\zeta^2\hat{Q}^2 + \zeta\hat{Q}^2\zeta - \frac{1}{2}\hat{Q}^2\zeta^2 = -\frac{1}{2}[\,\zeta,[\zeta,\hat{Q}^2]\,]\ . \tag{3.25}$$

With this in mind, the terms of Eq. (3.24) are grouped by order to provide the expansion for operator $\hat{N} = \hat{N}_0 + \hat{N}_1 + \hat{N}_2 + \cdots$ as

$$\hat{N}_0 = \hat{D}_0\ , \tag{3.26a}$$

$$\hat{N}_1 = \hat{D}_1 - \zeta_x\frac{d}{dx}\ , \tag{3.26b}$$

$$\hat{N}_n = \hat{D}_n + \zeta_x^2\hat{D}_{n-2}\ ,\quad \text{for } n \geq 2\,. \tag{3.26c}$$

Useful expressions for the numerical implementation of each $\hat{N}_n$ can be obtained by substituting the forms for $\hat{D}$ in (3.19) into (3.26). Milder showed that by making use of (3.25) and

$$\hat{Q}^2 = -k^2 - \frac{\partial^2}{\partial x^2}\ , \tag{3.27}$$

the first three terms of $\hat{N}$ can be cast into a symmetrical form at each order in the expansion. (An operator is symmetrical when the operations it represents are the same carried out from right to left or from left to right. Milder [1991] showed that symmetry of the operator implies reciprocity of the operator expansion solution.) This symmetry is not directly apparent when using commutator notation, but becomes so upon expansion of the commutators; up to second order, the resulting forms lead to a more efficient numerical implementation as well. At third order, considerable effort is required to show that the term $\hat{N}_3$ is indeed symmetric; this can be done by addition of terms which taken in combination with those in (3.28d) result in a manifestly symmetric expression, and new residual terms which can be shown to be symmetric after further manipulation using (3.25) and (3.27). However, this approach does not lead to a more compact form. The terms of $\hat{N}$ are given below as compact symmetric forms to second order, and as the "standard" form obtained from (3.19) and (3.26) for third order:

$$\hat{N}_0 = \hat{Q}\ , \tag{3.28a}$$

$$\hat{N}_1 = -\hat{Q}\zeta\hat{Q} - \frac{d}{dx}\Big(\zeta\frac{d}{dx}\Big) - k^2\zeta\,, \tag{3.28b}$$

$$\hat{N}_2 = -\frac{1}{2}\hat{Q}\zeta^2\hat{Q}^2 + \hat{Q}\zeta\hat{Q}\zeta\hat{Q} - \frac{1}{2}\hat{Q}^2\zeta^2\hat{Q} = -\frac{1}{2}\hat{Q}\,[\,\zeta\,,[\zeta,\hat{Q}\,]\,]\,\hat{Q}\ , \tag{3.28c}$$

$$\hat{N}_3 = -\hat{Q}\zeta\hat{Q}\zeta\hat{Q}\zeta\hat{Q} - \tfrac{1}{2}\hat{Q}^2\zeta^3\hat{Q}^2 + \tfrac{1}{2}\hat{Q}\zeta\hat{Q}\zeta^2\hat{Q}^2 + \tfrac{1}{2}\hat{Q}^2\zeta^2\hat{Q}\zeta\hat{Q}$$
$$+ \tfrac{1}{2}\hat{Q}\zeta^2\hat{Q}^2\zeta\hat{Q} - \tfrac{1}{6}\hat{Q}\zeta^3\hat{Q}^3 + \tfrac{1}{2}\zeta\hat{Q}^2\zeta^2\hat{Q}^2 - \tfrac{1}{2}\zeta^2\hat{Q}^2\zeta\hat{Q}^2 + \tfrac{1}{6}\zeta^3\hat{Q}^4 . \qquad (3.28d)$$

The use of these expressions in computing scattering from a 1-D Dirichlet surface is addressed in the next section, along with a brief description of the numerical implementation of the method.

3.3 Numerical Implementation of the Monte Carlo Method

The scattering cross section for the operator expansion, the integral equation, and other methods are obtained using a Monte Carlo technique. Scattering calculations are performed for single surface realizations and are then averaged to provide estimates of the cross section. The rough surface profiles used in this work are random realizations generated by a spectral method [Thorsos, 1988], [Macascill and Ewart, 1984]. The method produces periodic surfaces; here a nonperiodic subset of each generated surface is retained. For each surface realization and incident angle θ_i, the incident field p_i and its scaled normal derivative p_i' are evaluated on the rough surface. Then p' is computed by the operator expansion (or by any other means) and used to compute the total scattered intensity in the far field of the scattering region. The intensity is then averaged over realizations to provide an estimate of the cross section, and then of the scattering strength, defined in Sec. 2.3. The following sections outline the procedure in more detail, with particular emphasis given to the operator expansion method.

3.3.1 Using $\hat{N}$ in the scattering integral

Operator $\hat{N}$ is used in the scattering integral in the same way operator $\hat{Q}$ was used in the flat surface problem described in Sec. 3.2.1. Essentially, the surface values of the normal derivative of the scattered field are estimated by applying $\hat{N}$ to the surface values of the negative incident field. Writing scattering integral (2.13) over transverse coordinate x, the scattered field above the rough surface is given by

$$p_s(\mathbf{r}) = -\int_S G_0(\mathbf{r},\mathbf{r}')\; p'(x', \zeta(x'))\, dx' . \qquad (3.29)$$

The rough surface values of the scaled normal derivative of the total field are expressed as the sum of the incident and scattered field derivatives as $p' = p_i' + p_s'$, where $\hat{N}$ is used to estimate p_s':

$$p_s'(x, \zeta(x)) = \hat{N}\, p_s(x, \zeta(x)) = -\hat{N}\, p_i(x, \zeta(x)) . \qquad (3.30)$$

The series expansion for $\hat{N}$ leads to a series solution for p':

$$p' = p_i' - (\hat{N}_0 + \hat{N}_1 + \hat{N}_2 + \cdots) p_i = p_0' + p_1' + p_2' + \cdots \quad . \tag{3.31}$$

Once p' is determined, the scattered field can be evaluated anywhere above the rough surface using (3.29) and (2.3). In the far field of the surface, we use the scattering amplitude F defined in (2.19)

$$F(\mathbf{k}_s) = \frac{e^{i\pi/4}}{\sqrt{8\pi k}} \int_S \exp[-i\,\mathbf{k}_s \cdot \mathbf{r}']\, p'(\mathbf{r}')\, dx' \tag{3.32}$$

to find the cross section (combining (2.18) and (2.20)) given by

$$\sigma(\theta_i, \theta_s) = \langle |F|^2 \rangle \frac{\sin\theta_i}{2\rho c E_f} \quad . \tag{3.33}$$

When the series (3.31) for p' is evaluated to a given order, the procedure outlined above leads to the "truncated" series solution for the cross section given by (2.22). To obtain the "consistent" series (2.23), p_n' is evaluated at each order n separately, and then used in (3.32) to find each F_n term in the scattering amplitude series $F = F_0 + F_1 + \cdots + F_n + \cdots$. Finally, the product terms are computed and summed as given by (2.23). The procedure required to evaluate series (2.23) is much less efficient than the procedure for (2.22), and is only used to assess the importance of the higher order cross terms which distinguish the two series. Fortunately, it turns out that the truncated series (2.22) often makes better use of the n'th order surface field in the operator expansion method; see Sec. 4.4 (Gaussian spectrum) and Sec. 5.3 (Pierson-Moskowitz spectrum).

3.3.2 Tapered plane wave incident field

The incident field for the infinite randomly rough surface problem can be quite general, with the single restriction that it ensonify a limited portion of the surface, as discussed in Sec. 2.2. This restriction is compatible with numerical simulations which must use a finite surface length. Following Thorsos [1988] we use a modified Gaussian tapered plane wave given by

$$p_i(\mathbf{r}) = \exp\left(i\,\mathbf{k}_i \cdot \mathbf{r}\,[1 + w(\mathbf{r})] - b^2(\mathbf{r}) / g^2 \right), \tag{3.34a}$$

with

$$w(\mathbf{r}) = \left[2b^2(\mathbf{r})/g^2 - 1 \right] / (kg \sin\theta_i)^2, \qquad b(\mathbf{r}) = x - z\cot\theta_i, \tag{3.34b}$$

where $\mathbf{k}_i = k_{ix}\hat{\mathbf{x}} + k_{iz}\hat{\mathbf{z}}$ is the mean incident wave vector, and where the taper parameter g determines the width of the tapered wave. By adjusting the ratio L/g, where L is the

length of the surface, the incident field at the ends of the surface can be made very small in order to reduce edge effects to a negligible level. Then, the incident flux E_f for the tapered plane wave (3.34) is

$$E_f = \frac{\sin\theta_i}{2\rho c} g \sqrt{\frac{\pi}{2}} \left[1 - \frac{(1+2\cot^2\theta_i)}{2(kg\sin\theta_i)^2} \right]. \tag{3.35a}$$

In some cases it is useful to study scattering using less tapering to obtain better angular resolution in the far field. In general, the flux also depends on the surface length L:

$$E_f = \frac{\sin\theta_i}{2\rho c} g \sqrt{\frac{\pi}{2}} \,\mathrm{erf}(A) \left[1 - \frac{(1+2\cot^2\theta_i)}{2(kg\sin\theta_i)^2} - \frac{(1-2\cot^2\theta_i)}{2(kg\sin\theta_i)^2} \frac{A\exp(-A^2)}{\sqrt{\pi}\,\mathrm{erf}(A)} \right], \tag{3.35b}$$

with $A = \frac{L}{\sqrt{2}g}$, and where erf is the error function.

The incident field form (3.34) leads to the following expression for the scaled normal derivative of the incident field on the rough surface $z = \zeta(x)$:

$$p_i'(\mathbf{r}) = p_i(\mathbf{r}) \left[i[1+w(\mathbf{r})](-\zeta_x k_{ix} + k_{iz}) + \frac{2b(\mathbf{r})}{g^2}(\zeta_x + \cot\theta_i)\left(1 - \frac{2i\,\mathbf{k}_i\cdot\mathbf{r}}{(kg\sin\theta_i)^2}\right) \right]. \tag{3.36}$$

The surface slope first enters into the expression for $\hat{N}$ at first order. For consistency, ζ_x dependent terms in (3.36) are not included when computing the zeroth order estimate of p' in (3.31).

3.3.3 Even (inversion symmetric) and odd (inversion antisymmetric) series

The derivation of the expansion for $\hat{N}$ has been performed for the scattering geometry of Fig. 3.4 (see also Fig. 2.1 and Fig. 4.1), in which down-going incident energy is scattered into up-going waves. Milder [1991] showed that inverting the scattering geometry leads to a useful symmetry property which significantly simplifies the operator expansion solution. We arrive at the same result by deriving the expansion for the down-going wave operator $\hat{N}_-$ for the current geometry, redrawn in Fig. 3.4. In this section, we denote the up-going wave operator $\hat{N} \equiv \hat{N}_+$ for clarity.

Operator $\hat{N}_-$ computes the scaled normal derivative of down-going fields; we write $\hat{N}_- p_- = p_-'$. The expansion for $\hat{N}_-$ is obtained by writing (3.2) for p_- in a downward wave expansion, with $k_z = -\sqrt{k^2 - k_x^2}$ and $\mathrm{Im}(k_z) \le 0$, and following the steps taken in the derivation of $\hat{N}_+$. For example, the z-derivative of down-going field p_- on a flat surface is

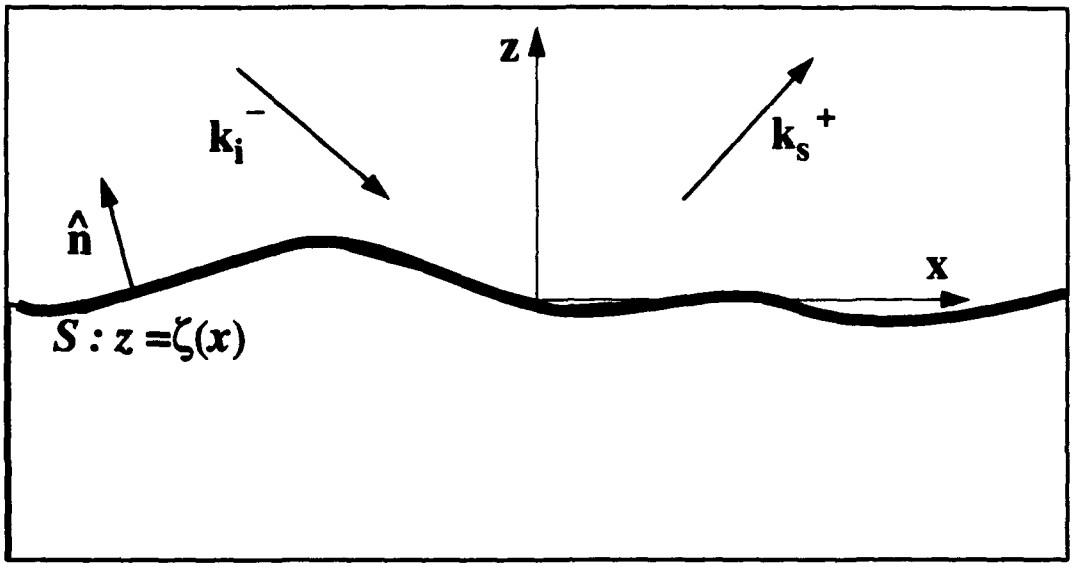

Figure 3.4 : Scattering geometry used in the derivation of the operator expansion.

$$\left[\frac{\partial p_-(\mathbf{r})}{\partial z}\right]_{z=z_0} = -\hat{Q}\, p_-(x,z_0)\ , \tag{3.37}$$

with $\hat{Q}$ defined in (3.4) for positive k_z (up-going waves). This negative sign carries through to the expansion for $\hat{N}_-$, which we write using the terms in the expansion for $\hat{N}_+$ given by (3.28):

$$\hat{N}_- = -\hat{N}_0+\hat{N}_1-\hat{N}_2+\hat{N}_3-\cdots\ , \tag{3.38}$$

since the n'th term in the series (3.28) for $\hat{N}_+$ contains $n+1$ powers of $\hat{Q}$.

This expression can be used to generate two alternative forms of the OE solution. The down-going operator applied to the incident field p_i simply evaluates the scaled normal derivative of the incident field on the rough surface

$$\hat{N}_- p_i = p_i' \quad <=> \quad (\hat{N}_0-\hat{N}_1+\hat{N}_2-\hat{N}_3+\cdots)p_i + p_i' = 0\ . \tag{3.39}$$

Then, by adding or subtracting (3.39) from (3.31), which we now denote as the "standard" solution p_{std}', the scaled normal derivative of the total field can be written using three different series:

$$p_{std}' \equiv p_i' - \hat{N}_+ p_i = p_i' - (\hat{N}_0+\hat{N}_1+\hat{N}_2+\cdots)p_i\ , \tag{3.40}$$

$$p_{odd}' \equiv 2p_i' - (\hat{N}_+ - \hat{N}_-)p_i = 2p_i' - 2(\hat{N}_1+\hat{N}_3+\cdots)p_i\ , \tag{3.41}$$

$$p_{even}' \equiv -(\hat{N}_+ + \hat{N}_-)p_i = -2(\hat{N}_0+\hat{N}_2+\cdots)p_i\ . \tag{3.42}$$

Note that in (3.41) all of p_i' expressed in (3.36) is included at first order, and no zeroth

order component of p_i' appears in the even series solution (3.42). We recognize that $2p_i'$ is the Kirchhoff solution, and that the odd series operator applied to $-p_i$ provides a correction to the standard Kirchhoff approximation. These even and odd series solutions[†] are obviously simpler to evaluate than the standard series (3.31) to any given order. Yet, the short series (3.41) and (3.42) provide solutions which are similar in accuracy to that of the standard series, and typically prove to be nearly as accurate as the standard solution taken to next higher order. Further details are presented in Chapters 4 and 5, where numerical examples illustrate that use of these shorter forms results in a reduction in computational expense while retaining, or, particularly in the case of Pierson-Moskowitz surfaces, improving upon the accuracy of the standard series solution evaluated at a given order.

3.3.4 Evaluating $\hat{N}p_i$ using the Fast Fourier Transform (FFT)

The series for $\hat{N}$ is written as a sequence of operations involving products with the surface height function $\zeta(x)$ and nonlocal operations by $\hat{Q}$. Each term in the expansion for $\hat{N}$ in (3.28) can be factored for a more efficient evaluation. For example, $\hat{N}_2$ can be written as

$$\hat{N}_2 = \hat{Q}\left(-\tfrac{1}{2}\zeta^2\hat{Q} + (\zeta\hat{Q} - \tfrac{1}{2}\hat{Q}\zeta)\zeta\right)\hat{Q} \quad . \tag{3.43}$$

Operator $\hat{Q}$ (3.4) (and higher powers of $\hat{Q}$ as well) is straightforwardly implemented as a subroutine using a sequence of Fast Fourier Transform (FFT) operations, with an intermediate product by a complex function of transverse wavenumber. The usual FFT requirement of 2^n points leads to minor modifications for a scattering problem posed on a surface divided into an arbitrary number of partition intervals. The surface height, slope, and complex arrays used in the computation of OE terms are extended by zero-padding to a power of two. Thus the computational surface length used in evaluating the operator expansion solution is typically longer than the original rough surface length. The incident field taper effectively reduces all field quantities to zero at the original surface extremities, making additional tapering of these quantities unnecessary. Nevertheless, when the surface is not periodic, the discontinuity in the rough surface height (and slope) at the original surface endpoints can introduce error into the results because the operator expansion solution is evaluated by repeated convolution with the Fourier transform of the surface height. Before extending surface height

[†] Milder refers to (3.41) as the inversion antisymmetric solution, and to (3.42) as the inversion symmetric solution. We call Eqs. (3.41) and (3.42) the short forms, collectively, and even and odd solutions, respectively.

and slope arrays it is preferable to apply a taper to the height function at the ends of the rough surface *where the incident energy is very small*; this procedure does not require renormalizing the surface height spectrum since the tapered portion of the surface does not contribute significantly to the scattering. We use a cosine taper, typically applied to 10% of the surface length at each end. Such tapering improves the third order operator expansion estimates of the surface field and hence of the scattering cross section (especially for low grazing angles when scattering levels are low) but has almost no effect on lower order terms.

The surface sampling density (number of points per wavelength) requirements of the operator expansion method depend on the order to which the solution is computed. In general, convergence studies in which the surface profile sampling density is increased until no significant change in the scattering results are obtained indicate that through second order the operator expansion requires about the same surface partition density as the integral equation method. However, third order computations often require more points per wavelength for comparable accuracy; in general, it is convenient to use twice the density for third order calculations because of the use of FFTs in the implementation. A table of parameter values for the numerical examples presented in this dissertation is included in the Appendix.

The use of a finite surface, here determined by the tapered incident field, leads to finite angular resolution in the scattering results which is coarsest within a few degrees of grazing. Thus, the scattering cross section obtained for a finite surface will not vanish at grazing as it must for the infinite surface. Tests in which the surface length is increased confirm that the accuracy statements made for shorter surfaces are consistent with results for longer surfaces with better angular resolution, with one exception. For all cases examined, the operator expansion solution requires more care in a small range of angles (less than about 3°) near grazing, especially for computing scattering at grazing (0° and 180°). This near-grazing behavior is not a consequence of the finite angular resolution discussed above, but rather is related to a need for greater wavenumber domain sampling density to achieve the same degree of accuracy obtained for other scattering angles. The wavenumber domain sampling density is proportional to the length of the computational surface used in the FFT. Tests in which the computational surface is lengthened (in powers of two) by zero padding show that, for any given order, the near-grazing operator expansion solution converges more slowly with increasing computational surface length than the solution in other angular directions. Extending the computational surface by zero padding does not change the scattering problem itself, because both the rough surface profile and the incident field remain unchanged; the integral equation solution for the unpadded surface is still the exact result. Simply extending the number of intervals in the computational surface to the

nearest power of two may not provide sufficiently accurate results near grazing, in some cases giving scattering strength errors of up to 3 dB at grazing. In such cases, doubling that number of computational intervals usually reduces the errors at grazing to about 0.5 dB, but convergence tests in which the computational surface is successively lengthened are the only reliable way of determining the best solution obtainable by the operator expansion for any given problem. The surfaces in the computations in this thesis have not, in general, been extended beyond the nearest power of two. One example presented in Fig. 5.10 for surfaces with a Pierson-Moskowitz height spectrum illustrates typical results obtained using different computational surface lengths.

3.4 The Mean Plane Methods

3.4.1 Introduction

The operator expansion solution is constructed in Sec. 3.2 as a sequence of operations on the scattered field. First, the scattered field is continued from the rough surface to a reference plane, chosen for convenience to be the mean plane $z = 0$. There the vertical derivative of the scattered field is evaluated, and this vertical derivative field is then continued back to the rough surface where it is related to the normal derivative field through the known tangential derivative of the scattered field along the surface. The entire procedure relies on an upward directed plane wave representation of the scattered field which becomes available after the first continuation step by Fourier transforming the scattered field expressed on the mean plane. One may wonder why that plane wave representation is not directly used to solve for the far-field scattered field needed in the determination of the scattering cross section. In this section we outline an algorithm that computes the scattering amplitude directly from the values of $p_s(x,0) = \hat{Z}^{-1} p_s(x, \zeta(x))$. In Sec. 4.6 we examine the accuracy of this method, and find that the solution performs better than the standard field perturbation series in kh; the $\hat{Z}^{-1}$ solution converges more rapidly, and better matches the statistical fluctuations of the exact solution for an average over a finite set of surface realizations. However, the $\hat{Z}^{-1}$ solution does not converge as rapidly as the $\hat{N}$ solution, nor is it as accurate for larger kh values, including some cases when the Kirchhoff approximation is accurate. In building the expansion for $\hat{N}$, Milder used a second continuation step; the continuation back to the rough surface (by application of $\hat{Z}$) improves the solution by reducing its dependence on the normalized height kh. Though the solution based on the use of $\hat{Z}^{-1}$ alone is not as widely accurate as the $\hat{N}$ solution, we examine it because of its connection to standard perturbation theory, and because it plays an important role as a building block of the operator expansion solution.

A second variant on the OE method which takes explicit advantage of the plane wave representation of the scattered field effectively replaces the truncated continuation operator $\hat{Z}$ with the exact expression (3.6). This solution directly evaluates the normal derivative on the rough surface using the spectral representation; consequently, it cannot be fully implemented using FFTs. This solution method is presented in Sec. 3.4.3.

3.4.2 Direct evaluation of the scattering amplitude using $\hat{Z}^{-1}$

Knowing the scattered field on a plane enables computation of the field anywhere above the plane, and in particular in the far-field of the scattering surface. Choosing the reference plane to be the mean plane $z_0 = 0$, we apply the continuation operator $\hat{Z}^{-1}$ to the rough surface values of the scattered field to obtain an estimate of the scattered field on the mean plane as

$$p_s(x,0) = \hat{Z}^{-1}\, p_s(x, \zeta(x)) \,. \tag{3.44}$$

The Helmholtz-Kirchhoff integral (2.10) on the mean plane is written as

$$p_s(\mathbf{r}) = - \int_{z=0} \left[G_0(\mathbf{r},\mathbf{r}') \frac{\partial p_s(\mathbf{r}')}{\partial z'} - p_s(\mathbf{r}') \frac{\partial G_0(\mathbf{r},\mathbf{r}')}{\partial z'} \right] dx'. \tag{3.45}$$

The scattered field satisfies an unknown boundary condition on this surface, but the vertical derivative is easily obtained from the values of $p_s(x,0)$ using operator $\hat{Q}$ defined in (3.4):

$$\left[\frac{\partial p_s(\mathbf{r})}{\partial z} \right]_{z=0} = \hat{Q}\, p_s(x,0) \,. \tag{3.46}$$

Using the large argument form for the Hankel function we write

$$\lim_{r \gg r'} G_0(\mathbf{r},\mathbf{r}') = \frac{e^{ikr}}{\sqrt{r}} \frac{e^{i\pi/4}}{\sqrt{8\pi k}} \exp[-i\,\mathbf{k}_s \cdot \mathbf{r}'] \tag{3.47}$$

and

$$\lim_{r \gg r'} \frac{\partial G_0(\mathbf{r},\mathbf{r}')}{\partial z'} = \frac{e^{ikr}}{\sqrt{r}} \frac{e^{i\pi/4}}{\sqrt{8\pi k}} (-ik_{sz}) \exp[-i\,\mathbf{k}_s \cdot \mathbf{r}'] \,. \tag{3.48}$$

Thus, we write the scattering amplitude as

$$F(\mathbf{k}_s) = -\frac{e^{i\pi/4}}{\sqrt{8\pi k}} \int_{z=0} \exp[-ik_{sx}x'] \left(\hat{Q} + ik_{sz} \right) p_s(x',0)\, dx'. \tag{3.49}$$

Expanding $\hat{Q}$ using the definition (3.4) we find

$$F(\mathbf{k}_s) = (-2ik_{sz}) \frac{e^{i\pi/4}}{\sqrt{8\pi k}} \int_{z=0} \exp[-ik_{sx}x']\, p_s(x',0)\, dx'$$

$$= (-2ik_{sz}) \frac{e^{i\pi/4}}{\sqrt{8\pi k}} \tilde{p}_s(k_x) \ , \qquad (3.50)$$

where we see the direct relationship between the scattering amplitude F and the plane wave coefficients $\tilde{p}_s$ evaluated from the mean plane field. It is important to emphasize that the scattering amplitude F evaluated using the mean plane method, that is, using $\hat{Z}^{-1}$ alone, is not equivalent to the OE solution for F (3.32), nor is the estimate for the plane wave amplitudes $\tilde{p}_s(k_x)$ the same in the two methods, though the notation in (3.50) does not distinguish between the two solutions. We note that (3.50) can also be obtained using the "image" Green function $G_1(\mathbf{r}, \mathbf{r}')$ (which is zero on the mean plane) in (3.45), following the Rayleigh-Rice perturbation development in Sec. 2.5.

3.4.3 Using $\hat{Z}^{-1}$ to compute the rough surface normal derivative field

The plane wave coefficients $\tilde{p}_s(k_x)$ defined in Sec. 3.4.2 can also be used to directly solve for the normal derivative of the scattered field on the rough surface in a different way than is done using $\hat{N}$. We replace steps 2, 3, and 4 in Fig. 3.3 by applying the scaled normal derivative to the plane wave representation (3.2) and then evaluating the field on the rough surface:

$$p_s'(x, \zeta(x)) = \left[\hat{\mathbf{n}} \cdot \nabla \ p_s(\mathbf{r}) \right]_{z = \zeta(x)}$$

$$= \int_{-\infty}^{+\infty} dk_x \ \exp[ik_x x] \exp[ik_z \zeta(x)] \left(-\zeta_x ik_x + ik_z\right) \tilde{p}_s(k_x) \ . \qquad (3.51)$$

Recall that $\tilde{p}_s(k_x)$ is found using $\hat{Z}^{-1}$:

$$\tilde{p}_s(k_x) = \frac{1}{2\pi} \int_{-\infty}^{+\infty} dx' \exp[-ik_x x'] \hat{Z}^{-1}[-p_i(x, \zeta(x))] \ . \qquad (3.52)$$

The surface field p_s' in (3.51) could be used instead of $\hat{N}p_s$ in (3.29) to compute the scattered field above the surface. This solution may also reduce the height dependence of the $\tilde{p}_s(k_x)$ representation by taking the solution back to the rough surface, but the effect of the higher order terms included in (3.51) is unknown. Only numerical tests can determine the relative accuracy of the solution given by (3.51) compared with the standard OE solution using $\hat{N}$, but this has not been done. The integral in (3.51) cannot be evaluated using an FFT because of the exponentiated surface height. Therefore, the solution (3.51) is much slower to evaluate numerically.

3.4.4 Comparing the $\hat{Z}^{-1}$ method to the Rayleigh-Rice perturbation method

The solution produced by simply applying the operator $\hat{Z}^{-1}$ to $p_s(x, \zeta(x))$ is very similar to the perturbation theory solution, but is not a consistent expansion in powers of kh, as we'll see below. Numerical tests indicate that this difference results in improved convergence and accuracy over the standard perturbation solution. Nevertheless, the $\hat{Z}^{-1}$ solution still retains a fundamental dependence on kh which limits its applicability to surfaces with small height, even when the rms surface slope is small. (Thus, the $\hat{Z}^{-1}$ solution is not as useful as the OE solution using $\hat{N}$.) To compare the $\hat{Z}^{-1}$ solution with the perturbation solution we must develop the perturbation method using the scattered field instead of the total field as done in Sec. 2.5.

Following the procedure of Sec. 2.5, we write the scattered field integral (2.10) on the mean plane and use the image Green function G_1 to obtain

$$p_s(\mathbf{r}) = \int_{z=0} p_s(x',0) \frac{\partial G_1(\mathbf{r},\mathbf{r}')}{\partial z'} dx' , \tag{3.53}$$

recognizing that the reflected field p_r is included in this formulation. Note that the incident field surface integral is not zero when using the image Green function, as can be seen by developing (2.27) for the incident field:

$$\begin{aligned} p_i(\mathbf{r}) &= \int_{V_3} P(\mathbf{r}') G_0(\mathbf{r},\mathbf{r}') dv' + \int_{z=0} p_i(x',0) \frac{\partial G_1(\mathbf{r},\mathbf{r}')}{\partial z'} dx' \\ &= p_i(\mathbf{r}) + p_r(\mathbf{r}) + \int_{z=0} p_i(x',0) \frac{\partial G_1(\mathbf{r},\mathbf{r}')}{\partial z'} dx' . \end{aligned} \tag{3.54}$$

Therefore,

$$\int_{z=0} p_i(x',0) \frac{\partial G_1(\mathbf{r},\mathbf{r}')}{\partial z'} dx' = -p_r(\mathbf{r}) . \tag{3.55}$$

The integral (2.31) for the field p_{si} is then decomposed as

$$\begin{aligned} p_{si}(\mathbf{r}) &= \int_{z=0} p(\mathbf{r}) \frac{\partial G_1(\mathbf{r},\mathbf{r}')}{\partial z'} dx' \\ p_{si}(\mathbf{r}) &= \int_{z=0} p_s(x',0) \frac{\partial G_1(\mathbf{r},\mathbf{r}')}{\partial z'} dx' + \int_{z=0} p_i(x',0) \frac{\partial G_1(\mathbf{r},\mathbf{r}')}{\partial z'} dx' \\ &= \int_{z=0} p_s(x',0) \frac{\partial G_1(\mathbf{r},\mathbf{r}')}{\partial z'} dx' - p_r(\mathbf{r}) , \end{aligned} \tag{3.56}$$

which clarifies the relation between p_s and p_{si}.

To develop the scattered field perturbation solution we write the Taylor series for the scattered field about the flat surface, evaluate it on the rough surface, and use operator $\hat{Q}$ to denote the vertical derivative on the mean plane (set $z_0 = 0$ in (3.4)) :

$$p_s(x, \zeta(x)) = \left[1 + \zeta\hat{Q} + \frac{\zeta^2\hat{Q}^2}{2} + \cdots\right] p_s(x,0) \ . \tag{3.57}$$

We write the scattered field as a power series in kh, absorbing the factors of $(kh)^n/n!$ into the terms as in (2.21),

$$p_s(\mathbf{r}) = p_{s0}(\mathbf{r}) + p_{s1}(\mathbf{r}) + p_{s2}(\mathbf{r}) + \cdots \ , \tag{3.58}$$

and substitute this expansion into the Taylor series (3.57) to obtain the following set of boundary conditions for the field:

$$\begin{aligned}
p_{s0}(x,0) &= p_{s0}(x, \zeta(x)) \ , \\
p_{s1}(x,0) &= p_{s1}(x, \zeta(x)) - \zeta\hat{Q}\, p_{s0}(x,0) \ , \\
p_{s2}(x,0) &= p_{s2}(x, \zeta(x)) - \zeta\hat{Q}\, p_{s1}(x,0) - \tfrac{1}{2}\zeta^2\hat{Q}^2 p_{s0}(x,0) \ , \\
&\cdots
\end{aligned} \tag{3.59}$$

Backsubstitution yields to third order:

$$p_{s0}(x,0) = p_{s0}(x, \zeta(x)) = -p_i(x,0) \ , \tag{3.60a}$$

$$p_{s1}(x,0) = p_{s1}(x, \zeta(x)) - \zeta\hat{Q}\, p_{s0}(x,0) \ , \tag{3.60b}$$

$$p_{s2}(x,0) = p_{s2}(x, \zeta(x)) + \left(\zeta\hat{Q}\,\zeta\hat{Q} - \tfrac{1}{2}\zeta^2\hat{Q}^2\right) p_{s0}(x,0) \ , \tag{3.60c}$$

$$p_{s3}(x,0) = p_{s3}(x, \zeta(x)) + \left(-\zeta\hat{Q}\,\zeta\hat{Q}\,\zeta\hat{Q} + \tfrac{1}{2}\zeta\hat{Q}\,\zeta^2\hat{Q}^2 + \tfrac{1}{2}\zeta^2\hat{Q}^2\zeta\hat{Q} - \tfrac{1}{6}\zeta^3\hat{Q}^3\right) p_{s0}(x,0). \tag{3.60d}$$

In contrast to the total field formulation, the Dirichlet boundary condition on the scattered field $p_s(x, \zeta(x)) = -p_i(x, \zeta(x))$ gives nonzero contributions at all orders; in particular, because $p_{s0}(x,0) \neq 0$, even order derivatives ($\hat{Q}^{2n}$) are not zero.

A direct comparison can now be made between solutions; inspection of the series (3.17) for $\hat{Z}^{-1}$ shows that the operations are the same as those in the perturbation method (3.60). However, the operator $\hat{Z}^{-1}$ is applied to the *complete* rough surface field (hence all orders of $\hat{Z}^{-1}$ are applied to the complete rough surface field), whereas the perturbation method requires expanding all rough surface fields in powers of kh and combining orders consistently. One consequence of this difference is that the $\hat{Z}^{-1}$ solution (and also the $\hat{N}$ solution) contains incoherent energy at lowest order where the perturbation solution does not. It turns out that this results in faster convergence of the

operator expansion solution and better matching of the statistical fluctuations for a finite number of surface realizations. (See Sec. 4.6 for numerical examples.)

3.5 Comments on Milder's derivation

Our derivation of the operator expansion solution differs from that of Milder's in two fundamental respects:

A- Milder used a variational differentiation technique to solve for the expansion for $\hat{D}$, obviating the need to find an explicit series for operator $\hat{Z}^{-1}$. However, the backsubstitution method used in Sec. 3.2.4 is a very straightforward approach and provides an alternative path to the same solution. We review Milder's technique in Sec. 3.5.1 for completeness, and because of its elegance in solving for the operator expansion.

B- To avoid making the Rayleigh hypothesis Milder did not apply the (scaled) normal derivative operator $\hat{N}$ to the scattered field directly, but as we'll see in Sec. 3.5.2 his approach is no less restrictive. On the other hand, in transforming an exact integral identity, Milder does show how the usual Rayleigh assumption can be relaxed. Some theoretical questions regarding convergence of the operator expansion series do remain, but numerical results in Chapters 4 and 5 indicate that for many practical problems of interest the operator expansion series converges rapidly to an accurate solution.

We now examine each of these points in turn.

3.5.1 Deriving the expansion for $\hat{D}$ using variational differentiation

Operator $\hat{D}$ is the essential component of the nonlocal operator solution to the scattering problem. In Sec. 3.2 the series for $\hat{D} = \hat{Z}\hat{Q}\hat{Z}^{-1}$ was obtained using the series for $\hat{Z}$ and $\hat{Z}^{-1}$ which are both written in terms of powers of operator $\hat{Q}$ and surface height $\zeta(x)$. Operator $\hat{Z}$ is defined using a Taylor series expansion of an up-going field about the mean plane. In an analogous way, operator $\hat{D}$ can be defined using an "operator Taylor series" about the flat surface solution for the vertical derivative operator.

The operators used in the operator expansion method all map functions of transverse coordinate x to other functions of x. These operators (like functionals) depend on functions of x; each operator $\hat{Z}$, $\hat{Z}^{-1}$, $\hat{D}$, and $\hat{N}$, depends on the particular choice of rough surface height $\zeta(x)$. We can express these properties mathematically

by defining an operator $\hat{A}$ by its action on complex functions of x:

$$\hat{A}_{\xi}[f(x)] = g(x).$$

Operator $\hat{A}$ depends on function $\xi(x)$ (which we later equate with surface height $\zeta(x)$) and operating on $f(x)$ produces $g(x)$. To understand how $\hat{A}$ depends on ξ we examine the notion of variational derivative and the variational Taylor series. The familiar Taylor series of a function $p(x)$ expanded in the neighborhood of the point x_0 is given by

$$p(x_0+\Delta x) = p(x_0) + \Delta x \left[\frac{\partial p(x)}{\partial x}\right]_{x=x_0} + \frac{(\Delta x)^2}{2!}\left[\frac{\partial^2 p(x)}{\partial x^2}\right]_{x=x_0} + \cdots . \quad (3.61)$$

By analogy, and by extending the concept of a functional Taylor series [Ishimaru, Vol. II, App. 20B, 1978], we define the operator Taylor series for $\hat{A}$, where we suppress the argument function $f(x)$ for clarity, and now denote the functional dependence of $\hat{A}$ in braces as $\hat{A}_{\xi} \equiv \hat{A}\{\xi\}$. Here, $\hat{A}$ is expanded for a variational (functional) excursion $\Delta\xi$ about the function ξ_0:

$$\hat{A}\{\xi_0+\Delta\xi\} = \hat{A}\{\xi_0\} + \delta_{\xi}\hat{A}\{\xi_0,\Delta\xi\} + \frac{\delta_{\xi}^2\hat{A}\{\xi_0,\Delta\xi\}}{2!} + \cdots . \quad (3.62)$$

The term $\hat{A}\{\xi_0\}$ is simply the operator $\hat{A}$ evaluated for function ξ_0. The term $\delta_{\xi}\hat{A}\{\xi_0,\Delta\xi\} \equiv \delta\hat{A}$ represents the variational derivative of $\hat{A}$ with respect to function $\xi(x)$ evaluated at $\xi_0(x)$, for an excursion $\Delta\xi(x)$, just as the term $\Delta x\left[\partial p(x)/\partial x\right]_{x=x_0}$ represents the derivative of p with respect to x evaluated at point x_0, for an excursion Δx. (The effect of the "product" with $\Delta\xi$ is implicit in the notation of (3.62).) Functions ξ, ξ_0, and $\Delta\xi$ are all independent functions of x. Here, ξ represents the general functional dependence of operator $\hat{A}$, ξ_0 is the particular choice of ξ about which to expand $\hat{A}$, and $\Delta\xi$ is the variational excursion about ξ_0 leading to the *first variation* $\delta\hat{A}$.

In the scattering problem, we choose to expand the operators about their flat surface expressions which are well known. In other words, we choose $\xi_0(x) = 0$ for all x. Furthermore, we choose the excursion $\Delta\xi$ to be the particular rough surface height profile for the problem: $\Delta\xi = \zeta$. Thus, the surface height enters naturally into the various operator expansions which have the exact flat surface solution as their zeroth order terms. We can then write the operator series for the scattering problem as

$$\hat{A}\{\zeta\} = \hat{A}\{0\} + \delta\hat{A}\{0,\zeta\} + \frac{1}{2}\delta^2\hat{A}\{0,\zeta\} + \cdots \quad (3.63)$$

which we simply denote by the series

$$\hat{A} = \hat{A}_0 + \hat{A}_1 + \hat{A}_2 + \cdots . \quad (3.64)$$

We are particularly interested in the series for operator $\hat{D}$ which we first write in its

general form:

$$\hat{D}\{\xi_0+\Delta\xi\} = \hat{D}\{\xi_0\} + \delta_\xi\hat{D}\{\xi_0,\Delta\xi\} + \frac{\delta_\xi^2\hat{D}\{\xi_0,\Delta\xi\}}{2!} + \cdots . \tag{3.65}$$

We know that the flat surface solution for the vertical derivative operator is $\hat{D}\{\xi_0=0\} = \hat{Q}$, but we need to evaluate the higher order terms in the series by solving for the variation $\delta\hat{D}$ given the representation (3.13), $\hat{D} = \hat{Z}\hat{Q}\hat{Z}^{-1}$. We use the form $\hat{D}\hat{Z} = \hat{Z}\hat{Q}$ for simplicity†. A small change in function ξ induces a variation in $\hat{D}$ and in $\hat{Z}$. For example, we write (3.65) to first order as $\hat{D}\{\xi_0+\Delta\xi\} \approx \hat{D}_0 + \delta\hat{D}$. Recalling that $\hat{Q}$ does not depend on ξ, we find to first order:

$$\begin{aligned}
&(\hat{D}_0+\delta\hat{D})(\hat{Z}_0+\delta\hat{Z}) = (\hat{Z}_0+\delta\hat{Z})\hat{Q} \\
\Leftrightarrow\ &\hat{D}_0\hat{Z}_0+\hat{D}_0\delta\hat{Z}+\delta\hat{D}\,\hat{Z}_0+\delta\hat{D}\,\delta\hat{Z} = \hat{Z}_0\hat{Q}+\delta\hat{Z}\,\hat{Q} \\
\Rightarrow\ &\delta\hat{D}\,\hat{Z}_0 = \delta\hat{Z}\,\hat{Q}-\hat{D}_0\delta\hat{Z}\ ,
\end{aligned} \tag{3.66}$$

recognizing that $\hat{D}_0\hat{Z}_0 = \hat{Z}_0\hat{Q}$, and neglecting the second order term $\delta\hat{D}\,\delta\hat{Z}$. Therefore, the first variation of $\hat{D}$ in terms of a variation in $\hat{Z}$ is given by

$$\delta\hat{D} = \delta\hat{Z}\,\hat{Q}\hat{Z}_0^{-1} - \hat{D}_0\delta\hat{Z}\,\hat{Z}_0^{-1} . \tag{3.67}$$

It is important to recognize that the symbols $\hat{D}_0$ and $\hat{Z}_0^{-1}$ in (3.67) are understood to be the operators $\hat{D}$ and $\hat{Z}^{-1}$ evaluated using function ξ_0.

Equation (3.67) can also be obtained using the usual rules of differentiation, bearing in mind that the operator terms do not commute. In this case, we must remember to defer evaluation of the operators at ξ_0 until *after* all differentiation operations are completed.

$$\begin{aligned}
&\delta(\hat{D}\hat{Z}) = \delta(\hat{Z}\hat{Q}) \\
\Leftrightarrow\ &\delta\hat{D}\,\hat{Z}+\hat{D}\,\delta\hat{Z} = \delta\hat{Z}\,\hat{Q} \\
\Rightarrow\ &\delta\hat{D} = \delta\hat{Z}\,\hat{Q}\hat{Z}_0^{-1} - \hat{D}_0\delta\hat{Z}\,\hat{Z}_0^{-1} .
\end{aligned} \tag{3.68}$$

The variation $\delta\hat{Z}$ is computed using (3.9) written in terms of ξ as follows:

$$\begin{aligned}
\delta\hat{Z} &= \sum_{n=0}^{+\infty}\frac{\delta(\xi^n)}{n!}\hat{Q}^n \\
&= \sum_{n=1}^{+\infty}\frac{n(\delta\xi)\xi^{n-1}}{n!}\hat{Q}^n
\end{aligned}$$

† This form is used to avoid computing $\delta\hat{Z}^{-1}$, but the variation of $\hat{Z}^{-1}$ can easily be obtained by evaluating $\delta(ZZ^{-1}=1)$ to find $\delta\hat{Z}^{-1} = -\hat{Z}^{-1}\delta\hat{Z}\,\hat{Z}^{-1}$.

$$= \delta\xi \left[\sum_{n=1}^{+\infty} \frac{(n-1)\xi^{n-1}}{(n-1)!} \hat{Q}^{n-1} \right] \hat{Q}$$

$$= \delta\xi \hat{Z}\hat{Q} \ . \tag{3.69}$$

By definition, $\delta\xi \equiv \Delta\xi$, and substituting expression (3.69) into (3.67) gives the first variation $\delta\hat{D}$ (having deferred the evaluation of $\hat{D}$ at ξ_0 in anticipation of a second differentiation with respect to ξ to follow below):

$$\begin{aligned} \delta\hat{D} &= (\Delta\xi \hat{Z}\hat{Q}\,)\hat{Q}\hat{Z}^{-1} - \hat{D}\,(\Delta\xi \hat{Z}\hat{Q}\,)\hat{Z}^{-1} \\ &= \Delta\xi \hat{Z}\hat{Q}^2\hat{Z}^{-1} - \hat{D}\,\Delta\xi\hat{D} \\ &= \Delta\xi \hat{D}^2 - \hat{D}\,\Delta\xi\hat{D} \\ &= [\,\Delta\xi, \hat{D}\,]\hat{D}\big|_{\hat{D}=\hat{D}_0} \ , \end{aligned} \tag{3.70}$$

using the commutator to simplify the notation. We continue the process to find the second variation of $\hat{D}$:

$$\begin{aligned} \delta^2\hat{D} &= \delta(\delta\hat{D}\,) = \delta(\Delta\xi\hat{D} - \hat{D}\,\Delta\xi)\hat{D} + [\,\Delta\xi, \hat{D}\,]\,\delta\hat{D} \\ &= \left((\Delta\xi\,\delta\hat{D} - \delta\hat{D}\,\Delta\xi\,) + [\Delta\xi, \hat{D}\,]^2 \right)\hat{D} \\ &= \left([\,\Delta\xi, [\,\Delta\xi, \hat{D}\,]\hat{D}\,] + [\,\Delta\xi, \hat{D}\,]^2 \right)\hat{D}\,\big|_{\hat{D}=\hat{D}_0} \ , \end{aligned} \tag{3.71}$$

where we recall that the excursion $\Delta\xi$ is *independent* of ξ, and thus is not differentiated.

The general series (3.65) for $\hat{D}\,\{\xi_0+\Delta\xi\}$ is now specialized to the scattering problem; setting $\xi_0 = 0$ and $\Delta\xi = \zeta$ the series for $\hat{D}$ is formally written as

$$\begin{aligned} \hat{D}\,\{\zeta\} &= \hat{D}\,\{0\} + \delta\hat{D}\,\{0,\zeta\} + \frac{1}{2}\delta^2\hat{D}\,\{0,\zeta\} + \cdots \\ &= \hat{D}_0 + \hat{D}_1 + \hat{D}_2 + \cdots \ . \end{aligned} \tag{3.72}$$

Evaluating operator $\hat{D}$ at $\xi_0 = 0$ in (3.70) and (3.71) we find to second order:

$$\hat{D}_0 = \hat{Q} \ , \tag{3.73a}$$

$$\hat{D}_1 = [\zeta, \hat{Q}\,]\hat{Q} \ , \tag{3.73b}$$

$$\hat{D}_2 = \frac{1}{2}\left([\zeta, [\zeta, \hat{Q}\,]\hat{Q}\,] + [\zeta, \hat{Q}\,]^2 \right)\hat{Q} \ . \tag{3.73c}$$

Expanding the commutators and with some rearrangement of terms, these expressions can be written as in (3.19) which was obtained by backsubstitution.

The commutator notation is compact, and becomes convenient once some simple algebraic properties are observed. For example, for any constant a, the commutator

$$[\zeta+a,\hat{Q}] = (\zeta+a)\hat{Q} - \hat{Q}(\zeta+a) = \zeta\hat{Q} - \hat{Q}\zeta + a\hat{Q} - \hat{Q}a = [\zeta,\hat{Q}] \qquad (3.74)$$

is independent of a because constants and operators commute. Thus, we see that a shift in the mean value of the surface height produces no change in the expansion for $\hat{D}$. This property of $\hat{D}$ (and hence of $\hat{N}$) is directly related to the fact that the location of the flat plane to which the scattered field is continued (Sec. 3.2.2) is arbitrary, indicating that the solution is predominantly dependent on derivatives of the surface height function (rather than the surface height itself).

The series for $\hat{D}$ is an operator (variational) Taylor series in which the n'th term is simply denoted

$$\hat{D}_n = \frac{1}{n!}\delta^n \hat{D}_0 \ , \qquad (3.75)$$

where the δ^n represents the n'th order variational derivative with respect to the surface height function. Applying δ to a commutator form results in a "product rule" property, illustrated by taking the variational derivative of $\hat{D}_1$ to find $\hat{D}_2$:

$$(2!)\,\hat{D}_2 = \delta^2\hat{D}_0 = \delta(\delta\hat{D}_0) = \delta\hat{D}_1 = \delta([\zeta,\hat{D}_0]\,\hat{D}_0) = [\zeta,\hat{D}_1]\,\hat{D}_0 + [\zeta,\hat{D}_0]\,\hat{D}_1 \ . \qquad (3.76)$$

Application of the product rule to find higher order terms quickly reveals the elegant recursive pattern (3.20), which provides a convenient way of expanding the series for $\hat{D}$ (and hence $\hat{N}$) to any desired order.

3.5.2 The operator expansion method and the Rayleigh hypothesis

In the derivation of the operator expansion in Sec. 3.2 we assumed outright that the (scaled) normal derivative of the scattered field p_s' could be obtained by applying operator $\hat{N}$ to the rough surface values of the scattered field p_s. Operator $\hat{N}$, derived here (and by Milder [1991]) for any field which satisfies the Rayleigh hypothesis, computes the normal derivative of such a field using an upward directed plane wave representation (3.2). In our derivation, that representation is assumed to exist for the scattered field, and moreover, can be obtained by Fourier transforming the values of the scattered field continued to a flat surface (3.3). This continuation is performed using an operator whose power series expansion is explicit (3.17), or which is implicitly included in operator $\hat{D}$ whose power series can be found using the method of variational differentiation used by Milder [1991] and reviewed in the preceding section.

It is well known, however, that the c[illegible]d scattered field has singularities below the rough surface, and when these appe[illegible] the region above the plane $z = \zeta_{min}$

the Rayleigh hypothesis is invalid, and the Rayleigh series (upward plane wave expansion (3.90) for the field scattered from a periodic surface) diverges for points below the height of the singularities. This fact would seem to place a validity limit on the operator expansion method closely linked to the validity of the Rayleigh hypothesis. However, theoretical work in functional analysis by a number of investigators has led to the surprising result that, even when the *infinite* Rayleigh series diverges, it is possible to approximate the boundary field with a *finite* sum of upward directed plane waves to arbitrary accuracy. It has been demonstrated that the up-going plane waves form a complete basis, and as such are able to represent (though not necessarily efficiently) the scattered field in the wells of the surface, where it may contain down-going components. Therefore, methods using upward wave expansions for the surface field are not *fundamentally* limited, but will have different ranges of applicability depending on the technique used to find the plane wave coefficients. We summarize some of these findings at the end of this section, but begin with a historical review of important developments in the study of the validity of the Rayleigh hypothesis, then discuss Milder's contribution to the question, and conclude with a discussion on the completeness of upward waves, accompanied by a few essential equations.

The Rayleigh hypothesis and singularities of the field

The Rayleigh Hypothesis (RH) is named after an approximation introduced by Rayleigh [1907, 1945] in his study of scattering by a sinusoidal surface grating, in which he assumed that the up-going plane wave representation for the scattered field, valid in the region entirely above the rough surface, can be extended all the way down to the surface. (Rayleigh made no attempt to justify his assumption, or to examine its validity.) The difficulty with this approximation has long been appreciated because of the apparent existence of down-going scattered waves inside the wells of the surface [Lippmann, 1953], but its effect was not understood until the validity of the hypothesis was tied to the location of singularities of the continued scattered field in the region below the rough surface.

The first significant step in this regard was taken by Petit and Cadilhac [1966], who were able to show that, for Dirichlet surfaces with a sinusoidal shape, the Rayleigh hypothesis is invalid for surfaces whose maximum slope exceeds the value $s_{max} > 0.448$. This result was obtained by analytic continuation of the boundary condition into the complex plane. Further progress was made by Millar [1969], who showed for periodic surfaces that the Rayleigh plane wave representation (infinite sum of upward directed plane waves) for the scattered field could be analytically continued from above the highest points on the surface into the wells and across the boundary (into the region below the surface) as far as the horizontal plane passing through the

uppermost singularities of the solution. The RH was thus shown to be valid if and only if these singularities lie beneath the lowest points of the surface. This investigation was conducted for arbitrary periodic surfaces whose shape is given by an analytic function; specialized to the sinusoidal profile, all singularities lie below the lowest surface points when the slope is given by $s_{peak} < 0.448$. Observing that the condition for validity is independent of frequency, Millar showed that the (uppermost) singularities can be located by treating the simpler potential problem, that is, the solution of the Laplace equation with the same boundary conditions (which is the Helmholtz equation specialized to the zero frequency case). This he solved using a conformal mapping between the original potential problem posed on a periodic surface and one posed on a closed cylinder. In a series of subsequent papers [Millar, 1971, and references therein] Millar refined and extended the technique to locate singularities of solutions to the Helmholtz equation for arbitrary analytic periodic profiles; when applied to sinusoidal surfaces, the results corroborated earlier findings.

Several investigators found simpler ways of determining the validity of the Rayleigh hypothesis for surface scattering, all based on examining the convergence of the upward plane wave series representation for the scattered field in the region between surface extrema (also called the selvedge region). Hill and Celli [1978] used an asymptotic (steepest descent) technique to examine the behavior of the plane wave coefficients ("diffracted order amplitudes") in the limit of large horizontal wave numbers (highly evanescent modes). A more detailed analysis by van den Berg and Fokkema [1979a, 1979b, 1980] resulted in a condition for the validity of the Rayleigh hypothesis by locating singularities of the scattered field analytically continued below the surface, for periodic gratings, closed cylinders, and for arbitrary nonperiodic analytic surfaces, respectively. They recovered the maximum slope validity condition of Petit and Cadilhac [1966] for sinusoidal surfaces. DeSanto [1981] also used a combination of analytic continuation and asymptotic analysis to examine the convergence of the up-going plane wave expansion inside the wells of an arbitrary periodic profile. Some nonanalytic (discontinuous derivatives) surfaces were examined, and earlier findings of Neviere and Cadilhac [1970] indicating that surfaces with corners pointed upward never allow satisfaction of the RH were confirmed. DeSanto's representation for the surface values of the Dirichlet scattered field differed from other approaches in that he used a plane wave expansion modified (multiplied) by the Kirchhoff approximation for the normal derivative, from which the usual Rayleigh plane wave coefficients for the scattered field could be determined. This approach reportedly "enhances numerical accuracy" [Whitman et al., 1980], but the analysis produced equivalent conditions for the validity of the RH to those of Hill and Celli [1978] and van den Berg and Fokkema [1980].

The singularities of the continued field are generally distributed in a complicated manner; they can be thought of as image sources of the scattered field as discussed in Sec. 3.2.2, although imaging techniques have not commonly been used to locate them. Nevertheless, their location is of considerable importance since the existence of singularities (sources) in the region above $z = \zeta_{min}$ leads to down-going scattered wave components at surface points below these singularities (and divergence of the Rayleigh series for such points), thus invalidating the Rayleigh hypothesis and casting doubt on the continuation procedure implicitly performed in the OE. The operator expansion is tied to the Rayleigh hypothesis question because a representation in up-going waves uniformly valid in the region above the plane passing through the lowest point on the surface underlies all aspects of the method. Fortunately, the impact of this restriction on the accuracy and applicability of the operator expansion method, in which only the leading orders are used, is readily investigated numerically. Numerical results seem to indicate that the series for $\hat{N}$ gives asymptotically convergent solutions for some cases in which the complete series might diverge, presumably when the Rayleigh hypothesis is invalid and when continuation is attempted through a singularity. Indeed, examples are presented in Sec. 4.5 for which the operator expansion solution for leading orders is quite accurate, though clearly beginning to diverge, in some situations for which the Rayleigh hypothesis is not valid.

Applying $\hat{N}$ directly to p_s forces making assumptions on the scattered field which are equivalent to imposing the Rayleigh hypothesis on p_s. However, Milder did not apply $\hat{N}$ directly to p_s in order to avoid making such assumptions. Moreover, Milder sought to demonstrate a general equivalence between an exact solution derived from what is known as the extinction theorem (or the Extended Boundary Condition (EBC) embodied in the integral theorem (2.9)) and the upward wave solution to the scattering problem given by the operator expansion. We find that general equivalence of these solutions is not assured, because convergence of (the complete series for) $\hat{N}$ has not been demonstrated for cases in which the Rayleigh hypothesis is not satisfied. However, a rigorous solution using an upward wave expansion for the scattered field can be obtained (even when the RH fails) because of the existence of a completeness theorem for up-going waves; we rely on the work of others for this result, and summarize their findings below. The identity derived by Milder indicates the sense in which the EBC solution and the rigorous upward wave solution are equivalent, but does not serve to show that the operator expansion method is formally exact. Nevertheless, as we shall show numerically in the following chapters, the operator expansion solution evaluated for leading orders is more widely valid than the Rayleigh hypothesis itself. We now discuss Milder's argument.

Milder's transformation of the extinction theorem

The scattered field above the rough surface is given by (3.29), and in the far field of the surface the scattering amplitude is given by (3.32). We first expand the total field scaled normal derivative $p' = p_i' + p_s'$ and write the scattering amplitude as two components

$$F(\mathbf{k}_s) = \frac{e^{i\pi/4}}{\sqrt{8\pi k}} \left[F_i(\mathbf{k}_s) + F_s(\mathbf{k}_s) \right] , \tag{3.77}$$

where only the integral over the scattered field derivative is unknown:

$$F_s(\mathbf{k}_s) = \int_S \exp[-i\,\mathbf{k}_s \cdot \mathbf{r}']\, p_s'(\mathbf{r}')\, dx' \equiv \int_S g_s(\mathbf{r}')\, p_s'(\mathbf{r}')\, dx' . \tag{3.78}$$

Milder develops an integral identity which allows solving for $F_s(\mathbf{k}_s)$ without using operator $\hat{N}$ directly on $p_s(\mathbf{r}')$. The exact integral identity (2.9) is transformed and used in (3.78) as follows.

We recall the scattered field form of the extinction theorem (2.9):

$$\int_S G_0(\mathbf{r}'', \mathbf{r}') \frac{\partial p_s(\mathbf{r}')}{\partial n'} ds' = \int_S p_s(\mathbf{r}') \frac{\partial G_0(\mathbf{r}'', \mathbf{r}')}{\partial n'} ds' , \quad \mathbf{r}' \in S, \ \mathbf{r}'' \in V_2 . \tag{3.79}$$

In order to transform this identity into one over functions of surface points $\mathbf{r}' \in S$ alone, (3.79) is multiplied by a function $u(x)$ specified on a plane $z = z_0 < \zeta_{\min}$ entirely below S, and integrated over all points on that plane:

$$\int_{z_0} dx''\, u(x'') \int_S ds'\, G_0(\mathbf{r}'', \mathbf{r}') \frac{\partial p_s(\mathbf{r}')}{\partial n'} = \int_{z_0} dx''\, u(x'') \int_S ds'\, p_s(\mathbf{r}') \frac{\partial G_0(\mathbf{r}'', \mathbf{r}')}{\partial n'} . \tag{3.80}$$

The function $u(x)$ is continuous and differentiable in x but otherwise arbitrary; we interchange orders of integration to obtain:

$$\int_S ds' \frac{\partial p_s(\mathbf{r}')}{\partial n'} \int_{z_0} dx''\, u(x'')\, G_0(\mathbf{r}'', \mathbf{r}') = \int_S ds'\, p_s(\mathbf{r}') \int_{z_0} dx''\, u(x'') \frac{\partial G_0(\mathbf{r}'', \mathbf{r}')}{\partial n'} . \tag{3.81}$$

The integral

$$\int_{z_0} dx''\, u(x'')\, G_0(\mathbf{r}'', \mathbf{r}') \equiv U(\mathbf{r}') , \quad \mathbf{r}' \in S , \tag{3.82}$$

results in a function $U(x, \zeta(x))$,[†] which can be interpreted as the rough surface values of a field $U(\mathbf{r})$ whose sources are a distribution $u(x)$ of monopoles on the plane $z = z_0$. The second integral over the $z = z_0$ plane in (3.81) simply gives the normal derivative of field $U(\mathbf{r})$, evaluated on the rough surface S:

$$\int_{z_0} dx'' \, u(x'') \frac{\partial G_0(\mathbf{r}'', \mathbf{r}')}{\partial n'} = \frac{\partial}{\partial n'} \int_{z_0} dx'' \, u(x'') \, G_0(\mathbf{r}'', \mathbf{r}') = \frac{\partial U(\mathbf{r}')}{\partial n'} \, . \tag{3.83}$$

Note that the field $U(\mathbf{r})$ is generated by a monopole layer alone; there are no dipole sources of U on the plane $z = z_0$. The usual Helmholtz integral for a field $U(\mathbf{r})$ in terms of surface values of U and its normal derivative is

$$U(\mathbf{r}) = \int_S \left[U(\mathbf{r}') \frac{\partial G_0(\mathbf{r}, \mathbf{r}')}{\partial n'} - G_0(\mathbf{r}, \mathbf{r}') \frac{\partial U(\mathbf{r}')}{\partial n'} \right] ds' \, , \tag{3.84}$$

and contains two terms; however, evaluating (3.84) on $z = z_0$ and comparing with (3.82), we see that on the plane $z = z_0$, $U(x, z_0) = 0$ and $\partial U(x, z_0)/\partial z = -u(x)$.

The exact integral identity (3.79) has thus been transformed without approximation into

$$\int_S U(\mathbf{r}') \frac{\partial p_s(\mathbf{r}')}{\partial n'} ds' = \int_S p_s(\mathbf{r}') \frac{\partial U(\mathbf{r}')}{\partial n'} ds' \, . \tag{3.85}$$

It is important to recognize that the function $U(x, \zeta(x))$ is not arbitrary; it is obtained from $U(\mathbf{r})$ which is by construction a purely up-going field for all points above the plane $z = z_0$. In fact, field $U(\mathbf{r})$ is guaranteed to satisfy the Rayleigh hypothesis since all of its sources are below the lowest point of the rough surface. Given the arbitrary source function $u(x, z_0)$, it is straightforward to compute the normal derivative $\partial U(\mathbf{r})/\partial n$; however, because $U(\mathbf{r})$ is purely up-going in the entire region between surface extrema, the normal derivative can be computed using $\hat{N}$ without knowledge of u, and without direct knowledge of the field $U(\mathbf{r})$ in the neighborhood of S. Thus, we have the following exact integral identity

$$\int_S U(\mathbf{r}') \, p_s'(\mathbf{r}') \, dx' = \int_S p_s(\mathbf{r}') \, \hat{N} \, [U(\mathbf{r}')] \, dx' \, . \tag{3.86}$$

Milder used this integral relation by replacing $U(\mathbf{r}')$ in (3.86) with the plane wave $g_s(\mathbf{r}') = \exp[-i \mathbf{k}_s \cdot \mathbf{r}']$ from (3.78) to find:

[†] Milder denoted function U by the symbol F which we reserve for the scattering amplitude.

$$F_s(\mathbf{k}_s) = \int_S g_s(\mathbf{r}')\, p_s'(\mathbf{r}')\, dx' = \int_S p_s(\mathbf{r}')\, \hat{N}\, [g_s(\mathbf{r}')]\, dx' \ . \tag{3.87}$$

However, we find that this equality is not rigorous, as discussed below.

Shortcomings of Milder's argument

In the steps above, the scattering problem appears to have been solved exactly without placing any restrictions on the scattered field. However, given the restrictions imposed on U, substituting g_s for U in (3.86) requires further justification. The function $g_s(\mathbf{r}') = \exp[-i\,\mathbf{k}_s \cdot \mathbf{r}']$ is the expression of a single down-going plane wave (recall that $k_{sz} \geq 0$) on the rough surface S, and therefore applying $\hat{N}$ to g_s is not fundamentally different from applying $\hat{N}$ to p_s. Indeed, this problem is equivalent to the scattering problem itself, in which the surface values of a down-going incident wave are to be interpreted as the surface values of an up-going (scattered) field whose normal derivative is sought on the rough surface. Operator $\hat{N}$ can no more be used to operate on $g_s(\mathbf{r}') = \exp[-i\,\mathbf{k}_s \cdot \mathbf{r}']$ than on $p_s(\mathbf{r}') = -\exp[+i\,\mathbf{k}_i \cdot \mathbf{r}']$ without apparently imposing the Rayleigh hypothesis on the problem, because both functions are arbitrary single *down-going* plane waves evaluated on the rough surface. While $\hat{N}$ is constructed to produce the correct (scaled) normal derivative of function U, it is not guaranteed to converge for a function which violates the Rayleigh hypothesis; and if p_s violates the RH, then so will g_s. Thus it seems that little is gained by trying to avoid applying $\hat{N}$ directly to the surface values of the scattered field; in fact, we can approximate F_s by evaluating either of the two forms:

$$F_s(\mathbf{k}_s) \approx \int_S g_s(\mathbf{r}')\, \hat{N}\, [p_s(\mathbf{r}')]\, dx' = \int_S p_s(\mathbf{r}')\, \hat{N}\, [g_s(\mathbf{r}')]\, dx' \ . \tag{3.88}$$

Equality of the two integrals is a consequence of the left-right symmetry of $\hat{N}$, which is itself a consequence of the fact that the operator expansion preserves reciprocity of the scattering solution [Milder, 1991].

It should be mentioned that the difficulty arising above can be foreseen by a simpler procedure than the one involving $u(x)$. Another way of removing the $\mathbf{r}''$ dependence in (3.79) is to examine the EBC integral theorem in the far field of the surface; after all, the desired scattering amplitude is also a far-field quantity. Taking the limit $|\mathbf{r}''| \gg |\mathbf{r}'|$ for points $\mathbf{r}''$ far *below* the surface, we obtain after canceling common factors

$$\int_S \exp[-i\,\mathbf{k}_t \cdot \mathbf{r}']\, p_s'(\mathbf{r}')\, dx' = \int_S (-\hat{\mathbf{n}}' \cdot i\,\mathbf{k}_t) \exp[-i\,\mathbf{k}_t \cdot \mathbf{r}']\, p_s(\mathbf{r}')\, dx' \ , \tag{3.89}$$

where the wavevector $\mathbf{k}_t = k_{tx}\hat{\mathbf{x}} + k_{tz}\hat{\mathbf{z}}$ has $k_{tz} \leq 0$ for propagating waves. After factoring out (and canceling) the predominant downward component $\exp[ikr'']/\sqrt{r''}$, the residual phase $\exp[-i\,\mathbf{k}_t\cdot\mathbf{r}']$ corresponds to the surface values of an *up-going* plane wave, which is not the desired down-going plane wave $g_s(\mathbf{r}')$ appearing in (3.78). The similarity between (3.89) and (3.85) is evident because the field U in (3.85) is a combination of up-going plane waves; neither of these equations is directly applicable to (3.78).

Though $\hat{N}$ does not appear in the earlier equation (3.85), substituting $g_s(\mathbf{r}')$ for $U(\mathbf{r}')$ there would also require justification. Equation (3.85) can be quickly verified[†] by applying Green's theorem (2.4) to two fields which satisfy the homogeneous Helmholtz equation in volume V_1 (such as p_s and U); however, a down-going plane wave has sources above surface S, and it is not appropriate to make the above substitution without a guarantee that a representation for $g_s(\mathbf{r}')$ exists in terms of homogeneous solutions, such as up-going plane waves. However, if the theorem of completeness of up-going waves is invoked, then substitution of $g_s(\mathbf{r}') = \exp[-i\,\mathbf{k}_s\cdot\mathbf{r}']$ for $U(\mathbf{r}')$ in (3.85) follows naturally because a representation for the boundary values of the down-going plane wave $g_s(\mathbf{r}')$ in terms of up-going waves does exist (and can be found by the least-squares method described below) *even if the Rayleigh hypothesis does not hold.* Because of the up-going wave restrictions placed on U, the normal derivative in the right hand side of (3.85) is understood to operate on the up-going representation for $U(\mathbf{r}') = g_s(\mathbf{r}')$, which we note *is not* the same as evaluating $\hat{\mathbf{n}}'\cdot\nabla(\exp[-i\,\mathbf{k}_s\cdot\mathbf{r}'])$. Milder's transformation of the EBC shows the sense in which the upward wave solution and the exact solution are related: only integrals over the surface fields are required to be equal; the surface fields themselves are not required to match at every point. As we shall see below, the theorem of completeness of up-going waves also indicates that the true boundary field can only be matched in an integrated least-square sense by the upward wave expansion.

In summary, the completeness of up-going waves justifies substituting $g_s(\mathbf{r}')$ for $U(\mathbf{r}')$ in (3.85) with the understanding that the normal derivative is to operate on the correct upward wave representation for $g_s(\mathbf{r}')$; in that case, (3.85) written for $g_s(\mathbf{r}')$ is exact. Operator $\hat{N}$ may be used to perform the normal derivative operation as in (3.87) and (3.88), but because there is no reason to assume that the upward wave representation used by $\hat{N}$ is the same as the one obtained by the rigorous least-squares method[††], the result is always going to be approximate when the Rayleigh hypothesis is not valid.

[†] Milder [1991, Eq. (56)] made a similar observation in his discussion on reciprocity and self-adjointness of the normal derivative operator under integration over surface values of homogeneous fields.

[††] No detailed comparison between the plane wave coefficients $\tilde{p}_s(k_x)$ internally used by $\hat{N}$ and those obtained by the rigorous least-squares method has been performed, but the operator expan-

($\hat{N}$ is rigorous when the RH is valid.) Nevertheless, numerical studies in Chapters 4 and 5 indicate that the far-field solutions obtained using leading orders of $\hat{N}$ are accurate well beyond the limits of validity of the Rayleigh hypothesis, and are far more rapidly computed than by any rigorous method. We now conclude this section with a brief discussion on the completeness theorem for upward directed plane waves and on the associated least-squares method of finding the series expansion.

Completeness of up-going waves — Least-squares convergence

We present equations in this section for periodic surfaces following most of the literature on this topic. We assume, following Millar [1973], that the extension of the theory to nonperiodic surfaces presents no fundamental problems. By analogy to (3.2), we write the field scattered from a surface of period $\Lambda = 2\pi/K$ as an infinite sum of upward directed plane waves (Rayleigh series), only a finite number of which are propagating waves, the remainder being evanescent:

$$p_s(\mathbf{r}) = \sum_{n=-\infty}^{+\infty} A_n \, \phi_n(\mathbf{r}) \ , \tag{3.90}$$

where the A_n are the complex plane wave coefficients, and the ϕ_n are the upward directed plane waves

$$\phi_n(\mathbf{r}) = \exp[i\alpha_n x + i\beta_n z] \ , \quad n = 0, \pm 1, \pm 2, \cdots \tag{3.91}$$

with $\alpha_n = k_{ix} + nK$, $\beta_n = +\sqrt{k^2 - \alpha_n^2}$, and $\mathrm{Im}(\beta_n) > 0$ for upward decaying evanescent waves. The series representation (3.90) is always convergent everywhere above the highest point on the surface $z = \zeta_{max}$; indeed, the evanescent waves decay rapidly away from the surface. The Rayleigh hypothesis consists of assuming that the same representation is also valid in the wells of the surface, all the way down onto the surface itself. From the work of Millar and others described earlier, we know that the Rayleigh series (3.90) is convergent for all surface points when the Rayleigh hypothesis is valid, that is when all singularities of the solution (3.90) lie below the lowest points of the surface. In this case, the unknown coefficients A_n can be found by a number of methods, the simplest of which sets up a system of linear equations by truncating the series to $J = 2M + 1$ terms and using the boundary condition to specify the surface field at J points in one surface period interval. This is called the Point Matching Method (PMM). The Fourier Series Method (FSM) consists of a similar procedure, but is implemented in Fourier space; since the true boundary field and the truncated series field evaluated on the boundary are both periodic functions, their Fourier series coefficients can be equated.

---

sion coefficients are not obtained by least-squares optimization.

When the Rayleigh hypothesis is not valid, the series (3.90) does not converge for surface points below the height of the singularities of the continued field, and the success of such numerical solutions is no longer assured. However, the desired upward wave coefficients A_n can still be approximated to arbitrary accuracy, providing an arbitrarily accurate representation of the scattered field at any point above the surface, including in the wells. This assertion rests on a theorem of completeness of the set of upward directed plane waves $\{\phi_n\}$ which guarantees that there exists a linear combination of $J = 2M + 1$ elements of the set that converges on the boundary to the values prescribed by the boundary condition as $M \to \infty$, *in the mean-square sense* [Millar, 1973]. To explain the sense of this convergence, we define a sequence of truncated expansions for the scattered field, with the M'th term in the sequence written as

$$p_s^{(M)}(\mathbf{r}) = \sum_{n=-M}^{+M} B_n^{(M)} \phi_n(\mathbf{r}) \ . \tag{3.92}$$

The plane wave coefficients $B_n^{(M)}$ for each series representation of $p_s^{(M)}(\mathbf{r})$ in the sequence are chosen in such a way as to minimize the integrated squared error in matching the boundary condition with the truncated expansion (3.92). For those optimal coefficients

$$\int_{\Lambda} \left| p_s(\mathbf{r}') - p_s^{(M)}(\mathbf{r}') \right|^2 ds' = \varepsilon_{\min}^{(M)} \ . \tag{3.93}$$

In general, the coefficients $B_n^{(M)}$ which minimize $\varepsilon^{(M)}$ depend on the value of M.

It can be shown [Millar, 1973] that the sequence of truncated series expansions (3.92) evaluated on the rough surface converges to the true surface field $p_s(\mathbf{r}')$ as $M \to \infty$ in the mean-square sense, that is,

$$\lim_{M \to \infty} \varepsilon_{\min}^{(M)} = 0 \ . \tag{3.94}$$

The least-squares truncated series representation for the surface field $p_s^{(M)}(\mathbf{r}')$ does not, in general, converge *uniformly* to the true boundary field with respect to position along the surface because (3.94) is an integral result. However, because the scattered field above the surface is given by an integration over surface values, (3.94) implies that *the sequence of solutions* $p_s^{(M)}(\mathbf{r})$ *evaluated for points* $\mathbf{r}$ *in closed regions above the surface* S *converges uniformly to the exact scattered field* [Millar, 1973]. We must bear in mind that these properties hold even when the Rayleigh hypothesis is not valid, that is, when the infinite series (3.90) diverges for some points on (or above) the surface. Millar [1973] points out that a similar completeness theorem exists for the normal derivative of elements of the set $\{\phi_n\}$, and therefore the Neumann problem can be treated in the same way.

The completeness theorem is a powerful theoretical result, but it also leads to a rigorous numerical solution of the scattering problem in which the coefficients $B_n^{(M)}$ are found by least-squares to minimize the error in satisfying the boundary condition. It turns out that these coefficients converge to the Rayleigh coefficients

$$\lim_{M \to \infty} B_n^{(M)} = A_n \ , \tag{3.95}$$

even when the Rayleigh coefficients A_n do not lead to a convergent series expansion on the surface, and therefore cannot be found directly from (3.90) and the boundary condition. A least-squares method was first proposed by Meecham [1956b] to solve the problem of scattering from an echelette grating (he called it a variational method). Apparently Meecham was unaware that the solution obtained in this way converged uniformly to the exact field above the surface. The completeness theorem was first developed for surface scattering by Yasuura [1971], and Yasuura and Ikuno [1971], who also compared the PMM with a numerical method based on the least-squares approach which they called Improved Point Matching Method (IPMM) [Ikuno and Yasuura, 1973]. They show that the IPMM reduces to the PMM when the number of surface points I used in evaluating the boundary condition is equal to the number of basis functions $J = 2M + 1$. When $I \geq 2J$ they found that the IPMM has much broader validity than the PMM.

The completeness theorem was revisited and discussed with great clarity by Millar [1973], and reviewed by Petit [1980], Cadilhac [1980], and also by Hugonin, Petit, and Cadilhac [1981] who evaluated the performance of several numerical methods based on upward wave expansions: PMM, FSM, and LSAM (Least-Squares Approximation Method, which is very similar to the IPMM). Much of our discussion is guided by the insightful presentation of Hugonin et al. [1981], as well as by the work of Millar [1973]. Recently, Berman and Perkins [1990] have extended the least-squares approach, which they implemented both in coordinate space ("least-squares point matching") and Fourier space ("Rayleigh-Fourier method"), to fluid-fluid and fluid-solid interfaces with good results.

The coefficients $B_n^{(M)}$ generally depend on the value of M because the plane waves evaluated on the rough surface do not form an orthogonal set of basis functions. It is possible to form a new orthogonal basis whose elements are linear combinations of the original plane waves; this approach was taken by Meecham [1956b], and further discussed by Millar [1973]. The $B_n^{(M)}$ coefficients thus obtained do not depend on the number of basis functions used in the expansion, but there is no guarantee that such an expansion is as efficient (requires as few terms) as the series (3.92). Of course, any upward wave representation is not likely to be as efficient as a modal representation (an expansion in up- and down-going waves) for a field containing significant amounts of down-going energy, such as a field whose singularities are well above the lowest

surface points.

Summary

The validity of the operator expansion method seems to be constrained by the validity of the Rayleigh hypothesis because $\hat{N}$ is rigorously defined for fields which satisfy the RH — convergence of $\hat{N}$ is not assured when it is applied to the surface values of a field which does not satisfy the RH. However, the fact that $\hat{N}$ relies on an upward wave representation to represent the surface values of the scattered field is not in and of itself a fundamental limitation. Theoretical work in functional analysis demonstrates that upward directed plane waves form a complete basis, that is, a truncated expansion in up-going waves can represent the boundary values of the scattered field to arbitrary accuracy, in the mean-square sense. Such a representation can approximate the scattered field *at any point above the surface* to arbitrary accuracy, even in the wells of the surface when the Rayleigh hypothesis is invalid. A subtle but important distinction between the least-squares sequence approach and the (infinite) Rayleigh series methods is that the sequence of truncated least-squares series (3.92) converges to the exact scattered field (off the boundary) even when the infinite series (3.90) diverges. The difficulty with methods based on upward wave representations lies in finding the series coefficients for scattering problems over a wide range of scattering regimes.

The completeness theorem leads to a rigorous numerical method based on minimizing the error in matching the boundary condition. The operator expansion method uses a completely different method of estimating the plane wave coefficients; in fact, the coefficients are never explicitly evaluated. Though direct comparisons between the rigorously derived coefficients and those used internally by $\hat{N}$ have not been made, there is no theoretical reason to assume that these coefficients are the same, and hence no theoretical reason to believe that the operator expansion method is rigorous when the RH is not valid. However, numerical tests have shown that when the operator expansion solution converges rapidly for leading orders it always converges to the exact result without regard to the validity of the RH, and that in other cases where the series begins to diverge lower order solutions still provide useful results, indicating that the OE series is occasionally asymptotically convergent. Indeed, calculations for sinusoidal surfaces [Milder, 1991] [Milder and Sharp, 1992], and for randomly rough surfaces discussed in the next two chapters, show that many scattering problems which are well beyond the validity limits of the Rayleigh hypothesis are treated accurately by leading order operator expansion solutions.

CHAPTER 4

Accuracy of the Operator Expansion for Surfaces with a Gaussian Spectrum

4.1 Introduction to Chapter 4

The operator expansion method presented in Chapter 3 is an approximate numerical technique for computing scattering from rough surfaces. The solution is cast as a systematic series; in practice, only a few leading terms in the series are used. Milder [1991] presented the expansions for the first three terms (through second order) and we have derived one more term (third order, $\hat{N}_3$). Computing the third order solution presents additional numerical difficulties associated with the increase in complexity of the terms, and may not be practical for some applications. Nevertheless, the third order term is very helpful in studying the convergence of the OE, and also in examining the behavior of the short forms of the OE solution.

The issues discussed in the previous chapter regarding the link between the formal validity of the solution and the validity of the Rayleigh hypothesis are of academic interest, but have little bearing on the usefulness of the OE method. The latter is dependent on the accuracy of the leading order solutions, and Milder showed [Milder, 1991], [Milder and Sharp, 1992], through comparisons with exact solutions for sinusoidal and triangular sawtooth surfaces, that the method performs well. Furthermore, Milder showed that the OE reduces to the small perturbation result for surfaces with sufficiently small values of kh, and to the Kirchhoff approximation result for surfaces with oscillations long compared to the incident wavelength. This important reduction property indicates that the operator expansion method should be valid over a wide range of scattering parameters because the two classical methods are valid in complementary, but not necessarily overlapping, scattering regimes. Indeed, any method that can accurately compute scattering from multiscale surfaces must possess capabilities of both classical approximations. Before applying the OE to multiscale surfaces (Chapter 5) we first examine the performance of the operator expansion solution for scattering from single-scale randomly rough surfaces; in this chapter we study scattering from surfaces with a Gaussian spectrum.

The accuracy of the OE for scattering from randomly rough surfaces can be assessed through comparison to exact results, obtained by solving an integral equation. Here, we use a numerical solution of the first kind equation (2.14), or of an equivalent second kind equation, following Thorsos [1988]. The implementation of the solutions is identical to that presented by Thorsos, and will not be repeated here. However, a few

remarks on the equivalence of these numerical solutions are in order. Though the first and second kind equations are formally equivalent, agreement between the two *numerical* solutions to some prescribed accuracy will only be reached when the surface sampling density and incident field tapering are sufficient. With increasingly dense sampling, each numerical integral equation solution converges to the same result, but the implementation of the first kind solution often requires more surface partition density than second kind solution to reach the same level of accuracy. This difference is only typically noticeable when scattering strength comparisons are made to within 0.2 dB, or when total energy accuracy is required beyond 1%, for sampling densities of 5 points per wavelength. The OE is very accurate for some cases; thus, the second kind solution is used on those occasions when precise comparisons are desired for scattering from slightly rough surfaces sampled at less than 8 points per wavelength. At higher densities, or for rougher surfaces, the first kind solution is more efficient. (The second kind solution takes almost twice as long to compute as the first kind solution for a given number of points.) We do not distinguish between first or second kind solutions in the examples presented below because, before comparing with approximate solutions, the accuracy of the integral equation solution is determined by convergence studies and through comparison between first and second kind solutions. The error remaining in the integral equation solution is always verified to be much less than the error of an approximate solution whose accuracy is being evaluated.

The validity of the classical methods is well known for surfaces with a Gaussian spectrum [Thorsos, 1988] and [Thorsos and Jackson, 1989]; hence, it is natural to study the operator expansion method in this context. Section 4.2 presents a brief review of these results. In Sec. 4.3 we examine the accuracy and convergence rate of the standard OE series in the surface roughness regime for which the classical methods apply. Then, for somewhat rougher surfaces, we compare the alternative forms of the OE solution (the odd, even, and consistent series) to the standard series solution, and to the integral equation solution, in Sec. 4.4. In Sec. 4.5, the various OE solutions are examined as surface roughness is increased to well beyond the domains in which the classical approximations are valid. We observe that the OE method fails gradually, remaining accurate for some cases in which enhanced backscattering is observed. Finally, in Sec. 4.6 the mean plane solution obtained using just the $\hat{Z}^{-1}$ operator (Sec. 3.4) is investigated numerically, and compared to the classical solutions.

4.2 Accuracy of the classical approximations

The roughness regime depends on the incident and scattering angles θ_i and θ_s, and on the surface roughness in comparison to the acoustic wavelength. For surfaces with Gaussian statistics (see Sec. 6.1) and with a Gaussian spectrum given by

$$W(K) = \frac{lh^2}{2\sqrt{\pi}} e^{-K^2l^2/4}, \tag{4.1}$$

where K is the spatial wavenumber, two parameters define the surface roughness: the surface correlation length l, and the root-mean-square (rms) surface height h. The rms surface slope is given by $s = \sqrt{2}\, h/l$. An example of a single realization of a 1-D surface generated using the Gaussian spectrum (4.1) is presented in Fig. 4.1, along with the scattering geometry for the 2-D scattering problem.

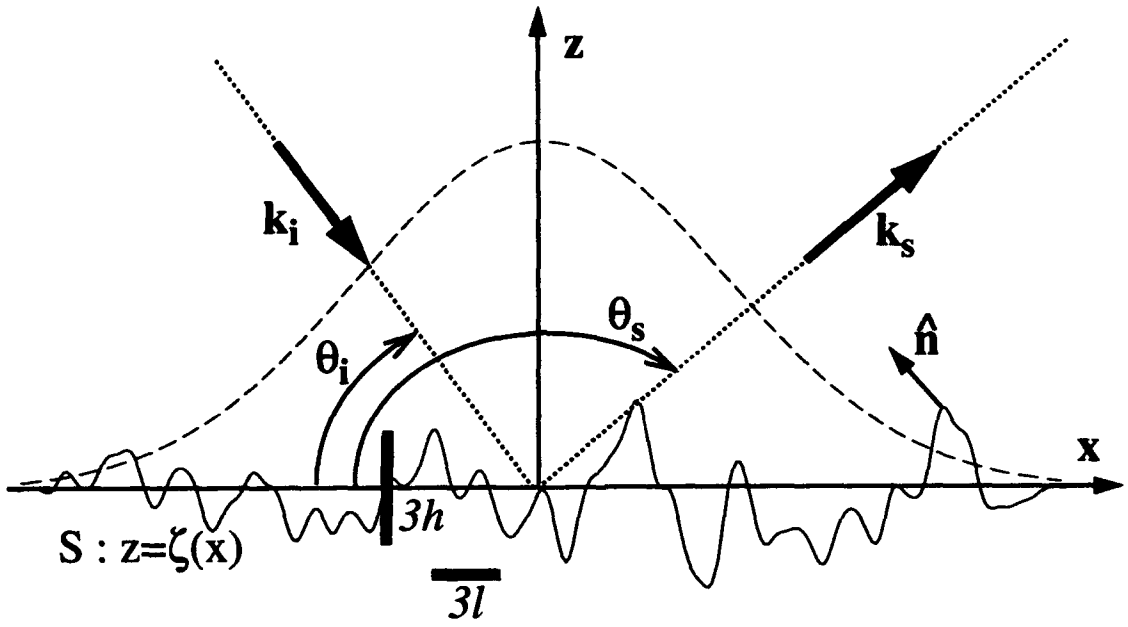

Figure 4.1 : Geometry for scattering from a 1-D rough surface. The surface height function $z = \zeta(x)$ is a realization of a Gaussian stochastic process, with a Gaussian spectrum given by (4.1). Bars of length three times the rms height $3h$ and correlation length $3l$ are indicated next to the surface for comparison; for illustrative purposes the ratio h/l is many times larger than that used in the calculations. The surface has been tapered at the ends using a 10% cosine taper. The incident field amplitude is typically made very small near the ends of the surface; the amplitude of the tapered plane wave incident field (evaluated on the mean plane) for $L/g = 4$ is plotted with a dashed line.

The *kl*-*kh* plane represents the parameter space for the (Gaussian spectrum) surface roughness. The locations of the numerical examples in this plane are shown in Fig. 4.2, along with the 1 dB validity contours for "bistatic" scattering for the two classical methods, as presented by Thorsos [1988], and Thorsos and Jackson [1989]. We define bistatic to mean "for all scattering angles, given a single incident angle". The solid curves mark the locus in the *kl*-*kh* plane for which the maximum error in the incoherent scattering strength computed by the perturbation method (at *any* scattering angle, for 45° incidence) is 1 dB. The Kirchhoff approximation validity region is not as sharply defined [Thorsos and Jackson, 1991], and scattering angles near grazing are

excluded from consideration [Thorsos, 1988]. With the same accuracy criterion of 1 dB, we use representative examples to illustrate that the operator expansion solution is accurate and rapidly convergent in both regions of *kl*-*kh* space for which the classical methods are valid, in the "gap" between those regions, and for parts of the *kl*-*kh* plane well above those regions.

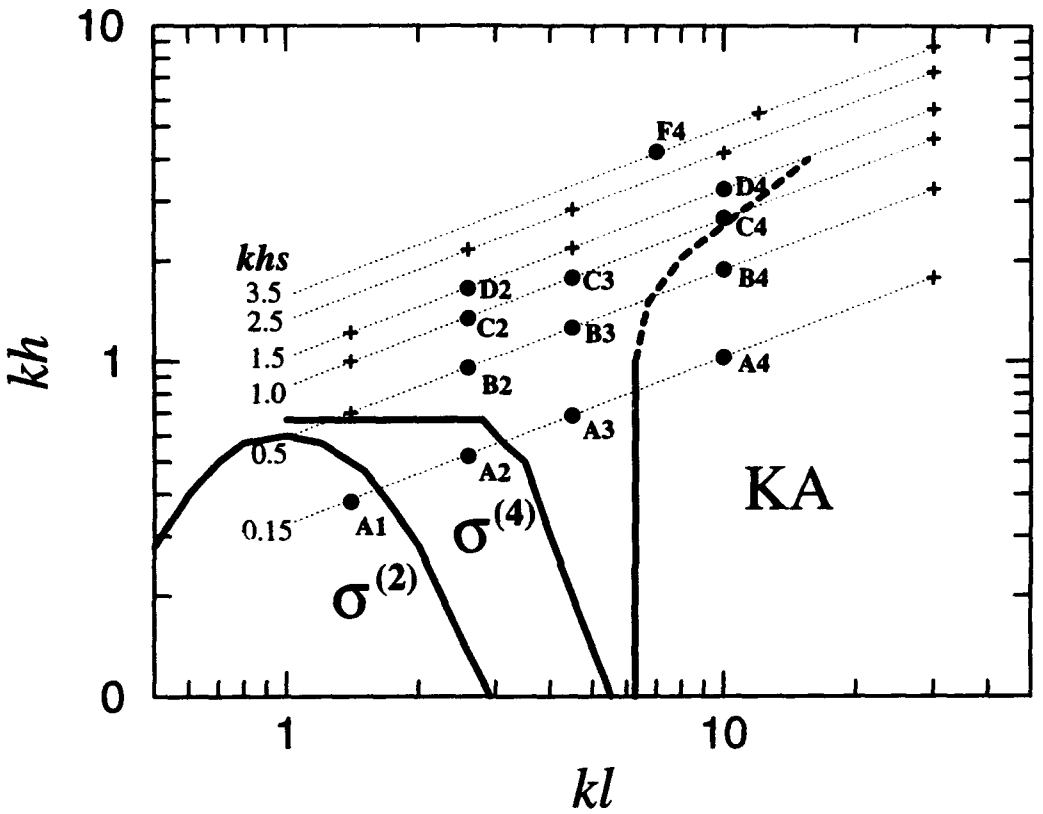

Figure 4.2 : The *kl*-*kh* plane, roughness parameter space for surfaces with Gaussian spectra. Located in the *kl*-*kh* plane are the numerical examples (on contours of the slope-height parameter *khs*), the validity regions for lowest order perturbation theory ($\sigma^{(2)}$), next order perturbation theory ($\sigma^{(4)}$), and the Kirchhoff approximation (KA). Examples discussed in the dissertation are marked by dots and labeled; other cases examined in detail but not discussed are marked by plus signs.

The examples are chosen on contours of constant slope-height parameter *khs* in order to study convergence and accuracy of the OE as a function of *khs*. Milder proposed the "Fresnel number" *khs* [Milder, 1991] as an indicator of the applicability of the OE, and found that the method performed well for scattering from 1-D [Milder 1991] and 2-D [Milder and Sharp, 1992] sinusoidal surfaces when $khs \lesssim 1.0$. We find that the single parameter *khs* is a useful general indicator of the roughness regime for the OE applied to randomly rough surfaces, but that the convergence properties and the accuracy at any given order also depend on the angular distance from the specular direction, and on the surface roughness parameters *kl* and *kh* (or alternatively, on the

rms slope and normalized height) separately. We now turn to a detailed examination of the examples; the essential results of this study are summarized in Chapter 9.

4.3 Accuracy of the OE for moderately rough surfaces

The examples in this section illustrate three fundamental numerical results using Gaussian spectrum surfaces of moderate roughness. First, through comparison with the numerically exact solution of an integral equation, the accuracy of the operator expansion solution is found to be very good over a wide range of incident and scattering angles. Second, the convergence of the operator expansion solution is rapid and monotonic over a wide range of scattering parameters. Therefore, for this roughness regime ($khs \approx 0.15$), the accuracy of the solution at any order can be inferred from the size of the next term in the series. Third, the operator expansion solution taken to first order in the surface field is comparable in accuracy to the classical methods in their respective validity regions, but it is also accurate for some examples in which neither classical method is accurate. These results will be useful in applying the operator expansion method to scattering from 2-D surfaces for which exact solutions are still extremely costly.

Case A1 -- $\sigma^{(2)}$ validity region

Case A1 was selected from the region within which lowest order perturbation theory, with cross section computed to order $(kh)^2$ and denoted $\sigma^{(2)}$, is accurate. Bistatic scattering strength curves computed over an ensemble of 50 surface realizations appear in Fig. 4.3, where $kl = 1.4$, $kh = 0.38$ and the incident grazing angle $\theta_i = 45°$. The rms surface slope $s = 0.384 \equiv \tan\gamma$, so that the rms slope angle $\gamma = 21°$. We first examine the scattering strength curves computed by the operator expansion method with orders defined by (2.22) and (3.40), and presented in Fig. 4.3a; we denote these solutions as OE_0, OE_1, and OE_2 at zeroth, first, and second orders, respectively. (This notation is not the same as that used by Milder [1991], in which the short series solutions (3.41) and (3.42) were designated by OE_n. Milder did not present results for the standard series solution.) In this region, convergence is so rapid that curves OE_1 and OE_2 are essentially identical when plotted on the scale shown. To better distinguish between orders the difference between each scattering strength curve and the second order curve OE_2 is presented in Fig. 4.3b. Note that the error in OE_0 is nearly completely corrected by the first order contribution, most significantly near grazing.

The convergence of the operator expansion series can be further appreciated by examining the contributions to the cross section from each individual order in the series

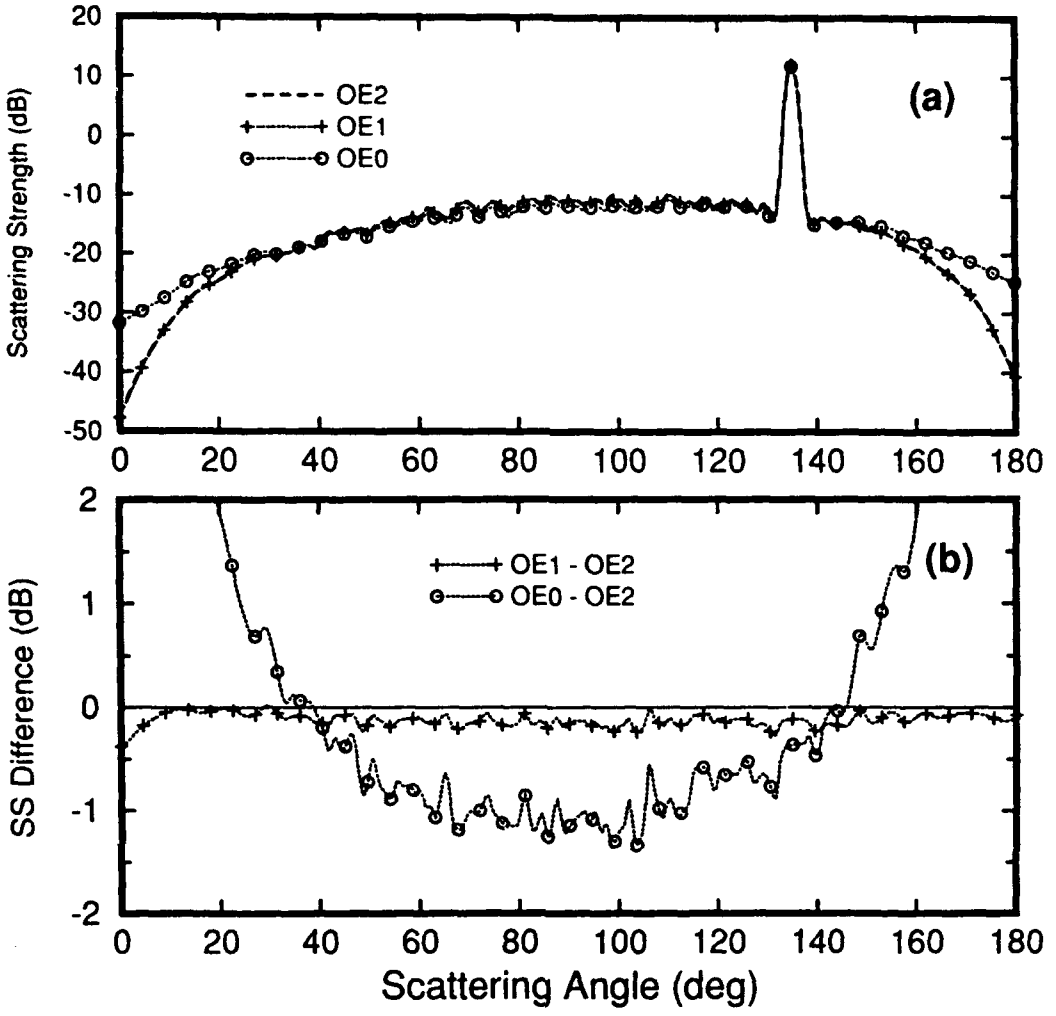

Figure 4.3 : Scattering results averaged over 50 surfaces using parameters for case A1, $kl = 1.4$, $kh = 0.38$, and $\theta_i = 45°$. The scattering strengths for the zeroth, first, and second orders of the Operator Expansion solution (OE_0, OE_1, and OE_2) indicate rapid convergence (a), the character of which is better illustrated by the difference between scattering strength curves (b).

for the surface field. These contributions are obtained by computing the $|F_n|^2$ terms in (2.22); denoted by ON_n, the curves for the first four terms are presented in Fig. 4.3c. (Note that $ON_0 \equiv OE_0$.) The relative amplitudes of the far field contributions from each order fall off monotonically over the full range of scattering angles. Experience with the operator expansion solution for surfaces with moderate roughness shows that a rapid rate of decay of the series terms with increasing order is always associated with convergence to the exact solution, except very near grazing as described below. Note that the ON_n series as defined does not consider the phases of the contributions at each order, and as such provides a conservative estimate of the convergence of the solution. Some cancellation between orders does occur (near grazing between zeroth and first orders, for example) and results in faster decay of the solution than is apparent from the ON_n series. Because the operator expansion is very accurate, the differences between the

OE scattering strength curves and the integral equation (IE) scattering strength are presented; these difference curves represent the error in the complete solution at each order. Furthermore, by using the IE solution as the reference curve, the fluctuations resulting from a finite number of surface realizations are reduced.

Differences between the OE_1 and OE_2 solutions and the integral equation solution appear in Fig. 4.3d and are typical for the $\sigma^{(2)}$ region. The first order solution is very accurate over all scattering angles except for a very narrow range a few degrees from grazing; the errors for all orders above zeroth reach about 1.5 dB at 0° and 180°. A discrepancy with the integral equation solution very near grazing is commonly observed in all cases, but the detailed structure of that difference depends on numerical parameters such as the surface length. As expected from the rapid convergence, the second order solution OE_2 differs little from OE_1 but is clearly more accurate on average.

In the regime where lowest order perturbation theory is accurate, it is of interest to compare the operator expansion and perturbation theory solutions in terms of their relative accuracy and rate of convergence. In Fig. 4.3e the difference between the integral equation solution and the Monte Carlo solution for the incoherent scattering strengths $\sigma^{(2)}$ and $\sigma^{(4)}$, computed to order $(kh)^2$ and $(kh)^4$, respectively, is presented. Even though formally averaged solutions exist for perturbation theory, it is more straightforward to compare a Monte Carlo perturbation solution to the integral equation solution because of the inevitable statistical fluctuations in the scattering curves. Nevertheless, the error in matching the fluctuations with the lowest order solution $\sigma^{(2)}$ is readily apparent, though the mean error is clearly less than 1 dB (the error threshold used to determine accuracy). Accurately matching both the mean and the fluctuations requires higher order contributions in perturbation theory as indicated by the $\sigma^{(4)}$ curve, whereas even the first order operator expansion solution matches the integral equation fluctuations very well; see Fig. 4.3d.

Two additional remarks are in order when comparing perturbation theory curves to the operator expansion or integral equation results. First, the Monte Carlo implementation of Rayleigh-Rice perturbation theory has an explicit $\sin^2\theta_s$ dependence for the cross section[†] at low grazing angles that is correct for the *infinite* length Dirichlet surface but incorrect for finite length surfaces. This behavior makes comparisons with finite length calculations difficult in the region very near grazing. Near grazing, the angular dependence of the infinite surface cross section creates a very steep falloff in

[†] This explicit dependence comes from expressing the solution in terms of a field on the mean plane, resulting in a factor of k_z in the scattering amplitude (3.50).

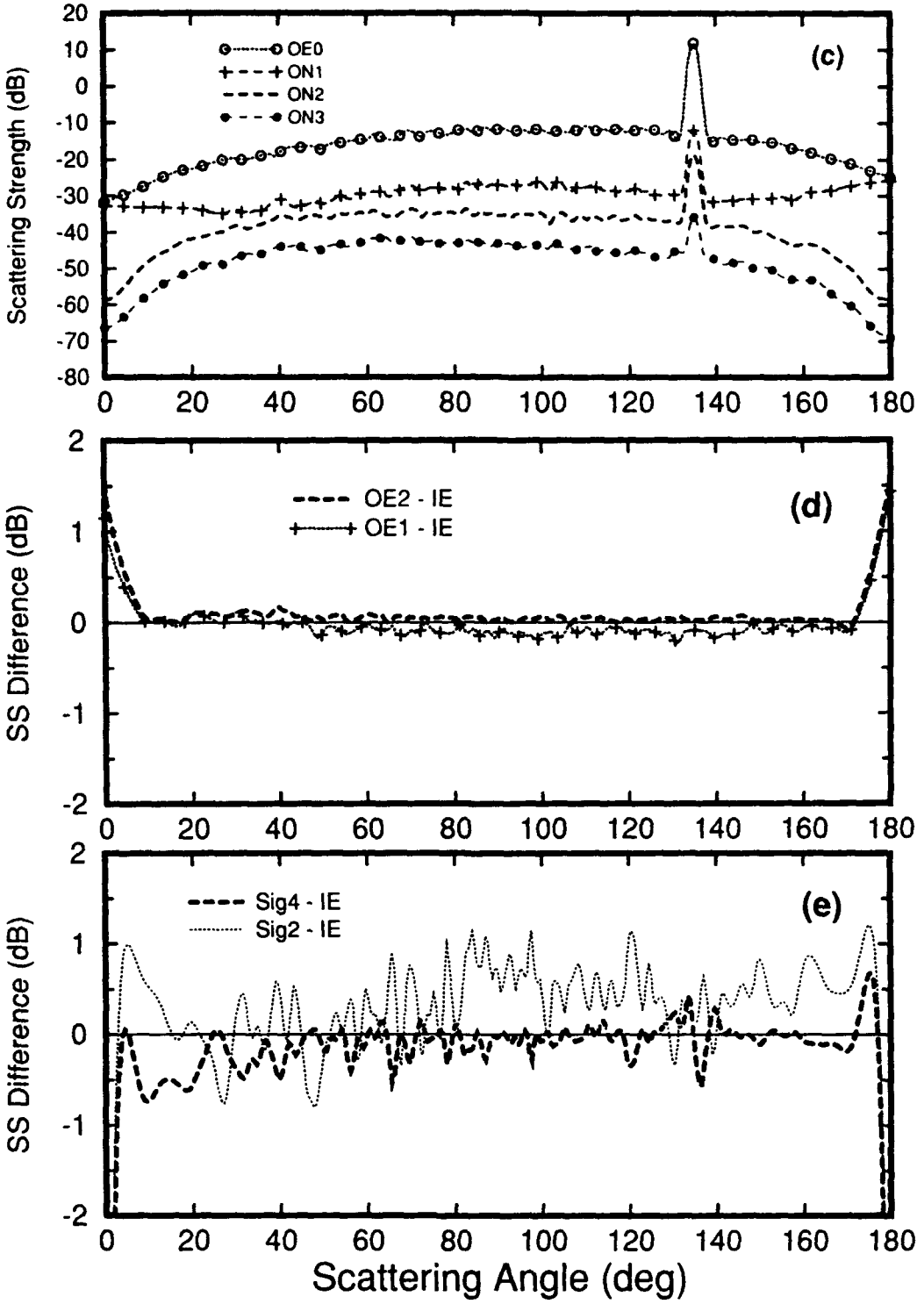

Figure 4.3 (continued) : The scattering strength contributions from the individual terms in the surface field series (denoted ON_n) can be used to examine convergence of the solution over all scattering angles (c). Differences between the OE solutions and the exact Integral Equation (IE) solution indicate that the operator expansion has converged to the right answer, except perhaps very near grazing (d). When lowest order perturbation theory ($\sigma^{(2)}$) is accurate, $\sigma^{(2)}$ and $\sigma^{(4)}$ (e) do not match the IE fluctuations as well and are less accurate on average than OE_1 and OE_2 (d).

scattering strength curves which is blurred by limited angular resolution in the other Monte Carlo methods. The integral equation result is the exact solution of the *finite* surface problem, and is used to assess the accuracy of the operator expansion solution over all scattering angles. Second, the cross section generally computed here by the integral equation and operator expansion methods is the total scattering cross section, meaning that both the coherent and incoherent parts of the scattered field are included. The total field is computed because it is of interest to evaluate the accuracy of the operator expansion estimate of the coherent field (and hence energy conservation) as well. The perturbation solution used in this work contains only the incoherent solution, and comparisons to other solutions near the specular direction are only performed for the incoherent component.

Case A2 -- $\sigma^{(4)}$ validity region

Case A2 is located in a scattering regime that requires terms of order $(kh)^4$ in the perturbation series for the scattering cross section in order to maintain 1 dB accuracy over the bistatic scattering range; the surface parameters are $kl = 2.6$ and $kh = 0.52$, resulting in rms surface slope $s = 0.283$. The operator expansion solution for the surface field contributions to the scattering strength again decays monotonically with increasing order over all scattering angles (Fig. 4.4a). The first order contribution ON_1 is well below OE_0 except near grazing where it once again proves very effective at correcting the significant error in OE_0. Indeed, Figs. 4.4b and 4.4c show through comparison with the integral equation that the accuracy of first order ion OE_1 is very good over most of the range of scattering angles but worsens in the back direction, finally underpredicting the scattering strength by 1 dB at 10°. The second order solution OE_2 is accurate over all angles, except within 5° of grazing; again, this inaccuracy close to grazing can be reduced by zero-padding the computational surface. In this example, the averaged perturbation result $\sigma^{(4)}$ has a deviation from the integral equation solution that is about 0.5 dB over most scattering angles, but $\sigma^{(4)}$ also fluctuates much more than the operator expansion solutions; see Fig. 4.4c. In this region, the first order operator expansion solution OE_1 is more accurate than $\sigma^{(4)}$ except near grazing in the back direction. The second order solution OE_2 is consistently better than $\sigma^{(4)}$, indicating that the broader range of applicability of the operator expansion solution results in faster convergence than that of the perturbation solution in the region where the latter is valid.

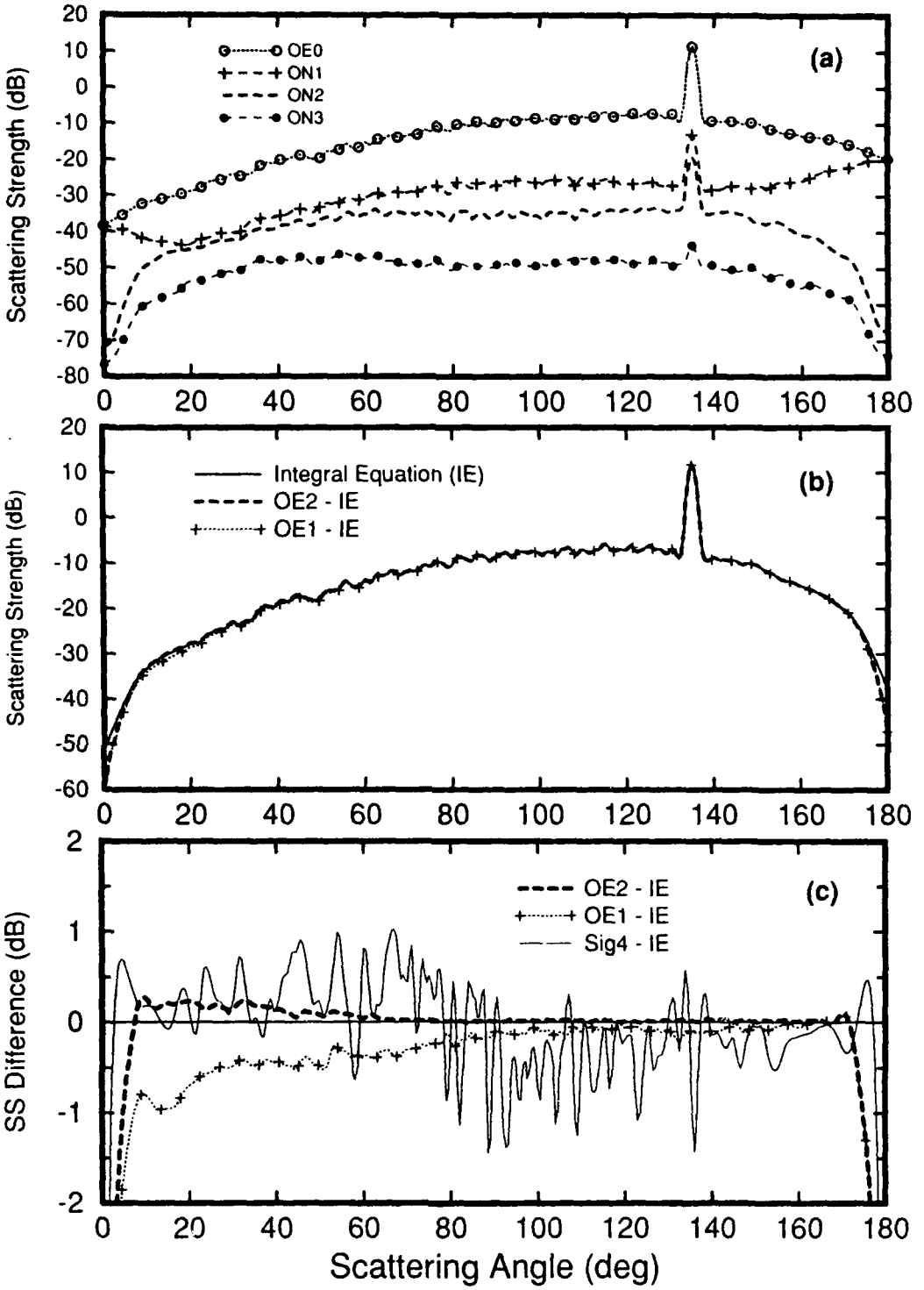

Figure 4.4 : Scattering results for case A2, located in the $\sigma^{(4)}$ validity region, with $kl = 2.6$, $kh = 0.52$, and $\theta_i = 45°$. Decay of the first four terms in the OE solution is rapid and monotonic over all scattering angles (a), leading to an accurate solution (b), better shown using scattering strength differences (c); the fluctuations in the IE solution are much better matched by the OE than by the perturbation solution $\sigma^{(4)}$, although the latter is accurate on average (avg error <1 dB).

Case A3 -- Gap region

Case A3 is selected from the "gap" region where neither $\sigma^{(4)}$ nor the Kirchhoff approximation are deemed accurate over the full range of scattering angles; the surface parameters for this case are $kl = 4.5$ and $kh = 0.69$, resulting in rms surface slope $s = 0.217$. A study of the cross section contributions in Fig. 4.5a from each order in the surface field indicates that the operator expansion solution converges rapidly over most of the scattering range, but that the decay of the terms with increasing order is not everywhere monotonic. Because the second order term is greater than the first order term in the region between 5° and 20°, we recognize that an accurate solution in that angular region will likely require computing the surface field to at least second order. Nevertheless, we suspect that second order should suffice, since the third order contribution lies well below the contributions from lesser orders. This example suggests that the effect of the second order contribution is better studied when compared with the complete first order solution; indeed, Fig. 4.5b illustrates that the amplitude of contribution ON_2 is everywhere less than solution OE_1, indicating that this new series falls off monotonically over the full range of scattering angles. This latter series (OE_1, ON_2, ON_3, ...) is a more appropriate indicator of convergence since first order (OE_1) is the lowest order for which the operator expansion solution exhibits the essentially correct behavior near grazing, having included an important cancellation beween zeroth and first order terms.

The differences between the operator expansion curves and the integral equation result appear in Fig. 4.5c. As expected from the convergence study, OE_1 is less accurate in the back direction but OE_2 is indeed very accurate over the whole range of scattering angles. The third order solution OE_3 is slightly less accurate than OE_2 for a small range of angles in the backscattering region (also apparent in Fig. 4.6c for case A4), and this behavior is the first hint of nonmonotonic convergence observed in other cases with greater surface roughness (see Sec. 4.5.1). From Fig. 4.5d, we observe that OE_1 is more accurate for this example than either $\sigma^{(4)}$ or the Kirchhoff approximation result (KA), where the formally averaged solutions for the two theories, [Thorsos, 1988] and [Thorsos and Jackson, 1989], are presented to assist in distinguishing the curves.

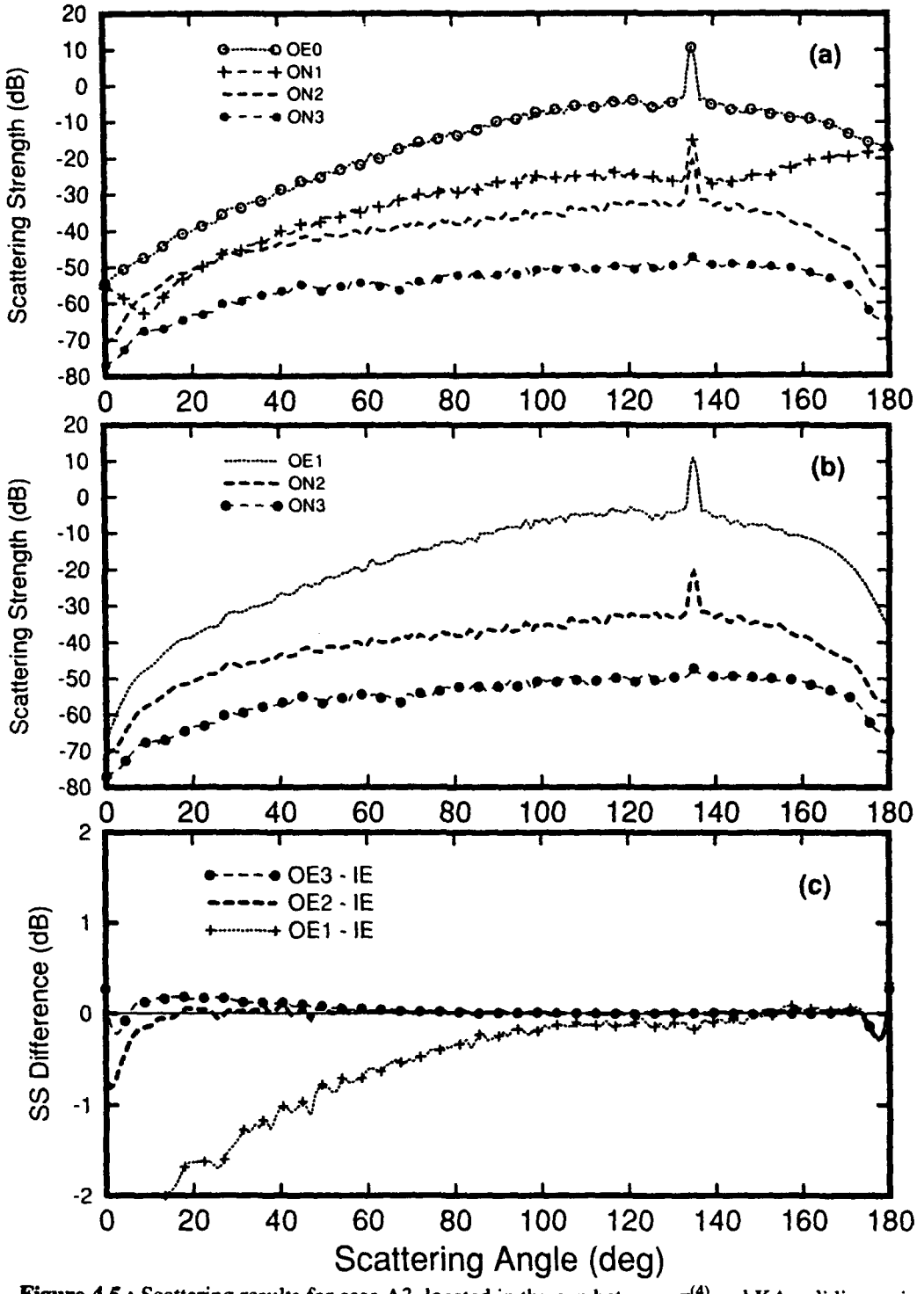

Figure 4.5 : Scattering results for case A3, located in the gap between $\sigma^{(4)}$ and KA validity regions, with $kl = 4.5$, $kh = 0.69$, and $\theta_i = 45°$. Decay of the first four terms in the ON series is not monotonic over all scattering angles (a). OE_1 is the lowest order solution that has essentially correct behavior near grazing; beginning with OE_1, the terms decay monotonically with increasing order over all scattering angles (b). The OE errors are obtained using the differences between the OE scattering strength curves and the integral equation (IE) curve (c).

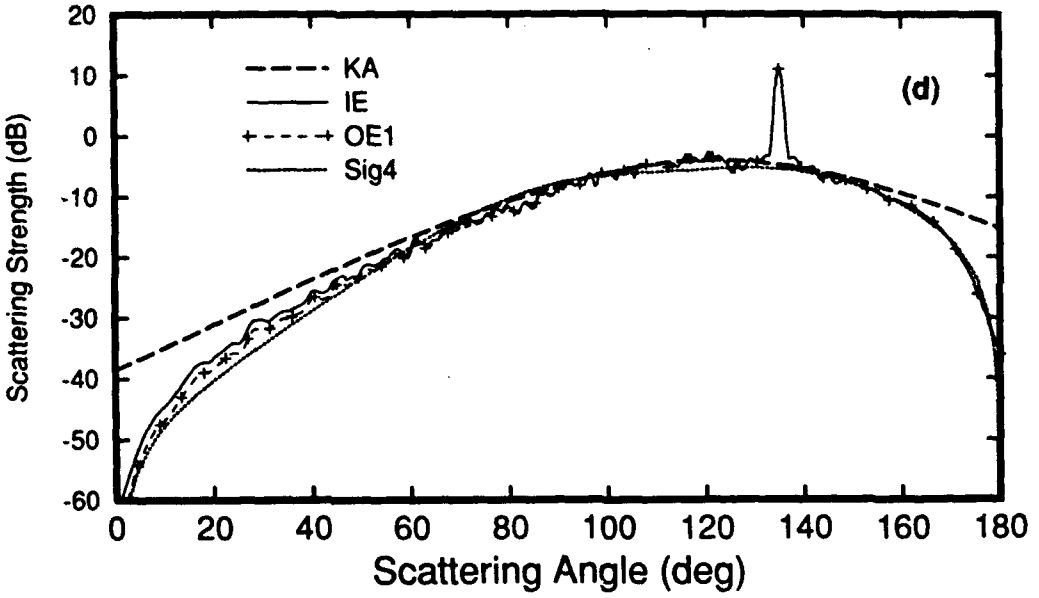

Figure 4.5 (continued) : In the gap between validity regions of the classical approximations, OE_1 is more accurate than either KA or $\sigma^{(4)}$ (d).

Case A4 -- Kirchhoff approximation validity region

Case A4 is selected from inside the Kirchhoff approximation validity region; the surface parameters for this case are $kl = 10.0$ and $kh = 1.03$, resulting in rms surface slope $s = 0.146$. In this regime the surfaces are smooth enough that most of the energy is scattered into the angular region near the specular direction; numerical studies over the full range of scattering angles are difficult to conduct since the dynamic range of the scattering strength is very large. Very low levels in the back direction require a more stringent choice of numerical parameters such as the incident wave taper width, surface length, surface partition density, or surface end taper; these parameters can be relaxed for computations emphasizing forward scattering. A study of the relative contributions from each order of the operator expansion solution in Fig. 4.6a reveals that the convergence of the operator expansion solution has a distinctly different character near specular than in the backscattering region. In the forward scattering direction the ON_n terms fall off at about 15 dB per order (beginning with OE_0 which is not shown), whereas the curves gather near grazing in the back direction. When the third order contribution lies well below the lower order curves, we infer that the solution should be accurate at second order; otherwise third (and possibly higher) order contributions become important. The comparison with the integral equation result in Fig. 4.6c indicates that the second order solution is indeed accurate down to the 10° grazing angle range, where the error reaches 1 dB. Note that the dynamic range of the solution is much greater than that required for most cases of practical interest; the scattering strength near 10° is about 80 dB below the level near the specular direction. In a manner reminiscent of the

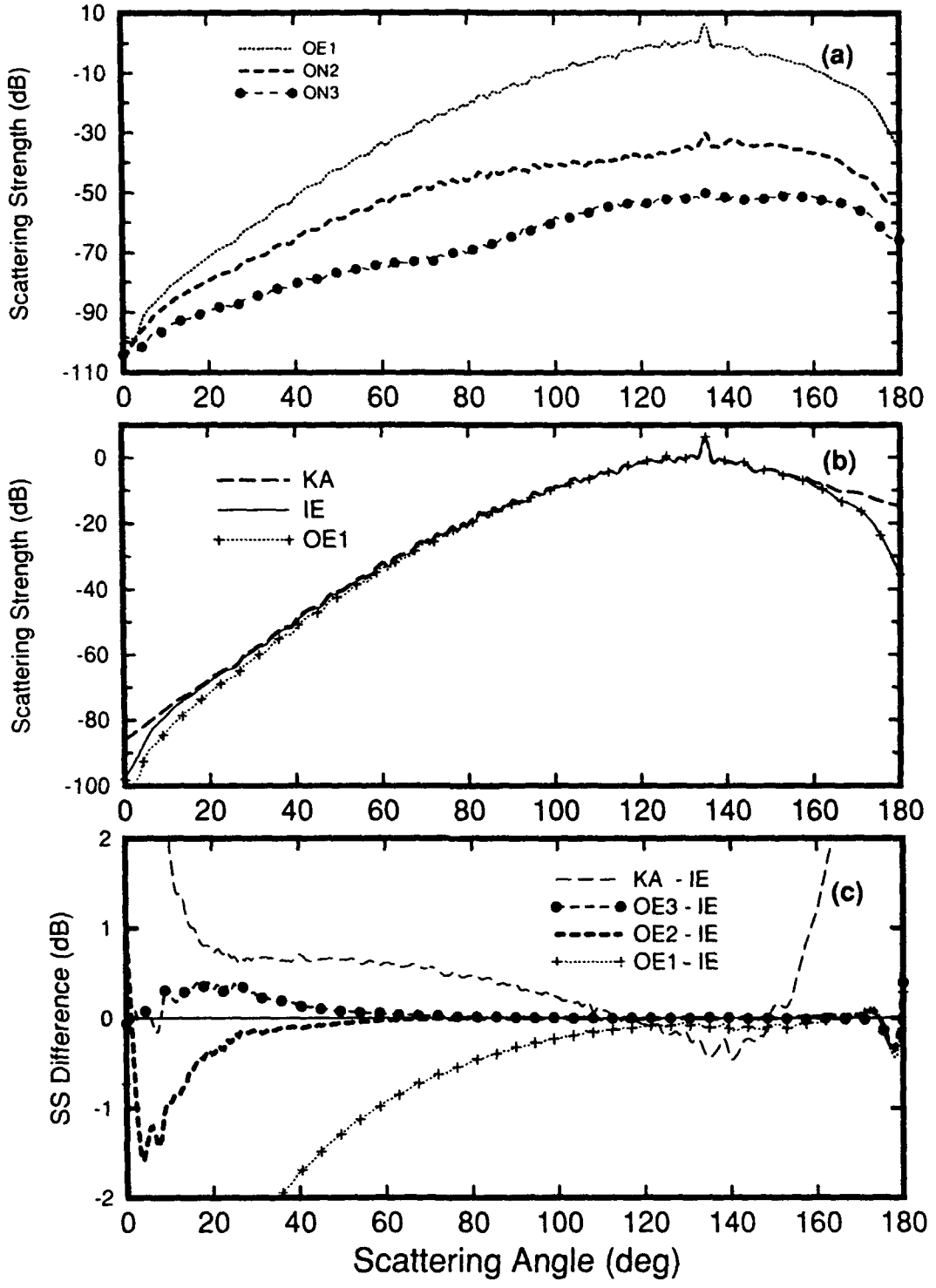

Figure 4.6 : Scattering results for case A4, located in the KA validity region, with kl = 10.0, kh = 1.03, and $\theta_i = 45°$. Decay of the ON_n series terms is rapid over a broad region around the specular direction (135°) but slows appreciably in the far backscatter region (a). Convergence to the exact integral equation solution (IE) is likewise rapid around the specular direction but less so in the back direction (b). The Kirchhoff approximation (KA) is not accurate in a scattering angle region within 20° from grazing, but the OE solution converges to nearly the exact result (c).

behavior of the perturbation theory solution [Thorsos and Jackson, 1989, Fig. 12], the lower order operator expansion solutions converge toward the exact curve from below, whereas the Kirchhoff approximation overpredicts the scattering strength by about 0.5 dB over the entire backscattering region, except near grazing where it is never accurate. The first order solution (OE_1) is not quite as accurate as the Kirchhoff approximation solution (KA) in the backscattering region, but OE_1 is more accurate than KA in the forward scattering region, in particular within 20° of grazing; see Figs. 4.6b and 4.6c.

Other angles of incidence

The cases examined above indicate that the operator expansion converges to the correct solution very rapidly in an angular scattering region broadly centered on the specular direction. The higher order corrections are predominantly important away from specular, especially near grazing in the back direction. Milder [1991] indicated that the operator expansion method is reciprocal at each order, and we have verified this property analytically through third order. We would then expect that the method would perform best for *incident* angles far from grazing, and perhaps converge more slowly for incident angles closer to grazing. We have observed this general trend in other calculations in which the incident angle θ_i was varied, using the surface parameters of the four examples studied above. The effect is best seen in cases with $kl \geq 4$ where convergence in the backscattering region is slower. For case A3 and $\theta_i = 90°$, the decay rate of the contributions in Fig. 4.7a is clearly very rapid; indeed, an improvement in convergence over the $\theta_i = 45°$ calculation is observed by comparing the error curves for OE_1 and OE_2 in Fig. 4.7b with the error curves for OE_2 and OE_3, respectively, in Fig. 4.5c.

Now turning to a lower angle of incidence, $\theta_i = 20°$, we see in Fig. 4.7c that convergence is much slower in the backscattering direction than in the forward direction; nevertheless, for this region of *kl*-*kh* parameter space the operator expansion solution is accurate at second order; see Fig. 4.7d. This general behavior is observed so long as the scattering angle is not too close to grazing. For angles of incidence in the range $20° \lesssim \theta_i \lesssim 90°$, the scattering strength inaccuracies observed very near grazing (for example in cases A1 and A2 for $\theta_s \lesssim 5°$) were essentially independent of θ_i. These errors likely depend on distant multiple scattering effects inadequately addressed by the operator expansion method.

In examining the character of the bistatic scattering error curves as a function of incident angle θ_i we observe that the accuracy and convergence of the operator expansion is tied to the angular separation from the specular direction: $|180° - \theta_i - \theta_s|$. Changing θ_i by tens of degrees essentially shifts the error curves by the same amount.

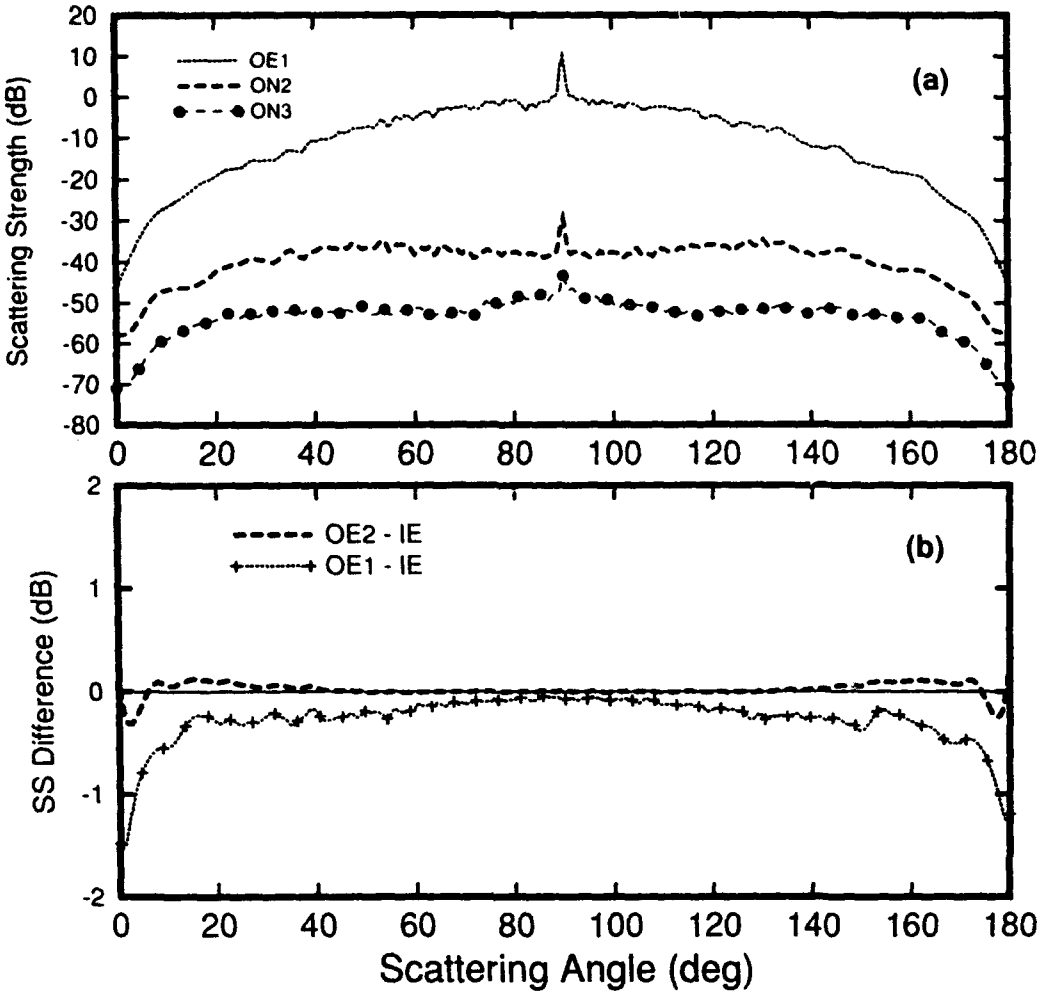

Figure 4.7 : Convergence and accuracy of the operator expansion solution as a function of angle of incidence for the surface parameters of case A3 (Fig. 4.5). $\theta_i = 90°$ (a) and (b). The OE_3 curve lies on the zero line in (b) and is omitted for clarity.

For example, in case A3 the error curve for OE_1 reaches 1 dB near $\theta_s = 90° - \theta_i$ for all values of θ_i, as long as $\theta_s \geq 5°$.

4.4 Evaluation of alternative series forms

4.4.1 Introduction

In defining the cross section in Sec. 2.3, we distinguished between a consistent expansion (2.23) in orders of the surface field expansion parameter and an inconsistent expansion (2.22) which used all terms available in a truncated series solution for the surface field. Earlier in this chapter, we studied the accuracy of this latter form since it is simpler to implement and was used by Milder [1991]. In Sec. 4.4.2 we examine the

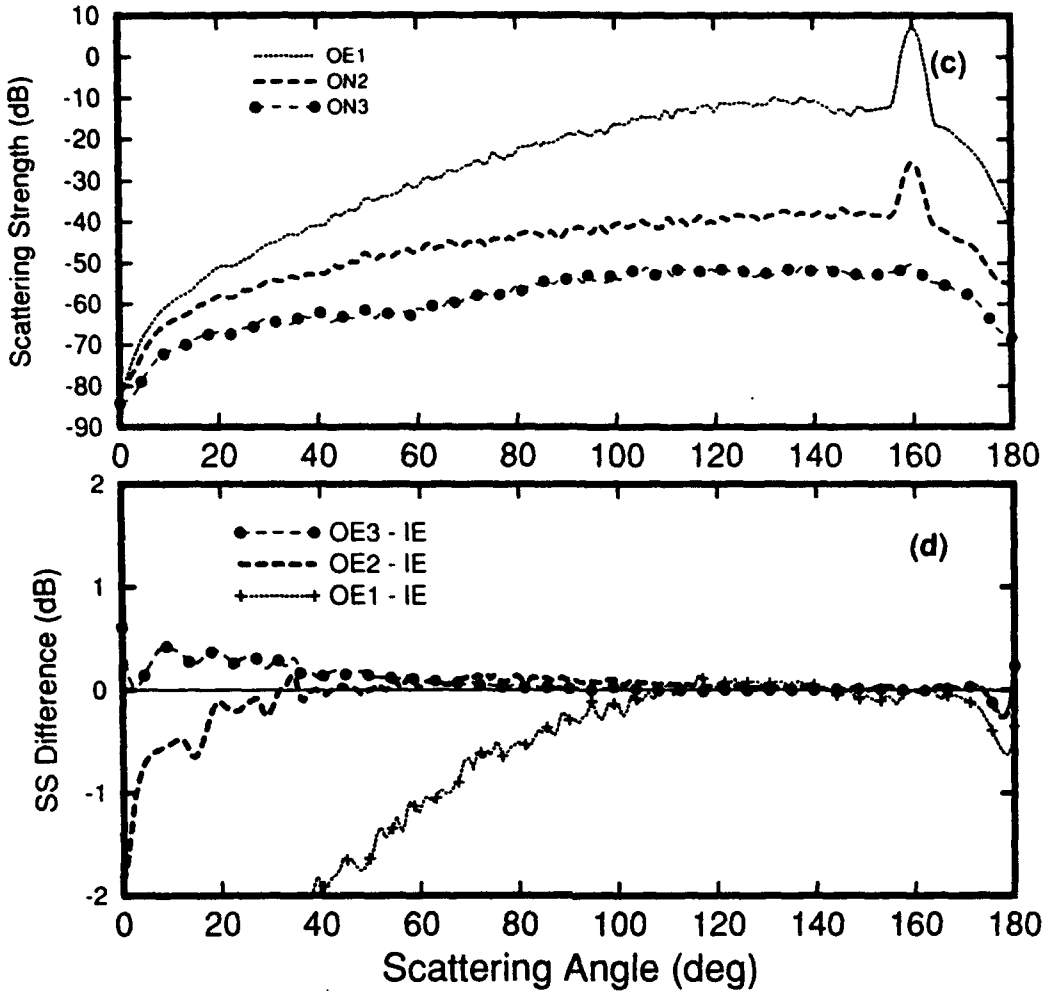

Figure 4.7 (continued) : Convergence and accuracy of the operator expansion solution as a function of angle of incidence for the surface parameters of case A3 (Fig. 4.5). $\theta_i = 20°$ (c) and (d).

consequence of that choice, and show that consistency occasionally improves the OE solution, but is not required to maintain accuracy. Indeed, as we'll see in examples below, the truncated series often uses the n'th order field more efficiently than does the consistent series.

Milder developed a further simplification to the standard OE series solution by taking advantage of a symmetry with respect to the sign of the surface height profile. Suitable treatment of scattering from the sign-reversed surface (Sec. 3.3.3) results in a reformulation of the standard solution (3.40) for the surface field (scaled) normal derivative into two alternative series (3.41) and (3.42) which only contain odd or even operator terms, respectively. Milder [1991] suggested that these short series might be good to order $n+1$ when computed to order n, because the next available term in the series is of order $n+2$. We find that the short series solutions do indeed exhibit the character of the standard solution taken to next order, even when that solution is inaccurate; see Sec. 4.4.3.

These alternative series solutions are easier to investigate for rougher surfaces than have been used in earlier sections; thus we take this opportunity to examine the convergence properties of the OE for larger values of the slope-height parameter *khs*. We begin with a study of the effect of consistency in the series expansion parameter on the accuracy of the OE solution for the scattering strength.

4.4.2 Relative accuracy of the consistent expansion

In this section we examine the relative accuracy of the second order consistent solution $OE^{(2)}$ (given by $I^{(2)}$ in (2.23) and denoted by OE(2) in the figures) and the truncated series solutions OE_1, OE_2, and OE_3, given by (2.22). Results are presented for cases whose slope-height parameter is $khs = 0.5$ (Fig. 4.8) and $khs = 1.0$ (Fig. 4.9). Calculations have also been performed for higher values of *khs* and the results are similar to those shown here, though the mean error and fluctuation levels generally increase with increasing *khs*.

The examples are representative of two regimes observed as a function of *kl*. These regimes are separated by a transition region and are distinguished by the way the OE_n series converges in the backscattering region (there is little sensitivity to *kl* in the forward scattering region): $kl \lesssim 3.5$ (relatively large slope regime), $3.5 \lesssim kl \lesssim 5$ (transition region), and $kl \gtrsim 5$ (relatively small slope regime). These regions are not precisely delimited; the bounding values of *kl* are to be used as a general indication. The incident angle is quite low ($\theta_i = 20°$, except for Fig. 4.9a in which $\theta_i = 30°$) allowing study of the OE solution in the far backscatter region, that is, for relatively large Bragg wavenumbers. We expect that these results can be used to infer accuracy of the OE for steeper incident angles. The difference (error) curves between the scattering strengths obtained by the various approximations and the integral equation solution are presented for each example; 50 surface realizations were used in the averages. We limit the discussion to Fig. 4.8, but include Fig. 4.9 to provide a quantitative illustration of the change in the OE results for a given change in the value of *khs*; the qualitative behavior of the solution for these rougher surfaces is essentially the same.

We first examine the accuracy and convergence of the standard OE_n series for $khs = 0.5$. In Fig. 4.8a, for $kl = 2.6$, $kh = 0.96$, and $s = 0.52$ (higher slope regime), convergence of the OE_n solution is nonmonotonic in the region of scattering angles $\theta_s \lesssim 90°$. The error curve for OE_2 shows it to only be marginally better than OE_1; however, the third order OE_3 is clearly more accurate. This is no longer the case in Fig. 4.8b, where $kl = 4.5$, $kh = 1.3$, and $s = 0.4$ (transition regime), where for scattering angles $\theta_s \lesssim 50°$ the OE_3 solution is less accurate than OE_2. This tendency increases

with increasing kl; the OE_n series may be only be asymptotically convergent in this (lower slope) regime. Figure 4.8c, for which $kl = 10$, $kh = 1.9$, and $s = 0.27$, illustrates this behavior quite dramatically.

In the three examples of Fig. 4.8 the $OE^{(2)}$ solution curve lies between OE_1 and OE_2. This relationship to the truncated series solution might have been anticipated, since $OE^{(2)}$ contains higher order terms than OE_1, and the OE_2 solution contains still higher order terms (see (2.22) and (2.23)). Though its position relative to the other operator expansion solutions does not depend on kl, the relative accuracy of $OE^{(2)}$ does. The consistent solution $OE^{(2)}$ is more accurate in the backscatter region than the truncated solution OE_2 in the "higher slope" regime, approximately when $kl \lesssim 4$. However, the truncated solution is better than the consistent solution over all scattering angles for $kl \gtrsim 4$. Note that the $OE^{(2)}$ solution is generally comparable to OE_1 (and slightly less accurate than OE_2) in the forward scattering direction, particularly near specular, independently of kl; the higher order contributions in OE_2 are apparently important in this regime, leading to greater accuracy for that solution. Similar results to those described for Fig. 4.8 can be observed in Fig. 4.9 for $khs = 1.0$.

In summary, the operator expansion solution for the cross section does not seem to require consistency in the expansion parameter to maintain accuracy. This is fortunate because the (inconsistent) truncated series is substantially more efficient to compute. We now turn to a study of the short series which provide yet another OE formulation which is even more efficient than the standard OE_n series.

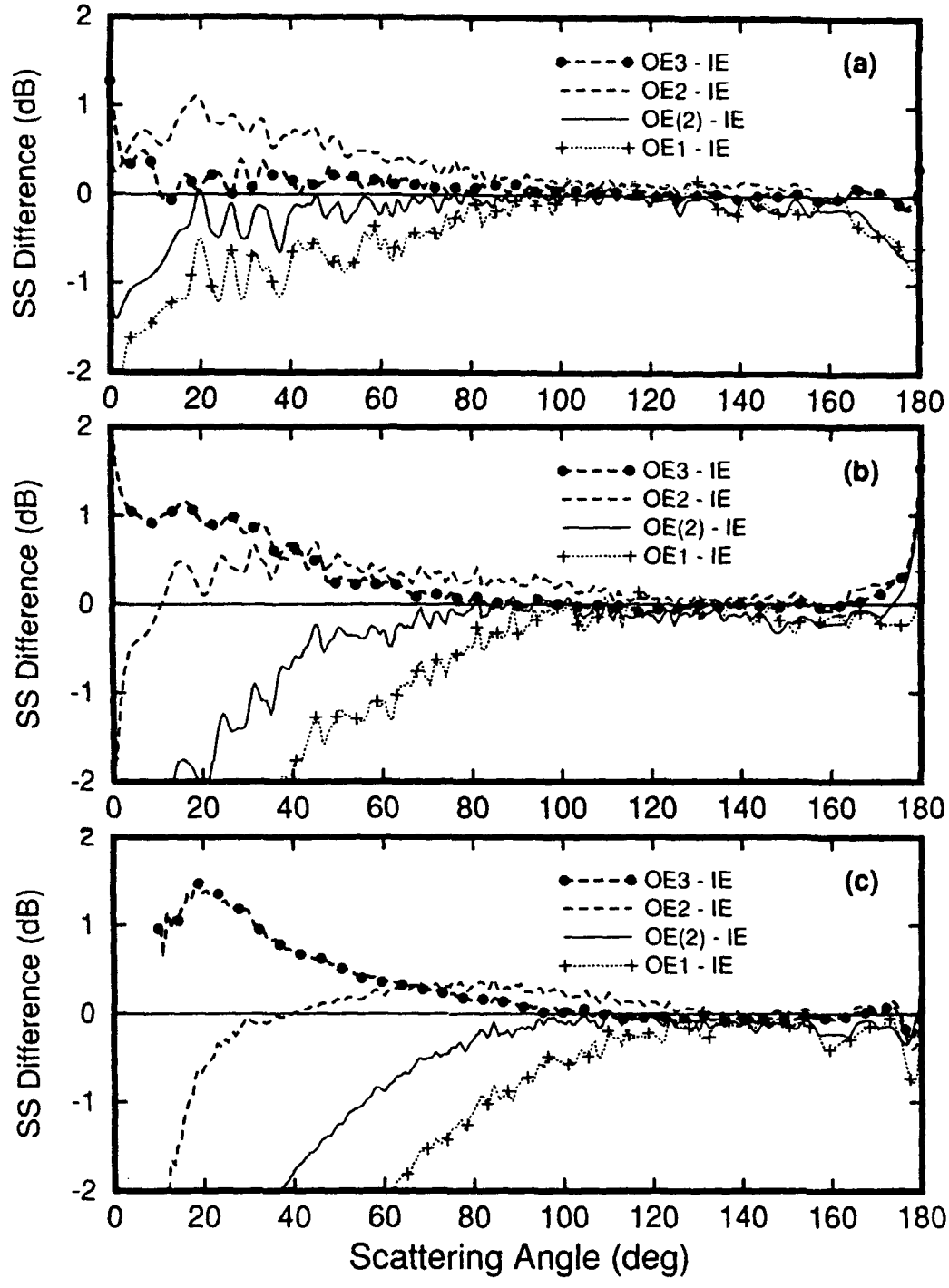

Figure 4.8 : Accuracy of the second order consistent solution $OE^{(2)}$ for $khs = 0.5$. Error curves for truncated series solutions OE_1, OE_2, and OE_3, and for consistent solution $OE^{(2)}$ (labeled OE(2) in figures) are presented for scattering from Gaussian spectrum surfaces averaged over 50 surface realizations, for $\theta_i = 20°$. (a) $kl = 2.6$, $kh = 0.96$ and $s = 0.522$ (case B2); (b) $kl = 4.5$, $kh = 1.26$ and $s = 0.396$ (case B3); (c) $kl = 10.$, $kh = 1.88$ and $s = 0.266$ (case B4).

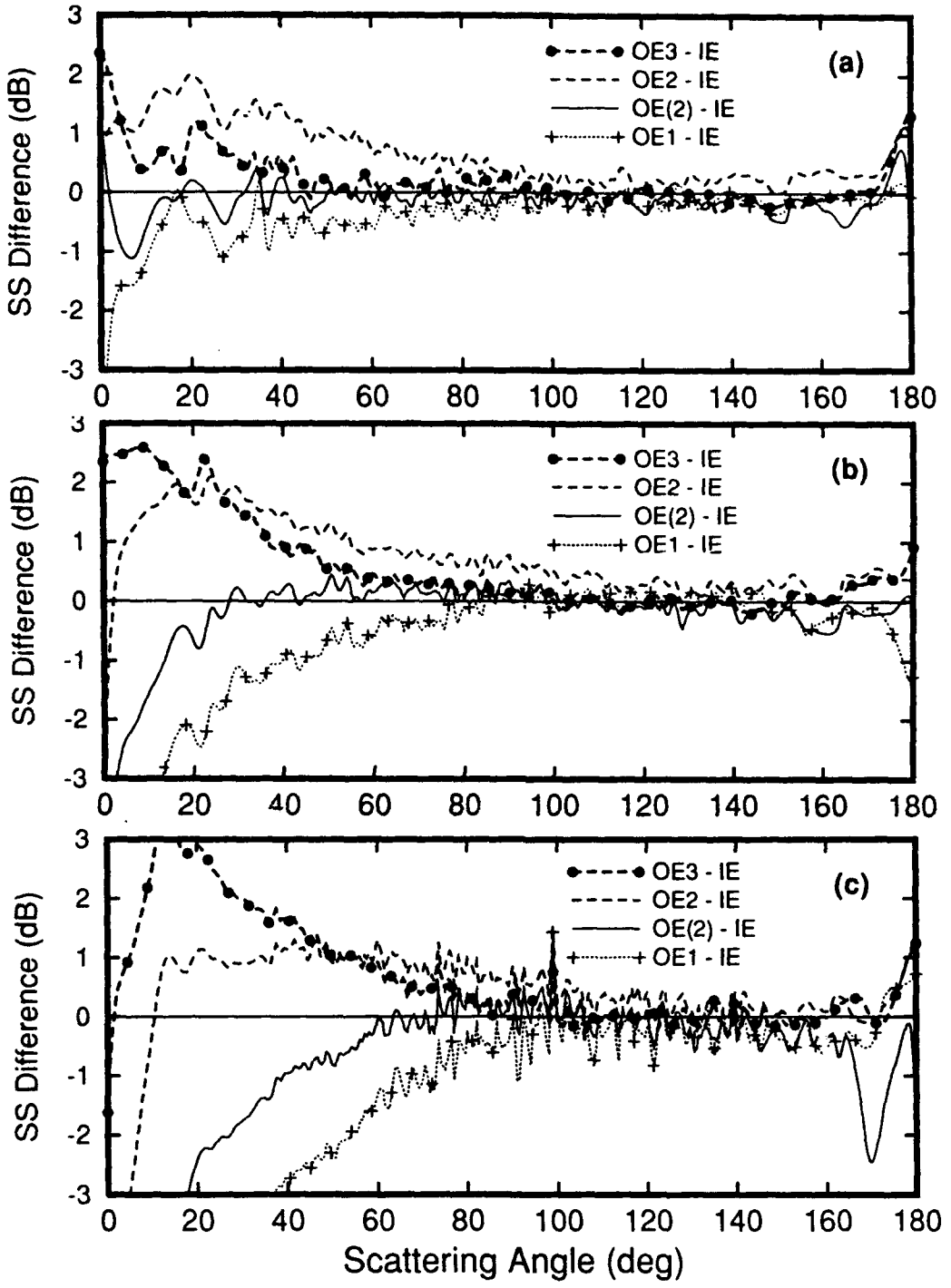

Figure 4.9 : Accuracy of the second order consistent solution $OE^{(2)}$ for $khs = 1.0$. Error curves for truncated series solutions OE_1, OE_2, and OE_3, and consistent solution $OE^{(2)}$ are presented for scattering from Gaussian spectrum surfaces averaged over 50 surface realizations. (a) $kl = 2.6$, $kh = 1.35$, $s = 0.734$, and $\theta_i = 30°$ (case C2); (b) $kl = 4.5$, $kh = 1.78$, $s = 0.559$, and $\theta_i = 20°$ (case C3); (c) $kl = 10.$, $kh = 2.67$, $s = 0.378$, and $\theta_i = 20°$ (case C4).

4.4.3 Accuracy of the odd and even series

General comments

We have calculated the standard (truncated) series operator expansion solutions and the short series solutions through third order in the surface field over a reasonably wide range of *kl*-*kh* values (see Fig. 4.2) and for several different incident angles. It is important to keep in mind that higher order calculations, particularly terms containing third order ($\hat{N}_3$) fields, demand more care in the numerical implementation. Repeated application of Fourier integral operators compound edge effects and deficiencies due to marginal sampling density in the spatial or wavenumber domains. Therefore, calculations involving surface fields above second order have an additional hidden cost not reflected in computation times nor visible in the scattering strength curves presented here, and may not be practical for routine use. Nevertheless, third order calculations are extremely valuable in examining the convergence of the operator expansion solution.

For each of the numerical cases, the integral equation (either first or second kind, or both) solution was also computed in order to evaluate the accuracy of the approximations. Typically, convergence of the OE is slower for scattering angles far from the specular direction, especially when scattering levels are low, that is, for larger values of *kl*. We also find that as *khs* is increased, the convergence rate of the OE generally decreases, and the accuracy of any given approximation also decreases for the most part, though there are notable exceptions addressed later. Indeed, the detailed behavior of the operator expansion solution in the *kl*-*kh* parameter space is complicated and can not be simply described. Nevertheless, the following example (case B3) provides a very typical view of how the short series solutions behave compared with the standard series solutions for $khs \leq 1.5$. Other calculations show that relative positions of the scattering strength curves for given approximations remain about the same with respect to each other as *kl* and *kh* are changed along a line of constant *khs*, but that the overall position of the group of approximate solution curves with respect to the exact integral equation curve (and hence the accuracy of any particular approximation) depends on the values of *kl* and *kh*.

The short series solutions will be designated in a manner similar to the standard series. In summary, both the scattering strength curves and the scattering strength error curves are denoted OE_n for solutions using I_n in (2.22), $\mathrm{OE}^{(n)}$ for solutions using $I^{(n)}$ in (2.23), EV_n for solutions using only even terms in the series presented in (3.42), and OD_n for the odd series (3.41). Note that the $\mathrm{OE}^{(n)}$ series is the only consistent solution considered here. The nominal order of the solution is given by index n which

represents the highest order surface field term used in the calculation. Finally, the ON_n curves are the scattering strength contributions due to the $|F_n|^2$ terms alone.

Detailed study of case B3

A representative example for $khs = 0.5$ is presented in Fig. 4.10, where the surface roughness parameters for case B3 are $kl = 4.5$, $kh = 1.26$, and $s = 0.4$, which corresponds to an rms slope angle $\gamma = 22°$. The behavior of the surface field series terms is evident from the scattering strength contributions ON_n in Fig. 4.10a; these decay rapidly with increasing order over all scattering angles except those in the backscattering region near grazing. An accurate solution is reached by second order; the scattering strength curve for calculation OE_2 lies within 1 dB of the integral equation solution over the full range of scattering angles, for incident angle $\theta_i = 20°$ (see Fig. 4.10b). Again, the accuracy of any operator expansion solution improves with higher incidence angle, though no examples of this behavior are presented for this case. In general, the accuracy depends on the angular distance from the specular direction (see Figs. 4.7 and 5.3).

The example of Fig. 4.10 illustrates several features of the operator expansion solution observed in all cases studied which we review before proceeding with the short series results. The relatively rapid decay of the terms in Fig. 4.10a in the angular range between $50° \leq \theta_s \leq 180°$ is tied to rapid convergence and good accuracy of the solution over that range of angles, as seen in Fig. 4.10b. In the backscattering region for $\theta_s \leq 50°$ (corresponding to 110° from the specular direction) the convergence is slower. Here the accuracy of any given calculation depends on the values of kl and kh; however, the *relative* positions of the individual solutions seem to remain about the same with respect to each other, though the relation of the group of solutions to the level of the integral equation solution changes.

The scattering strength errors for the short series solutions EV_0, OD_1, EV_2, and OD_3 are presented in Fig. 4.10c. The line types chosen to identify the short series solutions correspond to the standard series solution curves in Fig. 4.10b which they most resemble; note that the odd and even solutions of order n have the character (but not quite all the accuracy) of the standard solutions of order $n+1$.

An interesting way to compare the short series solutions to the standard solutions is to look at the solutions order by order. Fig. 4.11a contains three curves corresponding to the solutions which could be considered first order (EV_0, OE_1, and OD_1), either because of the highest order of included surface field terms or because of the solution character, and the error curve for $OE^{(2)}$ which is a second order approximation included

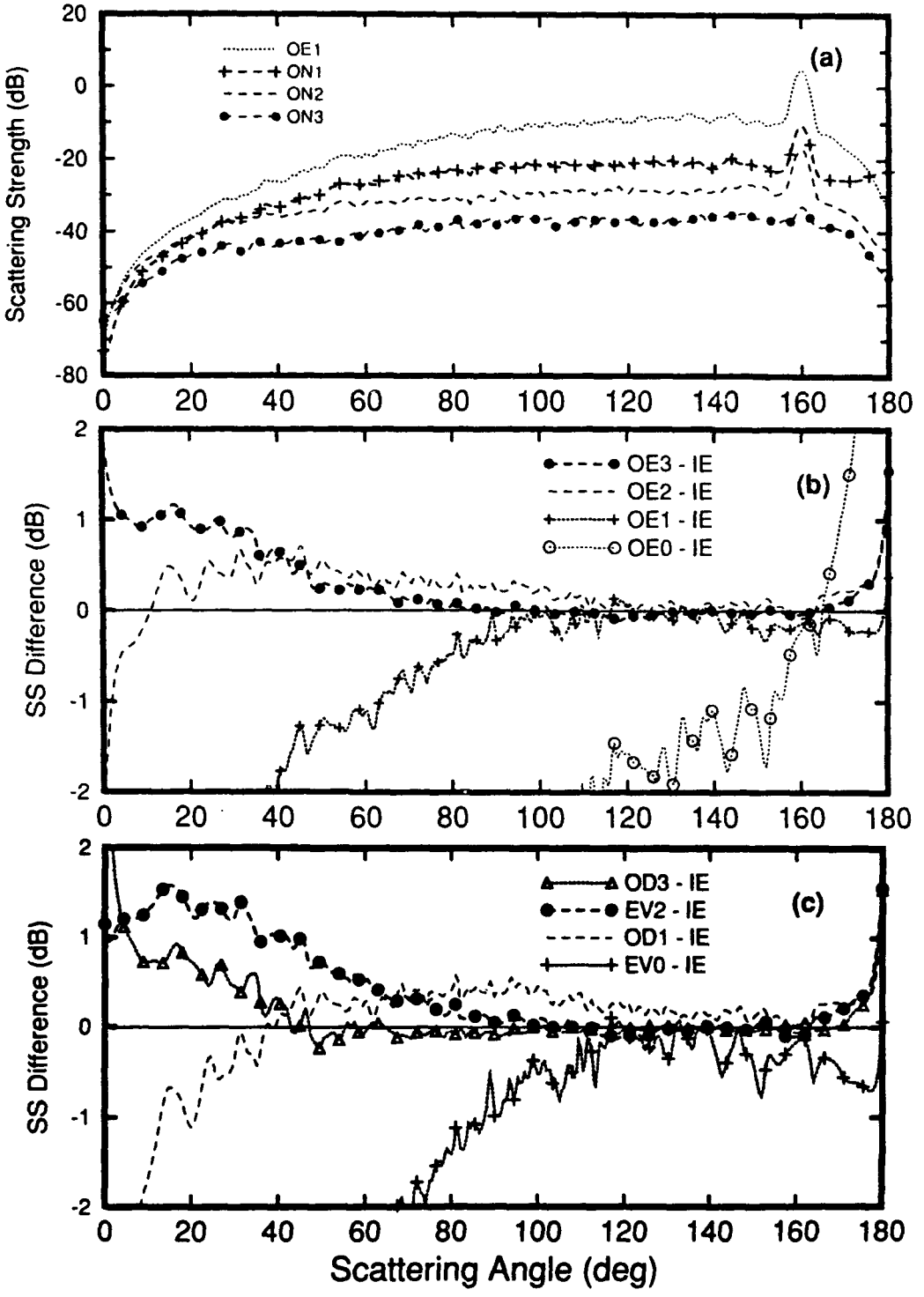

Figure 4.10 : Convergence and accuracy of the standard and short series solutions for case B3. a) Decay of the ON_n series; b) Accuracy of the standard series solutions OE_0, OE_1, OE_2, and OE_3; c) Accuracy of the short series solutions EV_0, OD_1, EV_2, and OD_3.

here for comparison. The accuracy of all approximations is good for the forward angles, $\theta_s \geq 90°$, but the performance of these solutions in the backscattering region $\theta_s \leq 90°$ is quite variable. Solutions which can be considered second order ($OE^{(2)}$, OD_1, OE_2, and EV_2) are presented in Fig. 4.11b. Considering the OD_1 solution for example, Figs. 4.11a and 4.11b indicate that the short series solution evaluated to first order appears to be more similar to the second order solutions OE_2 and $OE^{(2)}$ than to the first order solution OE_1. Similar observations can be made for EV_2 when comparing Figs. 4.11b and 4.11c. Admittedly, these comparisons are highly qualitative, but the obvious complexity of the relationship between solutions precludes making a more precise general statement. These characteristics are more easily discernible for power law surfaces (see Figs. 5.4 and 5.5).

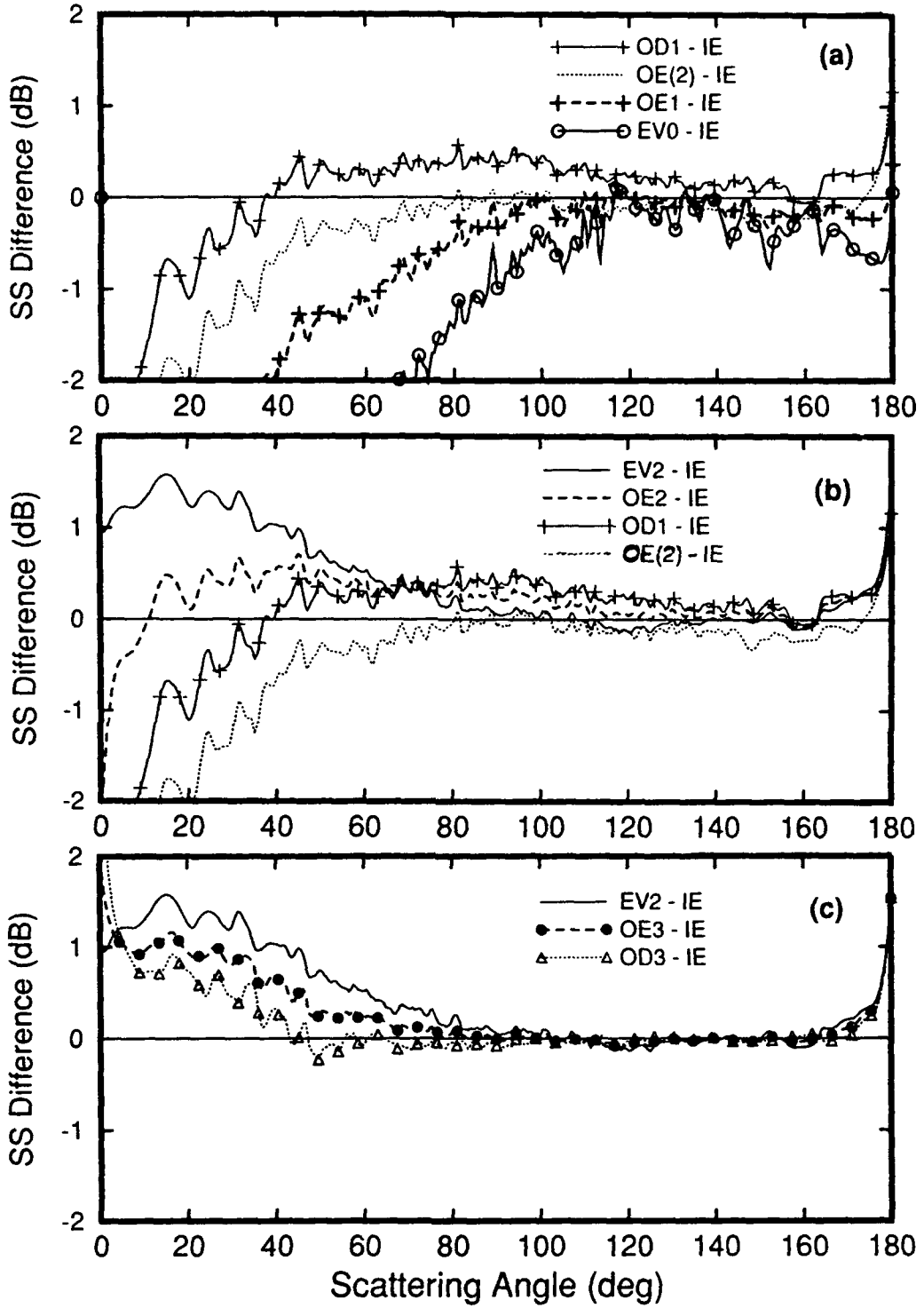

Figure 4.11 : Comparison of alternative series solutions to the standard series solutions order by order. a) first order; b) second order; c) third order.

4.5 OE behavior for rougher surfaces

4.5.1 General properties of the OE solutions for $khs \leq 1.5$

The general properties of the operator expansion solution have been discussed above, but we summarize them here and illustrate them by presenting solution curves from six numerical examples. These examples are picked using two values of kl, and are representative of two regimes discussed in Sec. 4.4.2, a relatively higher slope regime, and a relatively lower slope regime. Furthermore, the cases are chosen with $khs = 0.5,\ 1.0,$ and 1.5 to show how the OE solutions behave with changes in slope-height parameter. We include these examples for completeness, and because there is no better way to demonstrate the detailed behavior of the various OE approximations considered.

As the slope-height parameter khs is increased, the operator expansion generally converges more slowly, and a given approximation typically becomes less accurate. The convergence of the series for the normal derivative surface field is easily observed by examining the rate of decay of the ON_n series as a function of khs. As the decay rate slows overall, the third order solution ON_3 rises to the level of the second order term ON_2, and eventually exceeds it. The OE solution is perhaps beginning to diverge when this happens, although the fourth order term has not been computed to verify this trend. (A hint of the fourth order term's behavior can be obtained from looking at the relative accuracy of the OE_3 and OD_3 solutions; when OD_3 is more accurate than OE_3, the fourth order term ON_4 is likely to be smaller than the third order term ON_3.) The convergence seems to be asymptotic, because the leading orders do tend to converge before diverging. Accuracy of the OE solution is best studied by examining the scattering strength error curves obtained through comparison with the integral equation solution, which has been computed for the same set of surface realizations.

Typically, the convergence rate and accuracy degrade slowly with increasing roughness, that is, there is no clear threshold roughness above which the method fails catastrophically. Performance of the OE method is generally better in the forward scattering region, but behavior in the backscattering region is variable and depends quite strongly on the values of kl and kh. The slope-height parameter is generally a good indicator of the operator expansion's performance, but detailed behavior with respect to scattering angle depends on the separate values of kl and kh; experience with the method leads to a fairly reliable "calibration" of its performance with respect to the value of khs. The OE solution is not as accurate within a few degrees of grazing as it is elsewhere, and this is thought to be due to the numerical difficulties associated with the zero-crossing of the k_z filter function in $\hat{Q}$. However, the method is also expected to

have difficulties accurately treating strong distant multiple scattering, a phenomenon associated with the rise of scattered field singularities with increasing slope, discussed in Chapter 3 and in the following section. As roughness increases, the importance of distant multiple scattering increases for higher grazing angle scattering; indeed, numerical tests show that the range of angles over which the solution converges to an incorrect answer (or never converges) increases with increasing roughness. This behavior will be easily observed in the example presented in Sec. 4.5.2, when $khs = 3.5$, but can also be detected in Figs. 4.12-17 following below.

One notable exception to the general rule is that as khs increases beyond , the accuracy of the first order solution actually improves in the backscatter region, particularly in the regime for $kl \lesssim 4$. In this same region of scattering angles, the higher order solutions are usually not as accurate as the first order solution; this is a manifestation of the asymptotic convergence of the OE solution in this roughness regime. It is possible (but admittedly a speculation) that the importance of the (nonlocal) scattering physics included in the first order solution (OE_1) increases as khs is increased from 0.5 to 1.5, for example for $kl = 2.6$ (see Figs. 4.12, 4.13, and 4.14). Higher order terms (OE_2 and higher) likely emphasize more distant contributions which may also be important, but these are perhaps not handled as accurately by the OE at these roughness levels. The importance of correctly treating multiple scattering, and of the operator expansion method's ability to include some nonlocal contributions, is dramatically illustrated in the next section. First we examine the regime for $0.5 \leq khs \leq 1.5$. The decay of the ON_n series is presented in Fig. 4.12 for $kl = 2.6$, and in Fig. 4.15 for $kl = 10$. The accuracy of the standard series is presented in Fig. 4.13 and Fig. 4.16, for $kl = 2.6$ and $kl = 10$, respectively. Similarly, the accuracy of the short series is given by the curves in Figs. 4.14 and 4.17, for the same examples.

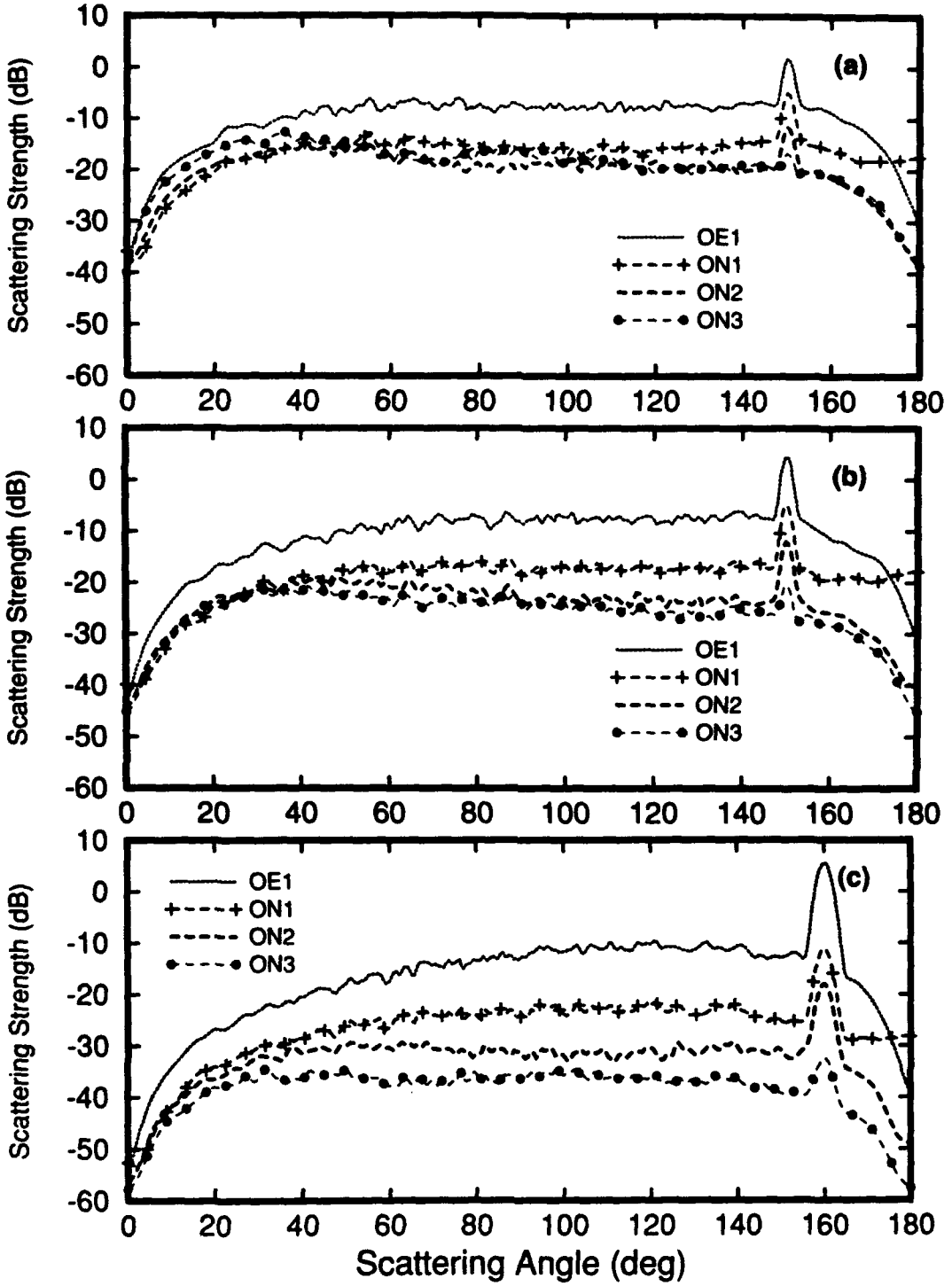

Figure 4.12 : Decay of the scattering strength contributions from individual orders of the surface field, for $kl = 2.6$.

a) Case D2: $kh = 1.66$, $s = 0.903$, $khs = 1.5$, $\theta_i = 30°$.

b) Case C2: $kh = 1.35$, $s = 0.734$, $khs = 1.0$, $\theta_i = 30°$.

c) Case B2: $kh = 0.96$, $s = 0.522$, $khs = 0.5$, $\theta_i = 20°$.

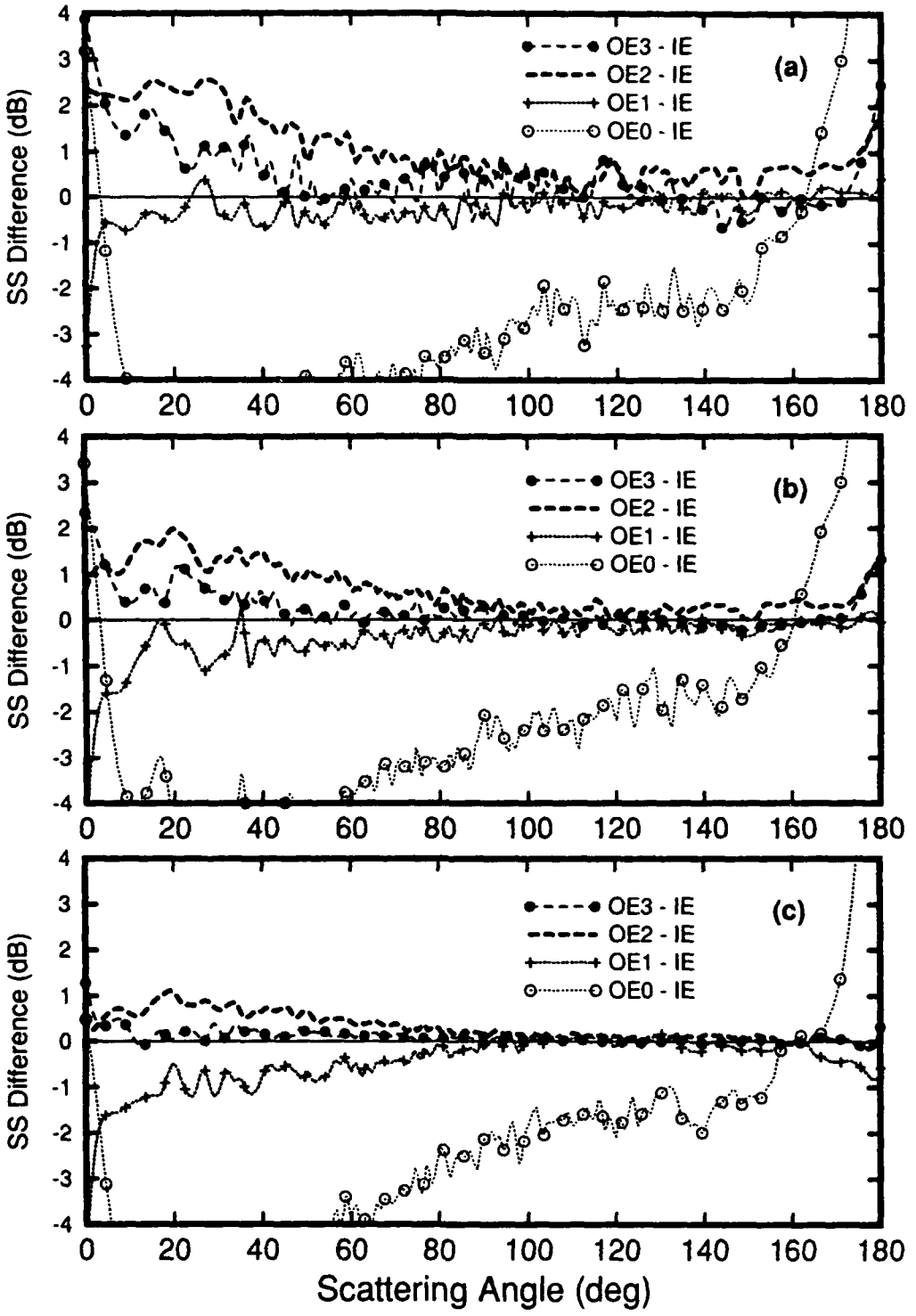

Figure 4.13 : Accuracy of the standard series solutions for cases D2, C2, and B2.

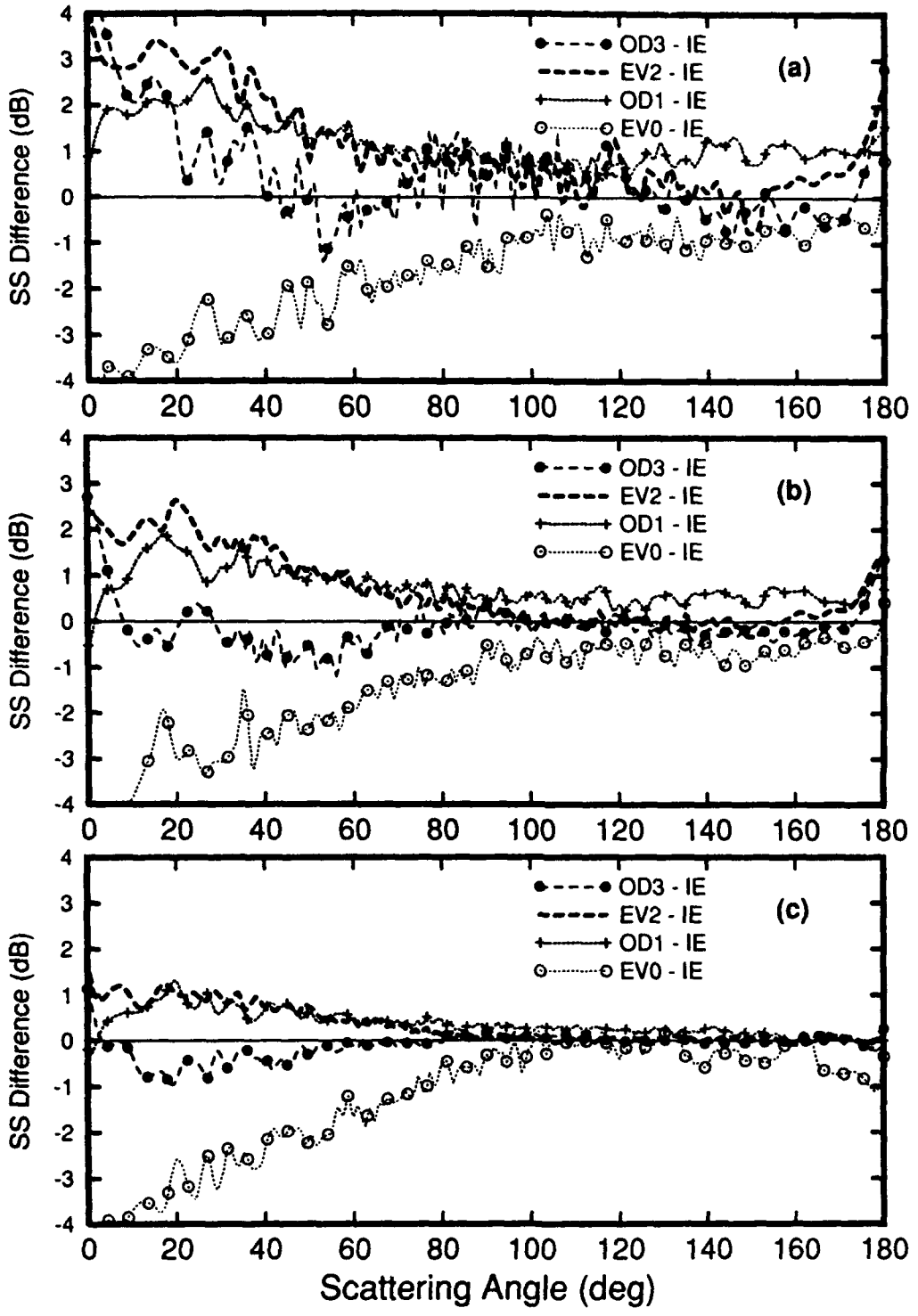

Figure 4.14 : Accuracy of the short series solutions for cases D2, C2, and B2.

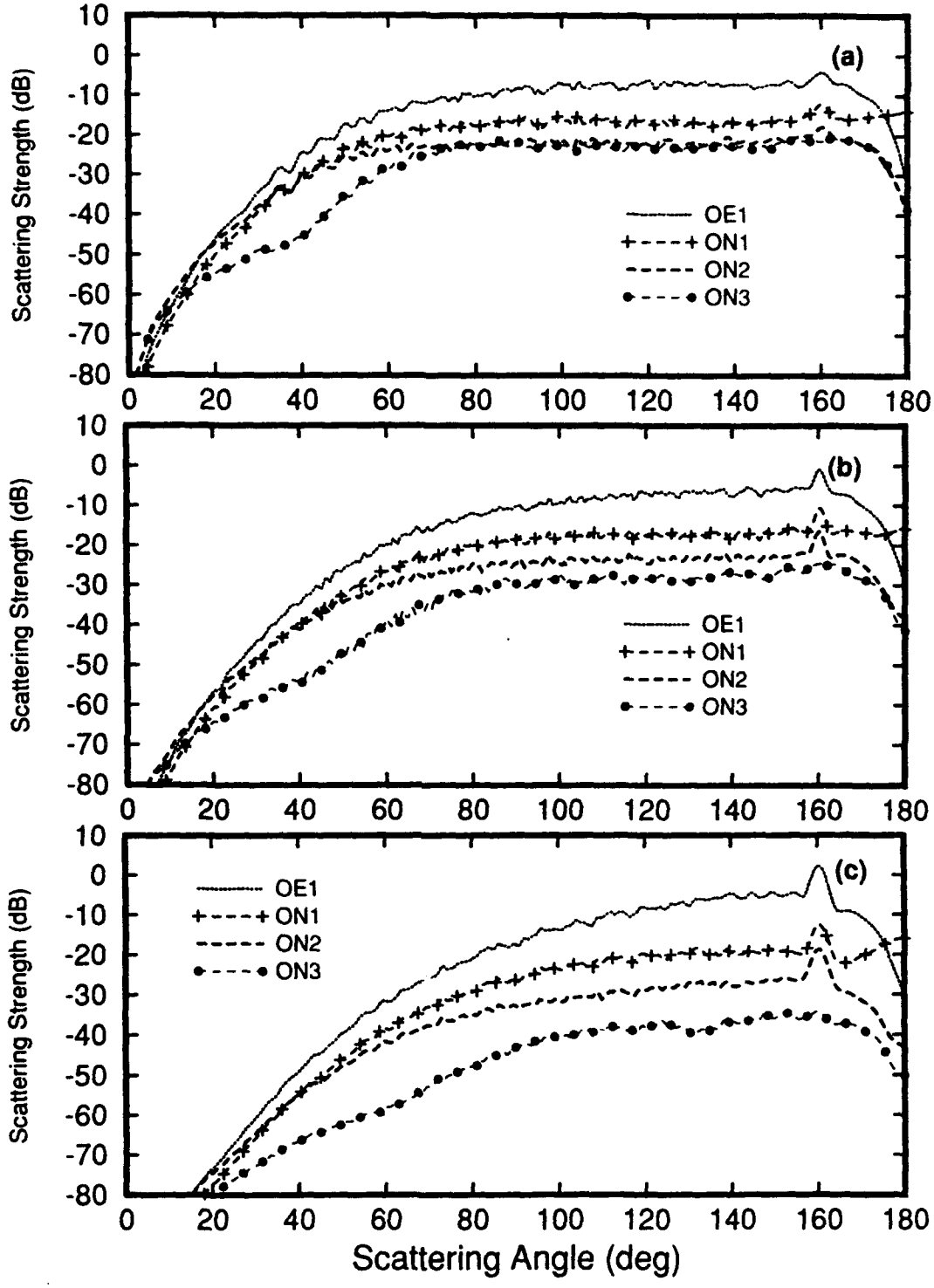

Figure 4.15 : Decay of the scattering strength contributions from individual orders of the surface field, for $kl = 10.0$ and $\theta_i = 20°$.

a) Case D4: $kh = 3.26$, $s = 0.461$, $khs = 1.5$.
b) Case C4: $kh = 2.67$, $s = 0.378$, $khs = 1.0$.
c) Case B4: $kh = 1.88$, $s = 0.266$, $khs = 0.5$.

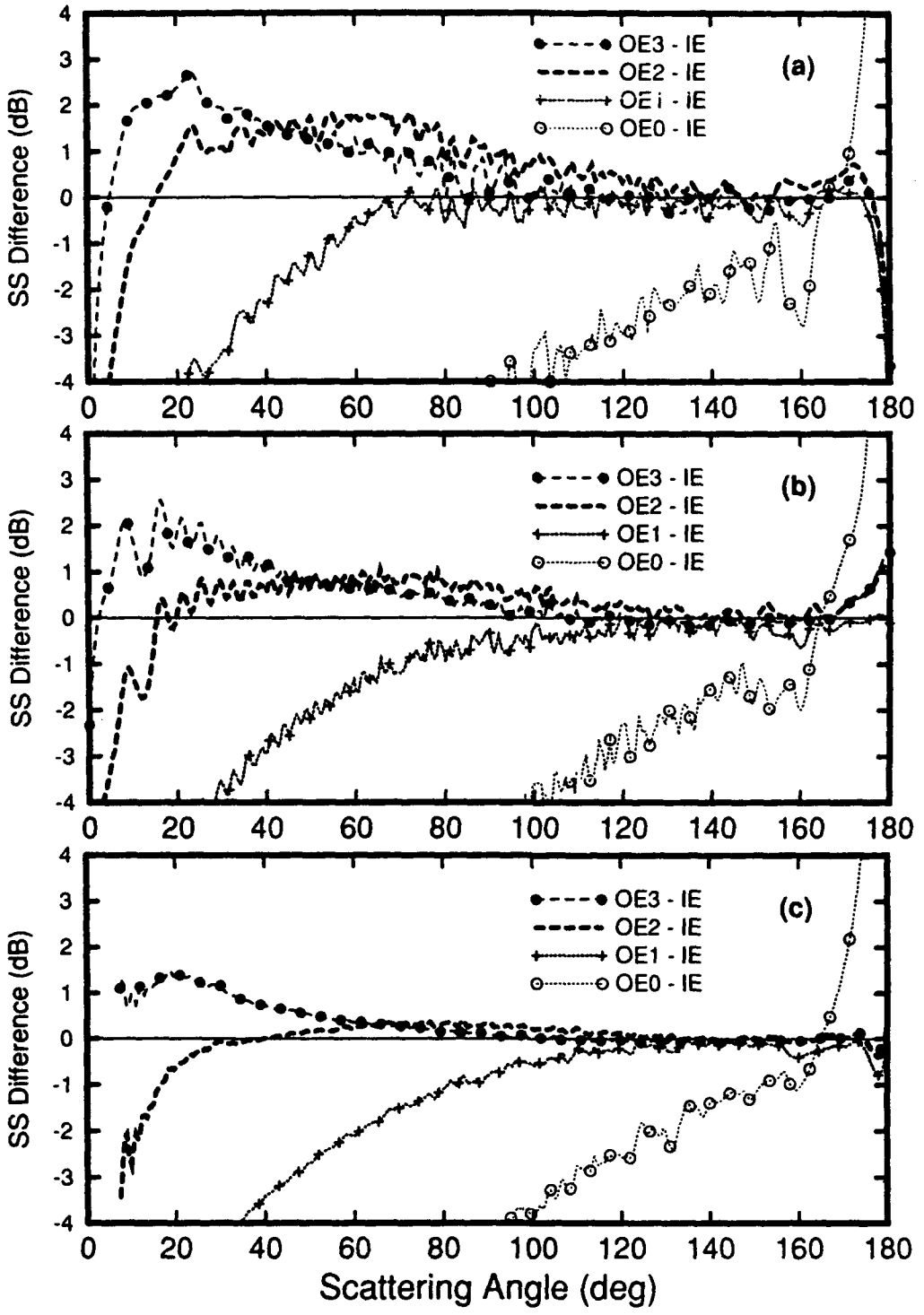

Figure 4.16 : Accuracy of the standard series solutions for cases D4, C4, and B4.

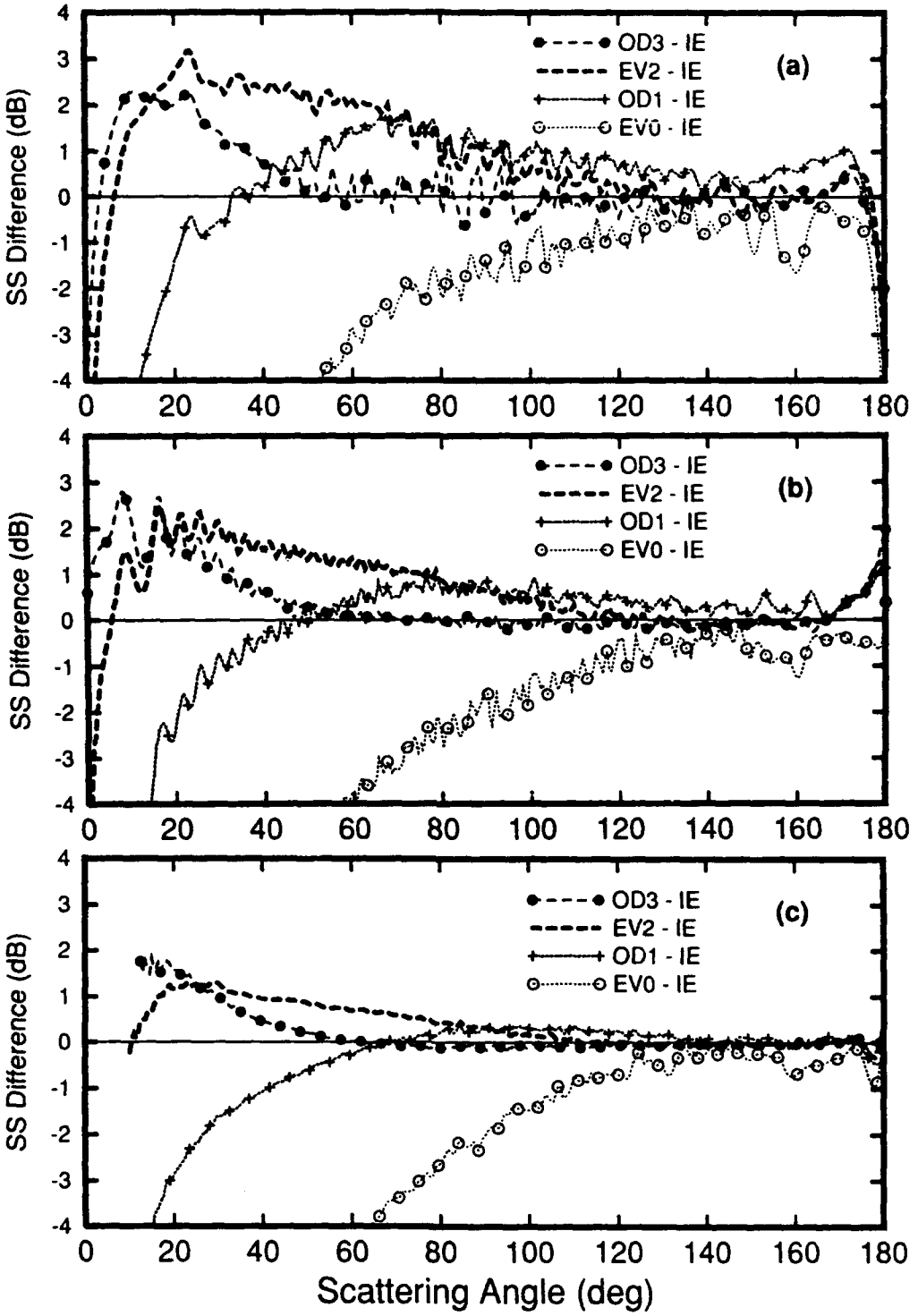

Figure 4.17 : Accuracy of the short series solutions for cases D4, C4, and B4.

4.5.2 Very rough surfaces — backscattering enhancement

A new physical regime exists for very rough Dirichlet surfaces in which multiple scattering plays an important role. Double-scattered reciprocal paths lead to an enhancement peak in the backscatter direction which can rise 3 dB above the average level [Thorsos and Jackson, 1991], [Ishimaru and Chen, 1990], in a manner analogous to the corresponding volume scattering problem [Tsang and Ishimaru, 1984]. Illustrative paths for the double scattering are sketched in Fig. 4.18. When such scattering processes contribute strongly to the cross section, the Rayleigh hypothesis is invalid because singularities of the (continued) scattered field must be present above the lowest points on the surface.

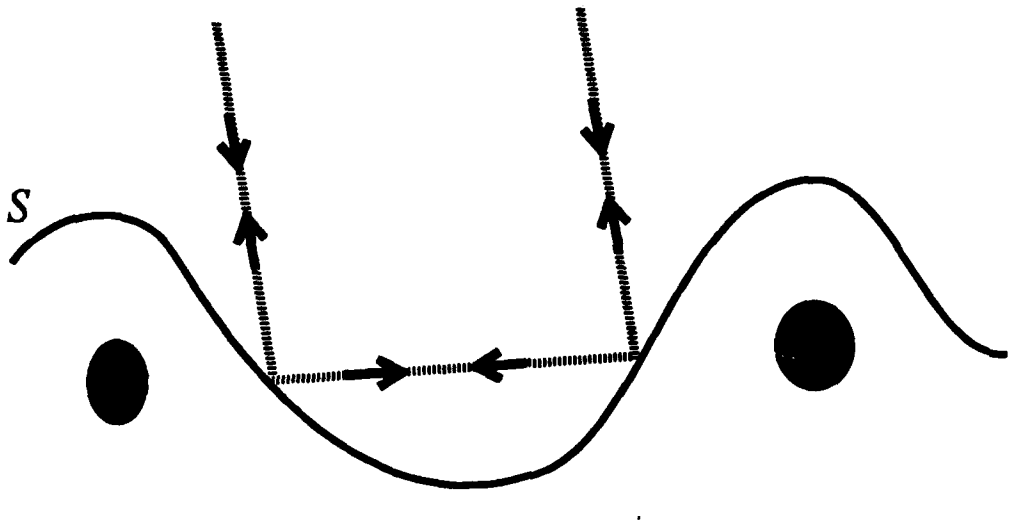

Figure 4.18 : Schematic depiction of double scattered paths and the location of associated singularities of the continued scattered field, for the roughness regime that supports backscattering enhancement.

Case F4, for which $kl = 7.0$, $kh = 4.2$, $s = 0.85$, and $khs = 3.56$, is rough enough that the enhancement peak is clearly visible in scattering strength contributions (Fig. 4.19a), and also in the scattering cross section curves (Fig. 4.20). The ON_n terms for $n > 0$ all contribute to the estimate of backscatter enhancement, indicating that even the first order OE solution includes nonlocal contributions distant enough to produce the enhancement peak. The scattering strength contributions from each order in the series for the surface field through third are presented in Fig. 4.19a. Each curve, except OE_0, has a distinct bump centered on the incident direction of $\theta_i = 60°$. It is interesting to observe that the width of the peaks decreases with increasing order; this behavior

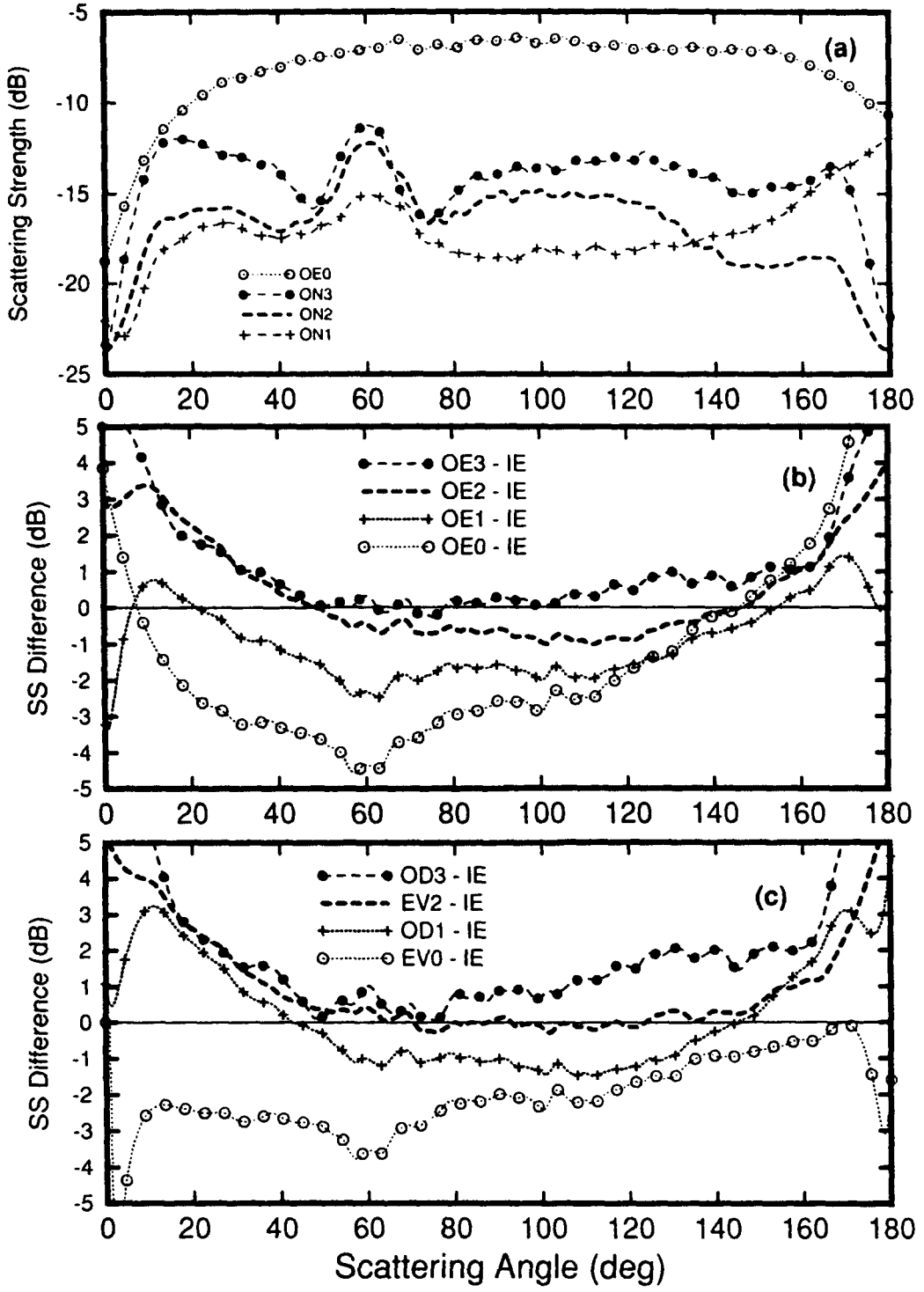

Figure 4.19 : Scattering results for an example in the backscattering enhancement regime (case F4, $\theta_i = 60°$, 500 surfaces). (a) Convergence of the operator expansion surface field — ON_n series. (b) Accuracy of the standard series solution — OE_n series. (c) Accuracy of the short series solution — OD_n and EV_n series.

indicates that the higher order OE terms treat more distant scattering than the lower order terms. (The width of the bump is inversely related to the average distance between multiple scattering points on paths that contribute to the backscatter enhancement.) Though the operator expansion series appears to be diverging beginning at second order, the error curves in Fig. 4.19b for the standard series and in Fig. 4.19c for the short series indicate that the second (ON_2) and third (ON_3) order contributions lead to approximations which improve in accuracy with increasing order, at least for the range of scattering angles 40° away from grazing. The surface roughness in this regime is such that a large number of realizations is required to reduce the fluctuations to an acceptable level; 500 surfaces were used in the calculations for case F4, an order of magnitude more than were used in most calculations presented earlier.

Until the backscattering enhancement regime is reached, the OE solution gradually slows its rate of convergence over most scattering angles; poor convergence is observed first in the angular region near grazing. By the time the slope-height parameter reaches $khs = 3.5$, the range of angles over which the solution converges to an accurate solution has been reduced to $40° \le \theta_s \le 140°$, when the incident angle is $\theta_i = 60°$. The backscattering enhancement peak is clearly seen in plots of the scattering cross section, presented for the integral equation, OE_3, and EV_2 in Fig. 4.20. The OE_3 solution is the better approximation near the peak, but the EV_2 solution is more accurate away from the peak in the range of scattering angles $80° \le \theta_s \le 150°$. The operator expansion is able to accurately calculate scattering for a case with $khs = 3.5$ which is just rough enough to exhibit backscattering enhancement, but the OE method is not capable of treating scattering from surfaces which are significantly rougher.

4.6 Accuracy of the $\hat{Z}^{-1}$ solution

The $\hat{Z}^{-1}$ solution, or "mean-plane" solution, is based on using the upward plane wave coefficients (3.3) available after the first continuation step from the rough surface to the mean plane. The method is presented in Sec. 3.4.2, and the solution for the scattering amplitude is given by (3.50) and (3.44) using the expansion for $\hat{Z}^{-1}$ given by (3.17). Unlike the OE solution based on using the $\hat{N}$ operator (of which $\hat{Z}^{-1}$ is a component), the mean-plane method does not reverse the continuation step taken by operator $\hat{Z}^{-1}$, and so does not reduce the height dependence introduced by the continuation. Consequently, the mean-plane solution has many of the characteristics of the standard perturbation solution (see Sec. 3.4.4 for a detailed comparison of the two methods), yet numerical comparisons (see below) indicate that the mean-plane method has some advantages over the perturbation method. For example, the $\hat{Z}^{-1}$ solution converges more rapidly than the perturbation solution, resulting in a more accurate result at any given order. Also, the mean-plane solution better matches fluctuations of the exact result for

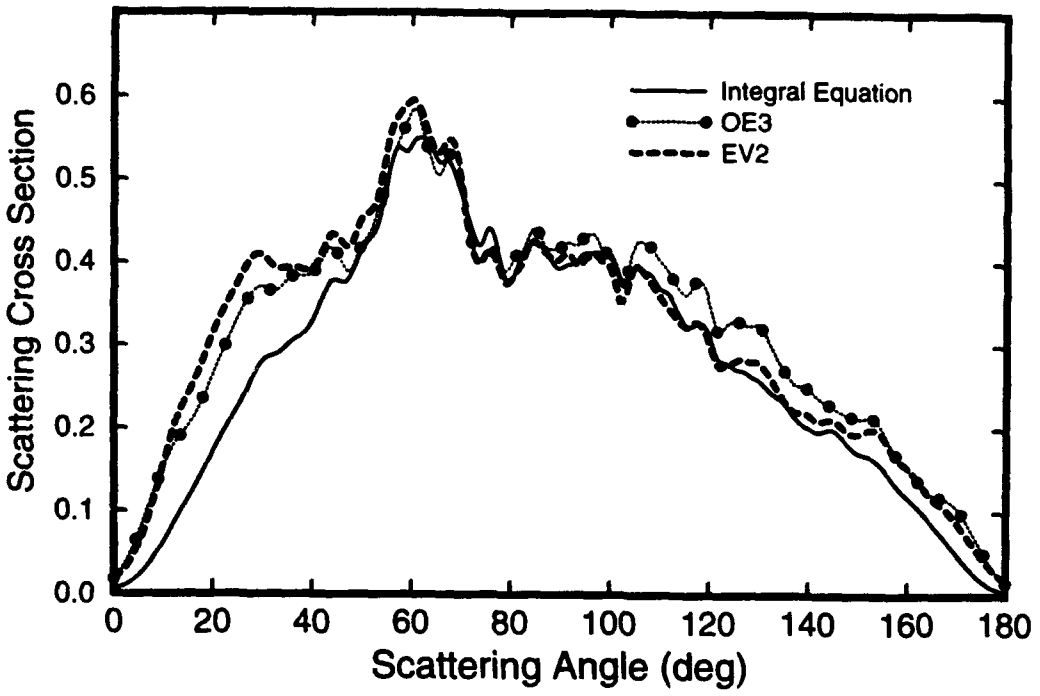

Figure 4.20 : Selected cross section curves from the backscatter enhancement example case F4, $\theta_i = 60°$, using 500 surface realizations.

a finite number of surface realizations. However, the mean-plane solution obtained using $\hat{Z}^{-1}$ is currently only implemented as a numerical method, and is not as easily averaged as the perturbation solution. Our goal here is merely to show numerically how the $\hat{Z}^{-1}$ method differs from the perturbation method which it greatly resembles, and to show the importance of the second (reverse) continuation step used in $\hat{N}$ but obviously absent in $\hat{Z}^{-1}$.

The $\hat{Z}^{-1}$ solution is computed for the four A-cases examined in Sec. 4.3, for which the slope-height parameter is $khs = 0.15$. The mean-plane method becomes inaccurate, and converges more slowly if at all, as the normalized height kh is increased beyond $kh \gtrsim 1.0$, even though khs is small for those cases. We begin by comparing the $\hat{Z}^{-1}$ and $\hat{N}$ solutions for each of the four examples A1-A4, then review the accuracy of the perturbation method for three of those cases. All examples are for the same incident angle ($\theta_i = 45°$) used in the computations in Sec. 4.3. The mean-plane solutions presented below are calculated using the truncated series (2.22) for the cross section.

The $\hat{Z}^{-1}$ method converges rapidly, and provides an accurate solution for case A1, with $kh = 0.38$, and $kl = 1.4$. The scattering strength contributions from each order in the series for the scattering amplitude computed using $\hat{Z}^{-1}$ (labeled Zn, where n is the

order of the calculation) are presented in Fig. 4.21a, and should be compared to the analogous plot for the operator expansion solution in Fig. 4.3c. Though the mean-plane method series decays uniformly over scattering angles, it is clear that the decay is not as rapid as for the operator expansion solution. Using the 1 dB bistatic error criterion, the mean-plane solution (labeled MPn) is accurate at first order (Fig. 4.21b) but is not quite as accurate as the operator expansion solution (Fig. 4.3d). We recall that the behavior of the mean-plane methods (both $\hat{Z}^{-1}$ and perturbation theory) very near grazing is controlled by the explicit factor of k_{sz} in the scattering amplitude (see Sec. 3.4.2) which results in the difference with the integral equation (IE) and operator expansion (OE) solutions.

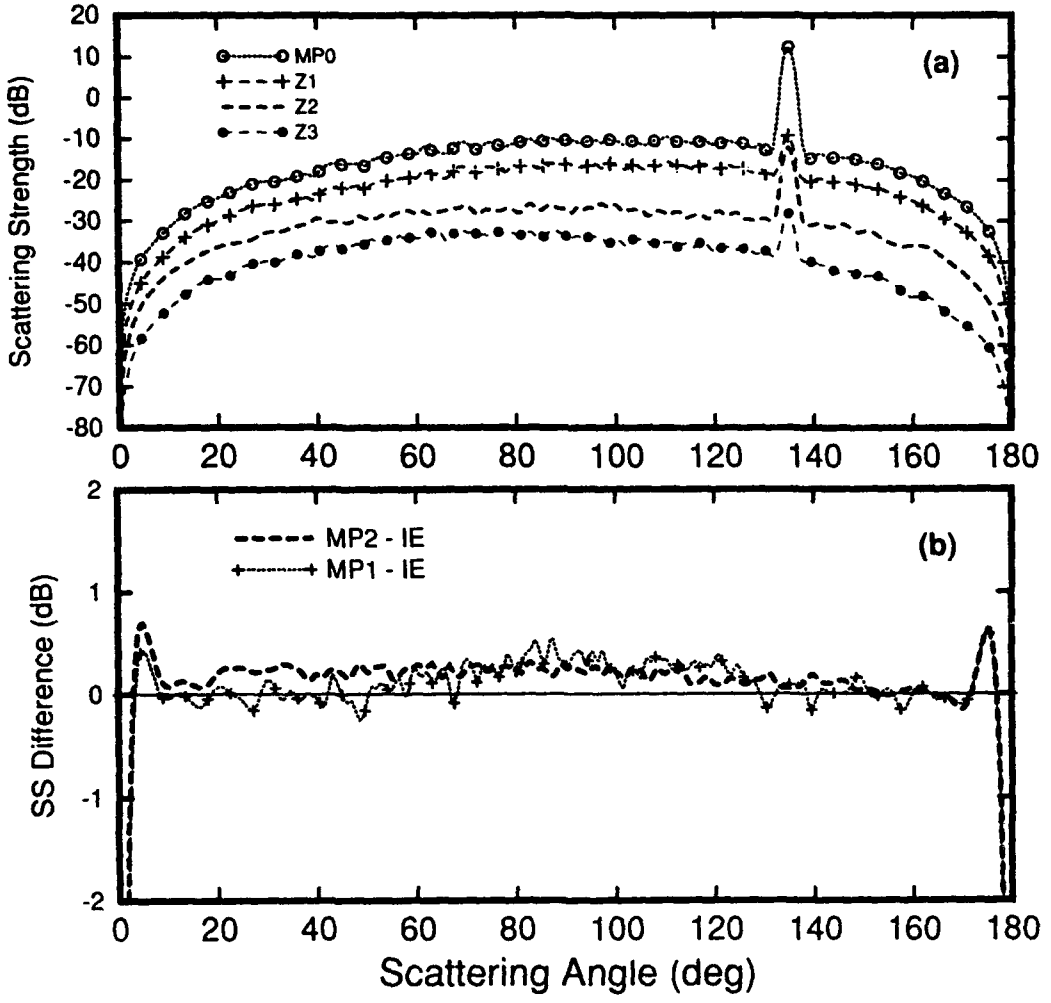

Figure 4.21 : Results of calculations using the $\hat{Z}^{-1}$ operator (mean-plane method) to compute scattering from the 50 surfaces used in Fig. 4.3 for case A1. (a) Scattering strength contributions from each term in the series for the scattering amplitude. (b) Error curves for the truncated series solution using the Mean-Plane (MP) method.

As kl increases, the OE solution converges more slowly in the backscattering region; see Sec. 4.3 for scattering from moderately rough surfaces, and Sec. 4.5.1 for scattering from rougher surfaces. The mean-plane solution also has this property, but its accuracy degrades more quickly than that of the OE solution, with increasing kl. For example, in case A2 with $kh = 0.52$ and $kl = 2.6$, the decay of the $\hat{Z}^{-1}$ series terms is not as rapid as it was in case A1; see Fig. 4.22a. The first order solution MP1 is not accurate over the entire range of scattering angles (see Fig. 4.22b), whereas the OE_1 solution is (see Fig. 4.4c).

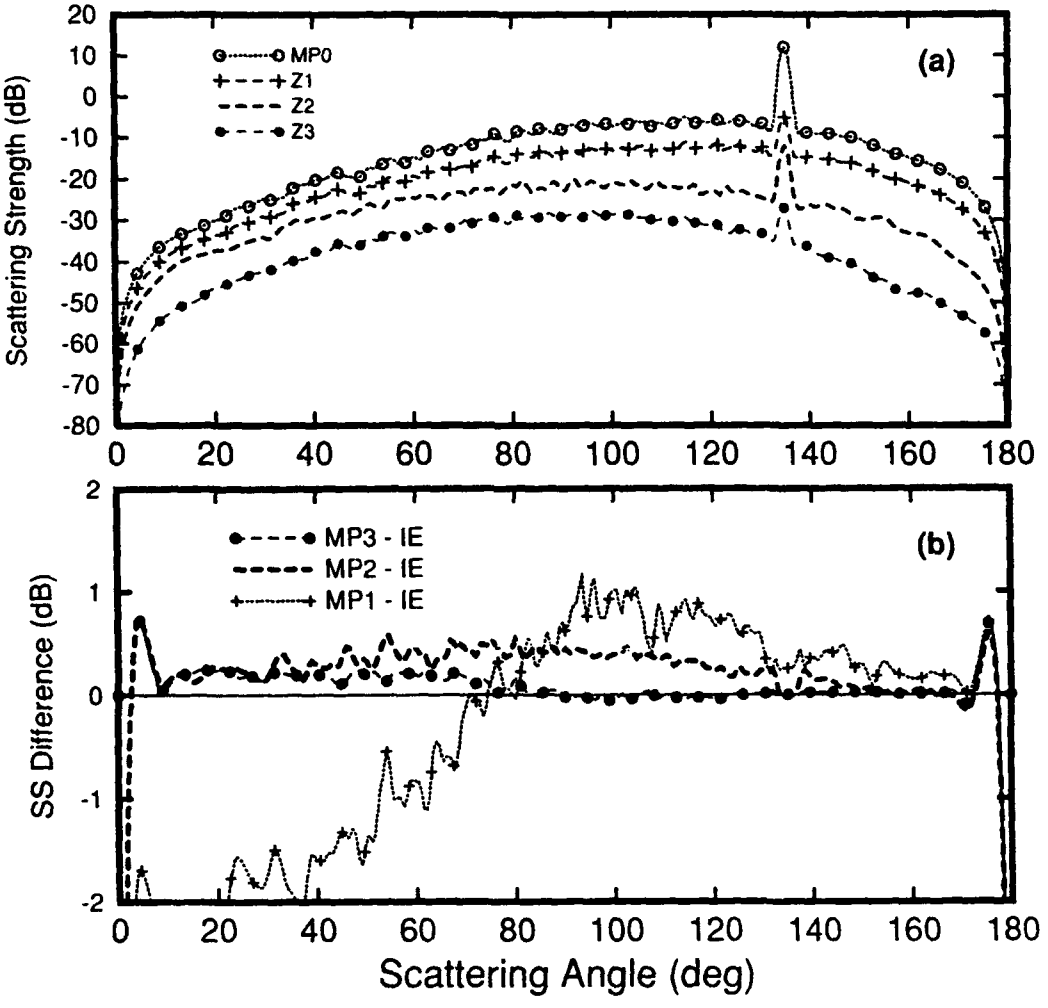

Figure 4.22 : Results of calculations using the $\hat{Z}^{-1}$ operator for case A2, with the parameters of Fig. 4.4. (a) Scattering strength contributions from each term in the $\hat{Z}^{-1}$ series for the scattering amplitude. (b) Error curves for the MP solution.

In addition to having poorer performance than the operator expansion method in the backscattering region, the mean-plane method also is less accurate in the near vertical direction. In Fig. 4.23b for case A3, with $kh = 0.69$ and $kl = 4.5$, the second order

$\hat{Z}^{-1}$ solution MP2 has more than 1 dB error for scattering angles near $\theta_s \approx 90°$.

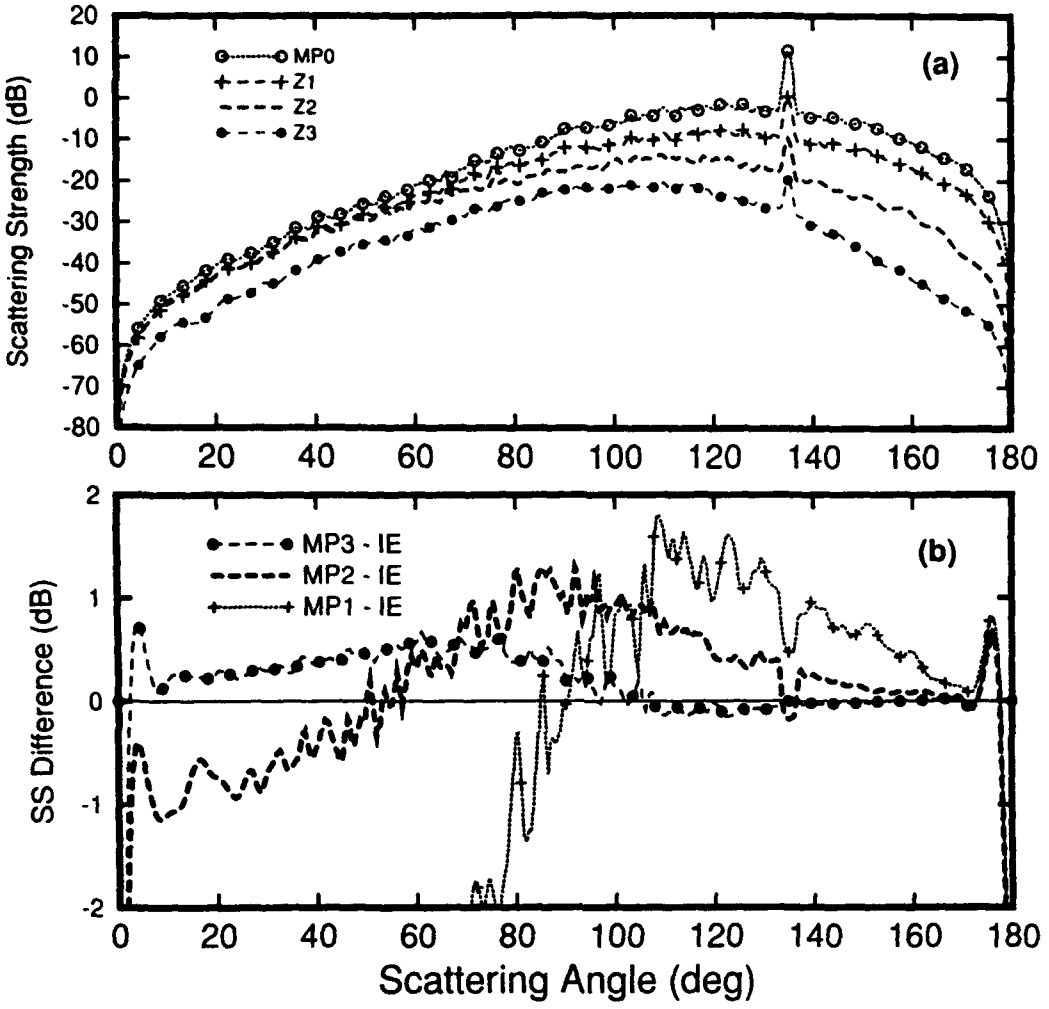

Figure 4.23 : Results of calculations using the $\hat{Z}^{-1}$ operator (mean-plane method) for case A3, with the parameters of Fig. 4.5. (a) Scattering strength contributions from each term in the Z^{-1} series for the scattering amplitude. (b) Error curves for the solution using the Mean-Plane (MP) method.

When kl is increased to $kl = 10$, with $kh \approx 1.03$ in case A4, the $\hat{Z}^{-1}$ series does not appear to be converging in the back direction, for angles $\theta_s \leq 90°$; see Fig. 4.24a. Nevertheless, the error curves in Fig. 4.24b do indicate convergence toward the correct solution. In the forward direction, the MP solution performs better than elsewhere; the third order solution MP3 is accurate over the forward scattering angles $\theta_s \geq 120°$. By comparison with Fig. 4.6, it is clear that the OE solution is much better than the $\hat{Z}^{-1}$ solution at treating scattering in this regime of larger kh values, when khs is still small.

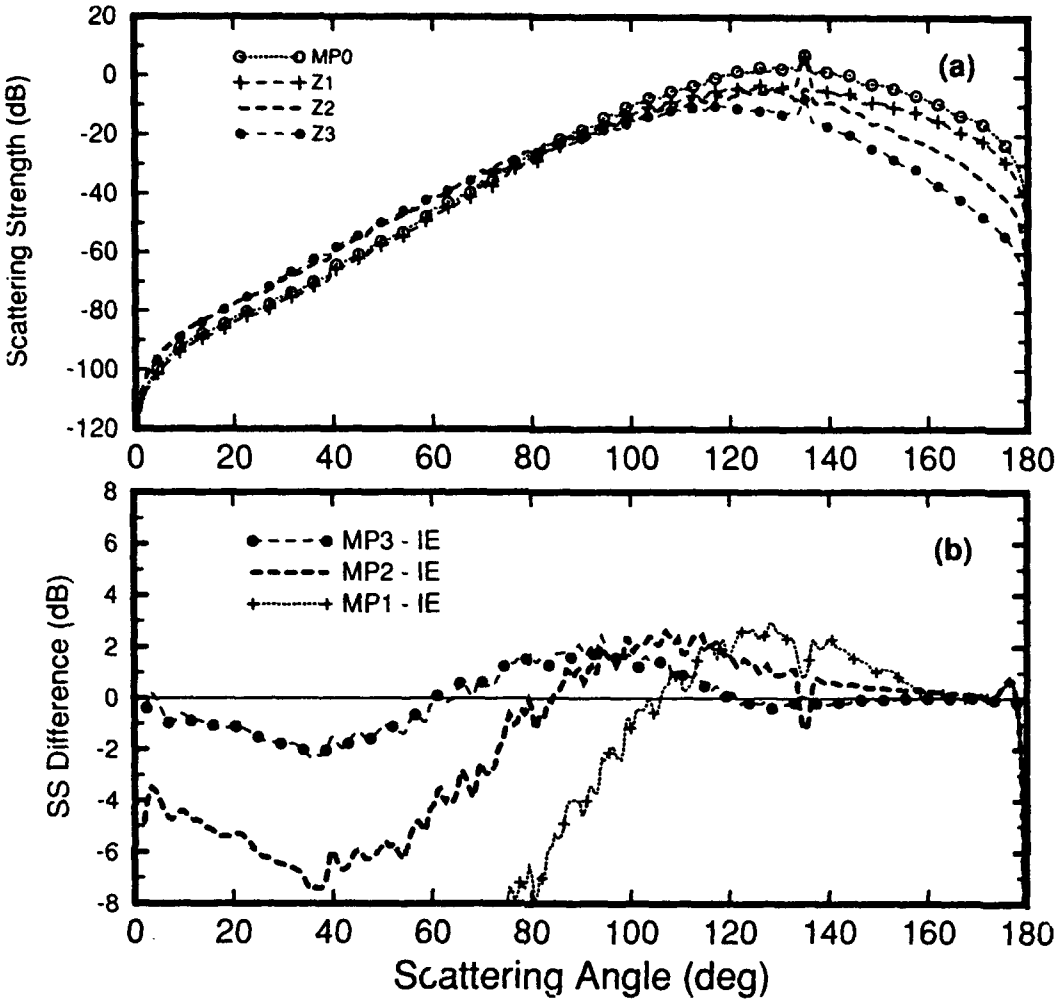

Figure 4.24 : Results of calculations using the $\hat{Z}^{-1}$ operator (mean-plane method) for case A4, with the parameters of Fig. 4.6. (a) Scattering strength contributions from each term in the $\hat{Z}^{-1}$ series for the scattering amplitude. (b) Error curves for the solution using the Mean-Plane (MP) method.

The Monte Carlo perturbation method error curves for lowest order ($\sigma^{(2)}$) and next order ($\sigma^{(4)}$) have been presented for case A1 in Fig. 4.3e, but we present them here in Fig. 4.25a for convenience in comparing with the $\hat{Z}^{-1}$ mean-plane method error curves for the same case, in Fig. 4.21b. The perturbation solution for case A2 is presented in Fig. 4.25b. It is clear by casual inspection of the error curves for the two methods that the mean-plane method is much more widely accurate than the perturbation method, at any given order. Note that the comparison is not directly equivalent for any but the lowest order (MP1 and $\sigma^{(2)}$) because the perturbation solution has been computed using the consistent expansion for the cross section (2.23), whereas the mean-plane method is computed using the truncated series (2.22); however, this difference actually favors the perturbation solution. Figure 4.25c illustrates the contrast between the two solutions MP2 and $\sigma^{(4)}$, which both contain terms of order no higher than $(kh)^4$, for case A3 located outside the validity region of $\sigma^{(4)}$. This calculation clearly illustrates the wider

accuracy of the mean-plane solution using operator $\hat{Z}^{-1}$; note that the scale in Fig. 4.25c is four times greater than in Figs. 4.25a and 4.25b. The method based on operator $\hat{Z}^{-1}$ might have been an attractive alternative to perturbation theory were it not for the existence of methods that are altogether less sensitive to the value of kh, such as, for example, the operator expansion method and the small slope approximation [Voronovich, 1985], which are accurate for large surface height when the surface slope is small.

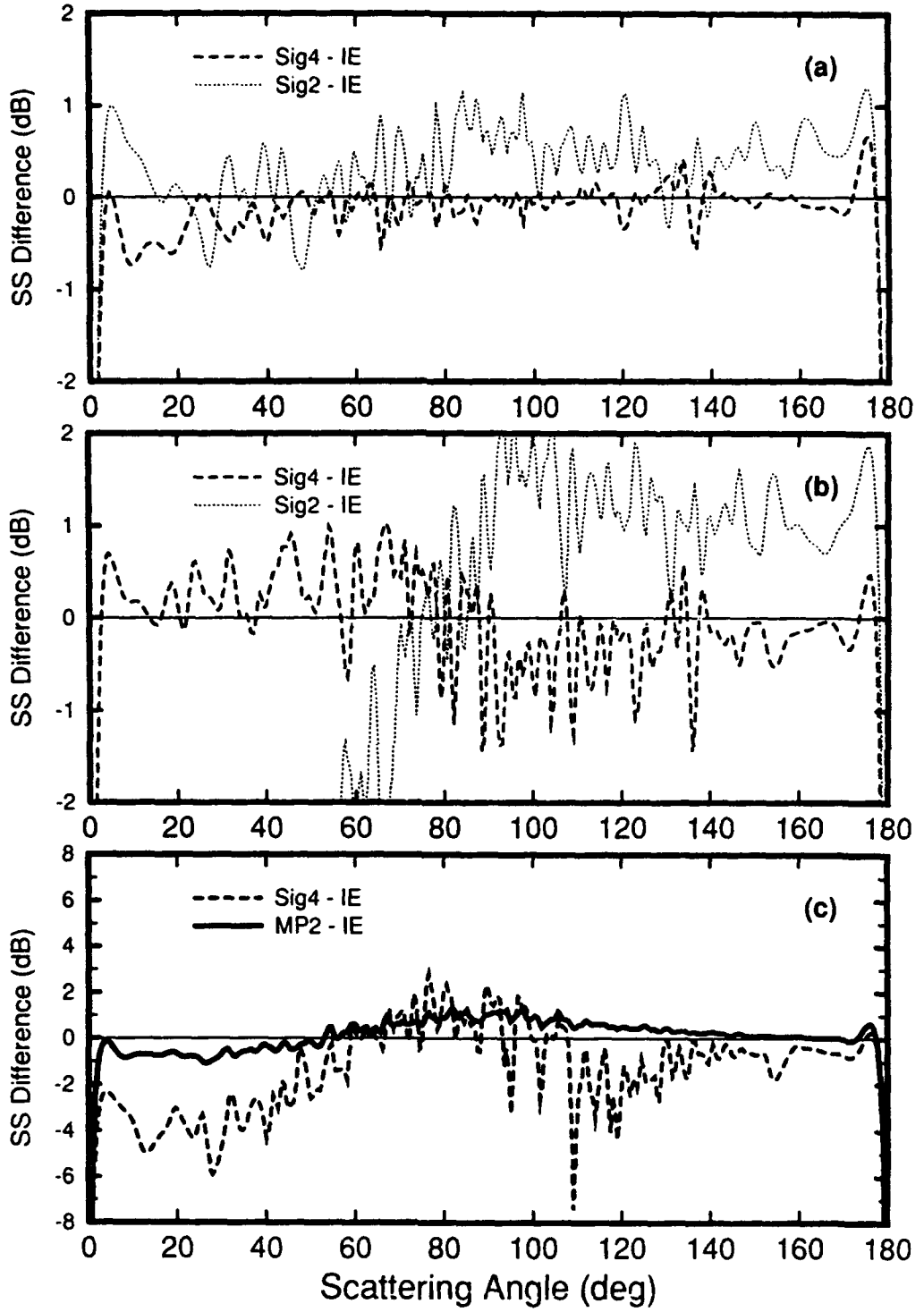

Figure 4.25 : Comparison between the perturbation method and the $\hat{Z}^{-1}$ mean-plane method. (a) Monte Carlo perturbation results for $\sigma^{(2)}$ and $\sigma^{(4)}$ (incoherent scattering), for case A1. (b) Monte Carlo perturbation results for $\sigma^{(2)}$ and $\sigma^{(4)}$ for case A2. (c) Error curves for the second order solution MP2 using the $\hat{Z}^{-1}$ method, and the perturbation solution $\sigma^{(4)}$, for case A3.

CHAPTER 5

Accuracy of the Operator Expansion for Surfaces with a Pierson-Moskowitz Spectrum

5.1 Introduction to Chapter 5

Many naturally occurring rough surfaces have surface height spectra that can be represented over a significant portion of the spectral band by a power law function of the spatial wave number. Such surfaces are rough at many length scales, and computing single-frequency scattering from such multiscale surfaces has been difficult since neither of the classical approximations (Kirchhoff approximation and perturbation theory) provides accurate results over the full range of scattering angles. In this chapter, we direct our study to relatively low frequency (200 to 1000 Hz) acoustic scattering from the ocean surface boundary and investigate the accuracy of the operator expansion method in this application. Scattering from the real ocean surface is a 3-D problem, additionally complicated by the presence of bubbles created by breaking waves and then carried to significant depths by surface circulation and mixing processes. Furthermore, gravity waves are nonlinear and nonsymmetrical (the waves do not look the same from above as they do from below). The OE method as currently developed can only compute scattering from a distinct boundary given an incident field known on the boundary, and does not account for variations in the neighboring medium. We use a simple sea surface model for the purpose of testing the OE method, and trust that the results of this study will carry over to more realistic applications, at least to realistic 2-D ocean surface shapes.

To model surfaces rough in one dimension (1-D)[†] we use a roughness spectrum derived from the Pierson-Moskowitz spectrum for a fully developed sea [Thorsos, 1990a]

$$W(K) = \left[\alpha / (4|K|^3)\right] \exp\left[-(\beta g^2)/(K^2 U^4)\right], \quad |K| \le K_c \tag{5.1}$$

and $W(K) = 0$ otherwise, and where the parameters $\alpha = 8.1 \times 10^{-3}$ and $\beta = 0.74$ are obtained from the Pierson-Moskowitz frequency spectrum [Pierson and Moskowitz, 1964]. Here $g = 9.81$ m/s^2 is the gravitational acceleration, and U is the wind speed (m/s) at a standard height of 19.5 meters. This power law spectrum is limited at low

[†] Recall that we specialize to 1-D surfaces because we rely on the solution of an integral equation (IE) to provide the exact result for the problem. The IE solution is too computationally intensive to be systematically applied to scattering from 2-D surfaces.

spatial wave numbers by a function of the wind speed U, and at high wave numbers by an upper cutoff K_c, about which more details are given below. The 1-D Pierson-Moskowitz spectrum (5.1) is plotted in Fig. 5.1 for wind speeds of 5, 10, 15, and 20 m/s, and a cutoff of $K_c = 2k$ for 200 Hz acoustic waves in water with a sound speed of 1500 m/s. Single surface realizations (each using the same sequence of random numbers) for the four wind speeds are also presented in Fig. 5.1.

A numerical study [Thorsos, 1990a] of scattering from 1-D Pierson-Moskowitz surfaces for a wind speed of 20 m/s (39 knots), and for incident angles between 10° and 20°, indicated that the Kirchhoff approximation accurately predicts the incoherent scattered field near the specular direction, but is inaccurate for backscattering. Conversely, perturbation theory with cross section computed consistently to fourth order in kh ($\sigma^{(4)}$) is very accurate in computing incoherent scattering over all scattering angles except near the specular direction. The operator expansion solution reduces to both classical approximations in their respective asymptotic limits, and numerical studies in chapter 4 using surfaces with a Gaussian spectrum indicate that the method is widely accurate for surfaces with small slope-height roughness parameter khs. This suggests that it might also perform well for low frequency scattering from ocean surfaces, for which khs is small.

It is important to note that without an upper wavenumber cutoff the rms slope for the Pierson-Moskowitz spectrum is unbounded. In this dissertation, we set the upper cutoff to no more than $K_c = 2k$ (maximum Bragg wave number) because integral equation studies have demonstrated numerically that retaining portions of the surface height spectrum above twice the acoustic wave number has little impact on the scattering results averaged over a set of surface realizations, for all scattering angles, though some differences are visible for scattering from single realizations. It is numerically advantageous to use a small value of K_c. A larger cutoff requires a significant increase in surface sampling density because the higher order operator expansion calculations effectively broaden the surface field spectrum through numerous convolutions with the Fourier transform of the surface height. The chosen cutoff of $2k$ results in a slope-height parameter value of about $khs = 0.25$ for 200 Hz scattering from 20 m/s surfaces. This value of the slope-height parameter is appropriate when including the full range of scattering angles, but it may effectively be lowered for scattering angles closer to the specular direction. In standard perturbation theory, the scattering results at any angle depend to first order on the value of the surface height spectrum at the Bragg wave number, indicating that an effective large-scale rms slope (obtained by cutting off the spectrum at near the Bragg wave number) might be a more appropriate value to use in describing the roughness regime for the OE (see for example Fig. 5.2). Numerical tests confirm that the OE converges more rapidly near specular, but no attempt has been

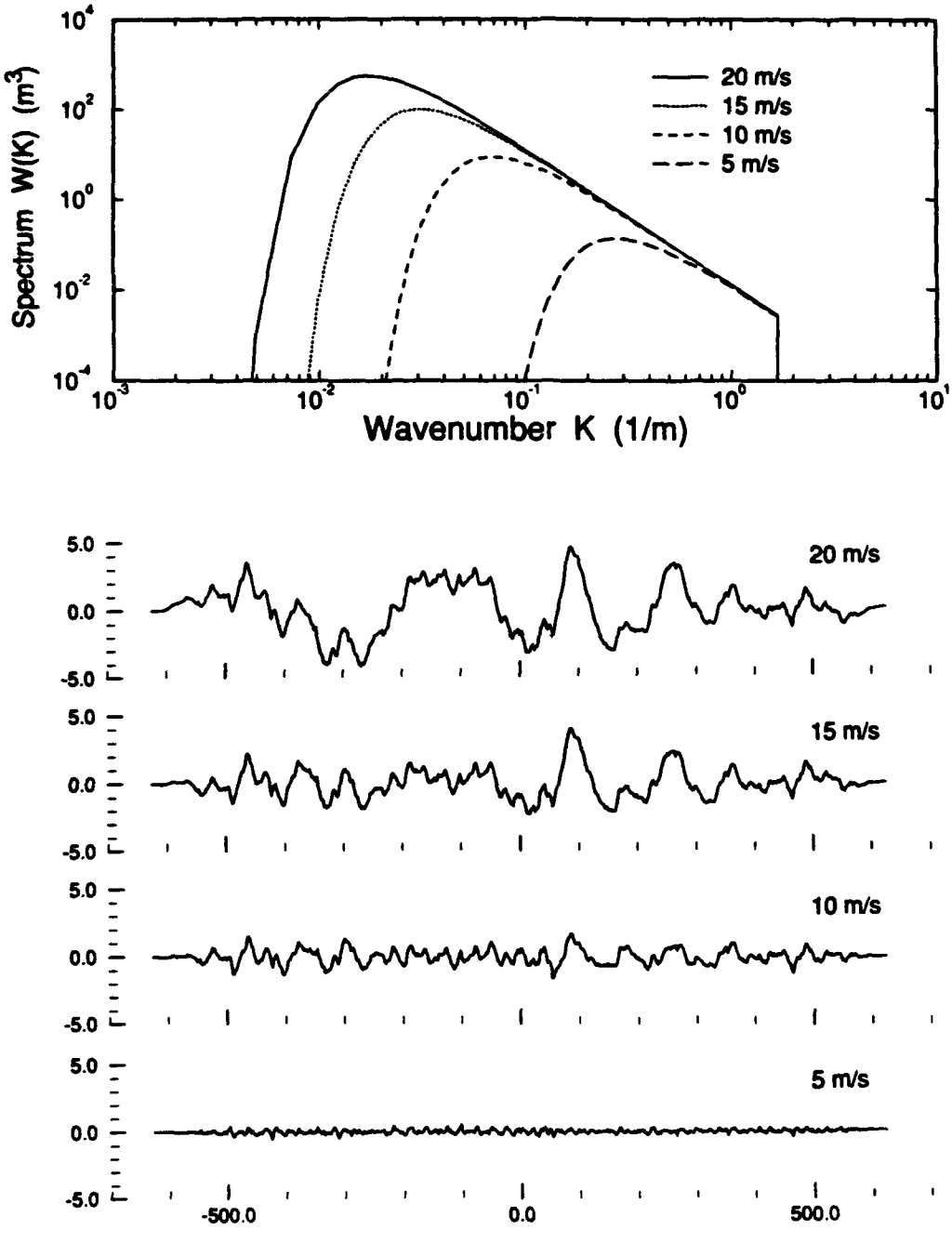

Figure 5.1 : The Pierson-Moskowitz spectrum, and individual surface realizations for four wind speeds: 5, 10, 15, and 20 m/s. The scales for the surface profiles are in meters.

made to relate the rate of convergence to a specific value of khs.

A cutoff of $K_c = k$ is used in Sec. 5.4 because the study emphasizes forward scattering. Again, integral equation studies[†] show numerically that including higher wavenumber components of the surface height spectrum does not change the results. Using a lower cutoff makes it possible to use longer surfaces (for better angular resolution) when studying scattering at low grazing incident angles. As discussed above, the smaller cutoff also reduces the rms slope for those surfaces, thereby lowering the slope-height parameter to a value that more accurately reflects the scattering regime for the operator expansion.

5.2 Low frequency scattering results — standard series

In this section, the standard series solution (3.40) of the operator expansion method is applied to 200 Hz scattering from 1-D Pierson-Moskowitz surfaces, with wind speeds between 5 and 20 m/s and for incident angles between 10° and 90°. In summary, the second order solution (OE_2) is accurate over the entire range of scattering angles for all incident angles tested, underpredicting the scattering strength by a maximum error of 0.5 dB near the backscattering direction for the most challenging case studied ($U = 20$ m/s and $\theta_i = 10°$). The first order solution (OE_1) is slightly less accurate over the entire range of scattering angles, reaching a maximum error of 2 dB near $\theta_s = 15°$, when $\theta_i = 10°$. The operator expansion solution for the coherent field is very accurate; the energy error for the total field is typically less than 2% for the first order solution OE_1, and less than 0.1% for the second order solution OE_2.

An example with 20 m/s wind speed and incident angle $\theta_i = 20°$ illustrates typical results obtained using the operator expansion. The convergence of the operator expansion solution for the surface field is evident when comparing the contributions from each order to the scattering strength, for an average computed from 50 surface realizations (Fig. 5.2a). The scattering strength curves for the first order solution (OE_1), the lowest order for which the proper angular behavior near grazing is obtained, and the second and third order contributions (ON_2 and ON_3) indicate that the ON_n series terms decay rapidly over all scattering angles, especially in the region near the specular direction. The convergence of the operator expansion solution to the integral equation result is illustrated in Fig. 5.2b which presents the scattering strengths for the zeroth and first orders plotted along with the Integral Equation solution (IE); higher orders are

[†] The OE solution shows a similar lack of sensitivity to the higher wavenumber surface components for this application to forward scattering.

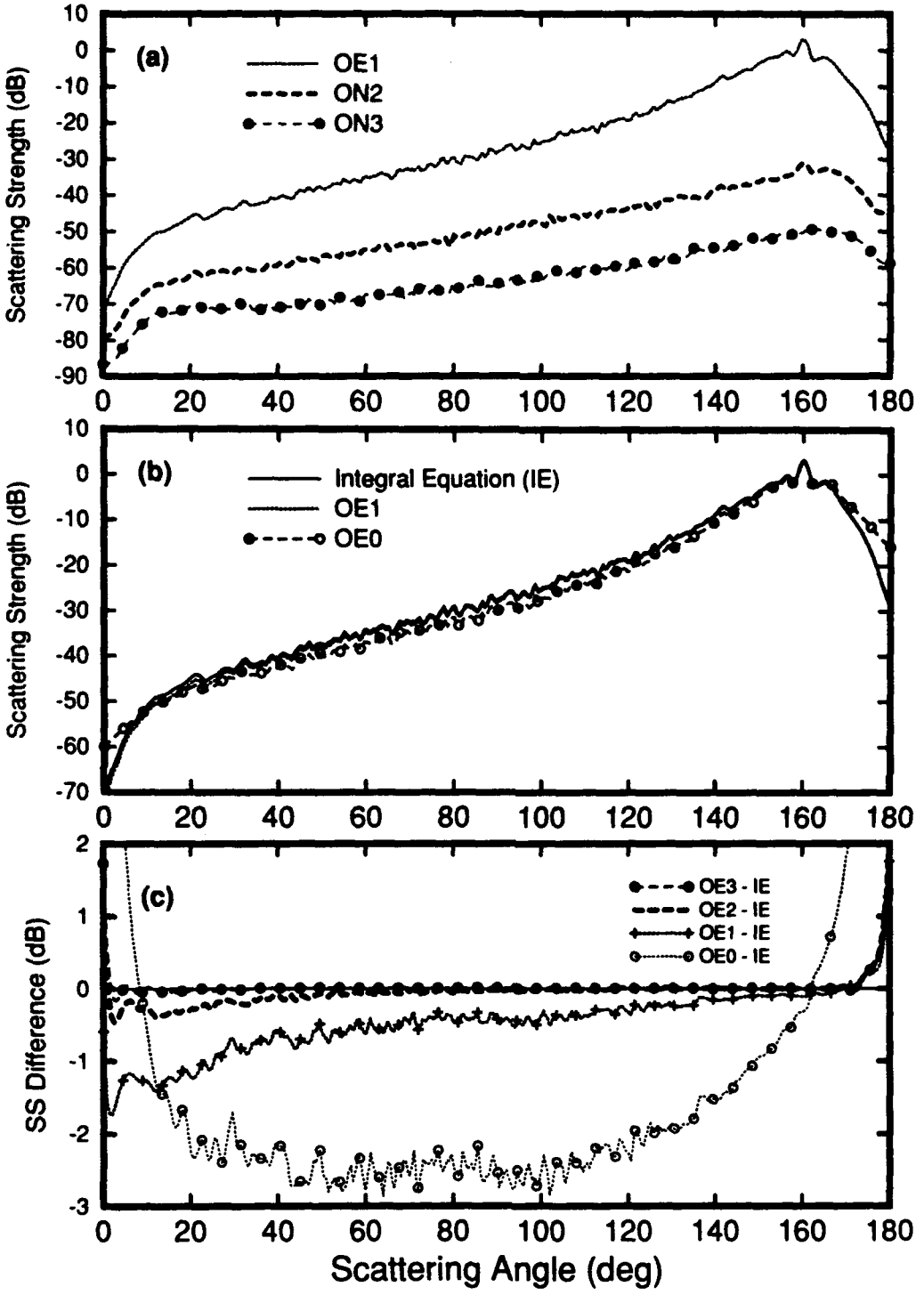

Figure 5.2 : Averaged results for 200 Hz scattering from 50 surfaces with a $U = 20$ m/s Pierson-Moskowitz spectrum and with $\theta_i = 20°$. The decay of the ON_n series is rapid and monotonic over all scattering angles (a). The scattering strengths for zeroth and first order solutions OE_0 and OE_1 are plotted against the integral equation solution (b). Accuracy of the OE solutions is illustrated in detail using scattering strength differences with the integral equation solution (c).

indistinguishable from the IE curve at this scale. As in the Gaussian examples, the difference between the operator expansion scattering strengths and the integral equation scattering strength provides a clear picture of the accuracy of the operator expansion solution for each order up through OE_3; see Fig. 5.2c. Within a few degrees of grazing the OE solution is not as reliable as elsewhere, though the maximum error is typically only 1-2 dB at grazing in either direction for the computational surface lengths used in the examples. This error can be reduced to about 0.5 dB by zero-padding the computational surface to twice the minimum number of intervals (2048); see Fig. 5.10.

The convergence rate of the operator expansion solution depends on the incident angle in a manner similar to that observed for single scale surfaces: the solution is generally more accurate when the incident angle is further from grazing. For $\theta_i = 90°$ the averaged first order solution (OE_1) reaches a maximum error of about 0.5 dB near $\theta_s = 20°$, compared to 0.7 dB when $\theta_i = 45°$, 1.3 dB for $\theta_i = 20°$, and 2 dB for $\theta_i = 10°$. The scattering strength differences (error curves) between the operator expansion solutions and the integral equation solution for $\theta_i = 10°$, 45°, and 90° are presented in Figs. 5.3a, 5.3b, and 5.3c, respectively. The curves in Fig. 5.3 indicate that for any given order (and for this surface roughness), the error in scattering strength is essentially determined by the angular distance away from the specular direction $|\,180° - \theta_i - \theta_s\,|$; from this and other examples it seems that scattering results for low grazing angles of incidence can be used to infer accuracy for higher incident grazing angles.

No fundamentally different behavior is noted as the incident angle is further reduced to near the rms surface slope angle, which is about 7° for these surfaces (for a cutoff of $K_c = 2k$), where multiple scattering between large surface features might be expected to occur. Examples emphasizing very low angle scattering are presented in Sec. 5.4.

5.3 Low frequency scattering results — alternative series

In this section, we investigate the accuracy of further simplifications introduced by Milder which involve only odd-termed (3.41), or only even-termed (3.42), operator series. Numerical examples illustrate that use of these shorter forms in computing scattering from Pierson-Moskowitz surfaces results in a reduction in computational expense while clearly improving upon the accuracy of the standard solution (3.40).

We also revisit the question regarding the relative merit of retaining consistency in the expansion for the cross section at the expense of computational efficiency which was addressed in Sec. 4.4.2 for scattering from surfaces with a Gaussian spectrum.

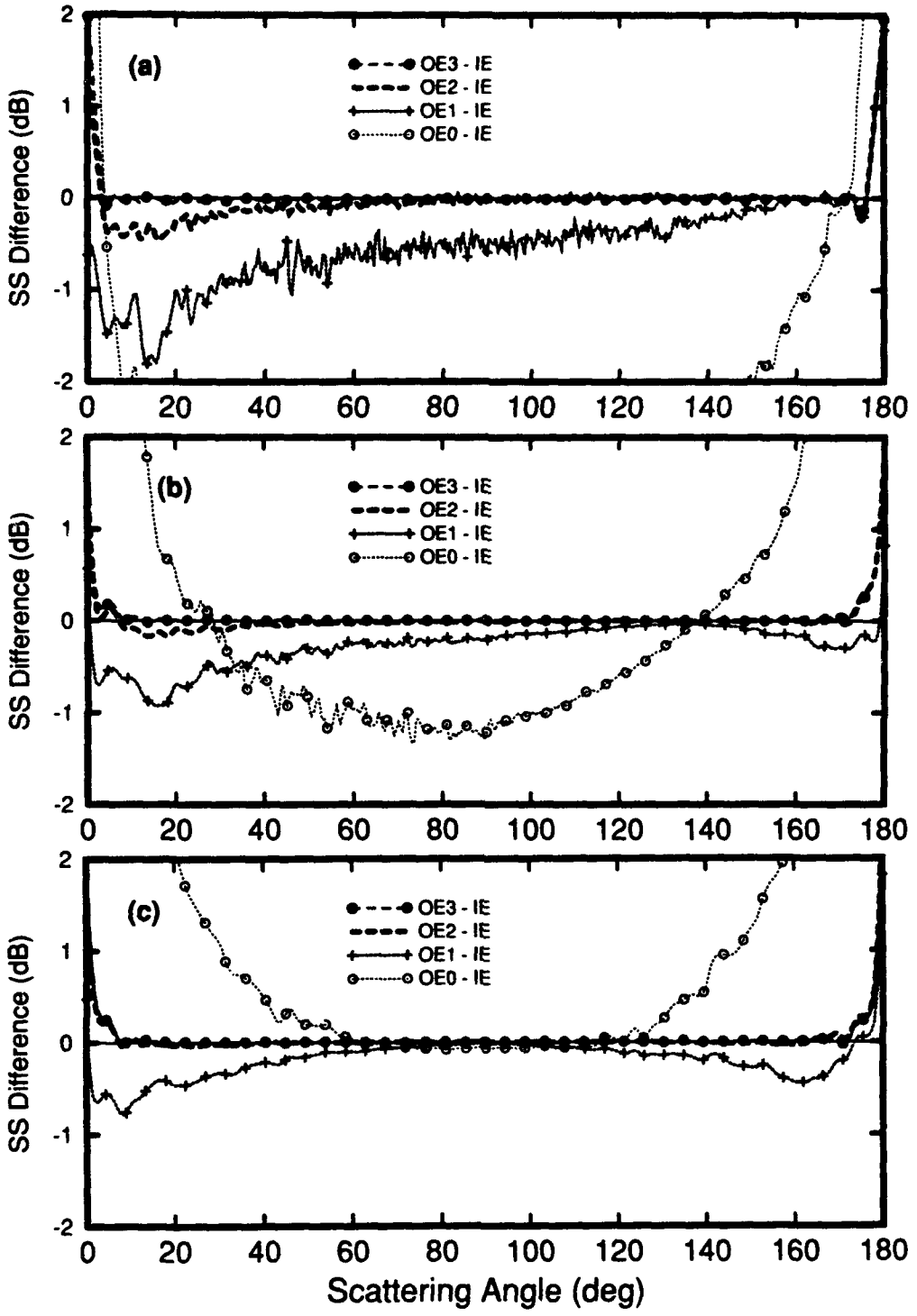

Figure 5.3 : Convergence and accuracy of the operator expansion solution as a function of angle of incidence for 200 Hz scattering from 20 m/s 1-D Pierson-Moskowitz surfaces. $\theta_i = 10°$ (a), $\theta_i = 45°$ (b), and $\theta_i = 90°$ (c).

Those findings suggested that consistency in the expansion parameter is not required in order to maintain accuracy; it turns out that the same is true for scattering from Pierson-Moskowitz surfaces. First we examine the accuracy of the short series solutions.

For this power law spectrum, the short series computed to order n are almost as accurate as the standard series taken to order $n+1$, providing a solution which is easier to compute and more accurate for any given order in the surface field. This behavior is dramatically illustrated by comparing the scattering strength for the even series solution EV_0 to the standard solution OE_0. Recall that OE_0 is never accurate for a significant range of angles near grazing (within about 15° for the parameters of Fig. 5.2), whereas OE_1 is essentially correct in this region. For the forward scattering angles ($90° \le \theta_s \le 180°$) we see through comparison with the integral equation solution that, for the 20 m/s surface and $\theta_i = 20°$, the operator expansion solution obtained using EV_0 is accurate over the full range of forward angles, *including* those between 165° and 180°; see Fig. 5.4.

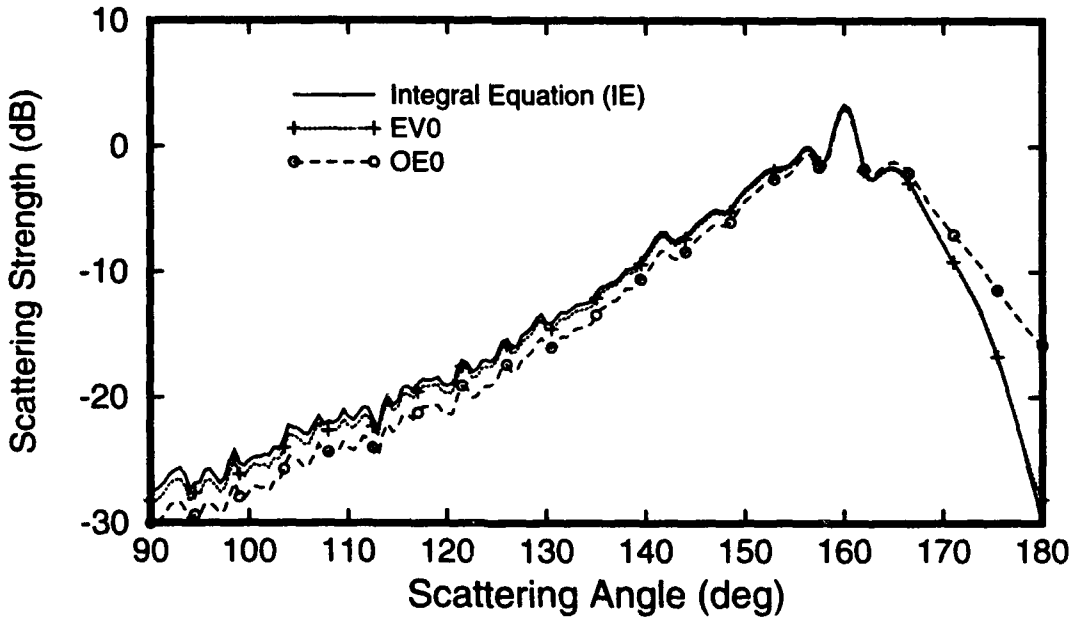

Figure 5.4 : Comparison between the zeroth order standard series solution (OE_0) and the zeroth order even series solution (EV_0) for forward scattering angles. The exact integral equation solution (IE) is also presented for reference.

Ranking the various operator expansion solutions by their relative accuracy for scattering from surfaces with a Pierson-Moskowitz spectrum is very easily accomplished because the standard OE solution approaches the exact scattering strength from below (Fig. 5.2c) over all scattering angles. The short series solutions (3.41) and (3.42) are consistently more accurate than the standard series (3.31), for any given order in the surface field. Qualitatively, the relative accuracy of the solutions is maintained over all scattering angles except for those very near grazing (less than about 3 degrees), for which the operator expansion solution is not as reliable. For the example of Fig. 5.2, where the wind speed is $U = 20$ m/s and the incident angle is $\theta_i = 20°$, the differences between the scattering strengths of the operator expansion solutions and the integral equation result are presented in Fig. 5.5. The error curves for the standard solutions OE_0, OE_1, and OE_2 are plotted in broken lines, and the error curves for the short forms EV_0, OD_1, and EV_2 are plotted using solid lines. It is easy to see that the short forms evaluated to order n in the surface field have the character and nearly all of the accuracy of the standard solution evaluated at order $n+1$.

We conclude this section by presenting the error curve for the second order consistent solution $OE^{(2)}$ (2.23c) compared with the first order truncated solution (2.22b) curves using the standard series for the scattering amplitude (OE_1), and using the odd series (OD_1); see Fig. 5.6. The $OE^{(2)}$ curve is more accurate than OE_1 but less accurate than OD_1 over all scattering angles. This example is typical for scattering from Pierson-Moskowitz surfaces, and clearly illustrates the lack of importance of retaining consistency in constructing the cross section in the operator expansion method. Comparing the curves in Fig. 5.6 with those in Fig. 5.5 we see that the second order truncated solution OE_2 is more accurate than the second order consistent solution $OE^{(2)}$, while being faster to compute. The short series solutions are faster yet, and are the most efficient forms of the operator expansion solution among those investigated.

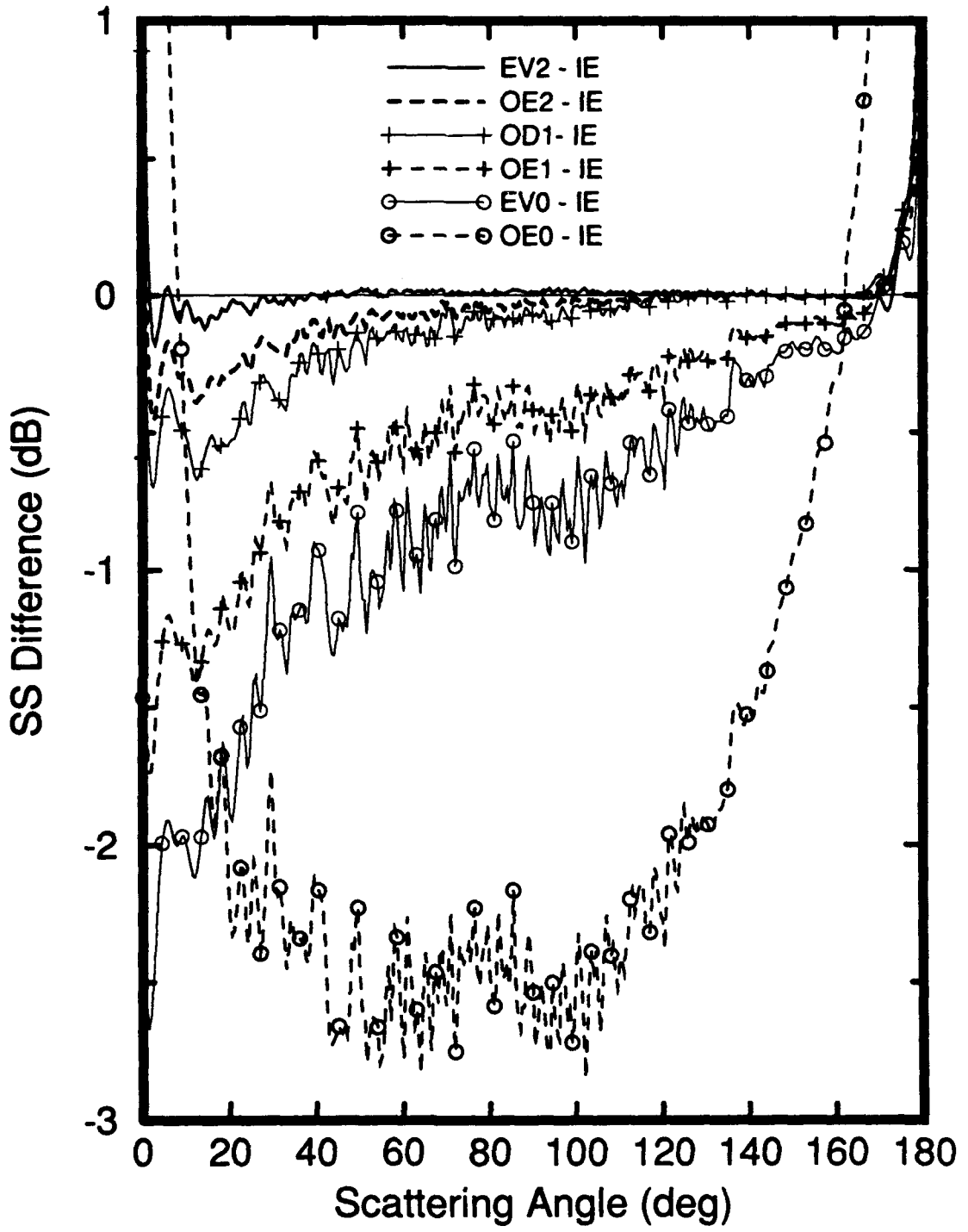

Figure 5.5 : Scattering strength errors for all operator expansion solutions up to second order in the surface field expansion, for the parameters of Fig. 5.2.

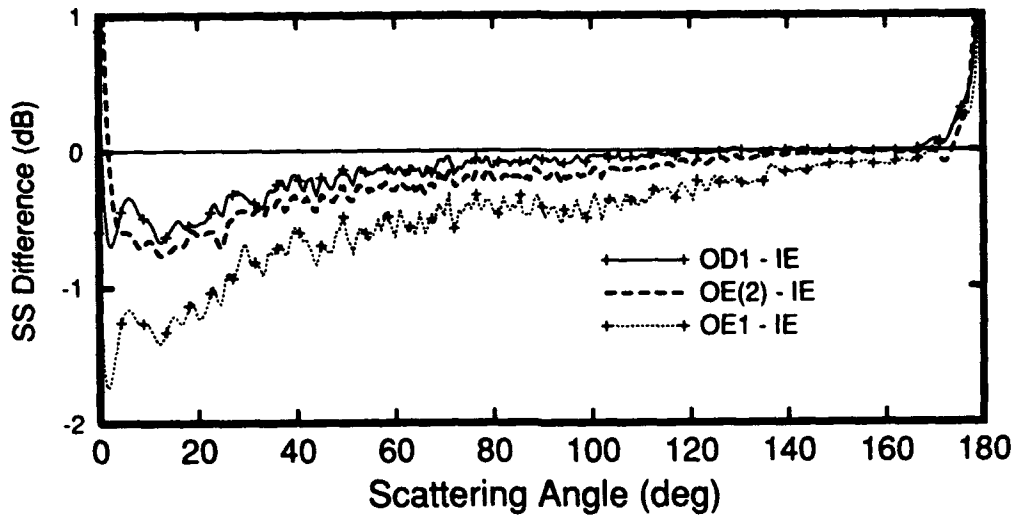

Figure 5.6 : Comparison between the consistent solution computed to second order in the surface field $OE^{(2)}$ and the truncated solutions computed to first order in the surface field (standard series solution OE_1 and odd series solution OD_1), for the parameters of Fig. 5.2.

5.4 Results for higher frequency, and very low grazing angles

In Sec. 5.4 we extend the operator expansion calculations to higher frequencies and lower incident grazing angles, for which the scattering regime is more stringent. This investigation is important because many sea surface scattering applications are characterized by low grazing angle propagation over a wide range of frequencies. Distant multiple scattering (an area of weakness for the OE) becomes increasingly likely in this regime. Recent studies of the accuracy of the "single backscattering multiple forward scattering" approximation [Thorsos, 1990b] indicate that for low grazing angle propagation, distant multiple scattering is only important in successive forward scattering, either propagating away from the source, or back toward the source; accurate results can be obtained using a single backscattering event in which the wave reverses direction, and this backscatter can be accurately treated using lowest order perturbation theory. Furthermore, backscatter from ocean surfaces is typically dominated by volume scattering from near surface bubbles, particularly for wind speeds above about 8 m/s. The accuracy of the OE method has also been found to degrade as the incident angle approaches grazing, though this behavior is worst in the backscattering region. We will therefore concentrate on studying the accuracy of the OE method in computing forward scattering from the ocean surface (the air-sea interface) at low grazing angles. The value of the slope-height parameter khs has been observed to give a general indication

of the accuracy of the operator expansion solution, and *khs* is proportional to the frequency of the acoustic wave; we will therefore extend the calculations to higher frequencies than previously considered.

Studies of low grazing angle surface scattering are difficult because significantly longer surfaces are required to maintain sufficient angular resolution in the scattering cross section. Since the sampling density along the surface is only a function of the acoustic frequency and the surface roughness (specifically, the value of the upper cutoff K_c), the number of surface partitions increases in proportion to the surface length. Thus, exact scattering calculations using the integral equation method used above [Thorsos, 1988] become very intensive as the incident grazing angle is reduced below about $\theta_i \lesssim 10°$, for $f \approx 400$ Hz.

The Parabolic Equation (PE) has long been used to compute propagation of energy in the ocean for angles relatively close to the horizontal direction [Tappert, 1977]. For that restricted range of angles, and to model "one-way" propagation (appropriate for weakly scattering media for which there is little scattering in the back direction), the parabolic equation is a good approximation to the Helmholtz Equation (HE). Many refinements to the standard PE approximation have led to algorithms that can accurately compute one-way wave propagation over a very wide range of angles about the forward (horizontal) direction. Recently, a parabolic equation approximation has been applied to surface scattering [Thorsos, 1987, 1993b], and an associated integral equation technique has been developed yielding a practical numerical solution to low grazing angle scattering. Within this approximation (which accurately matches the Helmholtz equation results for forward scattering for scattering angles within about 45° of grazing) an accurate numerical solution is now available which can readily treat scattering from surfaces an order of magnitude longer than previously possible with the technique based on the HE. We use this Parabolic Equation Integral Equation (PEIE) method to evaluate the accuracy of the operator expansion for low angle forward scattering. (The OE is still much faster to evaluate than the PEIE solution.)

Using the PEIE solution, the accuracy of the operator expansion solution has been examined over the range of scattering angles $135° \leq \theta_s \leq 180°$, for incident angles $5° \leq \theta_i \leq 20°$, with frequencies $f = 200$ Hz, 500 Hz, and 1000 Hz, and for 1-D Pierson-Moskowitz surfaces with 15 m/s wind speed. In these studies, the upper cutoff for the surface roughness spectrum is $K_c = k$; integral equation studies confirm that higher wavenumber components do not contribute significantly to forward scattering. The number of surface partitions used in computing scattering for $\theta_i = 10°$ and $f = 200$ Hz is 1000. For the most challenging case, $\theta_i = 5°$ and $f = 1000$ Hz, 20,000 surface partition intervals are used; typically, the number of intervals required to provide

adequate angular resolution and accuracy in the scattered field is inversely proportional to the square of the incident grazing angle, for angles near grazing. Results for all calculations are averaged over 50 surface realizations.

The first case we present is for incident angle $\theta_i = 10°$ and $f = 500$ Hz ($kh = 2.513$, $khs = 0.309$). The incoherent† contributions to the scattering strength for each of the surface field terms (beginning with the first order solution OE_1) in Fig. 5.7a indicate rapid decay over all forward angles in the range $135° \le \theta_s \le 180°$. The depression centered about the specular direction $\theta_{sp} = 170°$ visible in OE_1 is due to the gap in the 15 m/s surface height spectrum at low wave numbers, leading to a very small contribution. This effect is observed in perturbation theory as well, where there are no Bragg contributions in a spectral gap. (We observe that the depression is not visible in ON_2 and ON_3 because these contain only higher order contributions.) The error curves for the standard series solutions in Fig. 5.7b indicate that the OE solution is accurate at first order, though some error remains in OE_1 near the specular direction which requires higher order contributions because of the gap in the surface height spectrum. All OE solutions are somewhat unreliable within a couple of degrees from grazing, though for this set of parameters the OE solution converges to a very accurate solution near grazing. The OE_2 and OE_3 curves are actually more accurate than the PEIE solution for angles $\theta_s \lesssim 165°$, because the parabolic equation solution has a systematically increasing error as the scattering angle is decreased further from the forward horizontal direction (180°). In all examples presented in this section, the PEIE overpredicts the correct scattering strength obtained by exact solution of the HE by an amount that can be inferred from the difference between OE_3 and the zero line (PEIE) in Fig. 5.7b. Not surprisingly, the short series solutions converge more rapidly to the exact solution; see Fig. 5.7c.

† Only incoherent scattering strength is considered in the forward scattering examples because the strong (and broad) coherent signal masks some of the interesting behavior of the OE method. Typical physical scattering may have a much narrower coherent peak than is possible to obtain with tapered wave numerical simulations.

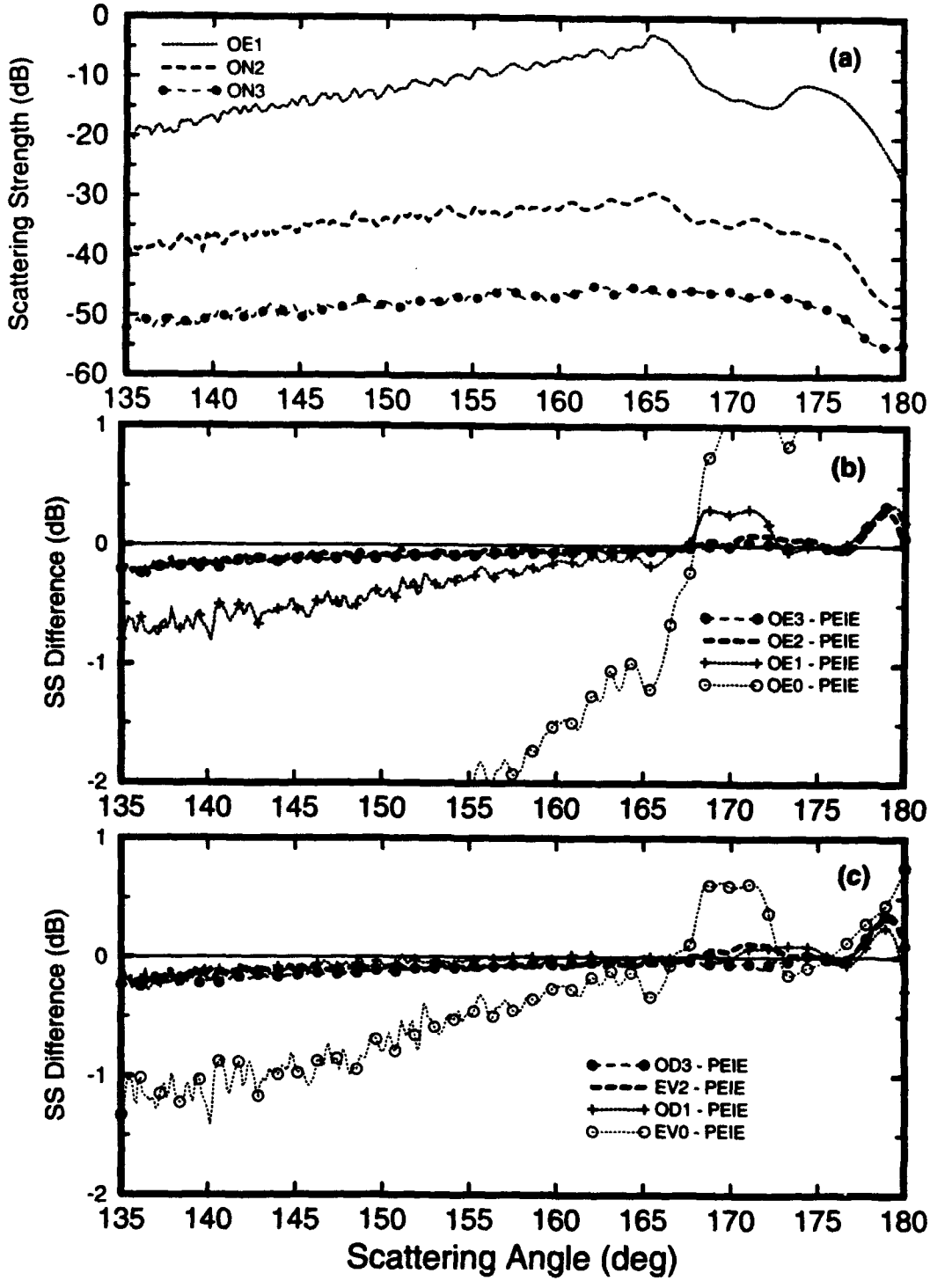

Figure 5.7 : Average (50 surfaces) scattering results for the operator expansion compared with the Parabolic Equation Integral Equation (PEIE) solution, for scattering from 15 m/s Pierson-Moskowitz surfaces with incident angle $\theta_i = 10°$ and acoustic frequency $f = 500$ Hz, using 2500 surface intervals. Scattering strength contributions from the ON_n series (a). Accuracy of the OE_n standard series solutions (b). Accuracy of the short series solutions (c).

The convergence of the OE solution changes somewhat as the incident angle is reduced to $\theta_i = 5°$, for the same frequency $f = 500$ Hz, so that the rms height and slope are the same as for the previous example. The specular direction is now only 5° from grazing, and higher order contributions are required to obtain an accurate solution from 175° to 180°. Note that the decay of the ON_n series (Fig. 5.8a) for 5° incidence is less rapid near grazing than for 10° incidence. This is reflected in the accuracy of the OE_1 solution, which begins to deviate from the exact solution near 172° and exceeds 1 dB error between 176° and grazing; see Fig. 5.8b. All short series solutions (except EV_0) are accurate over the entire range of forward angles studied (see Fig. 5.8c), except perhaps for OD_3 within 1° of grazing; the operator expansion solutions are relatively quite unreliable within a degree or two near grazing, producing results that occasionally vary by 1 or 2 dB depending on the particular set of surface parameters used.

Increasing the frequency to 1000 Hz ($kh = 5.03$, $khs = 0.673$) while maintaining 5° incidence still leads to an accurate operator expansion solution, but begins to show how the method's convergence degrades with increasing roughness. The decay of the OE_1, ON_2, ON_3 series is slower in the angular region $172° \le \theta_s \le 180°$ than for $f = 500$ Hz, and is not monotonic for this example (Fig. 5.9a) in the region very near grazing. The standard series error curves do not converge monotonically to the exact solution for scattering angles greater than $\theta_s \ge 172°$, which corresponds to the angular location of the edge of the gap in the scattering strength. As previously discussed, this gap is due to the lack of low wavenumber energy in the surface height spectrum, and contributions from higher order OE terms dominate in this angular region. Nevertheless, the OE solutions (first order and higher) are all accurate over the range of angles studied here, with OE_1 reaching 1 dB error at 135° (Fig. 5.9b). The short series are similarly accurate (Fig. 5.9c). Some very distant multiple scattering can occur for this last example, because the ratio between the wavelength of the surface waves at the peak of the spectrum for 15 m/s waves and the acoustic wavelength is $\lambda_{peak} / \lambda = 140$, but the slope of these large scale waves is very small. The number of surface partition intervals for this case is 20,000, and computations with further reduction of the incident angle, or increase of the acoustic frequency, have not been performed. Nevertheless, this study has shown that the operator expansion can give reliable results for a wide range of roughness regimes, in forward scattering from 1-D Pierson-Moskowitz Dirichlet surfaces.

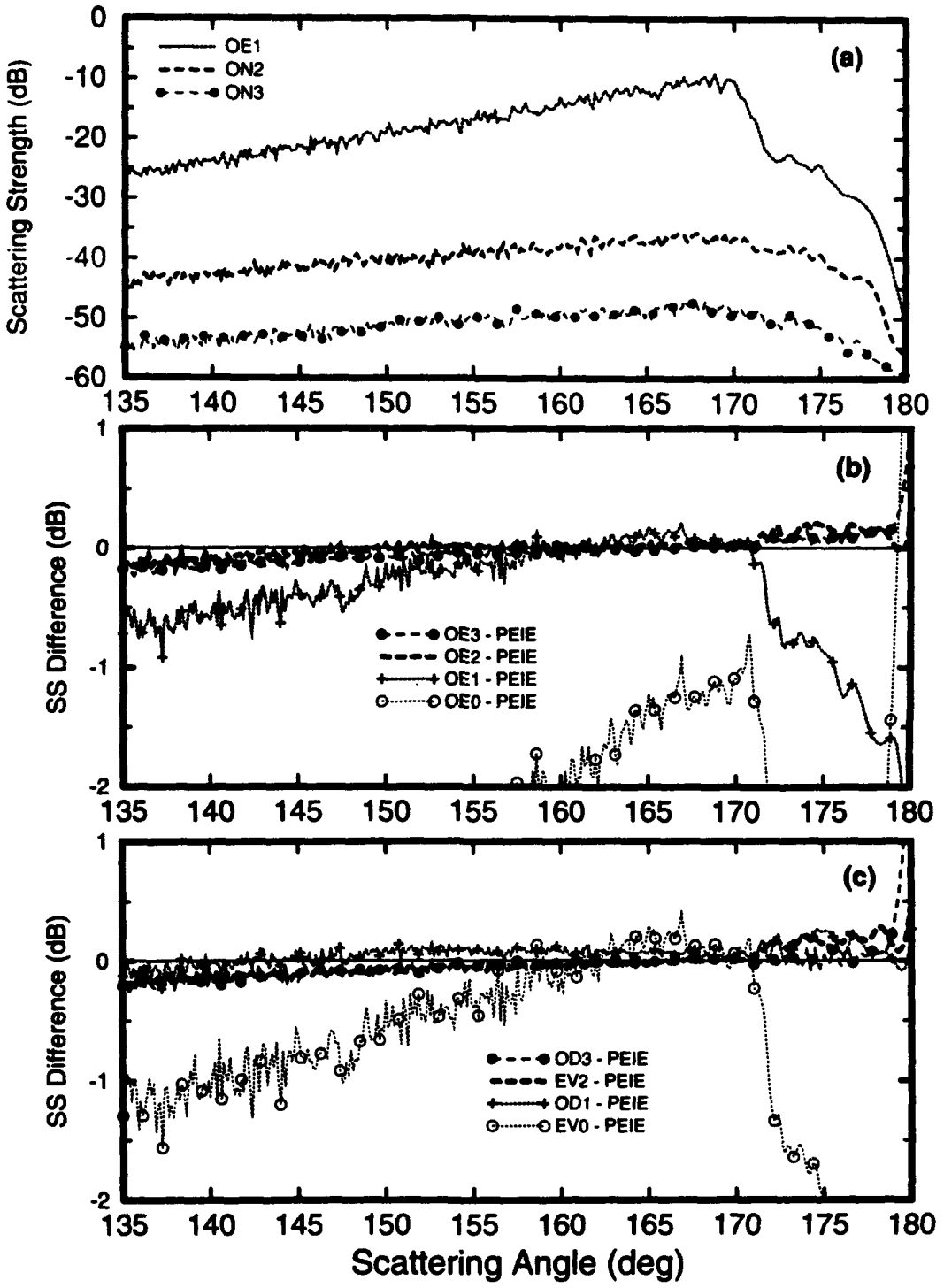

Figure 5.8 : Results for scattering from 15 m/s Pierson-Moskowitz surfaces at $\theta_i = 5°$, with $f = 500$ Hz, using 10,000 surface intervals. Scattering strength contributions from the ON_n series (a). Accuracy of the OE_n standard series solutions (b). Accuracy of the short series solutions (c).

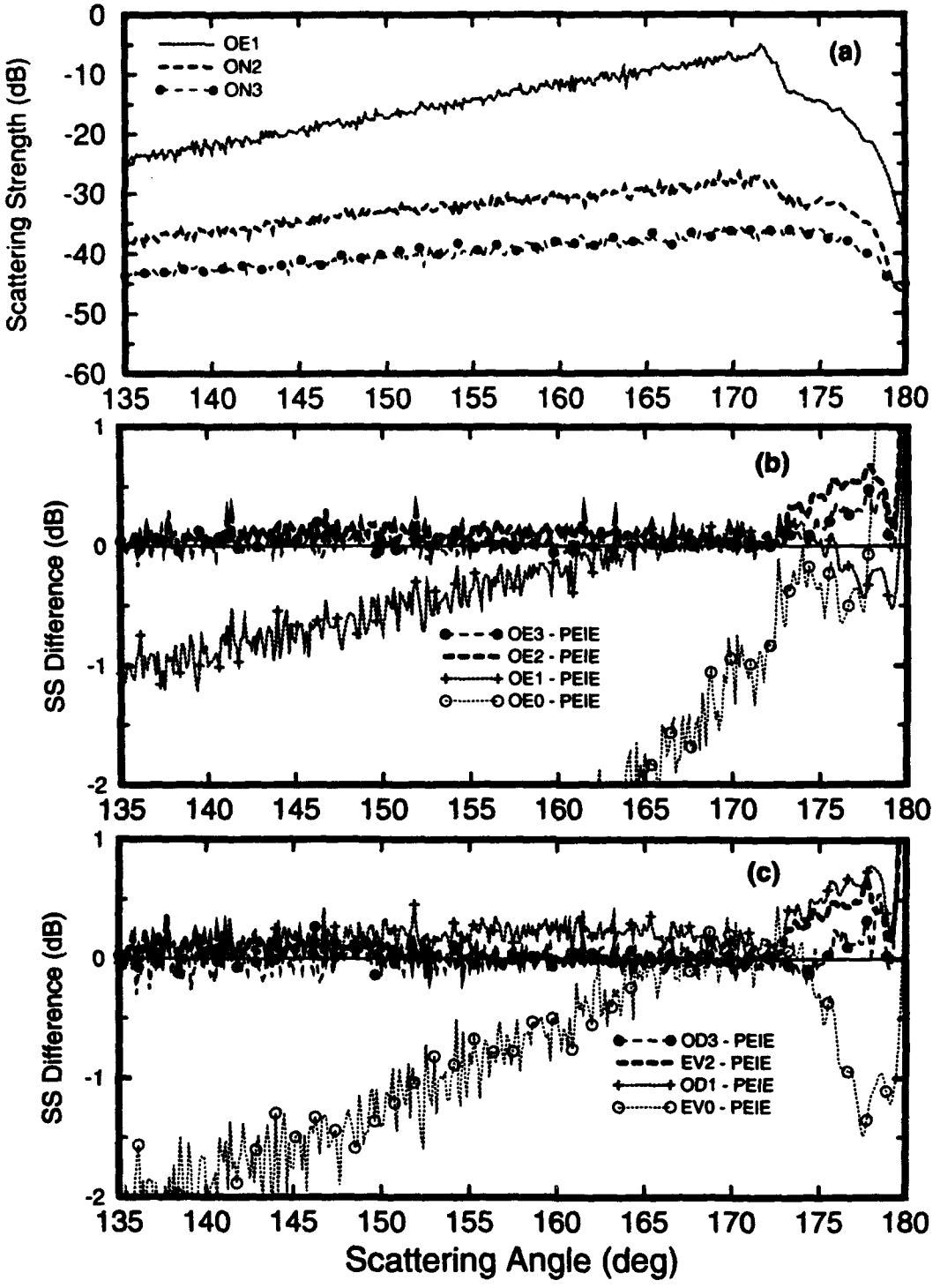

Figure 5.9 : Results for scattering from 15 m/s Pierson-Moskowitz surfaces at $\theta_i = 5°$, with $f = 1000$ Hz, using 20,000 surface intervals. Scattering strength contributions from the ON_n series (a). Accuracy of the OE_n standard series solutions (b). Accuracy of the short series solutions (c).

We conclude this section by illustrating the effects of extending the computational surface length by zero-padding the rough surface profile, a procedure discussed in Sec. 3.3.4. The error curves for the second order solution OE_2 for several different computational surface lengths are presented in Fig. 5.10. The same rough surface ensemble used in Fig. 5.2 is used here; each rough surface is divided into 1000 intervals. The shortest computational surface is therefore extended by zero-padding to 1024 intervals. The error at grazing for this surface length is about 2 dB, and is essentially independent of calculation order (except for OE_0 which has a much larger error near grazing due to its similarity to the Kirchhoff Approximation). The error in the angular region within a few degrees of grazing is significantly reduced by further extending the computational surface length (by zero-padding) to the next power of two, that is, 2048 intervals; at grazing, the error is about 0.5 dB for this surface length. Further reductions in numerical error are possible by continuing to lengthen the computational surface, but these improvements are modest and are not likely to be worth the additional computational cost. In many cases, using the minimum computational surface length is satisfactory, and all calculations in this dissertation (except for the ones used in Fig. 5.10) were performed by extending the number of surface intervals to the nearest power of two.

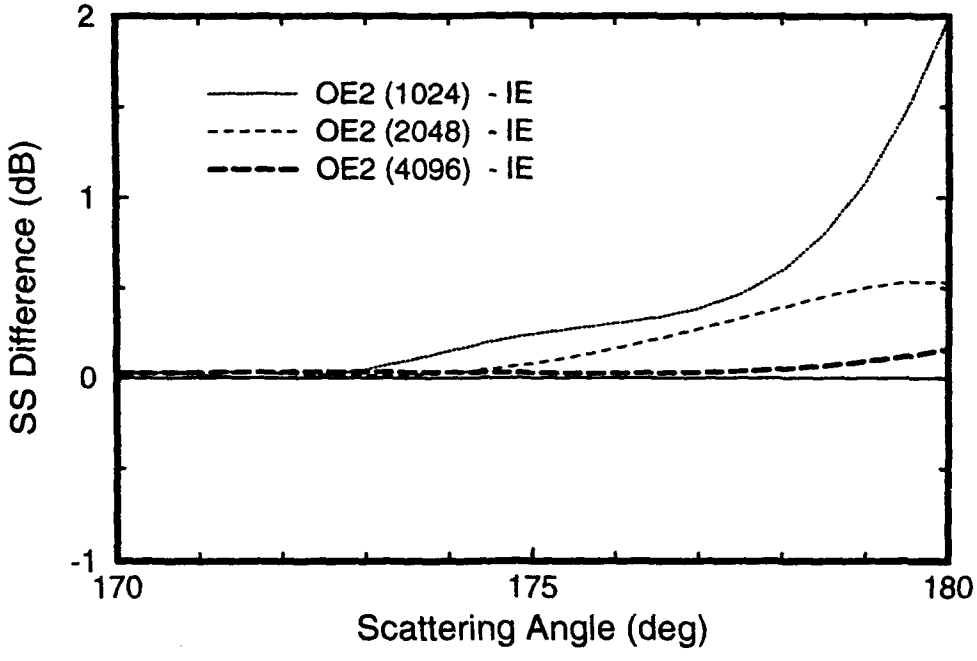

Figure 5.10 : The effect of computational surface length on near-grazing accuracy. The error curves are presented for OE_2 using 50 rough surface realizations with each rough surface divided into 1000 intervals. The computational surface for the operator expansion calculation was extended by zero-padding to 1024, 2048, and 4096 intervals.

CHAPTER 6

Formal Average of the Operator Expansion Solution

6.1 Introduction

The field scattered by a single randomly rough surface is itself a random function of space. Similarly, at any given point in space, the field scattered by each different surface realization is a random process. It is in this latter sense that we will consider the random scattering problem. The moments of the scattered field, obtained by averaging over the ensemble of random surfaces, are often of greater interest than the field scattered by a single "deterministic" surface. The operator expansion method has been derived and implemented to compute scattering from one surface profile at a time. To compute moments of the scattered field using the OE method we have resorted to numerically averaging the scattering results computed from many surface realizations taken from a stochastic ensemble of interest; this is known as the Monte Carlo method.

In this chapter we attempt to formally average the OE solution using the statistical properties of the surface height to evaluate certain moments of the field. Such expressions for the moments do not contain any random fluctuations since the average is taken over all members of the stochastic ensemble. If no additional approximations are made in performing the average analytically, the formally averaged result corresponds to the asymptotic limit of the Monte Carlo solution as the number of surface realizations is taken to be infinitely large, except for the fact that the formal average is for infinitely long surfaces. The angular behavior of the scattering cross section near grazing is limited by angular resolution in the Monte Carlo method because finite length surfaces are used in the calculations.

We succeed at finding an expression for the first and second moments of the scattering amplitude (leading directly to the scattering cross section) for the simplest OE approximation, the zeroth order even series solution EV_0. The expression for the second moment contains five integrations and as such is not practical, particularly since the EV_0 solution is not sufficiently accurate for many applications of interest (demonstrated numerically in Chapters 4 and 5). No important approximations were made in obtaining the formal average of the EV_0 solution, and analogous expressions for higher order approximations will be substantially more complicated. The usefulness of a formally averaged solution for the operator expansion is unquestioned, but finding an efficiently computable expression for the OE approximations remains a subject of research. We report our findings here as an introduction to the problem.

The scattered field at any point can be decomposed into two parts, the average field and the randomly fluctuating field:

$$p_s(\mathbf{r}) = \langle p_s(\mathbf{r}) \rangle + p_s^f(\mathbf{r}) . \tag{6.1}$$

The average, denoted by the brackets $\langle\ \rangle$, is performed over all surface profile realizations. The moments of the field are obtained by averaging the expressions relating the field to the surface height function $\zeta(x)$, and to the incident field. As we will see below, this procedure leads to the evaluation of moments of functions of the surface height.

The surface height is a random variable that we assume is stationary in space, that is, its statistical description is the same for all locations. The surface height is also assumed to have Gaussian statistics, which means that the ensemble of rough surfaces is entirely described by its two-point probability density function (pdf):

$$P_2(\zeta_1, \zeta_2) = \frac{1}{2\pi h^2 \sqrt{1 - C_{12}^2}} \exp\left[- \frac{(\zeta_1^2 - 2C_{12}\zeta_1\zeta_2 + \zeta_2^2)}{2h^2(1 - C_{12}^2)} \right] , \tag{6.2}$$

where $C_{12} \equiv C(x_1 - x_2)$ is the normalized correlation function of the surface height, and h is the rms surface height. The correlation function is denoted and defined as follows:

$$\begin{aligned} h^2 C(x_2 - x_1) &\equiv \langle \zeta(x_1)\zeta(x_2) \rangle \equiv \langle \zeta_1 \zeta_2 \rangle \\ &= \iint \zeta_1 \zeta_2 \; P_2(\zeta_1, \zeta_2) \; d\zeta_1 \, d\zeta_2 . \end{aligned} \tag{6.3}$$

Note that $\zeta(x)$ is a mean zero process, that is, $\langle \zeta \rangle = 0$. A Gaussian process is often defined by its spectrum, which is related to the correlation function by a Fourier transform [Papoulis, 1984].

A function of the surface height $f(\zeta)$ is also a random variable, but is not generally Gaussian. However, the pdf of $f(\zeta)$ is not needed to find the moments of f; they can be found using the pdf of ζ as follows [Papoulis, 1984]:

$$\langle f(\zeta) \rangle = \int f(\zeta) \, P(\zeta) \, d\zeta . \tag{6.4}$$

We will apply similar relations to find the average scattered field $\langle p_s \rangle$, called the coherent field, and the second moment of the field $\langle p_s p_s^* \rangle$ which is proportional to the average scattered intensity; in the far field of the ensonified surface patch, the second moment of the scattering amplitude F enters into the expression for the cross section (2.20). Here, the total scattering cross section σ is understood to be the sum of the coherent scattering cross section σ_C and the incoherent scattering cross section σ_I,

such that:

$$\sigma_I = \sigma - \sigma_C \ . \tag{6.5}$$

Thus, we are interested in both the first and second moments of the scattering amplitude. We begin by reviewing the expression for the scattering amplitude obtained by the operator expansion method for scattering from a single surface.

In the far field of the ensonified surface region, the scattering amplitude is given by (3.32)

$$F(\mathbf{k}_s) = A \int_S \exp[-i\,\mathbf{k}_s\cdot\mathbf{r}']\, p'(\mathbf{r}')\, dx' , \qquad \text{with} \quad A = \frac{e^{i\pi/4}}{\sqrt{8\pi k}} \ ,$$

where $p'(\mathbf{r}) = \sqrt{1+\zeta_x^2}\,(\hat{\mathbf{n}}\cdot\nabla\, p(\mathbf{r}))\big|_{z=\zeta(x)}$ is the scaled normal derivative of the total field on the rough surface. The OE method provides an estimate of $p'(\mathbf{r})$ using the nonlocal operator $\hat{N}$ whose series expansion is given by (3.28). Recall the three alternative series solutions for the total field derivative, (3.40), (3.41), and (3.42):

$$\begin{aligned} p'_{std} &= p_i' - (\hat{N}_0+\hat{N}_1+\hat{N}_2+\cdots)p_i \ , \\ p'_{odd} &= 2p_i' - 2(\hat{N}_1+\hat{N}_3+\cdots)p_i \ , \\ p'_{even} &= \quad -2(\hat{N}_0+\hat{N}_2+\cdots)p_i \ . \end{aligned}$$

In choosing the best series to average, we recognize that it is advantageous to use an expression with as few terms as possible because of the cross terms that appear in the expression for the second moment of the scattering amplitude. For example, at lowest order the standard series has two terms ($p_i' - \hat{N}_0 p_i$), but the even termed series has only a single term: $-2\hat{N}_0 p_i$. Numerical tests on surfaces with Gaussian or Pierson-Moskowitz spectral forms discussed in Chapters 4 and 5 have shown that the even (EV_n) and odd (OD_n) series (short series forms) are more efficient than the standard series; that is, they make better use of the n'th order surface field in providing an accurate solution. The EV_0 term is effectively a first order solution, and we'll examine its first and second moments below.

6.2 Coherent field — EV_0

The EV_0 estimate for the surface values of the scaled normal derivative is $p'_{EV_0} = -2\hat{N}_0 p_i = -2\hat{Q}p_i$, with $\hat{Q}$ defined by (3.4):

$$\hat{Q}\, p_i(x,\zeta(x)) = \int dk_x \exp[ik_x x]\,(ik_z) \int \frac{dx'}{2\pi} \exp[-ik_x x']\, p_i(x',\zeta(x')) \ ,$$

with $k_z = +\sqrt{k^2 - k_x^2}$ and $\mathrm{Im}(k_z) \geq 0$. We set the incident field to a tapered plane

wave (though we don't really need this degree of rigor in this limited development)

$$p_i(\mathbf{r}) = B(x)\exp[\,i\,\mathbf{k}_i\cdot\mathbf{r}\,], \qquad \mathbf{k}_i = k_{ix}\hat{\mathbf{x}} + k_{iz}\hat{\mathbf{z}}, \qquad k_{iz} \le 0,$$

where the taper function $B(x)$ changes arbitrarily slowly on the scale of the acoustic wavelength and also on the scale of the surface correlation length. With the scattering wavevector defined by $\mathbf{k}_s = k_{sx}\hat{\mathbf{x}} + k_{sz}\hat{\mathbf{z}}$, with $k_{sz} \ge 0$, the scattering amplitude for solution EV_0 is

$$F_{\mathrm{EV}_0}(\mathbf{k}_s,\mathbf{k}_i) = -2A \int_S dx_1 \exp[-ik_{sx}x_1 - ik_{sz}\zeta(x_1)] \int dk_x \exp[\,ik_x x_1\,]\,(ik_z)$$

$$\times \int_S \frac{dx_2}{2\pi} \exp[-ik_x x_2]\exp[\,ik_{ix}x_2 + ik_{iz}\zeta(x_2)\,]\,B(x_2). \qquad (6.6)$$

The averaging is only to be performed over functions of surface height, so all $\zeta(x)$ dependent terms are grouped together. Note that because the random variable ζ is assumed to be stationary, we drop the explicit x–dependence but label the surface heights differently if they are functions of different locations: for example, we write $\zeta(x_1) \equiv \zeta_1$. Taking the ensemble average of (6.6)

$$\langle F_{\mathrm{EV}_0}\rangle = -2A \int_S dx_1 \exp[-ik_{sx}x_1] \int dk_x \exp[\,ik_x x_1\,]\,(ik_z)$$

$$\times \int_S \frac{dx_2}{2\pi} \exp[\,i(k_{ix}-k_x)x_2\,]\,B(x_2)\,\langle \exp[\,ik_{iz}\zeta_2 - ik_{sz}\zeta_1\,]\rangle. \qquad (6.7)$$

We must now evaluate the second moment

$$M_0 = \langle \exp[-ik_{sz}\zeta_1]\exp[\,ik_{iz}\zeta_2\,]\rangle$$

which we will do using the probability density function for the surface height. In order to illustrate the more general method of evaluating moments of functions of several random variables, we do not take advantage of a special property of exponential functions of random variables. Later, in the evaluation of the incoherent scattering amplitude, a fourth moment will be evaluated using the special property mentioned above.

The moment M_0 is evaluated using the two-point pdf for the surface height as follows

$$M_0 = \iint \exp[-ik_{sz}\zeta_1]\exp[\,ik_{iz}\zeta_2\,]\,P_2(\zeta_1,\zeta_2)\,d\zeta_1\,d\zeta_2 \qquad (6.8)$$

$$= \exp\left[-\frac{h^2}{2}\left(k_{sz}^2 - 2C(x_1-x_2)k_{sz}k_{iz} + k_{iz}^2\right)\right] \qquad (6.9)$$

and yields another Gaussian form by Fourier transform of the Gaussian pdf (6.2). Because the correlation function C only depends on the difference between location coordinates, we change integration variables to sum and difference coordinates using the following transformation:

$$x = x_1 - x_2 \quad \text{and} \quad x' = x_1 + x_2 \tag{6.10}$$

giving

$$x_1 = \frac{x + x'}{2} \quad \text{and} \quad x_2 = \frac{x' - x}{2} \tag{6.11}$$

and $dx_1 dx_2 = \frac{1}{2} dx\, dx'$. Rearranging the integrals in (6.7) for the average scattering amplitude and changing variables we obtain:

$$\langle F_{EV_0} \rangle = -2A \int\int_S \int_S \frac{dk_x}{2\pi} dx_1\, dx_2\, (ik_z) \exp[\, ik_x(x_1 - x_2)\,] \exp[\, -ik_{sx} x_1\,]$$

$$\times \exp[\, ik_{ix} x_2\,]\; M_0(x_1 - x_2)\; B(x_2) \tag{6.12}$$

$$= -2A \int\int_{2S} \int_{2S} \frac{dk_x}{2\pi} \frac{dx\, dx'}{2} (ik_z) \exp[\, ik_x x\,] \exp[\, -ik_{sx}(x + x')/2\,]$$

$$\times \exp[\, ik_{ix}(x' - x)/2\,]\; M_0(x)\; B\left(\frac{x' - x}{2}\right) . \tag{6.13}$$

The surface correlation length is much shorter than the length of the ensonified portion of the surface, and the correlation function decays to negligible levels at distances of many correlation lengths. Thus, the integration limits for the difference coordinate x may just as well be extended from $2S$ to infinity. Similarly, because the taper function B changes very slowly on the scale of the surface height correlation length, the dependence on the difference coordinate may be dropped. We can therefore collect all quantities dependent on the sum coordinate x' and perform that integration:

$$\langle F_{EV_0} \rangle = -2A \int\int \frac{dk_x}{2\pi} dx\; (ik_z) \exp[\, ik_x x\,]\; \exp[\, -ik_{sx} x/2\,]\; \exp[\, -ik_{ix} x/2\,]\; M_0(x)$$

$$\times \int_{2S} \frac{dx'}{2} \exp[\, -ik_{sx} x'/2\,]\; \exp[\, ik_{ix} x'/2\,]\; B(x'/2) . \tag{6.14}$$

This last integral over the sum coordinate is the Fourier transform of the taper function, centered about the specular reflection condition: $2\pi \tilde{B}(k_{sx} - k_{ix})$. In the limit as the

taper width becomes infinitely large, a delta function evaluated in the specular direction is obtained.

6.3 Incoherent Scattering Amplitude

We wish to compute the EV_0 estimate for the scattering cross section given by (3.33)

$$\sigma(\theta_s, \theta_i) = \frac{\langle FF^* \rangle}{E_f'},$$

where the "normalized" energy flux E_f' incident on the surface is related to the actual energy flux E_f by:

$$E_f' = E_f \frac{2\rho c}{\sin\theta_i}.$$

If the taper function is assumed to have the modified Gaussian form defined in (3.34), and the taper parameter g is very large compared to the acoustic wavelength, the normalized flux E_f' for the Gaussian tapered plane wave becomes approximately $\sqrt{\frac{\pi}{2}}\, g$, as can be seen from (3.35).

Retaining the general form of the taper function $B(x)$, we write the expression for the squared magnitude of the scattering amplitude for the EV_0 approximation as

$$FF^* = 4A^2 \int_S dx_1 \exp[-ik_{sx}x_1 - ik_{sz}\zeta_1] \int dk_x \exp[ik_x x_1]\,(ik_z)$$

$$\times \int_S \frac{dx_2}{2\pi} \exp[-ik_x x_2] \exp[ik_{ix}x_2 + ik_{iz}\zeta_2]\, B(x_2)$$

$$\times \int_S dx_3 \exp[ik_{sx}x_3 + ik_{sz}\zeta_3] \int dk_x' \exp[-ik_x' x_3]\,(ik_z')^*$$

$$\times \int_S \frac{dx_4}{2\pi} \exp[ik_x' x_4] \exp[-ik_{ix}x_4 - ik_{iz}\zeta_4]\, B(x_4) \qquad (6.15)$$

which we now rearrange, again grouping the height dependent quantities together in preparation for averaging:

$$FF^* = 4A^2 \int \frac{dk_x}{2\pi} (ik_z) \int_S \int_S dx_1 dx_2 \exp[ik_x(x_1 - x_2)] \exp[-ik_{sx}x_1 + ik_{ix}x_2]$$
$$\times \exp[-ik_{sz}\zeta_1 + ik_{iz}\zeta_2] B(x_2)$$
$$\times \int \frac{dk_x'}{2\pi} (ik_z')^* \int_S \int_S dx_3 dx_4 \exp[-ik_x'(x_3 - x_4)] \exp[ik_{sx}x_3 - ik_{ix}x_4]$$
$$\times \exp[ik_{sz}\zeta_3 - ik_{iz}\zeta_4] B(x_4) . \quad (6.16)$$

It is clear that to compute the moment $<FF^*>_{EV_0}$ we need to evaluate the following fourth moment:

$$M_{00} = <\exp[i(-k_{sz}\zeta_1 + k_{iz}\zeta_2 + k_{sz}\zeta_3 - k_{iz}\zeta_4)]> = <e^{iX}> . \quad (6.17)$$

Since all the surface height variables are zero-mean Gaussian random variables, then X is also a zero-mean Gaussian variable, and we can evaluate M_{00} using the relationship

$$<e^{iX}> = e^{-\frac{1}{2}<X^2>} . \quad (6.18)$$

This relationship is obtained by Fourier transforming the single-point Gaussian pdf in the same way as was done earlier for moment M_0. Here, squaring X and rearranging terms we obtain:

$$X^2 = k_{sz}^2\zeta_1^2 + k_{iz}^2\zeta_2^2 + k_{sz}^2\zeta_3^2 + k_{iz}^2\zeta_4^2 - 2k_{sz}k_{iz}\zeta_1\zeta_2 - 2k_{sz}^2\zeta_1\zeta_3$$
$$+ 2k_{sz}k_{iz}\zeta_1\zeta_4 + 2k_{sz}k_{iz}\zeta_2\zeta_3 - 2k_{iz}^2\zeta_2\zeta_4 - 2k_{sz}k_{iz}\zeta_3\zeta_4 . \quad (6.19)$$

Taking the average of X^2, we obtain an expression in terms of all possible two-point correlation functions for the four coordinate locations:

$$<X^2> = 2h^2 \left[k_{sz}^2 + k_{iz}^2 - k_{sz}k_{iz}(C_{12} - C_{14} - C_{23} + C_{34}) - k_{sz}^2 C_{13} - k_{iz}^2 C_{24} \right] , \quad (6.20)$$

where

$$C_{ij} \equiv C(x_i - x_j) = C(x_j - x_i) = \frac{<\zeta(x_i)\zeta(x_j)>}{h^2} . \quad (6.21)$$

We can now write the desired second moment of F as:

$$<FF^*> = 4A^2 \iint \frac{dk_x\, dk_x'}{4\pi^2} (ik_z)(ik_z')^* \int_S \int_S \int_S \int_S dx_1 dx_2 dx_3 dx_4 \; e^{-\frac{1}{2}<X^2>} B(x_2)$$
$$\times B(x_4) \exp\left[i \left(k_x(x_1 - x_2) - k_x'(x_3 - x_4) - k_{sx}(x_1 - x_3) + k_{ix}(x_2 - x_4) \right) \right] . \quad (6.22)$$

We would like to take advantage of the fact that the correlation functions only depend on difference coordinates, but there are six pairs of difference coordinates to choose from, given the four spatial coordinates; thus, the choice of variable transformation to make is not an obvious one. We follow Uscinski [1985] in picking the following combinations, though we normalize the difference coordinates in a symmetrical way:

$$\mu = \frac{1}{4}\,(x_1 + x_2 + x_3 + x_4) \tag{6.23a}$$

$$u = \frac{1}{2}\,[\,(x_1 + x_2) - (x_3 + x_4)\,] \tag{6.23b}$$

$$v = \frac{1}{2}\,[\,(x_1 + x_4) - (x_2 + x_3)\,] \tag{6.23c}$$

$$w = \frac{1}{2}\,[\,(x_1 + x_3) - (x_2 + x_4)\,] \tag{6.23d}$$

leading to

$$x_1 = \frac{1}{4}\,(+2w + 2v + 2u + 4\mu) \tag{6.24a}$$

$$x_2 = \frac{1}{4}\,(-2w - 2v + 2u + 4\mu) \tag{6.24b}$$

$$x_3 = \frac{1}{4}\,(+2w - 2v - 2u + 4\mu) \tag{6.24c}$$

$$x_4 = \frac{1}{4}\,(-2w + 2v - 2u + 4\mu)\,. \tag{6.24d}$$

In terms of the new coordinates, the six possible difference coordinate pairs are given by

$$x_1 - x_2 = w + v \qquad x_1 - x_4 = w + u \qquad x_2 - x_3 = u - w \tag{6.25a}$$

$$x_3 - x_4 = w - v \qquad x_1 - x_3 = v + u \qquad x_2 - x_4 = u - v\,. \tag{6.25b}$$

Under the variable transformation the average of X^2 becomes

$$\begin{aligned} \langle X^2 \rangle = 2h^2 \big[\, & k_{sz}^2 + k_{iz}^2 - k_{sz} k_{iz} \big(C(w+v) - C(w+u) - C(u-w) + C(w-v) \big) \\ & - k_{sz}^2 C(v+u) - k_{iz}^2 C(u-v) \,\big]\,, \end{aligned} \tag{6.26}$$

and the other exponential term in (6.22) becomes

$$\begin{aligned} & \exp\left[i \left(k_x (w+v) - k_x'(w-v) - k_{sx}(v+u) + k_{ix}(u-v) \right) \right] \\ & \quad = \exp\left[i \left(w(k_x - k_x') + v(k_x + k_x' - k_{sx} - k_{ix}) + u(k_{ix} - k_{sx}) \right) \right]. \end{aligned} \tag{6.27}$$

Finally, under the variable transformation

$$dx_1\, dx_2\, dx_3\, dx_4 = J\, dw\, dv\, du\, d\mu \tag{6.28}$$

we change to sum and "difference" coordinates in (6.22) to obtain:

$$\langle F F^* \rangle = 4A^2 J \iint \frac{dk_x\, dk_x'}{4\pi^2} (ik_z)(ik_z')^* \int_{2S}\int_{2S}\int_{2S} du\, dv\, dw \quad e^{-\frac{1}{2}\langle X^2 \rangle}$$

$$\times \exp\left[i \left(w\,(k_x - k_x') + v\,(k_x + k_x' - k_{sx} - k_{ix}) + u\,(k_{ix} - k_{sx}) \right) \right]$$

$$\times \int_S d\mu\; B\left(\tfrac{1}{2}[-w - v + u + 2\mu]\right)\; B\left(\tfrac{1}{2}[-w + v - u + 2\mu]\right) . \qquad (6.30)$$

The dependence on all variables but μ can be dropped in the taper function B for the same reason cited in the development of (6.14), namely that the taper function is essentially constant over the range of u, v, or w for which these variables lead to non-negligible contributions in their integrals. The resulting integral over center of mass coordinate μ

$$\int_S B^2(\mu)\, d\mu \qquad (6.31)$$

cancels a similar term from the energy flux incident on the surface, which appears in the denominator of the expression for the cross section. The limits of integration for the integrals over u, v, and w can be extended to infinity as in (6.14), because the correlation functions will be negligibly small at ranges on the order of the surface length.

We are left with an expression for the total scattering cross section using the EV_0 approximation that has five integrals — an unwieldy solution, currently impractical to evaluate numerically for scattering from 1-D surfaces, let alone 2-D surfaces. Higher order operator expansion solutions will be considerably more complex, and yet are needed to provide a sufficiently accurate solution for most applications; based on the results of Chapters 4 and 5, approximation EV_0 does not seem accurate enough in general to be worth implementing in the form implied by (6.30). Further progress in reducing the expression, perhaps by making additional approximations in performing the integrals beyond those inherent in the EV_0 solution, must be made before the operator expansion has a useful formally averaged solution. Because the operator expansion method is so widely accurate this investigation remains a subject worthy of research.

CHAPTER 7

Dissertation Summary and Proposed Future Work

7.1 Introduction

Many kinds of energy propagate as waves, and these waves are modified by the changes in physical properties they encounter as they travel through a medium. In particular, an interface between two different media imposes boundary conditions on the wave field that often result in reflected and transmitted fields. Few physical surfaces are smooth; consequently, the interaction of waves with rough boundaries, called scattering, is a commonly occurring phenomenon. The essence of the rough surface scattering problem is to determine the field scattered by a rough boundary of known shape, given a known field incident upon it.

The deterministic problem treats scattering from a single surface, whereas in many situations an averaged solution is preferred, in which moments of the scattered field provide a more useful description of the scattering results. The exact solution of the rough surface scattering problem can only be obtained numerically, and then only for scattering from one surface at a time. Exact solutions of the stochastic problem are approached by averaging scattering results from a large number of individual realizations of the process; this procedure, called the Monte Carlo method, is very computationally intensive, even for computing 2-D scattering from 1-D surfaces.

Many approximations have been proposed to address the rough surface scattering problem, but most are restricted to treating a small range of roughness regimes. Very few methods can accurately treat scattering from multiscale surfaces (which commonly occur in nature) over a wide range of incident and scattering angles. In this dissertation, we study a new technique called the Operator Expansion (OE) method recently introduced by Milder [1991]. The OE method, currently only developed for scattering from surfaces with a Dirichlet boundary condition, has several important properties:

- Milder showed that the OE solution reduces analytically to the classical solutions to the surface scattering problem in their respective asymptotic limits, that is, to the perturbation solution in the limit of small rms surface height, and to the Kirchhoff approximation in the limit of very smooth surfaces (varying slowly on the scale of the acoustic wavelength). This reduction to *both* classical solutions must be a

property of any method that can accurately treat scattering from multiscale surfaces, yet has historically been very difficult to achieve.

- The OE solution is cast as an expansion in a systematic series, conveniently providing a self consistent accuracy check based on the convergence properties of the series.

- The OE solution is reciprocal at each order in the expansion. Reciprocity is a physical property of the scattering problem that is not always easy to retain in an approximation.

- The OE solution is implemented using Fast Fourier Transforms (FFTs) and is extremely fast to compute, even for 3-D scattering from 2-D surfaces.

These features make the OE method a very promising approximation and have motivated the current study of its accuracy. Milder tested the method for scattering from 1-D sinusoidal surfaces and wedge shaped gratings [Milder, 1991], and from 2-D sinusoidal surfaces [Milder and Sharp, 1992], and found that the method proved to be both fast and accurate for those surface types. We examine the method in computing scattering from randomly rough surfaces. In particular, the application to scattering from multiscale surfaces, such as those encountered in scattering of sound from the ocean surface, is of great interest. In this study, accuracy of the OE method is determined through comparison to the exact solution obtained through an integral equation technique; as discussed above, this solution is practically limited to treating scattering from 1-D surfaces. Our study was performed for 2-D scattering from 1-D surfaces, but the results are expected to carry over to 3-D scattering from 2-D surfaces.

Extensive numerical tests have shown that the operator expansion method is indeed accurate over a wide range of scattering parameters. These results are reported in Chapters 4 and 5, which treat scattering from randomly rough surfaces with Gaussian and Pierson-Moskowitz spectra, respectively. The broad range of validity of the OE method prompted a closer look at the derivation. We find that insight into the method's accuracy can be gained by examining the construction of the operator solution; this construction is performed in Chapter 3 in a somewhat less rigorous but more intuitive manner than in Milder's derivation. An extensive discussion of the differences between Milder's approach and our own also appear in Chapter 3. The basic equations governing the scattering problem and the two classical methods used to solve it are presented in Chapter 2.

The operator expansion method is currently developed as a numerical technique, that is, it computes scattering from one surface at a time. While this makes

comparisons with the exact integral equation solution particularly convenient, the OE method can only be used to compute moments of the scattered field using the Monte Carlo method. Most other approximations are formally averaged, that is, the statistical properties of the randomly rough surface height are used to analytically evaluate the moments of the scattered field. An attempt at formally averaging the lowest order operator expansion solution (even series solution EV_0) is presented in Chapter 6; the resulting expression for the scattering cross section is not simple enough to be practical. Thus, the OE method is currently seen as a very efficient numerical method providing an accurate solution to the surface scattering problem for rougher scattering regimes than can be treated with other approximations. The OE solution is much faster to compute than the exact integral equation solution and is practical for computing scattering from realistic 2-D surfaces, even when applied in a Monte Carlo approach.

A detailed summary of the work presented in the dissertation follows below.

7.2 Basic equations for rough surface scattering — Chapter 2

In Chapter 2, the basic equations governing acoustic scattering from rough surfaces are developed. The operator expansion method is well suited to computing 3-D scattering from 2-D surfaces, but the integral equation solution is only practical for solving scattering from 1-D surfaces; for consistency, all expressions are developed for 2-D scattering from 1-D surfaces.

In Sec. 2.2.2 Green's theorem is used to develop the Helmholtz-Kirchhoff scattering integrals which govern the surface scattering problem. Following Wolf [1973], Green's theorem is used to generate several important surface integral identities relating the incident, scattered, or total fields, and their normal derivatives. These integral theorems are the mathematical foundation of the scattering problem and provide the starting point for all approximations. These integral relations also lead to integral equations (Sec. 2.2.4) that can be solved numerically to provide the exact solutions used in this dissertation to assess the accuracy of approximate methods.

The problem of scattering from an infinite rough surface (in contrast to scattering from a finite object) poses formal difficulties which are addressed by considering ensonification by a source of finite extent. It is seen that the case of plane wave incidence can only be reached through a limiting process, in which the mathematical surface closing the integration surface is extended along with the ensonification region (Sec. 2.2.2).

It is often of interest to specialize the scattering solution to a region far from the ensonified surface; thus, the scattering amplitude is defined for the 2-D scattering geometry in Sec. 2.3. For stochastic problems, the average scattering results are often presented in terms of the the scattering cross section (here defined for a general incident field (2.18)), or in terms of the scattering strength which is the cross section expressed in dB. Methods that express the scattered field as systematic series expansions (such as the operator expansion or perturbation theory) have expansions for the cross section that contain cross terms of mixed orders. Typically, cross section series are organized by collecting terms of the same order in the field expansion parameter, but in the case of the operator expansion we find through numerical studies that consistency in the expansion parameter is not required to maintain accuracy of the solution. Indeed, the "truncated" series (2.22) which is more efficient computationally often proves to be more accurate than the consistent series (2.23). These two series solutions are presented in Sec. 2.3, and are numerically tested in Sec. 4.4 and Sec. 5.3.

For completeness, the two classical approximations, the Kirchhoff approximation (Sec. 2.4) and the small perturbation method (field perturbation, Sec. 2.5), are presented for scattering from a single surface. Through application of an integral theorem on the incident field developed earlier in the chapter, three forms of the Kirchhoff solution are presented. Though these forms are rigorously equivalent, they appear to be quite different; this example illustrates how reciprocal solutions can appear to be nonreciprocal. Rayleigh-Rice perturbation theory is presented for scattering from a single surface because the "Monte Carlo" development of the method is conveniently compared with the operator expansion solution in Chapter 3. It is seen through this comparison and through numerical tests in Chapter 4 that a subtle difference in the application of the perturbation method can result in a dramatic improvement in the accuracy of the solution. In Sec. 2.5 the mathematical foundation for this investigation is developed.

7.3 The operator expansion method — Chapter 3

The operator expansion method, introduced for the rough surface scattering problem by Milder [1991], was inspired by earlier work in surface hydrodynamics [Milder, 1990]. In the OE method, the Dirichlet (pressure release) scattering problem is solved using a nonlocal operator that computes the normal derivative of the scattered field given only the boundary values of the scattered field; these are known because they are tied to the incident field through the boundary condition. The nonlocal (scaled) normal derivative operator $\hat{N}$ that performs this transformation is expressed in a systematic series expansion whose terms contain powers of the surface height function and powers of a Fourier integral operator $\hat{Q}$ (3.4). In Chapter 3, we revisit the derivation of the

operator expansion and show how it is used to solve the Dirichlet scattering problem. Our presentation differs from that given by Milder in two fundamental respects. First, we derive the expansion for $\hat{N}$ assuming explicitly that the scattered field satisfies the Rayleigh Hypothesis (RH), though we then apply $\hat{N}$ in cases for which the RH may not hold. Second, the series expansion itself is obtained in a more straightforward but less rigorous way. Though our approach seems to make unnecessarily restrictive assumptions, the solution thus obtained is identical to Milder's. Furthermore, it provides an alternative way of deriving the expansion that we feel is simpler and more intuitive. The differences between our derivation and that of Milder's are extensively discussed in Sec. 3.5, and are summarized at the end of this section.

The operator expansion method solves the rough surface scattering problem much more efficiently than possible with an integral equation method by retaining only the most important parts of the nonlocal relationship between the surface values of scattered field and the surface values of its normal derivative (embodied in the integral relationships (2.9) or (2.15)). This is accomplished using an upward directed plane wave expansion of the scattered field (3.2), approximately obtained from its rough surface values. The up-going wave representation approach for solving the rough surface problem is introduced by first applying the solution technique to the problem of reflection of a down-going incident field by a flat surface (Sec. 3.2.1). In that unique situation, the decomposition of the scattered field into up-going plane waves can be simply and exactly obtained by Fourier transform of the surface values of the field. Once the plane wave representation for the field is known, the field or any of its derivatives can be evaluated anywhere the representation is valid, namely above the flat surface. The flat surface solution is expressed in terms of a Fourier integral operator $\hat{Q}$ (3.4), which transforms the surface values of the scattered field (given by the negative of the incident field) into the surface values of the vertical derivative of the field. The spectral technique thus developed is far more complicated than necessary to solve the problem of reflection by a flat surface, but illustrates the approach used in the rough surface case. Though the plane wave coefficients for the scattered field are never explicitly computed, representation of the surface values of the scattered field in up-going waves underlies the entire derivation.

The extension of the flat surface solution to the rough surface scattering problem (Sec. 3.2) involves the construction of a nonlocal vertical derivative operator $\hat{D}$ that reduces to $\hat{Q}$ when the surface is flat. Like operator $\hat{Q}$, operator $\hat{D}$ is applied to the surface values of the scattered field, specified through the Dirichlet boundary condition. Rough surface operator $\hat{D}$ is made up of three distinct operations performed sequentially. The scattered field is first analytically continued from the rough surface to a flat plane. On the flat plane, the vertical derivative of the field is obtained using operator

$\hat{Q}$. Finally, the vertical derivative field is continued back to the rough surface. The vertical derivative of the scattered field is then related to the desired normal derivative using the known tangential derivative of the surface field (the tangential derivative is known because the scattered field is known all along the surface). Thus, operator $\hat{D}$ (3.19) forms the essential part of the normal derivative operator $\hat{N}$ (3.26) by providing an estimate of the behavior of the scattered field in the neighborhood of the surface given only the values of the field on the surface.

The two analytic continuation operations (operators $\hat{Z}$ and $\hat{Z}^{-1}$) are expressed as series whose terms contain powers of the surface height function $\zeta(x)$ and powers of operator $\hat{Q}$, leading to a series expansion for the normal derivative operator $\hat{N}$ (3.28) in powers of ζ and $\hat{Q}$. Though each continuation operation is an expansion in surface height, the combination of the two continuations (away from and back to the rough surface) effectively reduces the height dependence of the OE solution, giving the method its broad range of accuracy. To illustrate the effect of the two-way continuation, a solution based on a single continuation using $\hat{Z}^{-1}$ is examined in Sec. 3.4. Since the continuation carries the scattered field to the mean plane, the plane wave coefficients for the upward wave representation can be found by Fourier transform, directly leading to the far-field scattering solution. The $\hat{Z}^{-1}$ method is developed analytically in Chapter 3 and numerically compared to the standard OE solution based on $\hat{N}$ (and to the exact integral equation solution) in Chapter 4; those results confirm that the two-way continuation greatly extends the range of accuracy and applicability of the operator expansion solution over the solution based on the one-way continuation.

The operator notation is very compact, and makes analytical comparisons between the OE and the small perturbation method very straightforward. Previously reported developments of "Monte Carlo perturbation theory" [Thorsos and Jackson, 1989] expand the total (incident plus scattered) field in small parameter *kh* (normalized surface height). When the development is carried out for the scattered field alone, and the solution written in operator notation using powers of ζ and $\hat{Q}$, the operations are shown to be identical to those in the $\hat{Z}^{-1}$ method described above (Sec. 3.4.4). However, a subtle difference in the application of the operations results in different lowest order solutions, and hence different higher order solutions as well. The zero order perturbation solution is the mean plane reflection, whereas the zero order solution in the $\hat{Z}^{-1}$ method places the *rough surface values* of the incident field on the mean plane, thus including roughness effects at lowest order. Numerical tests in Chapter 4 show that the $\hat{Z}^{-1}$ solution is much more widely accurate, and converges more rapidly, than the perturbation solution; indeed, were it not for the operator expansion method (based on the use of $\hat{N}$), the "modified" perturbation solution based on operator $\hat{Z}^{-1}$ might have been a very attractive method to pursue. However, Milder's operator expansion method which takes

advantage of two-way continuation is accurate over a much wider range of scattering regimes than the single continuation methods.

Milder [1991] showed that the OE solution can be simplified by exploiting a symmetry property of the expansion with respect to an inversion of the surface height function. By treating the analogous scattering problem for ensonification from below, or by simply developing the expansion for the nonlocal normal derivative operator for downward propagating waves (Sec. 3.3.3), two alternative series for the operator expansion estimate for the surface values of the scattered field normal derivative are obtained. These series contain only odd (3.41), or only even (3.42), order terms from the series for $\hat{N}$, thus providing series solutions that are expected to converge more rapidly than the standard solution (3.40). This expectation is confirmed and quantified in numerical tests conducted in Chapters 4 and 5.

The expansion for $\hat{N}$ is written in terms of powers of Fourier integral operator $\hat{Q}$; because $\hat{Q}$ is implemented using FFTs, the scattering solution is very efficiently computed. The OE solution for the scattered field is implemented in two steps. First, the rough boundary values of the normal derivative of the scattered field are computed using a few leading terms in the series for $\hat{N}$. Second, the scattered field is computed above the rough surface using the usual Helmholtz integral. Numerical implementation notes, including a description of the incident field (modified Gaussian tapered plane wave), use of the FFT, tapering of the surface height function, factoring of operator terms, and other such details are discussed in Sec. 3.3[†].

Chapter 3 concludes with a detailed discussion of the two principal mathematical differences between Milder's derivation of the OE solution and our own, and these are the method of finding the operator series expansion and the use of the Rayleigh hypothesis. The two derivations lead to the same expansion for $\hat{N}$, but we believe that the approach taken in Sec. 3.2 is more intuitive, though somewhat less rigorous.

Milder [1991] used a variational differentiation technique to solve for the expansion for nonlocal vertical derivative operator $\hat{D}$, obviating the need to find an explicit series representation for the continuation operator $\hat{Z}^{-1}$. However, the backsubstitution method (used in Sec. 3.2.4) is a very straightforward approach and provides an

[†] All numerical codes used in this work, including those which compute the rough surface values of the normal derivative using the Kirchhoff approximation, perturbation theory, the operator expansion, and the first and second kind integral equation solutions, and those that compute the Helmholtz integrals and random rough surface height profile realizations, were written by this author, with the exception of the FFT and matrix inversion routines which came from Numerical Recipes [Press et al., 1986], and LINPACK [Dongarra et al., 1979], respectively, and the PEIE method used in Chapter 5, which is courtesy of Eric Thorsos [1993b].

alternative path to the same solution. Furthermore, finding an explicit expansion for $\hat{Z}^{-1}$ allows us to analyze the OE solution; in particular, the solution based on operator $\hat{Z}^{-1}$ is found to be very closely related to the perturbation solution. We present an expanded discussion of Milder's variational technique in Sec. 3.5.2 for completeness, but also because of its elegance in solving for the operator expansion. Use of commutator notation further simplifies the expansion, and the variational derivative operating on commutator forms becomes particularly convenient for generating higher order terms in the expansion (3.20).

In our derivation, we have assumed that operator $\hat{N}$ can be directly applied to the rough surface values of the scattered field, even though the latter may not satisfy the Rayleigh hypothesis. The validity of this operation is in question because the derivation of $\hat{N}$ is performed for fields which do satisfy the RH, that is, fields whose singularities lie entirely below the plane passing through the lowest point on the rough surface (see Sec. 3.5.2). A field that satisfies the RH can be freely continued in the region between surface extrema, and such continuation is a fundamental part of the operator expansion derivation. Furthermore, a representation of the surface values of the scattered field in upward directed plane waves underlies the operator expansion method, and the validity of such a representation for the scattered field inside the wells of the surface (and in particular on the surface) is tied to the validity of the RH.

To avoid making the Rayleigh hypothesis Milder did not apply the normal derivative operator $\hat{N}$ to the scattered field directly, but it turns out that his approach is no less restrictive. We find that in his derivation the RH condition is imposed on an arbitrary down-going plane wave which, by analogy with the scattering problem, is equivalent to imposing the RH on the scattered field. On the other hand, in transforming an exact integral identity (the extended boundary condition (2.9)), Milder shows how the usual point-wise Rayleigh assumption can be relaxed when the solution for the scattered field off the rough surface is desired. In that case, the upward wave expansion for the surface values of the scattered field (and hence its normal derivative) need only match the true field specified by the boundary condition in an integral sense, that is, certain surface integrals over those quantities are equal (see Sec. 3.5.2).

A similar conclusion has been reached by others investigating the validity of the Rayleigh hypothesis, a study with a long and contentious history. A review of the RH issues arising in connection with the operator expansion method is presented in Sec. 3.5.2. The most important result from the work of Meecham [1956b], Yasuura [1971], Millar [1973], Petit [1980], and others, is that a *truncated* up-going plane wave representation can approximate the boundary values of the scattered field to arbitrary accuracy, in the mean-square sense (an integral statement). This "completeness"

property of up-going plane waves also guarantees that the scattered field off (above) the surface can be similarly approximated to arbitrary accuracy, even in the wells of the surface when the Rayleigh hypothesis is not satisfied. Thus, the up-going wave representation is not in itself fundamentally limited by the validity of the Rayleigh hypothesis; rather, the difficulty with methods based on such upward wave representations lies in finding the series coefficients for scattering problems over a wide range of scattering regimes.

The theory that demonstrates completeness of up-going waves also leads to a rigorous numerical method of finding the plane wave coefficients using a least-squares technique. The OE scattering solution is not obtained by solving a least-squares problem; the plane wave coefficients are never explicitly determined in the OE method, but are effectively approximated by the operator expansion series solution. (The coefficients could be obtained by evaluating an integral over the surface values of the normal derivative field in a manner similar to (3.32) for the scattering amplitude; see also (3.50).) The operator expansion method is not exact, but it does provide a very accurate solution over a wide range of scattering parameters. Furthermore, the OE solution is computed much more rapidly than possible with a rigorous method. We now turn to a summary of the numerical study of the accuracy of the operator expansion.

7.4 Accuracy of the OE for computing scattering from surfaces with a Gaussian spectrum — Chapter 4

The operator expansion method looks very promising analytically, but without numerical tests the accuracy of the solution is a matter of speculation, particularly when questions about the method's formal validity arise in connection with the Rayleigh hypothesis. In Chapters 4 and 5 we examine the accuracy of the operator expansion solution at several orders by comparison with the exact numerical solution of an integral equation, over a wide range of scattering regimes. Chapter 4 addresses scattering from random surfaces[†] with a Gaussian spectrum while Chapter 5 addresses scattering from multiscale surfaces with a power law spectrum (Pierson-Moskowitz). These tests indicate that the OE method is fast and accurate at computing acoustic scattering from Dirichlet boundaries for many situations of practical interest.

[†] All examples presented here are for average scattering; most cases use results from 50 surface realizations. Some fluctuations in the estimate for the scattering strength remain but are significantly reduced by examining the difference between the exact integral equation solution and an approximate solution.

Because the OE method is cast as a series solution, convergence of the series is examined as well as the accuracy at each order. For this purpose, we typically compute the surface field up through third order, one order higher than was presented by Milder. The third order term is substantially more complex than the second order term and also requires additional care in numerical implementation; it is more sensitive to edge effects and requires more surface sampling density than lower order terms for similar relative accuracy (see Sec. 3.3.4). For many applications a second order solution is sufficiently accurate, but the third order term is very useful in estimating the accuracy of the second order solution in the absence of an exact solution.

The accuracy of the classical methods (perturbation theory and Kirchhoff approximation, to which the OE solution reduces in appropriate limits) is well known for acoustic scattering from 1-D Dirichlet surfaces with a Gaussian spectrum [Thorsos, 1988], [Thorsos and Jackson, 1989]. We review these findings in Sec. 4.2, and use the *kl*-*kh* plane to map out the regions of validity of the classical methods and to guide our investigation of the accuracy of the OE (see Fig. 4.2). Milder [1991] proposed the "Fresnel number" *khs* (which we call the slope-height parameter) as a general descriptor for the OE roughness regime. To examine this single parameter's ability to describe the method's performance (convergence rate and accuracy) numerical cases were selected on contours of constant *khs* in the *kl*-*kh* plane. We find that the single slope-height parameter *khs* is a useful general indicator, but that convergence and accuracy of the OE solution also depend on the angular distance from the specular direction, and on the surface roughness parameters *kl* and *kh* separately.

Section 4.3 examines the performance of the OE for moderately rough surfaces, that is, for a roughness regime that includes the validity regions of both classical methods. Fig. 4.2 illustrates that the line for $khs = 0.15$ from which the first set of examples is chosen (A cases) conveniently spans the validity regions of the classical methods, also crossing a gap between those regions. The results for scattering from these surfaces confirm that the operator expansion method has capabilities of both classical approximations. Milder [1991] reduced the operator expansion solution to the perturbation solution for small *kh* (when perturbation theory is known to be accurate), but it is not clear from this analytical result how small *kh* must be for the operator expansion to be accurate as well. We find that the first order operator expansion solution (OE_1) is comparable in accuracy to $\sigma^{(4)}$ (the second order perturbation solution, that is, computed to order $(kh)^4$ in the cross section) over all scattering angles for the region in which $\sigma^{(4)}$ is accurate; see Figs. 4.3d, 4.3e, and 4.4c for the relative accuracy of the operator expansion and perturbation solutions for cases A1 and A2.

The first order operator expansion is also comparable in accuracy to the Kirchhoff approximation (KA) where the latter is accurate, that is, for surfaces with $kl > 6$ and for incident and scattering angles away from grazing (Fig. 4.6). However, unlike the Kirchhoff approximation, the OE_1 solution has the essentially correct angular dependence near grazing because important nonlocal effects are included in the solution. An example of the near-grazing behavior of OE_1 is presented in Fig. 4.5d, for case A3. However, we remark that when the scattering levels are very low in the backscattering region, higher orders of the OE are required to provide an accurate solution, even in some cases when the KA is accurate; see Fig. 4.6.

Significantly, the operator expansion solution is also accurate in regions of kl-kh roughness parameter space that lie outside the validity region boundaries of the classical approximations, for $khs = 0.15$. Figure 4.5 gives an example of scattering taken from the "gap region" and illustrates the relative accuracy of OE_1, KA, and $\sigma^{(4)}$ over all scattering angles, for incident angle $\theta_i = 45°$.

The operator expansion solution is cast as a series for which convergence is observed to result in accuracy of the solution. When $khs = 0.15$, the operator expansion solution converges very rapidly to the exact solution. The rapid convergence can be appreciated by looking at the scattering strength contributions from the first four terms in the series for the surface field. For case A1, the curves in Fig. 4.3c illustrate how the terms decay, computed over all scattering angles, for incident angle $\theta_i = 45°$. The solution converges so rapidly in this regime that the scattering strength results plotted over their full dynamic range are almost indistinguishable; for example, see the curves for case A2 in Fig. 4.4b. The differences between the integral equation scattering strength curve and the scattering strength curves for the operator expansion solutions are therefore presented with each example. The accuracy and convergence of the operator expansion solution can then be observed over all scattering angles; for case A3 and $\theta_i = 45°$, these differences are presented in Fig. 4.5c. For $\theta_i = 90°$ and $\theta_i = 20°$, the difference curves for case A3 are presented in Figs. 4.7b and 4.7d, respectively.

Milder [1991] indicated that the operator expansion solution is symmetrical, and hence reciprocal, order by order (we have verified this property through third order) and numerical results for a single angle of incidence show that higher order corrections are more important for scattering angles far from the specular direction, especially near grazing in the back direction. Alternatively, convergence is fastest near specular. Thus, it is not surprising that numerical tests for several angles of incidence indicate that the accuracy (and convergence) of the solution at any given order for a given roughness generally depends on the angular distance from the specular direction $|180° - \theta_i - \theta_s|$. Changing the incident angle by tens of degrees essentially shifts the scattering strength

error curves by the same amount, for scattering angles more than a few degrees from grazing.

Sec. 4.4 evaluates the accuracy of alternative series for the operator expansion solution. We begin by examining the consequence of choosing computational efficiency at the expense of retaining consistency in the series expansion for the cross section. Figs. 4.8 and 4.9 for $khs = 0.5$ and $khs = 1.0$, respectively, illustrate that consistency in the surface field series expansion parameter is not required to maintain accuracy of the scattering solution. This is fortunate because the inconsistent (truncated) cross section series (2.22) is far more efficiently computed than the consistent series (2.23).

Milder [1991] introduced the even (3.42) and odd (3.41) series solutions, and suggested that these short series might be good to order $n+1$ when computed to order n, because the next available term in the series is of order $n+2$. We find that the short series solutions do indeed exhibit some (but not all) of the character of the standard solution (3.40) taken to next order, even when that solution is inaccurate; see Sec. 4.4.3. This behavior, observed in case B3 ($khs = 0.5$, Fig. 4.10), is typical of that observed in many other calculations. Further examples are given in Sec. 4.5 which presents results for scattering from rougher surfaces.

Many properties of the OE observed for moderately rough surfaces continue to hold as the roughness increases. The convergence rate of the series for the surface field is useful in assessing the accuracy of the solution at any given order. When examined in the far field, the contributions from individual orders indicate convergence as a function of scattering angle. When decay of these terms (ON_n) is rapid, the OE solution always converges to an accurate result. When the decay is not rapid, or not monotonic, the accuracy of the solution at lower orders may still be good; the series appears to converge asymptotically in these cases. No clear threshold exists above which the OE method fails dramatically. Experience with the method leads to a good "calibration" of its performance (convergence and accuracy) with respect to the values of kh, kl, khs, and scattering angles. For a given value of khs, two regimes are observed in a variety of calculations: smaller kl (relatively larger slope), and larger kl (relatively smaller slope). These regimes are primarily distinguished by differences in behavior of the OE in the backscatter region. Detailed comparisons between OE solutions and the integral equation solution were conducted for many points in the kl-kh plane. Examples for $khs = 0.5$, 1.0, and 1.5 in Sec. 4.5 present results representative of the two kl regimes. These results are presented for completeness, and because the detailed behavior of the OE solution is best conveyed using the scattering strength error curves themselves.

A different physical regime exists for very rough surfaces in which multiple scattering plays an important role. Double-scattered reciprocal paths combine coherently leading to an enhancement peak in the backscatter direction that can rise 3 dB above the average level. It is perhaps surprising that the OE method can correctly compute such effects (in some cases), because the double scattering takes place over significant distances, requiring correct treatment of widely nonlocal interactions. Figs. 4.19 and 4.20 indicate that the OE solution is accurate over the range of scattering angles $40° \le \theta_s \le 140°$, including the backscatter region in case F4 ($khs = 3.6$, $kl = 7.0$, $kh = 4.2$, $s = 0.85$) with incident grazing angle $\theta_i = 60°$. Case F4 is just rough enough to exhibit backscatter enhancement; the OE method is unable to accurately treat scattering from surfaces which are much rougher. Studies in this regime often require averaging over large numbers of surface realizations to reduce the random fluctuations to acceptable levels; 500 surfaces were used in case F4.

Finally, Chapter 4 concludes with an investigation of the accuracy of the solution based on operator $\hat{Z}^{-1}$, the one-way continuation operator that continues the scattered field from the rough surface to the mean plane. The $\hat{Z}^{-1}$ solution is computed for each of the four A-cases ($khs = 0.15$), and compared with the standard OE solution, with the integral equation solution, and with the Monte Carlo perturbation solution. The $\hat{Z}^{-1}$ solution exhibits a strong height dependence, providing an accurate solution in case A1 ($kh = 0.52$), but barely converging in case A4 ($kh = 1.03$) to a solution that is much less accurate than the $\hat{N}$ solution which converges rapidly. The examples in Sec. 4.6 illustrate the tremendous difference the two-way continuation makes in constructing a widely accurate scattering solution.

The $\hat{Z}^{-1}$ solution is very similar analytically to the perturbation solution; the operations are the same, but the zeroth order solutions (and hence higher orders as well) are defined differently. The numerical examples show how this subtle difference dramatically improves the accuracy of the solution obtained. The $\hat{Z}^{-1}$ method converges more rapidly, and better matches the fluctuations of the exact solution for scattering from a finite number of surface realizations than the standard perturbation solution.

In summary, the operator expansion is accurate and rapidly convergent for scattering from surfaces with a Gaussian spectrum, over a wide range of scattering angles and over a wide range of surface roughness scales. This method is accurate in the validity regions of perturbation theory and the Kirchhoff approximation and beyond, strongly suggesting that the operator expansion method would be useful in computing scattering from multiscale surfaces; this expectation is confirmed in the numerical tests conducted in Chapter 5.

7.5 Accuracy of the OE for computing scattering from surfaces with a Pierson-Moskowitz spectrum — Chapter 5

The ocean surface is one of many naturally occurring interfaces which are rough on many scales. Scattering of acoustic waves from the ocean surface is a problem further complicated by the existence of variations in the sound speed in the water, which are due to the presence of bubbles, variations in temperature, pressure, and salinity, and to a lesser extent marine life, in the near surface region. In this dissertation the problem is restricted to interface scattering alone; we treat scattering of 200-1000 Hz acoustic energy from 1-D randomly rough surfaces consistent with a spectrum derived from the Pierson-Moskowitz spectrum for a fully developed sea. In this model, the 1-D surface height spectrum is inversely proportional to the cube of the spatial wave number with an upper wavenumber cutoff, and tapered at low wave numbers in a way that depends on the wind speed. This simplified model is used to assess the accuracy of the OE method, again through comparison with the integral equation solution. We expect that the results of this study will extend to scattering from realistic 2-D surfaces for which exact solutions are still very costly.

In Sec. 5.2, we study low frequency (200 Hz) scattering from surfaces with wind speeds between 5 and 20 m/s, and for incident angles $10° \le \theta_i \le 90°$. In this regime, the operator expansion series solution is rapidly convergent over all scattering angles, providing an accurate solution at second order, where the maximum error for OE_2 is about 0.5 dB (in the backscattering region) for incident angle $\theta_i = 10°$. The accuracy and convergence rate of the operator expansion solution up through third order are illustrated for $\theta_i = 20°$ and 20 m/s wind speed in Fig. 5.2. At any given scattering angle (except a couple of degrees from grazing where the OE solution is not quite as reliable), the scattering strength error decreases as the incident angle is increased, much as it did for Gaussian surfaces. This effect is demonstrated in Fig. 5.3, which presents scattering results for the same ensemble of 50 realizations of 20 m/s surfaces, for $\theta_i = 10°$, 45°, and 90°.

The accuracy of the alternative series formulations has also been examined for 1-D Pierson-Moskowitz surfaces. The greater efficiency of the short forms (odd and even series) is more clearly visible for Pierson-Moskowitz surfaces than for surfaces with a Gaussian spectrum. Figs. 5.4 and 5.5 indicate that the short series solutions are more accurate than the standard series computed to the same order, *over all scattering angles*. The character of the short series solutions computed to order n is very similar to that of the standard solution computed to order $n +$ ' this surface height spectrum, the odd and even series essentially get "an order fc

The short series also prove to be much more efficient at computing an accurate solution than the consistent series solution computed to the same order in the surface field. Fig. 5.6 illustrates this property for the second order consistent solution $OE^{(2)}$; even the first order solution OD_1 is more accurate than $OE^{(2)}$ over almost all scattering angles. This surprising lack of sensitivity of the OE solution to consistency in the expansion parameter is very different from the behavior of perturbation theory applied to scattering from Pierson-Moskowitz surfaces [Thorsos, 1990]. There it was shown that a major cancellation between terms containing fourth powers of the perturbation expansion parameter kh requires careful computation of both terms at that order, σ_{22} and σ_{13}, necessitating calculation of the second *and* third order fields to obtain the second term in the series for the incoherent cross section $\sigma^{(4)}$.

Many applications in ocean acoustics involve very low grazing angle propagation and scattering, and for higher frequencies than 200 Hz. The difficulty with testing scattering approximations in this regime using an integral equation technique has been the need for extremely long surfaces to preserve accuracy and angular resolution, and hence large numbers of surface partion intervals. The recent application of a parabolic approximation to the low grazing angle forward scattering problem [Thorsos, 1993b] has made testing of approximations possible in this regime. We apply the OE method to scattering from 15 m/s 1-D Pierson-Moskowitz surfaces for incident grazing angles as low as $\theta_i = 5°$ for acoustic frequencies as high as $f = 1000$ Hz. For that example 20,000 surface partition intervals are used. As for most numerical examples in the dissertation, 50 surface realizations are used in obtaining an average solution. We find that even for this case, the OE solutions (first order and higher) are accurate over the range of forward scattering angles studied: $135° \leq \theta_s \leq 180°$ (see Fig. 5.9). Some distant multiple scattering can occur for this example, because the ratio between the wavelength of the tallest surface waves (at the peak of the surface height spectrum) and the acoustic wavelength is $\lambda_{peak} / \lambda = 140$.

The OE solution for scattering angles within a few degrees of grazing requires more numerical care than elsewhere. The Fourier integral operator $\hat{Q}$ includes a wavenumber domain filter which goes to zero for $k_z = 0$, and relatively fine sampling in the wavenumber domain is required to properly represent the wave field in the neighborhood of the zero crossing. Extending the length of the computational surface by zero-padding the rough surface profile before Fourier transforming is a straightforward way of reducing the near-grazing error in the scattering strength; the error can be as large as 2 or 3 dB at grazing. An example representative of the results obtained for several choices of computational surface length is given in Fig. 5.10.

In summary, the operator expansion method is accurate and rapidly convergent for scattering from 1-D Pierson-Moskowitz surfaces used to model the ocean surface for wind speeds up to 15-20 m/s, for frequencies up to 1000 Hz. The numerical studies have all been carried out for surfaces rough in one dimension only because of computational constraints associated with the integral equation method. Nevertheless, the tie between the rapid convergence of the operator expansion series solution and its accuracy is expected to carry over to scattering from two-dimensional surfaces. The operator expansion is fast and accurate enough to be useful in treating moderate ($f \leq 1000$ Hz) frequency scattering from realistic two-dimensional sea surfaces. The method is likely to be useful at higher frequencies, but such tests have not been performed.

7.6 Formal average of the OE solution — Chapter 6

The operator expansion is currently applied in a Monte Carlo method, estimating moments of the scattered field by averaging scattering results computed from one surface at a time. A formal average of the lowest order even series solution EV_0 is performed in Chapter 6, but the solution obtained for the scattering cross section is not simple enough to be practical. The expression for the second moment of the scattering amplitude for scattering from a 1-D surface contains five integrations; without further reduction in complexity this unwieldy expression is of little practical value, particularly since this low order solution is not deemed sufficiently accurate for most applications.

The complexity of the average solution is a consequence of the OE method's nonlocal nature; this nonlocal property is also responsible for the method's accuracy. The simplest solution for the unknown surface field (specifically, the normal derivative of the scattered field) is obtained using the fundamental nonlocal derivative operator $\hat{Q}$ which contains two Fourier integrals, one over the transverse coordinate and one over the transverse wave number. A third integral (over the transverse coordinate) gives the scattered field above the surface. In the second moment, the product of two scattered field terms gives rise to a six-fold integral expression. A suitable coordinate transformation to sum and "difference" coordinates allows evaluation of the integral over the sum coordinate, leaving five integrals as mentioned above.

The second moment expression rapidly becomes more complex as higher order solutions are averaged. In essence, each higher order in the operator expansion for the surface field contains an additional product by the surface height function ζ and an additional operation by $\hat{Q}$, such that the n'th order operator has n factors of ζ and $n+1$ factors of $\hat{Q}$ arranged in alternating order in its intrinsically nonlocal term (see Eq. (3.28) for the complete list of terms in the expansion through third order). The

complexity of averaging higher order terms is prohibitively complex without application of some clever integration technique, or suitable approximation. The expressions in Chapter 6 are presented in order to outline the problem, and are not intended to be numerically evaluated.

7.7 Summary and ideas for future work

The operator expansion method [Milder, 1991] has been applied to computing acoustic scattering from 1-D randomly rough Dirichlet surfaces with Gaussian and Pierson-Moskowitz spectra. Through comparison with exact numerical results obtained by solution of an integral equation, the operator expansion method is found to provide a rapidly convergent and accurate solution over a wide range of incident and scattering angles and surface roughness parameters. The method achieves its accuracy through a cleverly constructed nonlocal operator that is expanded in a series containing powers of the surface height function and a Fourier integral operator. The latter is conveniently implemented in terms of FFTs, resulting in an algorithm that is very rapidly computed. Though the method only computes scattering from a single surface profile at a time, it is sufficiently fast to be practical in computing scattering from 2-D surfaces; the findings regarding the method's accuracy in scattering from 1-D surfaces are expected to carry over to scattering from 2-D surfaces.

The operator expansion method is a very promising technique, and the research for this dissertation has led to several interesting avenues worthy of further development:

- The method is currently only developed for scattering from Dirichlet surfaces, but the formalism of Chapter 3 may be useful in extending the method to other boundary conditions. Preliminary work on the Neumann boundary condition is encouraging[†].

- The method does not currently have a practical formal average. Such a result would enhance the method's usefulness.

- A few informal comparisons to other approximations that do have formally averaged solutions (such as the small slope approximation [Voronovich, 1985], for

[†] The formalism of Chapter 3 leads to a straightforward Neumann expansion in terms of the inverse operator Q^{-1}, which presents more of a challenge to implement. In a personal communication, Milder [1993] indicated that a straightforward numerical treatment of Q^{-1} is possible, leading to a useful OE solution for the Neumann boundary and consequently for electromagnetic scattering from a perfect conductor.

example) indicate that the OE method is more accurate. However, further tests are necessary to establish the relative accuracy of these methods.

- The OE has been tested for 1-D surfaces, but real applications exist primarily for scattering from 2-D surfaces. The extension to 2-D surfaces has been done by Milder and Sharp [1992], and others [Dubberley, 1992], but further validation through comparisons to theoretical and experimental results should be performed.

BIBLIOGRAPHY

Axline, R.M. and A.K. Fung, "Numerical computation of scattering from a perfectly conducting random surface," IEEE Trans. Antennas Propag. AP-26, 482-488, 1978; AP-28, p. 949, 1980.

Bahar, E., "Full-wave and physical optics solutions for scattered radiation fields by rough surfaces — Energy and reciprocity relationships," IEEE Trans. Antennas Propag. AP-26, 603-614, 1978.

Bahar, E., "Full-wave solutions for the scattered radiation fields from rough surfaces with arbitrary slope and frequency," IEEE Trans. Antennas Propag. AP-28, 11-21, 1980.

Bahar, E., "Scattering cross sections for random rough surfaces: Full wave analysis," Radio Sci. 16, 331-341, 1981.

Bahar, E., "Review of the full-wave solutions for rough surface scattering and depolarization: Comparisons with geometric and physical optics, perturbation, and two-scale hybrid solutions," J. Geophys. Res. 92, 5209-5224, 1987.

Bahar, E., "Examination of full-wave solutions and 'exact numerical results' for one-dimensional slightly rough surfaces," J. Geophys. Res. 96(C9), 17123-17131, 1991.

Baker, B.B. and E.T. Copson, *The Mathematical Theory of Huygens' Principle*, 2nd edition, Oxford University Press, London, 1950.

Bass, F.G. and I.M. Fuks, *Wave Scattering from Statistically Rough Surfaces*, International Series in Natural Philosophy, vol. 93, Pergamon Press, Oxford, 1979.

Beckmann P., and A. Spizzichino, *The Scattering of Electromagnetic Waves from Rough Surfaces*, Pergamon Press, New York, 1963.

Berman, D.H., "Simulations of rough interface scattering," J. Acoust. Soc. Am. 89(2), 623-636, 1991.

Berman, D. H., and J. S. Perkins, "Rayleigh method for scattering from random and deterministic interfaces," J. Acoust. Soc. Am. 88(2), 1032-1044, 1990.

Born, M., and E. Wolf, *Principles of Optics*, Pergamon Press, 1980.

Brekhovskikh, L. M., "Diffraction of waves at an uneven surface, I and II," J. Exptl.-Theoret. Phys. (USSR) 23, 275-304, 1952.

Broschat, S. L., L. Tsang, A. Ishimaru, and E. I. Thorsos, "A numerical comparison of the phase perturbation technique with the classical field perturbation and Kirchhoff approximations for random rough surface scattering," J. Electromagnetic Waves Applic. 2(1), 85-102, 1987.

Broschat, S. L., E. I. Thorsos, and A. Ishimaru, "The phase perturbation technique vs. an exact numerical method for random rough surface scattering," J. Electromagnetic Waves Applic. 3(3), 237-256, 1989.

Broschat, S. L., E. I. Thorsos, and A. Ishimaru, "A heuristic algorithm for the bistatic radar cross section for random rough surface scattering," IEEE Trans. Geosci. Remote Sensing 28(2), 202-206, 1990.

Broschat, S. L., and E. I. Thorsos, "A Numerical Study of the Small Slope Approximation for Rough Surface Scattering," Meeting Digest, ICO Topical Meeting on Atmospheric, Volume and Surface Scattering and Propagation, Florence, Italy, 1991 (paper in preparation)

Broschat, S.L., "The phase perturbation approximation for rough surface scattering from a Pierson-Moskowitz sea surface," IEEE Trans. on Geoscience and Remote Sensing, 31(1), 278-283, 1993.

Cadhilac, M., "Some mathematical aspects of the grating theory," in *Electromagnetic Theory of Gratings*, R. Petit editor, pp. 53-62, Springer-Verlag, Berlin, 1980.

Carsey, F. D. ed., *Microwave Sensing of Sea Ice*, Geophysical Monograph 68, American Geophysical Union, 1992.

Chen, J. S., and A. Ishimaru, "Numerical simulation of the second-order Kirchhoff approximation from very rough surfaces and a study of backscattering enhancement," J. Acoust. Soc. Am. 88(4), 1846-1850, 1990.

Chuang, S.L. and J.A. Kong, "Scattering of waves from periodic surfaces," Proc. IEEE 69, 1132-1144, 1981.

Claerbout, J. F., *Imaging the Earth's Interior*, Blackwell Scientific Publications, 1985.

Courant, R., and D. Hilbert, *Methods of Mathematical Physics*, Vol. II, *Partial Differential Equations*, by R. Courant, Interscience Publishers (Wiley), New York, 1962.

Dashen, R., and D. Wurmser, "A new theory for scattering from a surface," J. Math. Phys. 32(4), 971-985, 1991a.

Dashen, R., and D. Wurmser, "Approximate representations of the scattering amplitude," J. Math. Phys. 32(4), 986-996, 1991b.

Dashen, R., and D. Wurmser, "Applications of the new scattering formalism: The Dirichlet boundary condition," J. Math. Phys. 32(4), 997-1003, 1991c.

Dashen, R., F. S. Henyey, and D. Wurmser, "Calculations of acoustic scattering from the ocean surface," J. Acoust. Soc. Am. 88(1), 310-323, 1990.

DeSanto, J. A., "Theoretical methods in ocean acoustics," in *Ocean Acoustics*, edited by J. A. DeSanto, Springer-Verlag, Berlin, 7-77, 1979.

DeSanto, J. A., "Scattering from a perfectly reflecting arbitrary periodic surface: An exact theory," Radio Sci. 16(6), 1315-1326, 1981.

DeSanto, J. A., and G. S. Brown, "Analytical techniques for multiple scattering from rough surfaces," Progress in Optics XXIII, ed. E. Wolf, Elsevier, 1986.

Dongarra, J. J., J. R. Bunch, C. B. Moler, and G. W. Stewart, LINPACK *Users' Guide*, Soc. Indust. Appl. Math., Philadelphia, 1979.

Dubberley, J. R., "Operator expansion error estimation by higher-order terms," J. Acoust. Soc. Am. 91(4 Part 2), 2UW4, 1992.

Eckart, C., "The scattering of sound from the sea surface," J. Acoust. Soc. Am. 25, 566-570, 1953.

Ellis, D. D., J. R. Preston, and H. G. Urban, editors, *Ocean Reverberation*, Kluwer Academic Publishers, The Netherlands, 1993.

Garcia, N., V. Celli, N. R. Hill, and N. Cabrera, "Ill-conditioned matrices in the scattering of waves from hard corrugated surfaces," Phys. Rev. B 18(10), 5184-5189, 1978.

Geernaert, G. R., and W. J. Plant editors, *Surface Waves and Fluxes*, 2 vols., Kluwer Academic Publishers, The Netherlands, 1990.

Guinard, N.W., J.T. Ransone Jr., and J.C. Daley, "Variation of the NRCS of the sea with increasing roughness," J. Geophys. Res. 76, 1525- , 1971.

Harper, E. Y., and F. M. Labianca, "Perturbation theory for scattering of sound from a point source by a moving rough surface in the presence of refraction," J. Acoust. Soc. Am. 57, 1044-1051, 1975a.

Harper, E. Y., and F. M. Labianca, "Scattering of sound from a point source by a rough surface progressing over an isovelocity ocean," J. Acoust. Soc. Am. 58, 349-364, 1975b. (and erratum: JASA 59, p. 484, 1976)

Hill, N. R., and V. Celli, "Limits of convergence of the Rayleigh method for surface scattering," Phys. Rev. B 17, 2478-2481, 1978.

Holliday, D., "Resolution of a controversy surrounding the Kirchhoff approach and the small perturbation method in rough surface scattering theory," IEEE Trans. Antennas Propag. 35, 120-122, 1987.

Hugonin, J. P., R. Petit, M. Cadhilac, "Plane-wave expansions used to describe the field diffracted by a grating," J. Opt. Soc. Am. 71, 593-598, 1981.

Ikuno, H., and K. Yasuura, "Improved point-matching method with application to scattering from a periodic surface," IEEE Trans. Antennas Propag. AP-21, 657-662, 1973.

Ishimaru, A., *Wave Propagation and Scattering in Random Media*, 2 vols., Academic Press, New York, 1978.

Ishimaru, A., *Electromagnetic Wave Propagation, Radiation and Scattering*, Prentice Hall, New Jersey, 1991.

Ishimaru, A., and J. S. Chen, "Scattering from very rough surfaces based on the modified second-order Kirchhoff approximation with angular and propagation shadowing," J. Acoust. Soc. Am. 88(4), 1877-1888, 1990.

Jackson, D. R., D. Winebrenner, and A. Ishimaru, "Comparison of perturbation theories for rough-surface scattering," J. Acoust. Soc. Am. 83(3), 961-969, 1988.

Jackson, J. D., *Classical Electrodynamics*, Wiley, New York, 1975.

Kur'yanov, B.F., "The scattering of sound at a rough surface with two types of irregularity," Sov. Phys. Acoust., vol. 8, 252-257, 1963.

Kuttruff, H., *Ultrasonics Fundamentals and Applications*, Elsevier Science Publishing Co. Inc., New York, 1991.

Labianca, F.M. and E.Y. Harper, "Connection between various small- waveheight solutions of the problem of scattering from the ocean surface," J. Acoust. Soc. Am. 62, 1144-1157, 1977.

Lippmann, B. A., "Note on the theory of gratings," J. Opt. Soc. Am. 43(5), p. 408, 1953.

Liszka, E.G. and J.J. McCoy, "Scattering at a rough boundary - extensions of the Kirchhoff approximation," J. Acoust. Soc. Am. 71, 1093-1100, 1982.

Lou, S. H., *Application of Numerical Methods to Monte Carlo Simulations of Scattering of Waves by Random Rough Surfaces*, Ph.D. dissertation, Univ. of Washington, Seattle, 1991.

Lou, S. H., L. Tsang, C. H. Chan, and A. Ishimaru, "Application of the finite element method to Monte Carlo simulations of scattering of waves by random rough surfaces with the periodic boundary condition," J. Electromagnetic Waves and Appl. 5(8), 835-855, 1991a.

Lou, S. H., L. Tsang, and C. H. Chan, "Application of the finite element method to Monte Carlo simulations of scattering of waves by random rough surfaces: Penetrable case," Waves in Random Media 1(4), 287-307, 1991b.

Lysanov, Iu. P., "One approximate solution for the problem of the scattering of acoustic waves by an uneven surface," Soviet Phys. Acoust. 2, 190-197 (1956).

Macaskill, C. and T. E. Ewart, "Computer simulation of two-dimensional random wave propagation," IMA J. Appl. Math 33, 1-15, 1984.

Maradudin, A. A., T. Michel, A. R. McGurn, and E. R. Mendez, "Enhanced backscattering of light from a random grating," Annals of Physics 203, 255-307, 1990.

Marcuse, D., *Light Transmission Optics*, Van Nostrand Reinhold, New York, 1982.

McDaniel, S.T., "Sea surface reverberation: A review," J. Acoust. Soc. Am. 94(4), 1905-1922, 1993.

McDaniel, S.T. and A.D. Gorman, "Acoustic and radar sea-surface backscatter," J. Geophys. Res. 87, 4127-4136, 1982.

McDaniel, S.T. and A.D. Gorman, "An examination of the composite- roughness scattering model," J. Acoust. Soc. Am. 73(5), 1476-1486, 1983.

Meecham, W.C., "On the use of the Kirchhoff approximation for the solution of reflection problems," J. Rational Mech. Anal. 5(2), 323-334, 1956a.

Meecham, W. C., "Variational method for the calculation of the distribution of energy reflected from a periodic surface. I," J. Appl. Phys. 27(4), 361-367, 1956b.

Meecham, W. C., "Fourier transform method for the treatment of the problem of the reflection of radiation from irregular surfaces," J. Acoust. Soc. Am. 28(3), 370-377, 1956c.

Milder, D. M., "The effects of truncation on surface-wave Hamiltonians," J. Fluid Mech. 217, 249-262, 1990.

Milder, D. M., "An improved formalism for wave scattering from rough surfaces," J. Acoust. Soc. Am. 89(2), 529-541, 1991.

Milder, D. M., and H. T. Sharp, "An improved formalism for rough-surface scattering. II: Numerical trials in three dimensions," J. Acoust. Soc. Am. 91(5), 2620-2626, 1992.

Millar, R. F., "On the Rayleigh assumption in scattering by a periodic surface," Proc. Cambridge Phil. Soc. 65(3), 773-791, 1969.

Millar, R. F., "Singularities of two-dimensional exterior solutions of the Helmholtz equation," Proc. Cambridge Phil. Soc., 69(1), 175-188, 1971.

Millar, R. F., "The Rayleigh hypothesis and a related least-squares solution to scattering problems for periodic surfaces and other scatterers," Radio Sci. 8, 785-796, 1973.

Neviere, M., and M. Cadhilac, "Sur la validite du development de Rayleigh," Optics Commun. 2(5), 235-238, 1970.

Nieto-Vesperinas, M., and N. Garcia, "A detailed study of the scattering of scalar waves from random rough surfaces," Opt. Acta 28, 1651-1672, 1981.

Nutzel, B., H. Herwig, and A. Schmidt, "Acoustic and microwave backscattering of the sea surface," IEEE OCEANS, II:13-18, 1993.

Ogilvy, J. A., *Theory of Wave Scattering from Random Rough Surfaces*, Adam Hilger, Boston, 1991.

Papoulis, A., *Probability, Random Variables, and Stochastic Processes*, McGraw-Hill, 1984.

Petit, R. editor, *Electromagnetic Theory of Gratings*, Springer-Verlag, Berlin, 1980; includes "A tutorial introduction," by R. Petit, pp. 1-52.

Petit, R. and M. Cadhilac, "Sur la diffraction d'une onde plane par un reseau infiniment conducteur," C. R. Acad. Sci. Ser. B, 262(7), 468-471, 1966.

Pierson, W. J., and L. Moskowitz, "A proposed spectral form for fully developed wind seas based on the similarity theory of S. A. Kitaigorodskii," J. Geophys. Res. 69, 5181-5190, 1964.

Plant, W.J., "Comment on the full-wave controversy," J. Geophys. Res., 96, 17105-17106, 1991.

Press, W. H., B. P. Flannery, S. A. Teukolsky, W. T. Vetterling, *Numerical Recipes, the Art of Scientific Computing*, (FORTRAN version), Cambridge University Press, 1986.

Rayleigh, Lord (J. W. Strutt), "On the dynamical theory of gratings," Proc. Roy. Soc., Ser. A, vol. 79, 399-416, 1907.

Rayleigh, Lord (J. W. Strutt), *The Theory of Sound*, vol. 2, Dover, New York, 1945. (First edition printed 1877)

Rice, S. O., "Reflection of electromagnetic waves from slightly rough surfaces," Commun. Pure Appl. Math. 4, 351-378, 1951.

Rodriguez, E., "Beyond the Kirchhoff approximation," Radio Sci. 24(5), 681-693, 1989.

Rodriguez, E., and Y. Kim, "A unified perturbation expansion for surface scattering," Radio Sci. 27(1), 79-93, 1992.

Shen, J., and A. A. Maradudin, "Multiple scattering of waves from random rough surfaces," Phys. Rev. B, 22(9), 4234-4240, 1980.

Sommerfeld, A., *Optics*, Vol. IV of *Lectures on Theoretical Physics*, Academic Press, New York, 1954.

Soto-Crespo, J. M., M. Nieto-Vesperinas, and A. T. Friberg, "Scattering from slightly rough random surfaces: a detailed study on the validity of the small perturbation method," J. Opt. Soc. Am. A 7(7), 1185-1201, 1990.

Tappert, F. D., "The parabolic approximation method," in *Wave Propagation in Underwater Acoustics*, eds. J. B. Keller and J. S. Papadakis, Springer-Verlag, Berlin, 224-287, 1977.

Thompson, D.R. and R.D. Chapman, "Note on the reduction of the 'full- wave' method for rough surface scattering to the small-height limit," J. Geophys. Res., 98(C3), 4827-4831, 1993.

Thorsos, E. I., "Rough surface scattering using the parabolic wave equation," J. Acoust. Soc. Am. 82(S1), S103A, 1987.

Thorsos, E. I., "The validity of the Kirchhoff approximation for rough surface scattering using a Gaussian roughness spectrum," J. Acoust. Soc. Am. 83(1), 78-92, 1988.

Thorsos, E. I., "Acoustic scattering from a 'Pierson-Moskowitz' sea surface," J. Acoust. Soc. Am. 88(1), 335-349, 1990.

Thorsos, E. I., "The accuracy of the single backscattering, multiple forward scattering approximation for low grazing angle sea surface reverberation," J. Acoust. Soc. Am. Suppl. 1, vol. 88, S83-S84, 1990.

Thorsos, E. I., (accuracy of the small slope approximation) personal communication, 1993a.

Thorsos, E. I., Parabolic Equation Integral Equation method for rough surface scattering (paper in preparation), 1993b.

Thorsos, E. I., and D. R. Jackson, "The validity of the perturbation approximation for rough surface scattering using a Gaussian roughness spectrum," J. Acoust. Soc. Am. 86(1), 261-277, 1989.

Thorsos, E. I., and D. R. Jackson, "Studies of scattering theory using numerical methods," Waves in Random Media 3, S165-S190, 1991.

Thorsos, E.I. and D.P. Winebrenner, "An examination of the Full- Wave" method for rough surface scattering in the case of small roughness," J. Geophys. Res. 96(C9), 17107-17121, 1991.

Tsang, L., C. H. Chan, and H. Sangani, "Banded matrix iterative approach to Monte-Carlo simulations of scattering of waves by large-scale random rough surface problems: TM case," Electron. Let. 29(2), 166-167, 1993a.

Tsang, L., C. H. Chan, and K. Pak, "Monte Carlo simulation of a two-dimensional random rough surface using the sparse-matrix flat-surface iterative approach," Electron. Let. 29(13), 1153-1154, 1993b.

Tsang, L., and A. Ishimaru, "Backscattering enhancement of random discrete scatterers," J. Opt. Soc. Am. A 1, 836-839, 1984.

Urusovskii, I. A., "Sound scattering by a sinusoidally uneven surface characterized by normal acoustic conductivity," Soviet Phys. Acoust. 5(3), 362-369 (1960).

Uscinski, B. J., "Analytical solution of the fourth-moment equation and interpretation as a set of phase screens," J. Opt. Soc. Am. A 2(12), 2077-2091, 1985.

Valenzuela, G.R., "Theories for the interaction of electromagnetic and oceanic waves — A review," Boundary Layer Meteorol., 13, 61-85, 1978.

van den Berg, P. M., and J. T. Fokkema, "The Rayleigh hypothesis in the theory of reflection by a grating," J. Opt. Soc. Am. 69(1), 27-31, 1979a.

van den Berg, P. M., and J. T. Fokkema, "The Rayleigh hypothesis in the theory of diffraction by a cylindrical obstacle," IEEE Trans. Antennas Propag. AP-27(5), 577-583, 1979b.

van den Berg, P. M., and J. T. Fokkema, "The Rayleigh hypothesis in the theory of diffraction by a perturbation in a plane surface," Radio Sci. 15(4), 723-732, 1980.

Voronovich, A. G., "Small slope approximation in wave scattering by rough surfaces," Sov. Phys. JETP 62(1), 65-70, 1985.

Voronovich,, A. G., "The small-slope approximation in the theory of sound scattering by an uneven free surface," Dokl. Acad. Sci. USSR, Earth Sci. Sections 287(1-6), 186-190 (1987).

Wagner, R. J., "Shadowing of randomly rough surfaces," J. Acoust. Soc. Am. 41, 138-147, 1966.

Waterman, P.C., "Scattering by periodic surfaces," J. Acoust. Soc. Am., 57(4), 791-802, 1975.

Watson, K. M., and B. J. West, "A transport-equation description of nonlinear ocean surface wave interactions," J. Fluid Mech. 70(4), 815-826, 1975.

Weissman, D. E., W. J. Plant, S. Stolte, and J. P. Dugan, "The modulation and coherence functions between atmospheric turbulence at the sea surface and the microwave radar cross section," IEEE OCEANS, II:358-364, 1993.

West, B. J., K. A. Brueckner, R. S. Janda, D. M. Milder, and R. L. Milton, "A new numerical method for surface hydrodynamics," J. Geophys. Res. 92(C11), 11803-11824, 1987.

Whitman, G. M., D. M. Leskiw, and F. Schwering, "Rigorous theory of scattering by perfectly conducting periodic surfaces with trapezoidal height profile, TE and TM polarization," J. Opt. Soc. Am. 70, 1495-1503, 1980.

Winebrenner, D. P., *A Surface Field Phase-Perturbation Technique for Scattering from Rough Surfaces*, Ph.D. dissertation, Univ. of Washington, Seattle, 1985.

Winebrenner, D. and A. Ishimaru, "Investigation of a surface field phase perturbation technique for scattering from rough surfaces," Rad. Sci. 20, 161-170, 1985a.

Winebrenner, D. and A. Ishimaru, "Application of the phase-perturbation technique to randomly rough surfaces," J. Opt. Soc. Am. 2, 2285-2294, 1985b.

Wolf, E., "A generalized extinction theorem and its role in scattering theory," in *Coherence and Quantum Optics*, ed. L. Mandel and E. Wolf, 339-357, Plenum Press, New York, 1973.

Yasuura, K., "A view of numerical methods in diffraction problems," in *Progress in Radio Science 1966-1969*, vol. 3, edited by C. M. Minnis, Radio Waves and Circuits, 1971.

Yasuura, K., and H. Ikuno, "On the modified Rayleigh hypothesis and the mode-matching method," Summaries International Symposium on Antennas and Propagation, Sendai, Japan, 173-174, Institute of Electronics and Communication Engineers of Japan, Tokyo, Japan, 1971.

APPENDIX

Table of Numerical Parameters

TABLE 1 : Parameter values used in numerical computations.

Case [Freq (Hz)]	Figure(s)	θ_i(deg)	kl [U (m/s)]	kh	Number of Intervals	$\lambda/\Delta x$	L/g	Tp(%)
A1	4.3,21,25	45	1.4	0.38	800	10	5.0	0
A2	4.4,22,25	45	2.6	0.52	800	8	5.5	0
A3	4.5,7,23,25	45,20,90	4.5	0.69	600	5	5.5	0
A4	4.6	45	10.0	1.03	750	5	7.0	10
B2	4.8,12,13,14	20	2.6	0.96	1100	10	5.5	5
B3	4.8,10,11	20	4.5	1.26	800	6	6.0	10
B4	4.8,15,16,17	20	10.0	1.88	800	5	8.0	15
C2	4.9,12,13,14	30	2.6	1.35	1500	14	5.5	8
C3	4.9	20	4.5	1.78	1100	10	6.0	10
C4	4.9,15,16,17	20	10.0	2.67	1200	6	7.0	15
D2	4.9,12,13,14	30	2.6	1.66	1500	15	5.5	8
D4	4.9,15,16,17	20	10.0	3.26	1200	8	7.0	15
F4	4.19,20	60	7.0	4.2	512	12	6.0	15
[200]	5.2,3,4,5,6	20,45,90	[20]	1.79	1000	6	6.0	10
[200]	5.3	10	[20]	1.79	2000	6	6.5	10
[500]	5.7	10	[15]	2.51	2500	5	4.0	0
[500]	5.8	5	[15]	2.51	10000	5	4.0	0
[1000]	5.9	5	[15]	5.03	20000	5	4.0	0

The number of surface realizations used in the averaging for each case is 50, except in the backscattering enhancement case F4 when 500 surfaces were used. The parameter values presented below are for all computations *except* third order operator expansion calculations, OE_3 and ON_3. These calculations were done using twice the surface partition density (i.e., twice the number of points per wavelength $\lambda/\Delta x$, and hence twice the number of surface intervals) for the same surface profile used in the other calculations. The surface height function is spectrally interpolated to obtain the higher density. The incident field taper is expressed in terms of the surface length L and the taper width g defined in (3.34). The surface height taper discussed in Sec. 3.3.4 is listed in Table 1 as "Tp" and represents the percentage of the surface length L over which a half period cosine tapers the surface height at each end of the surface.

VITA

Peter Kaczkowski was born on May 6, 1956 in Asbestos, Quebec, Canada. He graduated with a Baccalaureat "C" (Math-Physics) from the Lycee International de Saint Germain en Laye, France, in 1973. He received a Bachelor of Science in Electrical Engineering from the University of Colorado in Boulder, Colorado, in 1977. After working for the Bureau of Electricity in Alameda, California, as a power distribution engineer, for Intel Corporation in Santa Clara, California, as an integrated circuit test engineer, and for Geoconsult in Denver, Colorado, as a geophysicist, he obtained a Master of Science in Geophysics from the Colorado School of Mines in Golden, Colorado, in 1986. He then taught physics and electronics at Sylvania Community College in Portland, Oregon, and began studies in the Ph. D. program in Electrical Engineering at the University of Washington in 1988. While in this program, he also worked as an electrical engineer at the Applied Physics Laboratory. His research interests include theoretical and experimental aspects of ocean acoustics, rough surface scattering, inverse problems, and electromagnetic methods in geophysics. He is a current member of the Acoustical Society of America, and a former member of the Society of Exploration Geophysicists and the European Association of Exploration Geophysicists.

Selected Publications

Kaczkowski, P., "Damped least squares inversion applied to ducted propagation of acoustic energy in the ocean", Master's Thesis, Department of Geophysics, Colorado School of Mines, 1986.

Kaczkowski, P. J., and E. I. Thorsos, "Application of the operator expansion method to scattering of low frequency sound from the ocean surface," IEEE OCEANS, I:421-426, 1993.

Kaczkowski, P. J., and E. I. Thorsos, "Application of the operator expansion method to scattering from one-dimensional moderately rough Dirichlet random surfaces," submitted to the Journal of the Acoustical Society of America, July 1993.

REPORT DOCUMENTATION PAGE

Form Approved
OPM No. 0704-0188

1. AGENCY USE ONLY *(Leave blank)*	2. REPORT DATE	3. REPORT TYPE AND DATES COVERED
	June 1994	Technical

4. TITLE AND SUBTITLE
A Study of the Operator Expansion Method and its Application to Scattering from Randomly Rough Dirichlet Surfaces

5. FUNDING NUMBERS
N00014-90-J-1252

6. AUTHOR(S)
Peter J. Kaczkowski

7. PERFORMING ORGANIZATION NAME(S) AND ADDRESS(ES)
Applied Physics Laboratory
University of Washington
1013 NE 40th Street
Seattle, WA 98105-6698

8. PERFORMING ORGANIZATION REPORT NUMBER
APL-UW TR9406

9. SPONSORING / MONITORING AGENCY NAME(S) AND ADDRESS(ES)
Office of Naval Research
800 N. Quincy Street
Arlington, VA 22217-5660
ATTN: Code 3210A

10. SPONSORING / MONITORING AGENCY REPORT NUMBER

11. SUPPLEMENTARY NOTES

12a. DISTRIBUTION / AVAILABILITY STATEMENT
Unlimited distribution

12b. DISTRIBUTION CODE

13. ABSTRACT *(Maximum 200 words)*

The Operator Expansion (OE) method, a new approximation introduced by Milder [J. Acoust. Soc. Am. 89(2), 529-541, 1991] for computing wave scattering from rough surfaces, is applied to acoustic scattering from one-dimensional randomly rough pressure release (Dirichlet) surfaces. The accuracy of the OE series solution is evaluated through comparison with exact numerical results obtained by solution of an integral equation. Studies of scattering from moderately rough surfaces with a Gaussian spectrum indicate that the first order OE solution is accurate when either small perturbation theory or the Kirchhoff approximation is accurate. The first order OE solution is also accurate in some cases when neither classical method is valid. In this moderate roughness regime, the OE series converges rapidly over all scattering angles for a broad range of incident angles, and numerical studies indicate that rapid convergence is always associated with an accurate solution. As roughness is increased, the OE series solution converges less rapidly overall but remains accurate for a wide range of scattering regimes, including some cases just rough enough to support backscattering enhancement.

Studies of scattering from surfaces with a Pierson-Moskowitz spectrum used to model the sea surface interface roughness indicate that the OE method is very rapidly convergent over all angles for low frequency (200 Hz) acoustic scattering for wind speeds up to at least 20 m/s, and that the OE solution is accurate for very low grazing angle forward scattering for frequencies at least as high as 1000 Hz.

(continued)

14. SUBJECT TERMS
Underwater Acoustics, Rough Surface Scattering, Sea Surface Scattering, Rough Interface Scattering, Operator Expansion Method, Kirchhoff Approximation, Small Perturbation Method, Monte Carlo Method, Rayleigh Hypothesis, Backscattering Enhancement, Pierson-Moskowitz Spectrum

15. NUMBER OF PAGES
185

16. PRICE CODE

17. SECURITY CLASSIFICATION OF REPORT	18. SECURITY CLASSIFICATION OF THIS PAGE	19. SECURITY CLASSIFICATION OF ABSTRACT	20. LIMITATION OF ABSTRACT
Unclassified	Unclassified	Unclassified	SAR

13. ABSTRACT (continued)

The accuracy of simpler forms of the OE solution (also proposed by Milder) is investigated; these odd- or even-termed series are shown to be more efficient than the standard series at computing accurate solutions. The derivation of the operator series expansion is modified to provide an alternative, more intuitive, development. The connection to the Rayleigh hypothesis is discussed. OE estimates for the cross section are currently obtained using a Monte Carlo technique. The formal average for the lowest order cross section is presented, but the resulting expression is complicated and is not deemed practical. However, the OE method's efficiency and accuracy in one-dimensional tests suggest that this new approximation would be very useful, even as a Monte Carlo technique, for computing scattering from two-dimensional surfaces over a wide range of roughness regimes.